Electronic Supplementary Material (ESI) for ChemComm.

Supplementary Information

For:

Multivalent NHS-Acrylates for Orthogonal Site-Selective Functionalisation of Peptides at Cysteines Residues

Mariama Djaló,[a] Maria J. S. A. Silva,[a] Hélio Faustino,[a,b] Sandra N. Pinto,[c] Ricardo Mendonça[d] and, Pedro M. P. Gois[a]*

[a] Research Institute for Medicines (iMed.ULisboa) Faculty of Pharmacy, Universidade de Lisboa, Lisbon (Portugal)

[b] Association BLC3 — Innovation and Technology Campus, Oliveira do Hospital, Portugal.

[c] iBB-Institute for Bioengineering and Biosciences and i4HB-Institute for Health and Bioeconomy, Instituto Superior Técnico, Av. Rovisco Pais, 1049-001 Lisboa, Portugal.

[d] Hovione FarmaCiencia SA, Sete Casas, 2674-506 Loures, Portugal

E-mail: pedrogois@ff.ulisboa.pt

Index

1. General Remarks

Commercially available reagents were used without further purification and all solvents were of HPLC quality, purchased from Sigma-Aldrich, Fluorochem, Alfa Aesar, TCI, Carlo Erba or Honeywell. *C*-Ovalbumin, Laminin fragment, Cys-Bombesin and Cys-Cys-Bombesin peptides were purchased from GeneCust. Dipeptides were kindly prepared by Ismael Compañón and Dr. Francisco Corzana from Departamento de Química, Centro de Investigación en Síntesis Química, Universidad de La Rioja. Reactions under N_2 atmosphere were performed in oven-dried glassware and anhydrous solvents. Anhydrous DCM and THF were obtained using a Pure Solv™ Micro 100 Liter solvent purification system with activated alumina column and anhydrous DMF was purchased from Carlo Erba. All reaction were monitored by thin layer chromatography using Merck silica gel $60F_{254}$ aluminium plates. Visualization of the former was conducted under UV-light or by staining with the developing agents: Ninhydrin (0.3 g in a mixture of n-butanol (100 mL) and conc. H_2SO_4 (3 mL)), $KMnO_4$ (3 g with 20 g of K_2CO_3 in a mixture of H_2O (300 mL) and 5% aq. NaOH (5 mL)), PMA (7 g in 100 mL EtOH) and bromocresol green (0.04 g in a mixture of EtOH (100 mL) and 0.1 M NaOH solution, added until blue), followed by heating. Flash chromatography was performed with Merck Geduran® Si 60 (0.040-0.063 mm) silica gel. All new compounds were characterized by IR, ^{1}H NMR, ^{13}C NMR, HRMS (ESI) and when applicable. NMR spectra were recorded in Bruker Fourier 300, 400 and 500 using $CDCl_3$, $(CD_3)_2CO$, D_2O or $(CD_3)_2SO$ as deuterated solvents. The NMR spectrometers are part of the National NMR Network (PTNMR) and are partially supported by Infrastructure Project Nº 022161c and ROTEIRO/0031/2013– PINFRA/22161/2016 (co-financed by FEDER through COMPETE 2020, POCI and PORL and FCT through PIDDAC). All coupling constants are expressed in Hz and chemical shifts (δ) in ppm. Multiplicities are given as: s (singlet), d (doublet), dd (double doublet), dt (double triplet), t (triplet), td (triple triplet), tt (triple triplet), q (quartet), quint (quintuplet) and m (multiplet). IR spectra were traced in a Bruker FTIR-ATR Alpha II. UV spectra were traced in Thermo Scientific Evolution 201 UV-visible spectrophotometer. Fluorescence measurements were taken on a SHIMADZU spectrofluorophotometer RF-6000 instrument. Low Resolution Mass spectra were recorded in LCQ Fleet Ion Trap Mass Spectrometer, Thermo Fisher Scientific, Germany. High Resolution Mass spectra were recorded in a Thermo Scientific Q Exactive hybrid quadrupole-Orbitrap mass spectrometer (Thermo Scientific™ Q Exactive™ Plus). The Liquid chromatography–mass spectrometry (LC-MS) runs were performed using a Dionex Ultimate 3000 UHPLC+ system equipped with a Multiple-Wavelength detector and a imChem Surf C18 TriF 100 Å 3 µm 100 x 2,1 mm column connected to Thermo Scientific Q Exactive hybrid quadrupole-Orbitrap mass spectrometer (Thermo Scientific™ Q Exactive™ Plus). Semi-preparative RP HPLC was performed on a Dionex Ultimate 3000 system using a Phenomenex Luna® 10 µm

C18(2) 100 Å, LC Column 250 x 10 mm. 2-(2-(2-methoxyethoxy)ethoxy)ethyl-4-methylbenzenesulfonate,[1] 2-(2-(2-methoxyethoxy)ethoxy)-N-methylethan-1-amine[1], ((oxybis(ethane-2,1-diyl))bis(oxy))bis(ethane-2,1-diyl) dimethanesulfonate,[2] 2-(2-(2-(2-azidoethoxy)ethoxy)ethoxy)ethyl methanesulfonate,[3] 2-(2-(2-(2-azidoethoxy)ethoxy)ethoxy)-N-methylethan-1-amine,[4] ethyl 3-(diethylamino)-3-oxopropanoate,[5] ethyl 3-(methyl(phenyl)amino)-3-oxopropanoate,[6] 7-(diethylamino)-2H-chromen-2-one,[7] 7-(diethylamino)-2-oxo-2H-chromene-3-carbaldehyde[7], maleimide **27**[8] and BCN-Doxorubicin **S27**[9] were prepared according to reported procedures.

2. Chemical synthesis

2.1. General procedure for the synthesis of ethyl oxopropanoate derivates S1-2

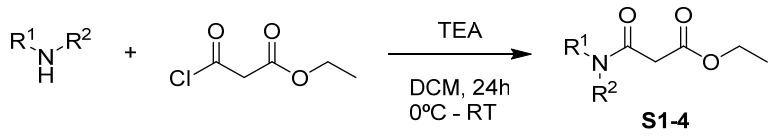

To a solution of amine (1.0 equiv) in dry DCM is added TEA (2.0 equiv) under argon and cooled to 0ºC. Afterwards, ethyl 3-chloro-3-oxopropanoate (1.0 equiv) in dry DCM was added dropwise. The solution was allowed to warm at rt and stirred for 24 h. The reaction was quenched with 1 M HCl, extracted with EtOAc, washed with sat. $NaHCO_3$ and brine then dried over Na_2SO_4. Organic phase was evaporated in vacuum to afford the desired products in moderate to good yields. The products were used in the next step without further purification.

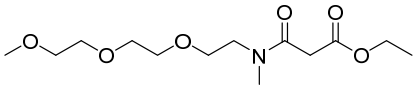

ethyl 11-methyl-12-oxo-2,5,8-trioxa-11-azatetradecan-14-oate S1 was attained as an orange residue with 30% yield. **^{1}H NMR** (300 MHz, Chloroform-*d*) δ 4.11 (qd, *J* = 7.1, 4.2 Hz, 2H), 3.65 – 3.43 (m, 13H), 3.40 (t, *J* = 5.3 Hz, 1H), 3.36 (s, 1H), 3.30 (t, *J* = 5.0 Hz, 3H), 3.00 (s, 1H), 2.89 (s, 1H), 1.19 (td, *J* = 7.1, 1.2 Hz, 3H). **^{13}C NMR** (75 MHz, $CDCl_3$) δ 167.9, 167.5, 166.6, 166.1, 70.7, 70.5, 70.2, 69.9, 69.2, 68.4, 61.2, 50.5, 50.3, 47.8, 41.4, 41.0, 37.4, 33.7, 14.0. **HRMS** Calculated for $C_{13}H_{26}NO_6^+$ $[M+H]^+$: 292.1755, found 292.1748. **FTIR** (cm^{-1}): 2874, 2105, 1738, 1645, 1404, 1289, 1111, 1033, 913, 728.

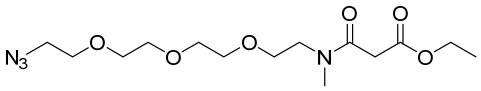

ethyl 1-azido-12-methyl-13-oxo-3,6,9-trioxa-12-azapentadecan-15-oate S2 was attained as an amber oil with 38% yield. **^{1}H NMR** (300 MHz, Chloroform-*d*) δ 3.84 (qd, *J* = 7.1, 4.3 Hz, 2H), 3.34 – 3.24 (m, 8H), 3.24 – 3.10 (m, 6H), 3.01 (s, 3H), 2.75 (s, 1H), 2.63 (s, 1H), 0.93 (td, *J* = 7.1, 1.2 Hz, 3H). **^{13}C NMR** (75 MHz, $CDCl_3$) δ 167.3, 166.8, 166.0, 165.5, 71.1, 71.1, 70.0, 69.8, 69.7, 69.6, 69.6, 68.4, 67.8, 60.4, 60.3, 58.0, 49.6, 47.1, 40.7, 40.3, 36.7, 32.9, 13.4. **HRMS** Calculated for $C_{14}H_{27}N_4O_6^+$$[M+H]^+$: 347.1925, found 347,1922. **FTIR** (cm^{-1}): 2876, 1738, 1647, 1400, 1250, 1105, 918, 845, 728, 647, 579.

2.2. General procedure for Knoevenagel Condensation to synthesize the carbamoyl acrylates

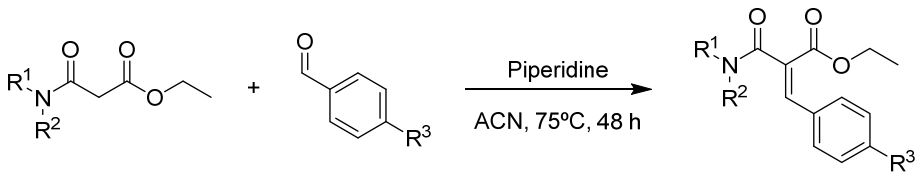

S3-S6

Equimolar mixtures of ethyl oxopropanoates **S3–6** and aldehydes in dry ACN were dissolved and a catalytic quantity of piperidine (0.1 equiv) was added. The mixtures were stirred under N_2 atm, at 75ºC for 48 h. Afterwards, solvent was evaporated in vacuum and the attained crudes were purified by flash chromatography to afford the desired products with moderate good yield.

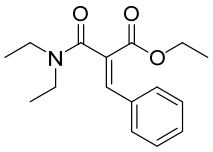

ethyl-2-(diethylcarbamoyl)-3-phenylacrylate S3 was purified by flash chromatography (SiO_2, 7:3 to 3:2 Hexane:EtOAc) to obtain the desired product in 75% yield as a green oil. **^{1}H NMR** (300 MHz, Chloroform-*d*) δ 7.59 (s, 1H), 7.49 – 7.43 (m, 2H), 7.26 (dd, *J* = 5.1, 1.9 Hz, 3H), 4.34 – 4.08 (m, 2H), 3.46 (q, *J* = 7.1 Hz, 2H), 3.14 – 3.03 (m, 2H), 1.23 (t, *J* = 7.1 Hz, 3H), 1.12 (t, *J* = 7.1 Hz, 3H), 0.80 (t, *J* = 7.2 Hz, 3H).**^{13}C NMR** (75 MHz, $CDCl_3$) δ 166.0, 164.6, 139.6, 133.0, 130.1, 129.5, 128.5, 128.0, 61.1, 42.5, 38.6, 13.9, 13.3, 11.7. **HRMS** calculated for $C_{16}H_{22}NO_3^+$ $[M+H]^+$: 276.1594, found 276,1087. **FTIR** (cm^{-1}): 2984, 2940, 1713, 1625, 1439, 1365, 1247, 1196, 1151, 1060, 1019, 946, 872, 759, 730, 691, 586, 495.

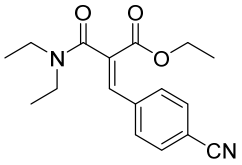

ethyl-3-(4-cyanophenyl)-2-(diethylcarbamoyl)acrylate S4 was purified by flash chromatography (SiO_2, 100% Hexane to 7:3 Hexane:EtOAc) to obtain the desired product in 59% yield as an amber oil. **^{1}H NMR** (300 MHz, Chloroform-*d*) δ 7.62 (d, *J* = 1.3 Hz, 5H), 4.38 – 4.21 (m, 2H), 3.56 – 3.45 (m, 2H), 3.18 – 3.06 (m, 2H), 1.31 (t, *J* = 7.2 Hz, 3H), 1.17 (t, *J* = 7.2 Hz, 3H), 0.86 (t, *J* = 7.2 Hz, 3H).**^{13}C NMR** (75 MHz, $CDCl_3$) δ 165.3, 164.0, 138.1, 137.4, 136.1, 133.2, 132.2, 131.4, 131.2, 129.9, 128.9, 118.0, 113.2, 63.6, 61.7, 59.7, 53.4, 42.6, 38.8, 14.7, 14.3, 13.1, 13.0, 12.6, 11.0. **HRMS** calculated for $C_{17}H_{21}N_2O_3^+$ $[M+H]^+$: 301.1547,

found 301,1548. **FTIR** (cm^{-1}): 2986, 2932, 2229, 1716, 1625, 1443, 1365, 1247, 1200, 1153, 1062, 1017, 922, 835, 732, 460.

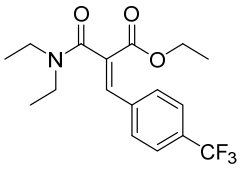

ethyl-2-(diethylcarbamoyl)-3-(4-(trifluoromethyl)phenyl)acrylate S5 was purified by flash chromatography (SiO_2, 100% Hexane to 7:3 Hexane:EtOAc) to obtain the desired product in 59.3% yield as a green oil. **^{1}H NMR** (300 MHz, Chloroform-*d*) δ 7.65 (dd, *J* = 17.5, 7.9 Hz, 5H), 4.35 (d, *J* = 8.7 Hz, 2H), 3.55 (q, *J* = 7.3, 6.6 Hz, 2H), 3.18 (d, *J* = 8.1 Hz, 2H), 1.35 (td, *J* = 7.3, 2.1 Hz, 3H), 1.22 (td, *J* = 7.1, 1.9 Hz, 3H), 0.92 (td, *J* = 7.0, 2.0 Hz, 3H).**^{13}C NMR** (101 MHz, $CDCl_3$) δ 165.5, 164.3, 137.8, 136.6, 136.6, 132.2, 131.9, 131.6, 131.2, 130.9, 130.6, 129.8, 129.5, 128.8, 128.8, 128.5, 127.6, 125.5, 125.5, 125.4, 125.4, 124.9, 122.2, 119.5, 61.6, 42.6, 38.7, 13.9, 13.4, 11.8. **HRMS** calculated for $C_{17}H_{21}F_3NO_3^+$ $[M+H]^+$: 344.1468, found 344.1467. **FTIR** (cm^{-1}): 2932, 2561, 1707, 1584, 1447, 1320, 1241, 1159, 1113, 1066, 1014, 928, 887, 829, 767, 707, 664, 604, 503, 443.

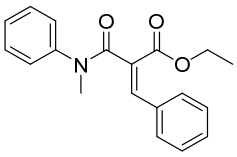

ethyl-2-(methyl(phenyl)carbamoyl)-3-phenylacrylate S6 was purified by flash chromatography (SiO_2, 100% Hexane to 3:2 Hexane:EtOAc) to obtain the desired product in 13.9% yield as an amber oil. **^{1}H NMR** (400 MHz, Chloroform-*d*) δ 7.42 (s, 5H), 7.37 (s, 1H), 7.21 – 7.09 (m, 4H), 6.70 (dd, *J* = 7.6, 1.7 Hz, 1H), 4.29 (dd, *J* = 11.0, 5.5 Hz, 2H), 3.38 (s, 3H), 1.35 (t, *J* = 7.1 Hz, 3H). **^{13}C NMR** (101 MHz, $CDCl_3$) δ 166.9, 164.8, 142.8, 140.9, 133.9, 130.4, 129.7, 129.1, 129.0, 128.8, 127.9, 126.0, 61.6, 37.1, 14.4. **HRMS** calculated for $C_{19}H_{20}NO_3^+$ $[M+H]^+$: 310.1438, found 310.1435. **FTIR** (cm^{-1}): 3052, 2990, 2944, 1711, 1647, 1594, 1495, 1443, 1388, 1326, 1252, 1198, 1132, 1068, 1027, 918, 852, 769, 732, 670, 606, 536, 493.

2.3. General procedure of Saponification for the synthesis of carbamoyl acrylic acids

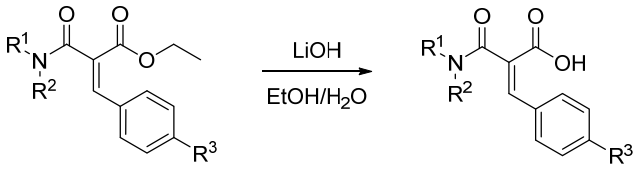

S7-S10

LiOH (2.0 equiv) was added to a solution of carbamoyl acrylate in EtOH/H_2O (10:0.7). The reaction mixture was stirred overnight at rt. Afterwards, solvent was evaporated in vacuo, treated with 1 M NaOH and extracted with DCM. The aqueous phase pH was adjusted to 3 with 1 M HCl and extracted 3x with DCM to afford the desire products with no further purification.

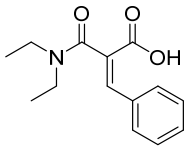

2-(diethylcarbamoyl)-3-phenylacrylic acid S7 was attained as a yellow solid with 77% yield. **^{1}H NMR** (400 MHz, Chloroform-*d*) δ 10.51 (s, 1H), 7.74 (s, 1H), 7.57 – 7.49 (m, 2H), 7.39 – 7.31 (m, 3H), 3.62 (dq, *J* = 14.3, 7.1 Hz, 1H), 3.45 (dq, *J* = 14.7, 7.4 Hz, 1H), 3.24 – 3.08 (m, *J* = 7.3 Hz, 2H), 1.19 (t, *J* = 7.2 Hz, 3H), 0.87 (t, *J* = 7.1 Hz, 3H). **^{13}C NMR** (101 MHz, $CDCl_3$) δ 168.8, 166.8, 141.8, 133.1, 130.7, 130.1, 128.9, 127.5, 43.1, 39.3, 13.6, 12.1. **HRMS** calculated for $C_{14}H_{18}NO_3^+$ $[M+H]^+$: 248.1281, found 248.1277. **FTIR** (cm^{-1}): 2969, 2938, 2864, 2728, 2520, 2458, 1707, 1573, 1491, 1445, 1381, 1351, 1270, 1237, 1198, 1078, 946, 883, 847, 763, 695, 664,593, 492, 446.

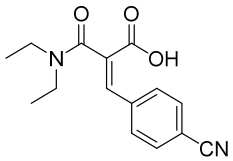

3-(4-cyanophenyl)-2-(diethylcarbamoyl)acrylic acid S8 was attained as a pale yellow solid with 59% yield. **^{1}H NMR** (300 MHz, Chloroform-*d*) δ 7.68 (s, 1H), 7.64 (s, 4H), 3.46 (q, *J* = 7.2 Hz, 2H), 3.38 – 3.28 (m, 2H), 1.21 (dt, *J* = 16.6, 7.2 Hz, 3H), 0.89 (t, *J* = 7.2 Hz, 3H). **^{13}C NMR** (101 MHz, $CDCl_3$) δ 139.0, 137.5, 132.6, 130.3, 113.9, 70.8, 67.2, 60.6, 43.2, 42.4, 41.4, 39.4, 29.8, 14.3, 13.9, 13.8, 12.8, 12.2. **HRMS** calculated for $C_{15}H_{17}N_2O_3$+ $[M+H]^+$: 273.1234, found 273.1232. **FTIR** (cm^{-1}): 3460, 3393, 2930, 2757, 2584, 2505, 2227, 1705, 1588, 1445, 1361, 1260, 1204, 1101, 1019, 942, 889, 833, 651, 592, 550.

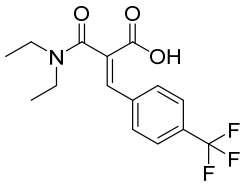

2-(diethylcarbamoyl)-3-(4-(trifluoromethyl)phenyl)acrylic acid S9 was attained as a dark amber solid with 74% yield. **^{1}H NMR** (300 MHz, Chloroform-*d*) δ 7.76 (s, 1H), 7.64 (q, *J* = 8.4 Hz, 4H), 3.71 – 3.37 (m, 2H), 3.17 (p, *J* = 7.1 Hz, 2H), 1.20 (t, *J* = 7.1 Hz, 3H), 0.90 (t, *J* = 7.1 Hz, 3H). **^{13}C NMR** (101 MHz, $CDCl_3$) δ 167.1, 166.6, 139.4, 136.5, 132.3, 132.0, 131.7, 131.4, 130.0, 130.0, 127.8, 125.8, 125.7, 125.7, 125.6, 125.1, 122.4, 119.7, 43.2, 39.4, 13.5, 12.0. **HRMS** calculated for $C_{15}H_{17}F_3NO_3^+$ $[M+H]^+$: 316.1155, found: 316.1154. **FTIR** (cm^{-1}): 3460, 2918, 2561, 1709, 1588, 1437, 1320, 1241, 1161, 1113, 1068, 1017, 930, 829, 666, 662, 590, 437.

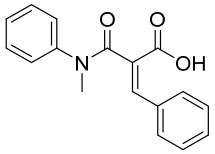

2-(methyl(phenyl)carbamoyl)-3-phenylacrylic acid S10 was attained as a amber residue with 87% yield. **^{1}H NMR** (400 MHz, Chloroform-*d*) δ 7.47 – 7.35 (m, 6H), 7.20 – 7.13 (m, 1H), 7.10 (dd, *J* = 8.3, 6.6 Hz, 2H), 6.69 (dd, *J* = 7.5, 1.8 Hz, 2H), 3.36 (s, 3H). **^{13}C NMR** (101 MHz, $CDCl_3$) δ 169.1, 167.1, 142.7, 142.5, 133.7, 130.7, 129.8, 129.5, 129.2, 129.1, 128.8, 128.5, 128.0, 126.0, 126.0, 37.2. **HRMS** calculated for $C_{17}H_{16}NO_3^+$ $[M+H]^+$: 282.1125, found: 282.1121. **FTIR** (cm^{-1}): 2924, 1709, 1617, 1592, 1495, 1450, 1396, 1326, 1233, 1202, 1128, 913, 769, 689, 695, 579.

2.4. General procedure for the synthesis of carbamoyl NHS acrylates

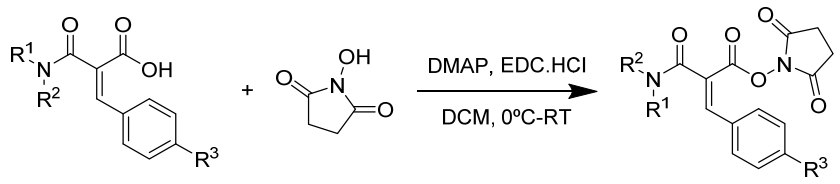

1-4

To a 0.2 molar solution of acid (1.0 equiv) in dry DCM was added 1-hydroxypyrrolidine-2,5-dione (1.2 equiv) under argon and cooled to 0 °C. Then, *N*,*N*-dimethylpyridin-4-amine (DMAP, 0.1 equiv) and 3-(((ethylimino)methylene)amino)-*N*,*N*-dimethylpropan-1-amine hydrochloride (EDC.HCl, 1.0 equiv) were added to the solution. The reaction was stirred for 1 h at 0 °C and 23 h at room temperature. The reaction mixture was filtered and concentrated under reduced

pressure. The thereby obtained crude was purified by flash chromatography to obtain the desired NHS ester in moderate yields.

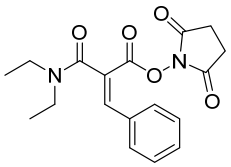

2,5-dioxopyrrolidin-1-yl-2-(diethylcarbamoyl)-3-phenylacrylate 1 was purified by flash chromatography (SiO_2, 3:2 to 3:7 Hexane:EtOAc) to attain a pale yellow solid with 51% yield. **^{1}H NMR** (400 MHz, Chloroform-*d*) δ 7.88 (s, 1H), 7.59 (d, *J* = 7.1 Hz, 2H), 7.47 – 7.35 (m, 3H), 3.67 – 3.41 (m, 2H), 3.24 (qd, *J* = 7.4, 3.4 Hz, 2H), 2.86 (s, 4H), 1.20 (t, *J* = 7.1 Hz, 3H), 0.95 (t, *J* = 7.2 Hz, 3H).**^{13}C NMR** (75 MHz, $CDCl_3$) δ 168.9, 164.1, 160.7, 144.9, 132.6, 131.7, 130.6, 129.1, 123.3, 43.2, 39.4, 25.8, 13.8, 12.2. **HRMS** calculated for $C_{18}H_{21}N_2O_5^+$ $[M+H]^+$: 345.1445, found 345.1441. **FTIR** (cm^{-1}): 3544, 2986,1738, 1631, 1485, 1437, 1363, 1270, 1206, 1177, 1070, 1014, 957, 887, 769, 701, 647, 567, 489, 404.

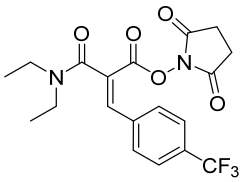

2,5-dioxopyrrolidin-1-yl-2-(diethylcarbamoyl)-3-(4-(trifluoromethyl)phenyl)acrylate 2 was purified by flash chromatography (SiO_2, 7:3 to 1:1 Hexane:EtOAc) to attain a pale yellow powder with 51% yield. **^{1}H NMR** (300 MHz, Chloroform-*d*) δ 7.89 (s, 1H), 7.76 – 7.63 (m, 4H), 3.55 (d, *J* = 7.4 Hz, 2H), 3.25 (q, *J* = 7.2 Hz, 2H), 2.88 (s, 4H), 1.20 (t, *J* = 7.1 Hz, 3H), 0.97 (t, *J* = 7.2 Hz, 3H). **^{13}C NMR** (75 MHz, $CDCl_3$) δ 168.8, 163.5, 160.4, 160.3, 143.5, 143.3, 141.9, 141.7, 135.9, 133.1, 133.0, 132.6, 132.5, 131.4, 131.4, 129.7, 129.1, 127.0, 125.9, 125.8, 125.5, 125.2, 125.0, 121.9, 43.3, 39.5, 25.7, 12.9, 11.3. **HRMS** calculated for $C_{19}H_{20}F_3N_2O_5^+$ $[M+H]^+$: 413.1319, found 413.1313. **FTIR** (cm^{-1}): 2975, 1740, 1629, 1420, 1320, 1210, 1169, 1132, 1070, 1016, 839, 652, 414.

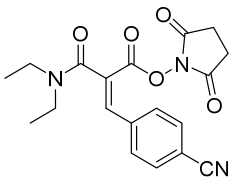

2,5-dioxopyrrolidin-1-yl-3-(4-cyanophenyl)-2-(diethylcarbamoyl)acrylate 3 was purified by flash chromatography (SiO_2, 7:3 to 1:1 Hexane:EtOAc) to attain a pale green oil with 18% yield. **^{1}H NMR** (300 MHz, Chloroform-*d*) δ 7.85 (s, 1H), 7.75 – 7.66 (m, 4H), 3.54 (q, *J* = 7.3 Hz, 2H), 3.24 (q, *J* = 7.2 Hz, 2H), 2.88 (s, 4H), 1.19 (t, *J* = 7.1 Hz, 3H), 0.96 (t, *J* = 7.1 Hz, 3H).

^{13}C NMR (101 MHz, $CDCl_3$) δ 172.8, 138.0, 137.7, 132.6, 132.2, 132.1, 130.1, 129.7, 127.4, 118.4, 113.6, 43.3, 39.4, 25.5, 13.7, 12.2. **HRMS** calculated for $C_{19}H_{20}N_3O_5^+$ $[M+H]^+$: 370.1397, found 370.1392. **FTIR** (cm^{-1}): 3439, 2942, 2230, 1705, 1600, 1429, 1229, 1204, 1072, 1023, 794, 647, 553, 406.

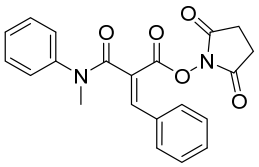

2,5-dioxopyrrolidin-1-yl-2-(methyl(phenyl)carbamoyl)-3-phenylacrylate 4 was purified by flash chromatography (SiO_2, 7:3 to 1:1 Hexane:EtOAc) to attain a amber viscous oil with 18% yield. **^{1}H NMR** (400 MHz, Chloroform-*d*) δ 7.50 (s, 1H), 7.48 – 7.33 (m, 5H), 7.22 – 7.08 (m, 3H), 6.80 – 6.66 (m, 2H), 3.34 (s, 3H), 2.86 (s, 4H). **^{13}C NMR** (101 MHz, $CDCl_3$) δ 172.6, 169.1, 164.7, 160.3, 145.2, 142.2, 133.0, 131.5, 130.0, 129.2, 128.9, 128.1, 126.0, 123.8, 37.2, 25.7. **HRMS** calculated for $C_{21}H_{19}N_2O_5^+$ $[M+H]^+$: 379.1288, found 379.1283. **FTIR** (cm^{-1}): 2949, 1707, 1639, 1594, 1495, 1400, 1207, 1070, 957, 763, 695, 647, 565, 402.

2.5. Synthesis of Coumarin NHS-activated acrylates

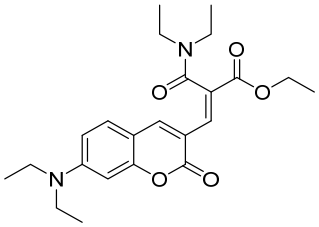

ethyl-3-(7-(diethylamino)-2-oxo-2H-chromen-3-yl)-2-(diethylcarbamoyl)acrylate S11 was prepared according to *2.2. General procedure for Knoevenagel Condensation to synthesize the carbamoyl acrylates*2.2, to afford an orange residue with 47% yield. **^{1}H NMR** (300 MHz, Chloroform-*d*) δ 8.04 (s, 1H), 7.86 (d, *J* = 0.7 Hz, 1H), 7.25 (d, *J* = 9 Hz, 1H), 6.57 (dd, *J* = 8.9, 2.5 Hz, 1H), 6.45 (d, *J* = 2.5 Hz, 1H), 4.39 – 4.14 (m, 2H), 3.41 (t, *J* = 7.1 Hz, 8H), 1.35 – 1.27 (m, 3H), 1.20 (td, *J* = 7.1, 5.8 Hz, 9H), 1.01 (t, *J* = 7.1 Hz, 3H). **^{13}C NMR** (75 MHz, $CDCl_3$) δ 166.7, 164.7, 161.5, 157.0, 152.0, 143.1, 133.4, 130.5, 127.7, 113.5, 109.6, 108.7, 97.2, 61.5, 45.2, 43.3, 39.2, 14.4, 14.0, 12.7, 12.6. **HRMS** calculated for $C_{23}H_{31}N_2O_5^+$ $[M+H]^+$: 415.2227, found 415.2226. **FTIR** (cm^{-1}): 2979, 2940, 2880, 1720, 1615, 1577, 1516, 1441, 1357, 1254, 1192, 1134, 1068, 1035, 944, 913, 823, 790, 730, 645, 470.

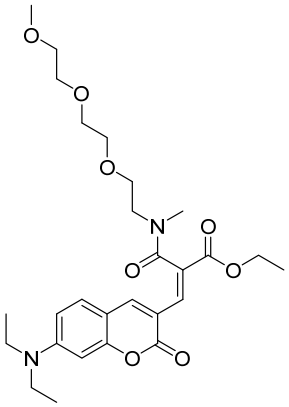

ethyl-13-((7-(diethylamino)-2-oxo-2H-chromen-3-yl)methylene)-11-methyl-12-oxo-2,5,8-trioxa-11-azatetradecan-14-oate S12 was prepared according to *2.2. General procedure for Knoevenagel Condensation to synthesize the carbamoyl acrylates*, to afford an orange oil that was used in the next step without further purification. **HRMS** calculated for $C_{27}H_{39}N_2O_8^+$ $[M+H]^+$: 519.2701, found 519.2698.

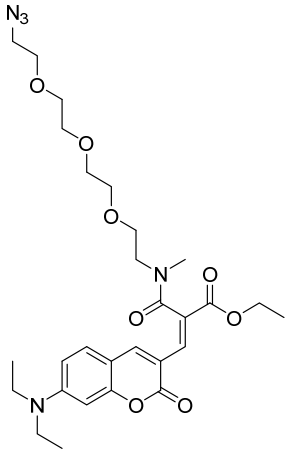

ethyl-1-azido-14-((7-(diethylamino)-2-oxo-2H-chromen-3-yl)methylene)-12-methyl-13-oxo-3,6,9-trioxa-12-azapentadecan-15-oate S13 was prepared according to *2.2. General procedure for Knoevenagel Condensation to synthesize the carbamoyl acrylates*, to afford an orange oil that was used in the next step without further purification. **HRMS** calculated for $C_{28}H_{40}N_5O_8^+$ $[M+H]^+$: 574.2871, found 574.2872.

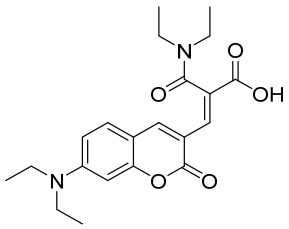

3-(7-(diethylamino)-2-oxo-2H-chromen-3-yl)-2-(diethylcarbamoyl)acrylic acid S14 (0.162 g, 0.391 mmol) was dissolved in a mixture of Dioxane:H_2O 1:1 (2.0 mL) and then LiOH

(0.023 g, 0.978 mmol) was added and the mixture was stirred overnight at RT. Afterwards, solvent was evaporated in vacuum, treated with 1 M NaOH and extracted with DCM. The aqueous phase pH was adjusted to 3 with 1 M HCl and extracted 3x with DCM to afford the desire product **S14** with 50% yield, as a orange residue. **^{1}H NMR** (300 MHz, Chloroform-*d*) δ 8.06 (s, 1H), 7.98 (d, *J* = 0.7 Hz, 1H), 7.25 (d, *J* = 7.2 Hz, 1H), 6.58 (dd, *J* = 8.9, 2.6 Hz, 1H), 6.46 (d, *J* = 2.4 Hz, 1H), 3.50 – 3.14 (m, 6H), 1.29 – 1.17 (m, 9H), 1.04 (t, *J* = 7.1 Hz, 3H). **^{13}C NMR** (101 MHz, $CDCl_3$) δ 168.2, 166.7, 161.4, 157.2, 152.1, 143.5, 135.4, 131.4, 130.7, 126.3, 113.0, 109.7, 108.8, 108.7, 97.2, 45.2, 43.4, 39.4, 29.8, 14.3, 14.0, 12.7, 12.6. **HRMS** calculated for $C_{21}H_{27}N_2O_5^+$ $[M+H]^+$: 387.1914, found 387.1906. **FTIR** (cm^{-1}): 2961, 1715, 1581, 1511, 1453, 1352, 1252, 1132, 1113, 1002, 872, 789, 614, 466.

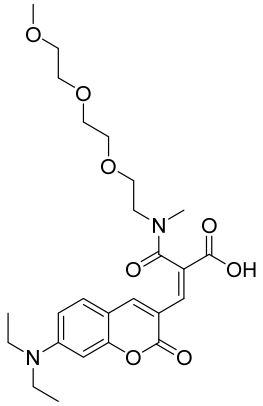

13-((7-(diethylamino)-2-oxo-2H-chromen-3-yl)methylene)-11-methyl-12-oxo-2,5,8-trioxa-11-azatetradecan-14-oic acid S15 (0.057 g, 0.110 mmol) was dissolved in a mixture of Dioxane:H_2O 1:1 (0.6 mL) and then LiOH (6.56 mg, 0.274 mmol) was added and the mixture was stirred overnight at RT. Afterwards, solvent was evaporated in vacuum, treated with 1 M NaOH and extracted with DCM. The aqueous phase pH was adjusted to 3 with 1 M HCl and extracted 3x with DCM to afford an orange oil. The compound was used for the next step with no further purification. **HRMS** calculated for $C_{25}H_{35}N_2O_8^+$ $[M+H]^+$: 491.2388, found 491.2380.

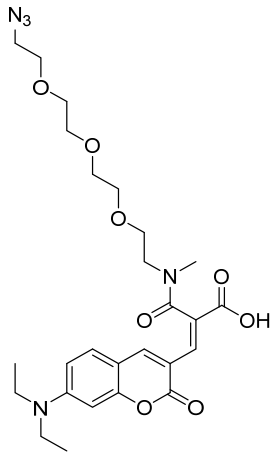

1-azido-14-((7-(diethylamino)-2-oxo-2H-chromen-3-yl)methylene)-12-methyl-13-oxo-3,6,9-trioxa-12-azapentadecan-15-oic acid S16 (0.067 g, 0.116 mmol) (0.057 g, 0.110 mmol) was dissolved in a mixture of Dioxane:H_2O 1:1 (0.7 mL) and then LiOH (6.95 mg, 0.290 mmol) was added and the mixture was stirred overnight at RT. Afterwards, solvent was evaporated in vacuum, treated with 1 M NaOH and extracted with DCM. The aqueous phase pH was adjusted to 3 with 1 M HCl and extracted 3x with DCM to afford an orange oil. The compound was used for the next step with no further purification. **HRMS** calculated for $C_{26}H_{36}N_5O_8^+$ $[M+H]^+$: 546.2558, found 546.2557.

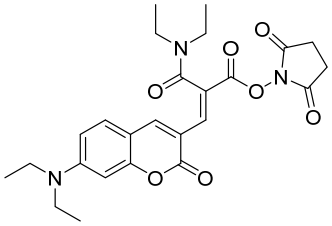

2,5-dioxopyrrolidin-1-yl-3-(7-(diethylamino)-2-oxo-2H-chromen-3-yl)-2 (diethylcarbamoyl)acrylate 29 was prepared according to *2.4. General procedure for the synthesis of carbamoyl NHS acrylates* to afford an orange powder with 63% yield. **^{1}H NMR** (400 MHz, Chloroform-*d*) δ 8.16 (d, *J* = 4.6 Hz, 2H), 7.27 (d, *J* = 9.5 Hz, 1H), 6.61 (dd, *J* = 9.0, 2.4 Hz, 1H), 6.46 (d, *J* = 2.4 Hz, 1H), 3.53 – 3.29 (m, 6H), 2.87 (s, 4H), 1.24 (q, *J* = 6.5 Hz, 9H), 1.10 (t, *J* = 7.1 Hz, 3H). **^{13}C NMR** (101 MHz, $CDCl_3$) δ 169.0, 164.6, 161.2, 160.3, 157.5, 152.7, 144.5, 138.5, 131.3, 131.2, 121.0, 112.2, 110.0, 108.8, 97.2, 45.3, 43.6, 39.6, 25.7, 14.1, 12.6, 12.6, 1.1. **HRMS** calculated for $C_{25}H_{30}N_3O_7^+$ $[M+H]^+$: 484.2078, found 484.2079. **FTIR** (cm^{-1}): 2946, 1736, 1621, 1513, 1445, 1355, 1252, 1190, 1132, 1062, 792, 650, 526, 404.

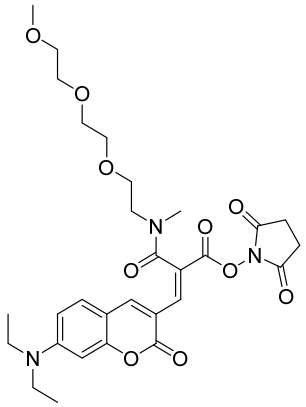

2,5-dioxopyrrolidin-1-yl-13-((7-(diethylamino)-2-oxo-2H-chromen-3-yl)methylene)-11 methyl-12-oxo-2,5,8-trioxa-11-azatetradecan-14-oate 34 was prepared according to *2.4. General procedure for the synthesis of carbamoyl NHS acrylates*. The compound was purified by flash chromatography (SiO_2,100% DCM to 1:1 DCM:EtOAc) to afford an orange oil with 7% yield over three steps. **^{1}H NMR** (300 MHz, Chloroform-*d*) δ 8.15 – 8.12 (m, 1H), 8.05 – 7.84 (m, 1H), 7.40 – 7.28 (m, 1H), 6.60 (dt, *J* = 9.1, 2.3 Hz, 1H), 6.45 (d, *J* = 2.3 Hz, 1H), 3.76 – 3.40 (m, 23H), 3.37 (d, *J* = 0.6 Hz, 1H), 3.34 (d, *J* = 1.2 Hz, 2H), 3.15 (s, 1H), 3.08 (d, *J* = 1.7 Hz, 1H), 3.01 (s, 0H), 2.87 – 2.79 (m, 4H), 1.31 – 1.19 (m, 13H). **^{13}C NMR** (75 MHz, $CDCl_3$) δ 172.3, 170.7, 169.2, 165.9, 161.2, 139.5, 131.6, 120.4, 112.1, 97.2, 77.6, 77.4, 77.2, 76.7, 72.0, 70.5, 59.1, 47.3, 45.3, 37.6, 29.8, 25.8, 25.6, 25.5, 12.6. **HRMS** calculated for $C_{29}H_{38}N_3O_{10}^+$ $[M+H]^+$: 588.2552, 588.2538. **FTIR** (cm^{-1}): 2944, 2891, 1707, 1610, 1571, 1513, 1427, 1355, 1219, 1206, 1134, 1070, 1000, 905, 817, 732, 650, 471.

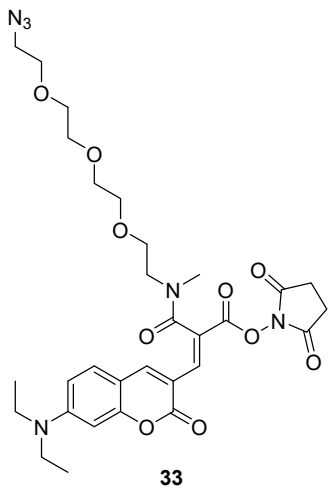

33

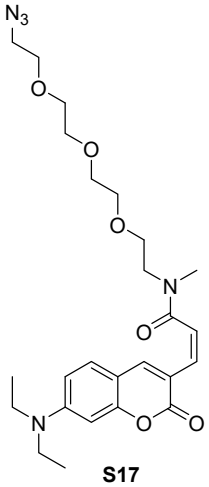

S17

2,5-dioxopyrrolidin-1-yl-1-azido-14-((7-(diethylamino)-2-oxo-2H-chromen-3-yl)methylene)-12-methyl-13-oxo-3,6,9-trioxa-12-azapentadecan-15-oate 35 was prepared according to *2.4. General procedure for the synthesis of carbamoyl NHS acrylates*. Compound **33** was isolated with flash chromatography (SiO_2,100% DCM to 1:1 DCM:EtOAc), followed by preparative TLC (SiO_2, 1:1 DCM:EtOAc), and used directly for bioconjugation with cys-

bombesin **22**, that was then isolated by semi-preparative (in the isolation process compound **33** partially decarboxilates). **HRMS** calculated for $C_{30}H_{39}N_6O_{10}^+$ [**33**+H]$^+$: 643.2722, found 643.2716, calculated for $C_{25}H_{36}N_5O_6^+$ [**S17**+H]$^+$: 502.2660, found 502.2656.

2.6. Synthesis of 1,4-thiazepane-3-carboxylate products from cysteine methyl-ester in organic conditions

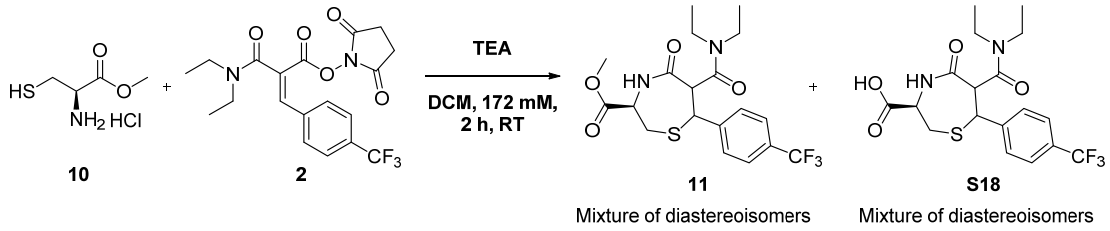

To a solution of methyl *L*-cysteinate hydrochloride **10** (93 mg, 0.688 mmol) in DCM (4.0 mL) was added triethylamine (240 µL, 1.720 mmol) and then, 2,5-dioxopyrrolidin-1-yl-2-(diethylcarbamoyl)-3-(4-(trifluoromethyl)phenyl)acrylate **2** (284 mg, 0.688 mmol). After 2 h, the reaction was quenched with 5 mL of 1 M HCl. The resulting organic phase was further washed with, NaOH 1 M and brine. Afterwards, the organic phase was dried over Na_2SO_4, filtered and the solvent evaporated under vacuum. The resulting crude mixture had three diastereoisomers mixture as confirmed by ^{1}H NMR (d.r. 1:3:5). Then, the crude was purified by silica column (100% DCM to 95:5 DCM:MeOH) to afford the isolated diastereoisomers as: green oils, white or yellow powder.NOESY NMR experiments were not conclusive to determine the relative configuration of each isolated diastereoisomer (data not shown). Nonetheless, HMBC spectra confirmed that the obtained products are seven-member heterocycles.

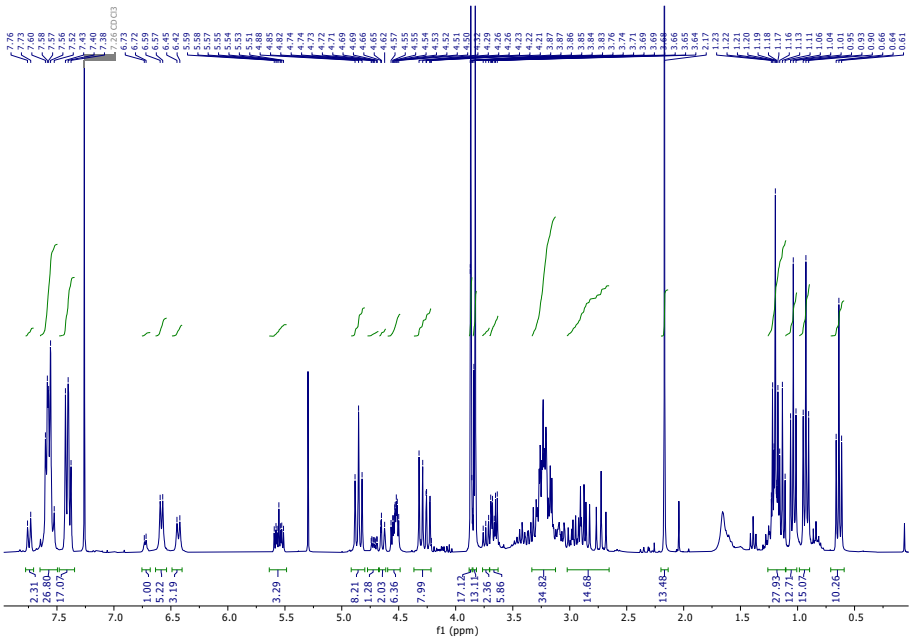

Figure S 1. ^{1}H-NMR spectrum in $CDCl_3$ of reaction crude mixture of Cys-methyl ester **10** with **2** under organic conditions (TEA, DCM).

LC-MS to the crude mixture was acquired for 15 min in positive mode and the HPLC runs were carried out with a gradient of A (Milli Q water containing 0.1% v/v Formic acid, FA) and B (acetonitrile containing 0.1% v/v FA, Honeywell HPLC-grade). The mobile phase was t = 0 min, 5% B; t = 1 min, 5% B; t = 10 min, 95.5% B; t = 11 min, 95.5% B; t = 12 min, 5% B; t = 15 min, stop, at a flow rate of 0.2 mL/min. From the LC-MS we observe two products: the desired 1,4-thiazepan-5-one **11** (*m/z* = 433.1393 $[M+H]^+$) and 1,4-thiazepan-5-one **S18** (*m/z* 419.1237 $[M+H]^+$).

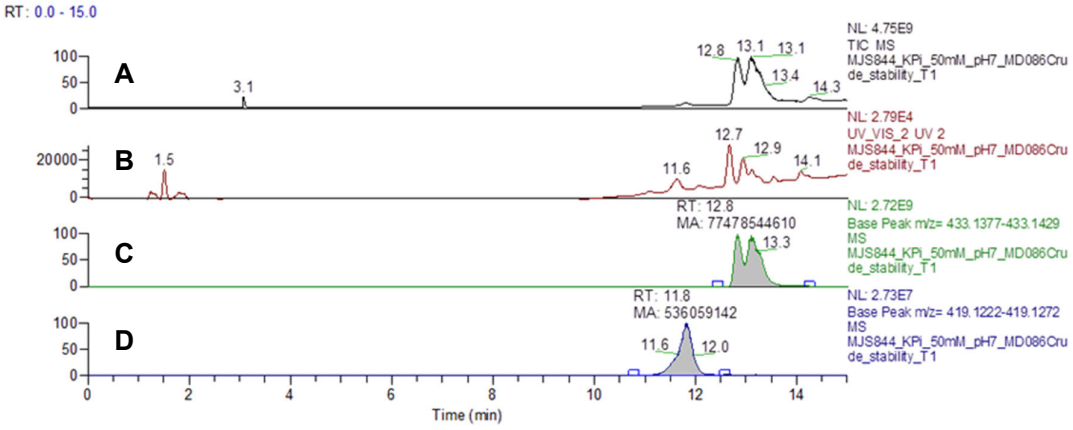

Figure S 2. LC-MS chromatograms of **2** with methyl *L*-cysteinate **10** and HRMS spectra: **A.** Total Ion Current (TIC) chromatogram; **B.** Detection at 254 nm chromatogram; **C.** Extracted Ion Chromatogram (EIC) of base of peak at m/z 433.1403 [**2**+H]+, with three superimposed peaks; **D**. Extracted Ion Chromatogram (EIC) of base of peak at m/z 419.1247 [**S18**+H]+.

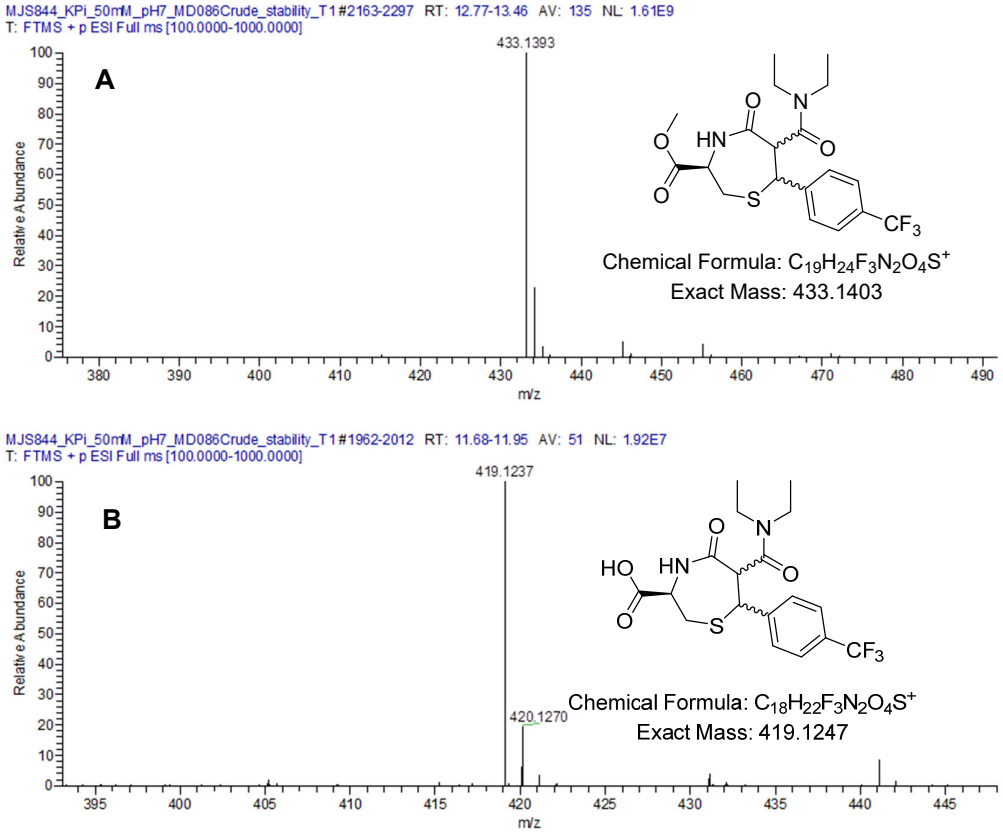

Figure S 3. ESI$^+$-HRMS spectra of: **A.** TIC peak at RT 12.8-13.5 min and **B.** TIC peak at RT 12.8 min with the corresponding products **2**. (Calculated for $C_{19}H_{24}F_3N_2O_4S$ [**2**+H]$^+$: 433.1403, found 433.1393) and hydrolysed **2-COOH** (Calculated for $C_{18}H_{22}F_3N_2O_4S$ [**S18**+H]$^+$: 419.1247, found 419.1237).

Characterization of isolated fractions:

Fraction A (9.6 mg, 22 µmol, 4% yield) as a yellow solid: **^{1}H NMR** (300 MHz, Chloroform-*d*) δ 7.80 – 7.70 (m, 2H), 7.54 (d, *J* = 8.3 Hz, 2H), 6.70 (d, *J* = 4.8 Hz, 1H), 4.71 (ddd, *J* = 9.3, 4.9, 1.7 Hz, 1H), 4.69 – 4.61 (m, 2H), 3.87 (s, 3H), 3.41 (dtt, *J* = 20.8, 14.0, 7.2 Hz, 2H), 3.25 – 3.05 (m, 2H), 3.07 – 2.90 (m, 2H), 1.31 – 1.09 (m, 6H), 0.93 – 0.79 (m, 2H). **^{13}C NMR** (75 MHz, $CDCl_3$) δ 169.7, 169.6, 166.6, 143.2, 129.3, 125.4, 59.5, 58.7, 53.9, 42.1, 40.3, 31.4, 29.8, 14.0, 12.8. **HRMS** Calculated for $C_{19}H_{24}F_3N_2O_4S$ [M+H]$^+$: 433.1403 found 433.1393. **FTIR** (cm^{-1}): 3299, 2916, 2852, 1732, 1666, 1435, 1386, 1326, 1305, 1266, 1221, 1165, 1109, 1068, 1016, 973, 847, 781, 676, 485.

HMBC correlation

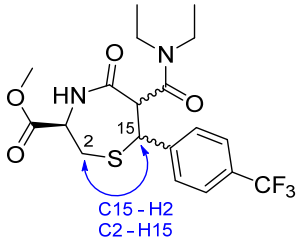

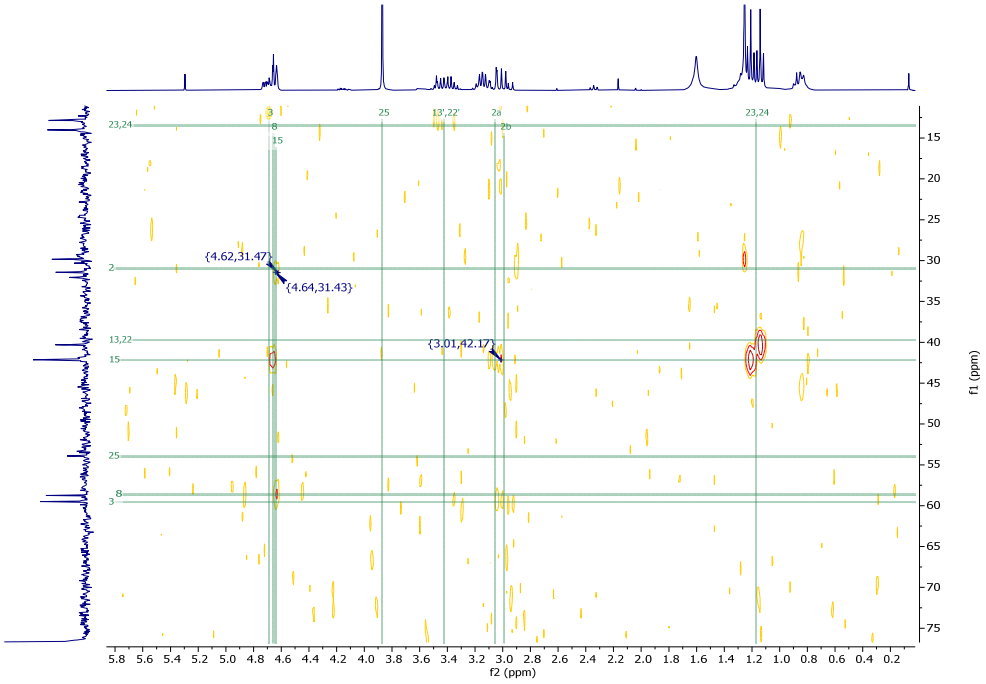

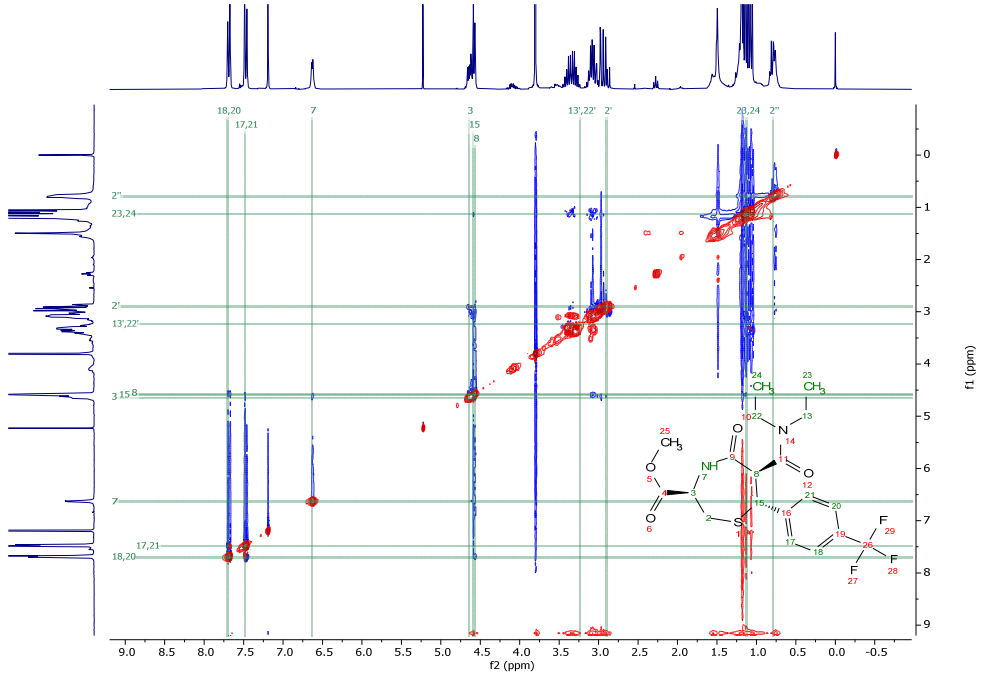

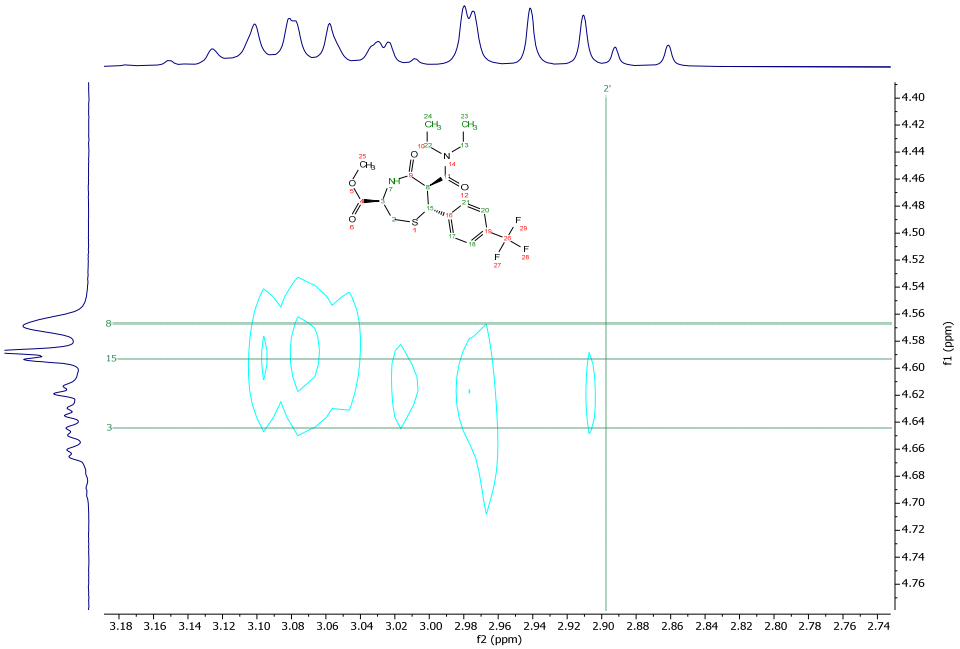
2'
8
15
3
f2 (ppm)
f1 (ppm)

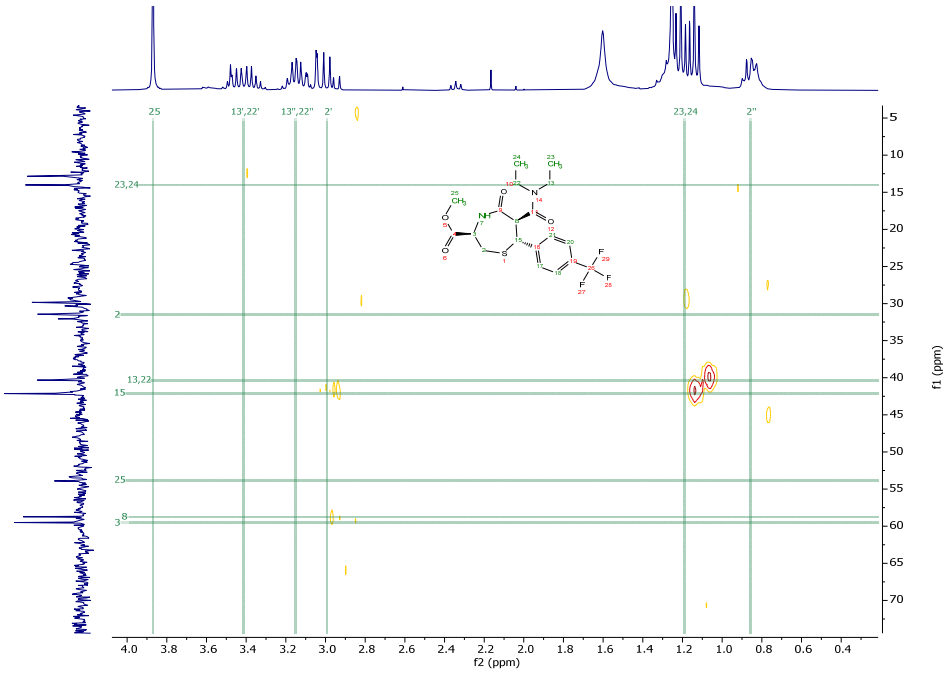
25
13',22'
13'',22''
2'
23,24
2''
23,24
2
13,22
15
25
3
8
f2 (ppm)
f1 (ppm)

Fraction B (66.5 mg, 154 µmol, 27% yield) as a green oil: **^{1}H NMR** (300 MHz, Chloroform-*d*) δ 7.57 (d, *J* = 8.2 Hz, 2H), 7.38 (d, *J* = 8.0 Hz, 2H), 6.44 (d, *J* = 7.6 Hz, 1H), 5.53 (dddd, *J* = 12.3, 7.7, 4.7, 1.0 Hz, 1H), 4.83 (d, *J* = 9.6 Hz, 1H), 4.24 (dd, *J* = 9.6, 1.2 Hz, 1H), 3.81 (s, *J* = 0.9 Hz, 3H), 3.74 – 3.59 (m, 2H), 3.28 (ddq, *J* = 20.5, 13.5, 7.1 Hz, 2H), 2.93 (dq, *J* = 14.5, 7.2 Hz, 1H), 2.72 (t, *J* = 12.5 Hz, 1H), 1.02 (td, *J* = 7.1, 1.0 Hz, 3H), 0.64 (t, *J* = 7.1 Hz, 3H). **^{13}C NMR** (75 MHz, Acetone) δ 171.3, 169.0, 167.2, 147.1, 130.4, 130.1, 129.7, 129.3, 128.6, 126.8, 126.5, 126.4, 126.4, 126.3, 125.2, 123.2, 61.6, 53.2, 52.5, 45.0, 42.6, 41.3, 35.5, 14.3, 13.0. **HRMS** Calculated for $C_{19}H_{24}F_3N_2O_4S$ $[M+H]^+$: 433.1403 found 433.1395. **FTIR** (cm^{-1}): 3318, 2960, 1746, 1631, 1439, 1324, 1214, 1132, 1111, 1107, 1018, 850, 792, 726, 604.

<u>HMBC correlation</u>

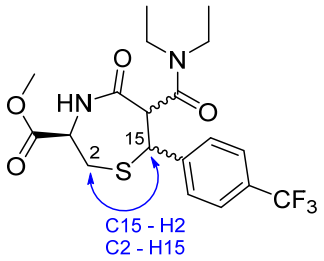

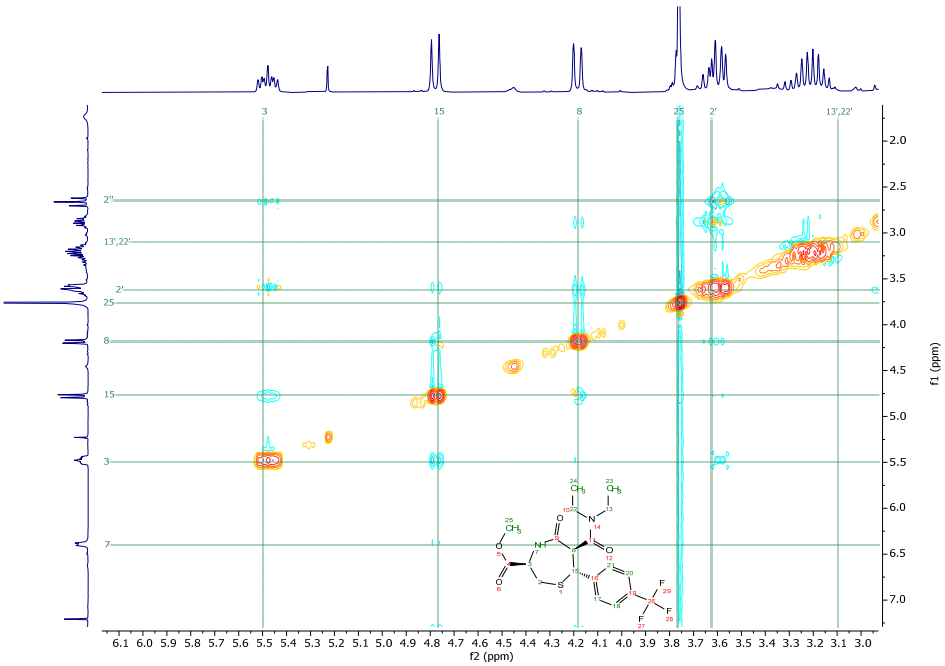

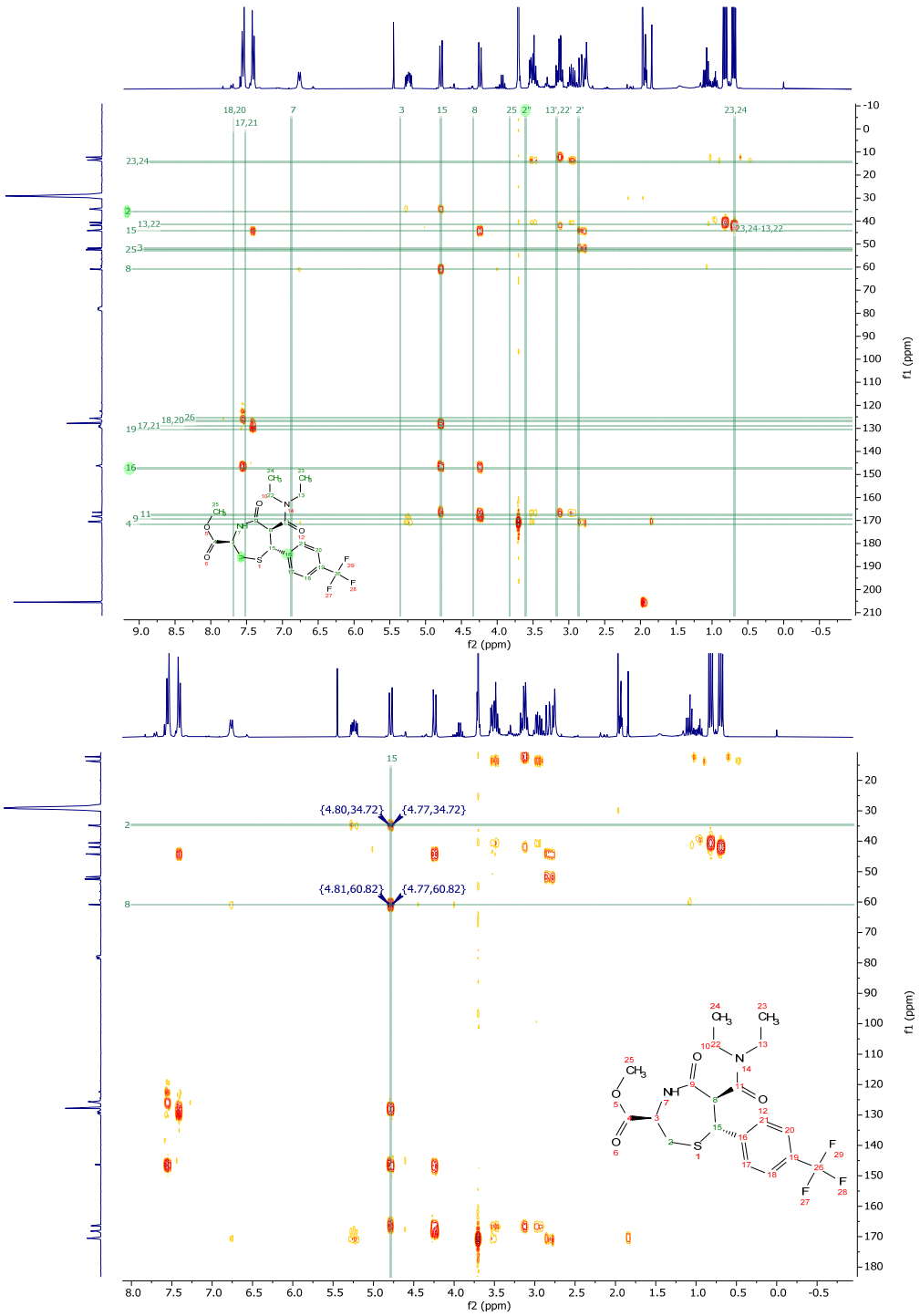
18,20
17,21
7
3
15
8
25
2'
13',22'
2'
23,24
23,24
13,22
23,24-13,22
f2 (ppm)
f1 (ppm)
{4.80,34.72}
{4.77,34.72}
{4.81,60.82}
{4.77,60.82}
f2 (ppm)
f1 (ppm)

Fraction C (125 mg, 289 µmol, 50% yield) as a white powder: **^{1}H NMR** (300 MHz, Chloroform-*d*) δ 7.55 (d, *J* = 8.7 Hz, 2H), 7.40 (d, *J* = 8.1 Hz, 2H), 6.55 (d, *J* = 6.7 Hz, 1H), 4.85 (d, *J* = 9.4 Hz, 1H), 4.53 (ddd, *J* = 9.3, 6.7, 4.2 Hz, 1H), 4.30 (d, *J* = 9.5 Hz, 1H), 3.85 (s, 3H), 3.31 – 3.11 (m, 4H), 2.85 (dd, *J* = 14.6, 9.4 Hz, 1H), 1.17 (t, *J* = 7.1 Hz, 3H), 0.91 (t, *J* = 7.1 Hz, 3H). **^{13}C NMR** (75 MHz, $CDCl_3$) δ 169.6, 168.9, 165.3, 145.0, 127.6, 125.8, 125.8, 56.4, 55.8, 53.7, 42.9, 42.2, 40.8, 34.2, 30.5, 30.2, 30.0, 14.6, 12.5. **HRMS** Calculated for $C_{19}H_{24}F_3N_2O_4S$ $[M+H]^+$: 433.1403 found 433.1393. **FTIR** (cm^{-1}): 3363, 2973, 2942, 1738, 1659, 1439, 1386, 1324, 1252, 1124, 1165, 1066, 1017, 986, 878, 831, 672, 635, 585, 474.

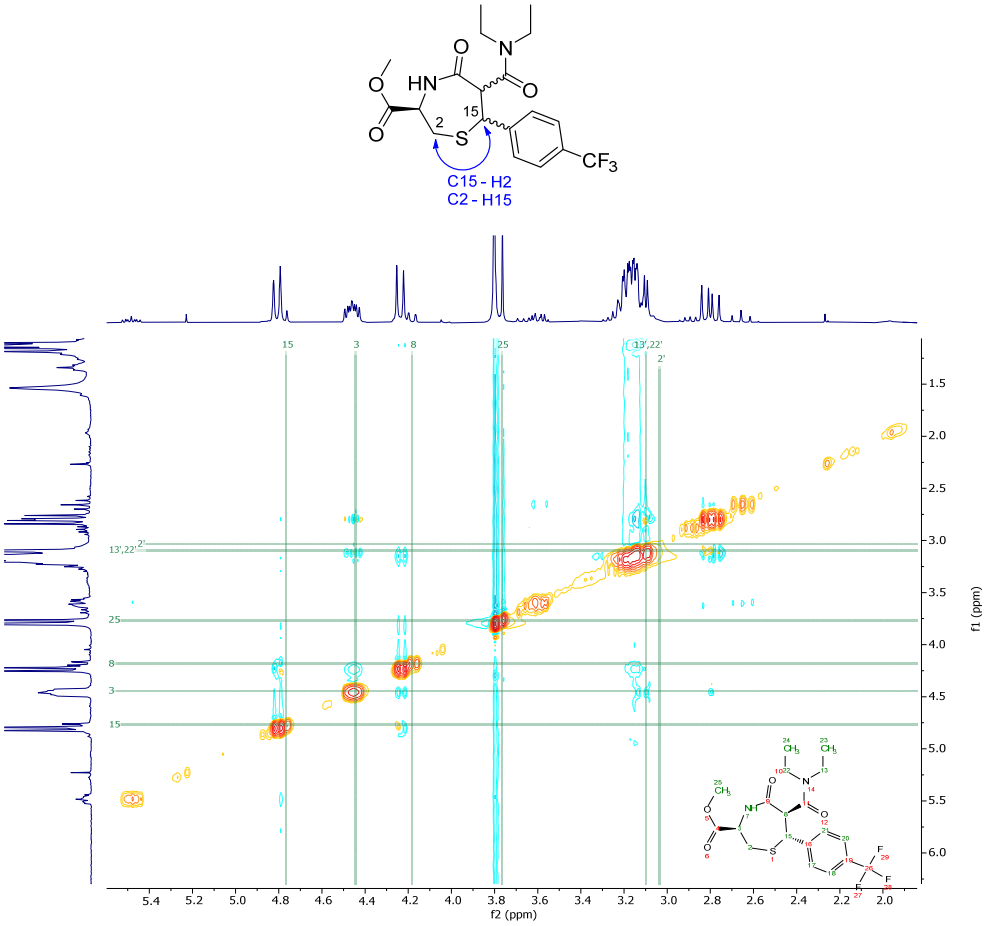

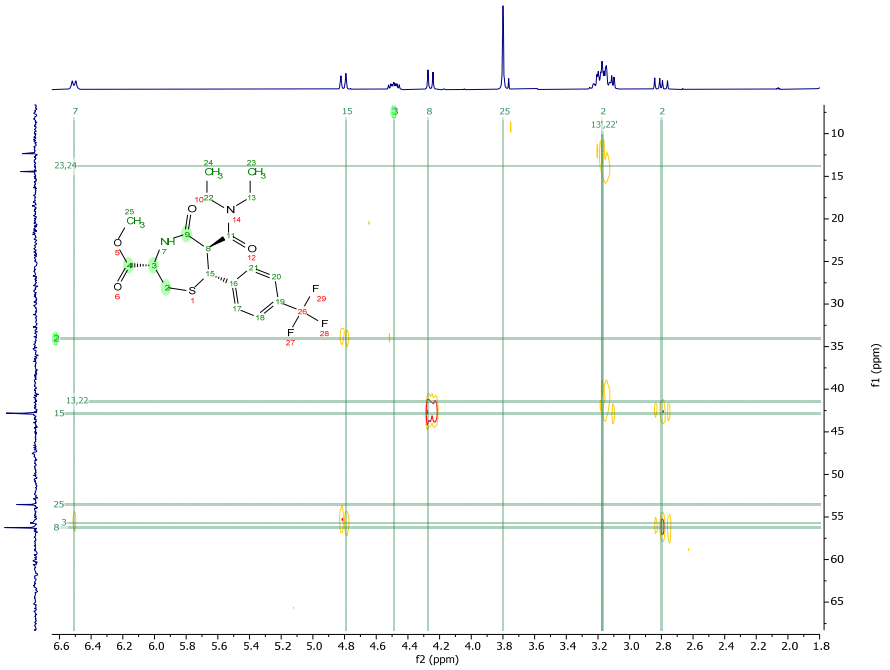

3. 1,4-thiazepane-3-one stability studies

Solutions of 1,4-thiazepan-5-one **11-fraction C** (10 mM in ACN) (5.0 µL, 0.050 µmol) in 1% ACN/KPi 50 mM, pH 4.5 and 7.0 (1.0 mL) were prepared and incubated at 25ºC for one week. 20 µL aliquots were taken over time for LC-MS analysis. The HPLC runs were carried out with a gradient of A (Milli Q water containing 0.1% v/v Formic acid, FA) and B (acetonitrile containing 0.1% v/v FA, Honeywell HPLC-grade). The mobile phase was t = 0–1 min, 5% B; t = 10–11 min, 95.5% B; t = 12 min, 5% B; t = 15 min, stop at a flow rate of 0.2 mL/min. 1,4-thiazepan-5-one **11-fraction C**: RT 12.9 min, 1,4-thiazepan-5-one **11-fraction C** methyl ester hydrolysis product: RT 11.6 min, detection at 254 nm, TIC and EIC.

A calibration curve based on EIC intensity (base peak *m/z* 433.1403, within 6 ppm range) was traced for quantification of remaining 1,4-thiazepan-5-one **11** over time.

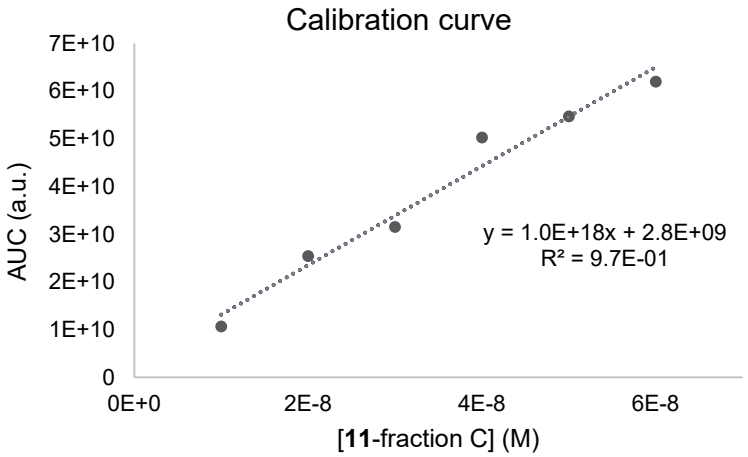

Figure S 4. 1,4-thiazepan-5-one **11**-fraction **C** calibration curve of EIC intensity (base peak *m/z* 433.1403, within 6 ppm range) *vs* **11**-fraction **C** concentration (M).

3.1. Stability at pH 4.5

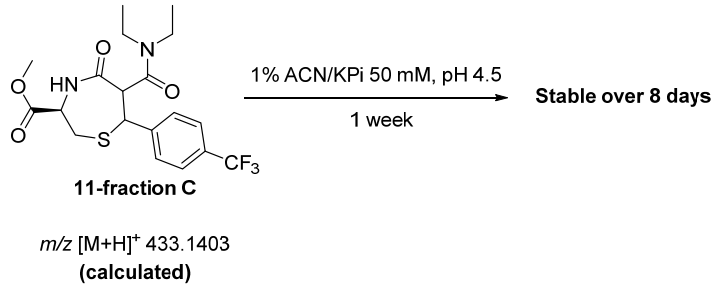

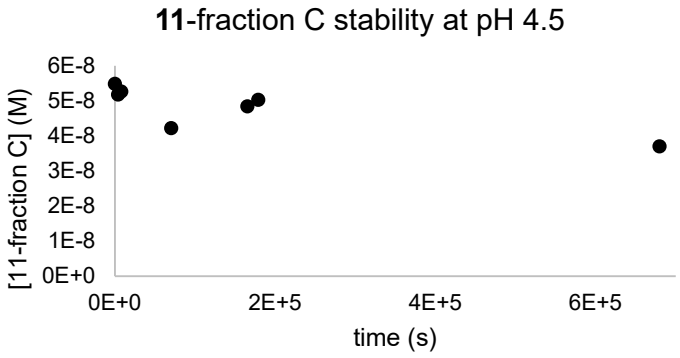

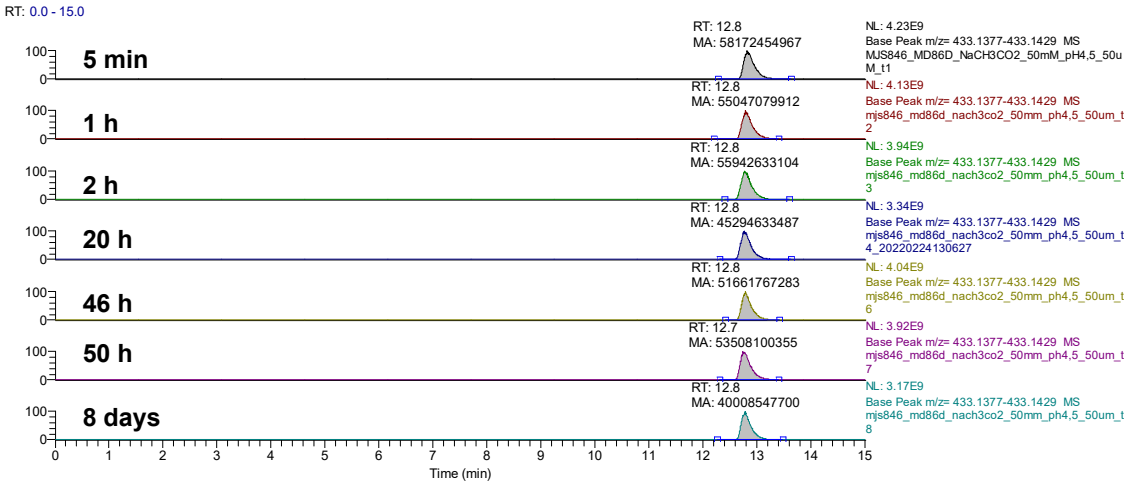

Figure S 5. EIC of 1,4-thiazepan-5-one **11**-fraction **C** in 1% ACN/KPi 50 mM, pH 4.5 over time (base peak *m/z* 433.1403, within 6 ppm range).

3.2. Stability at pH 7.0

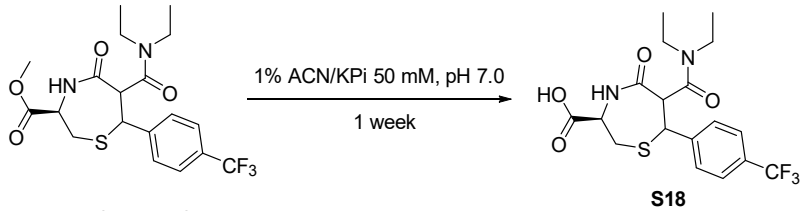

11-fraction C

m/z $[M+H]^+$ 433.1403
(calculated)

S18

m/z $[M+H]^+$ 419.1247
(calculated)

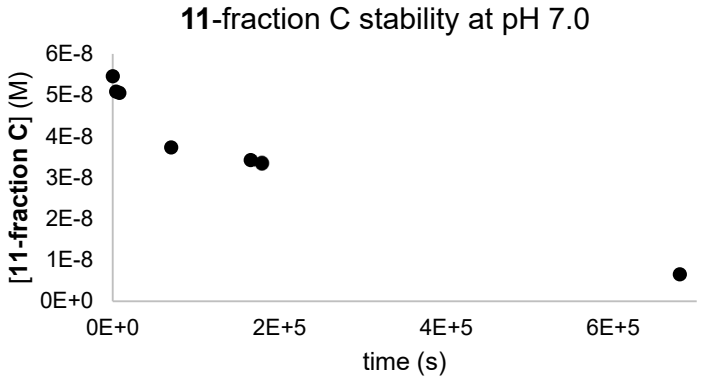

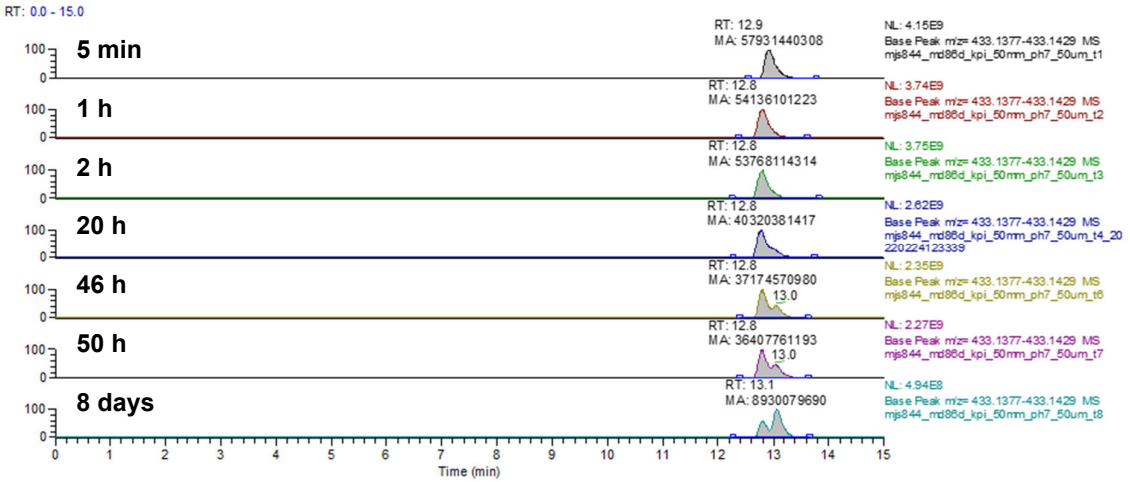

Figure S 6. EIC of 1,4-thiazepan-5-one **11**-fraction **C** in 1% ACN/KPi 50 mM, pH 7.0 over time (base peak *m/z* 433.1403, within 6 ppm range).

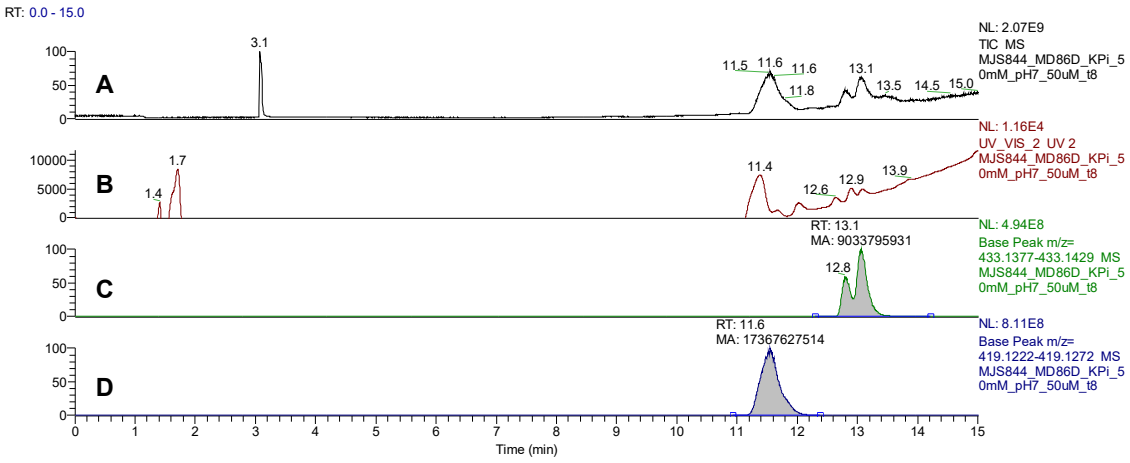

Figure S 7. LC-MS analysis of 1,4-thiazepan-5-one **11**-fraction **C** after 8 days incubation time. **A)** Total Ion Current (TIC) chromatogram; **B)** Detection at 254 nm chromatogram; **C)** Extracted Ion Chromatogram (EIC) of base of peak at *m/z* 433.1403 $[11+H]^+$; **D)** Extracted Ion Chromatogram (EIC) of base of peak at *m/z* 419.1247 $[\mathbf{S18}+H]^+$.

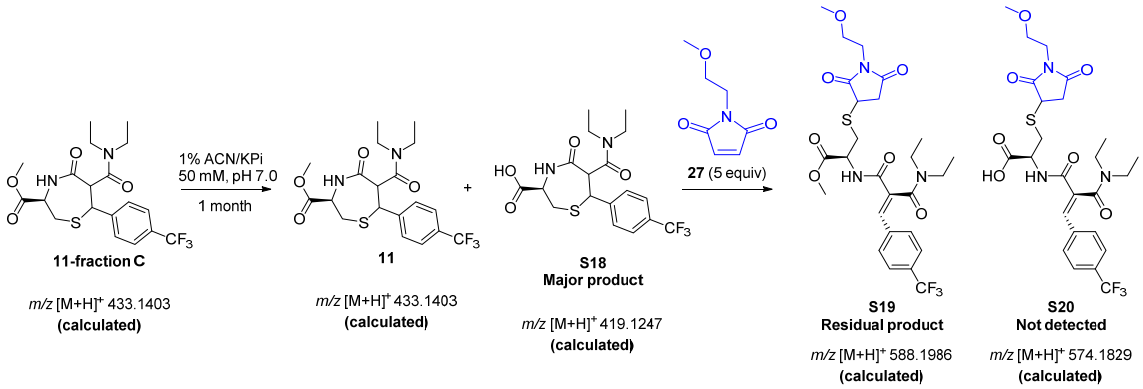

To an aliquot (200 µL) of solution of 1,4-thiazepan-5-one **11-fraction C** (10.0 nmol) in 1% ACN/KPi 50 mM, pH 7.0 incubated at 25ºC for one month was added maleimide **27** (1.67 µL, 50.0 nmol). A 20 µL aliquot was taken after 1 h reaction time for LC-MS analysis using the same mthod. 1,4-thiazepan-5-one **11-fraction C**: RT 12.8 and 13.1 min, **S18**: RT 11.4 min, **S19**: RT 13.9 min, **S20**: not detected. Detection at 254 nm, TIC and EIC.

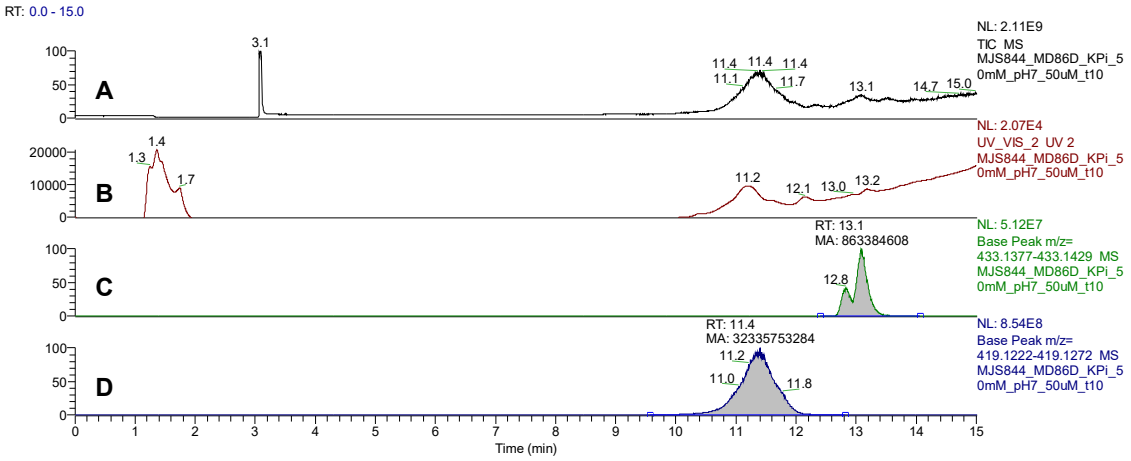

Figure S 8. LC-MS analysis of 1,4-thiazepan-5-one **11**-fraction **C** after 1 month incubation in KPi 50 mM, pH 7.0. **A)** Total Ion Current (TIC) chromatogram; **B)** Detection at 254 nm chromatogram; **C)** Extracted Ion Chromatogram (EIC) of base of peak at *m/z* 433.1403 $[11+H]^+$; **D)** Extracted Ion Chromatogram (EIC) of base of peak at *m/z* 419.1247 $[\mathbf{S18}+H]^+$.

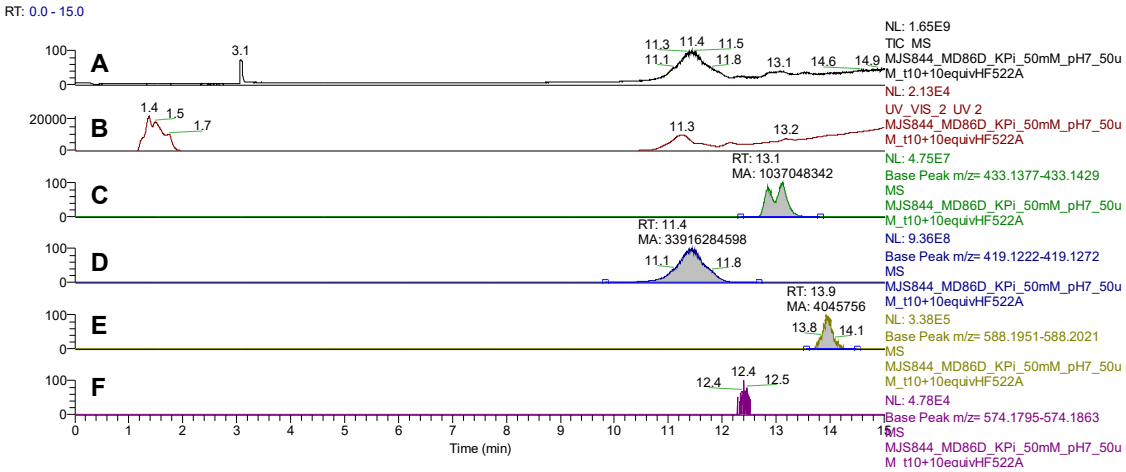

Figure S 9. LC-MS analysis of 1,4-thiazepan-5-one **11**-fraction **C** with 1 month incubation in KPi 50 mM, pH 7.0 after 1 h reacting with maleimide **27** (5 equiv). **A)** Total Ion Current (TIC) chromatogram; **B)** Detection at 254 nm chromatogram; **C)** Extracted Ion Chromatogram (EIC) of base of peak at *m/z* 433.1403 $[11+H]^+$; **D)** Extracted Ion Chromatogram (EIC) of base of peak at *m/z* 419.1247 $[\mathbf{S18}+H]^+$; **E)** Extracted Ion Chromatogram (EIC) of base of peak at *m/z* 588.1986 $[\mathbf{S19}+H]^+$ showing a peak with very low intensity compared to 1,4-thiazepan-5-one species; **F)** Extracted Ion Chromatogram (EIC) of base of peak at *m/z* 574.1829 $[\mathbf{S20}+H]^+$ showing a negligible peak.

3.3. Stability at pH 7.4 in presence of GSH (1 mM)

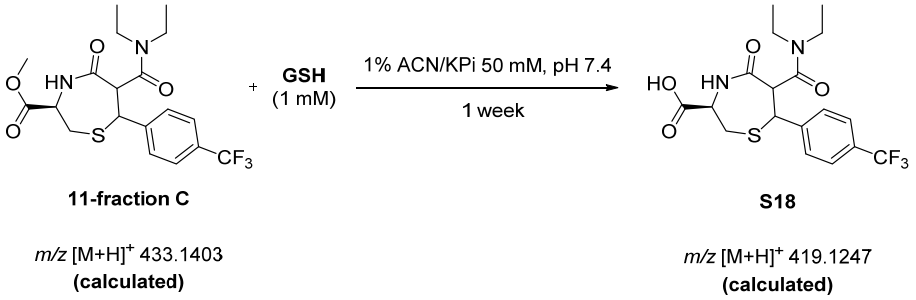

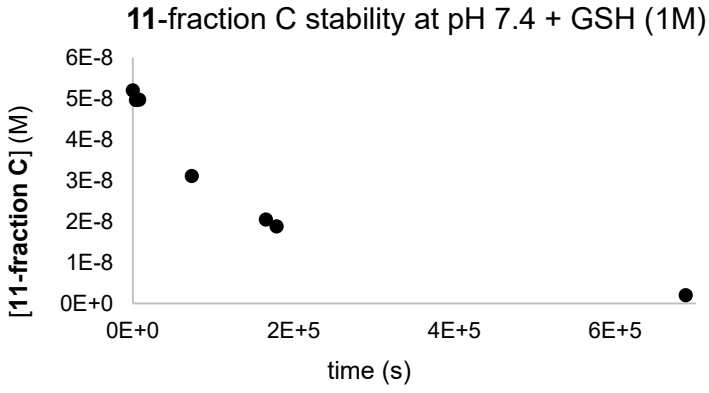

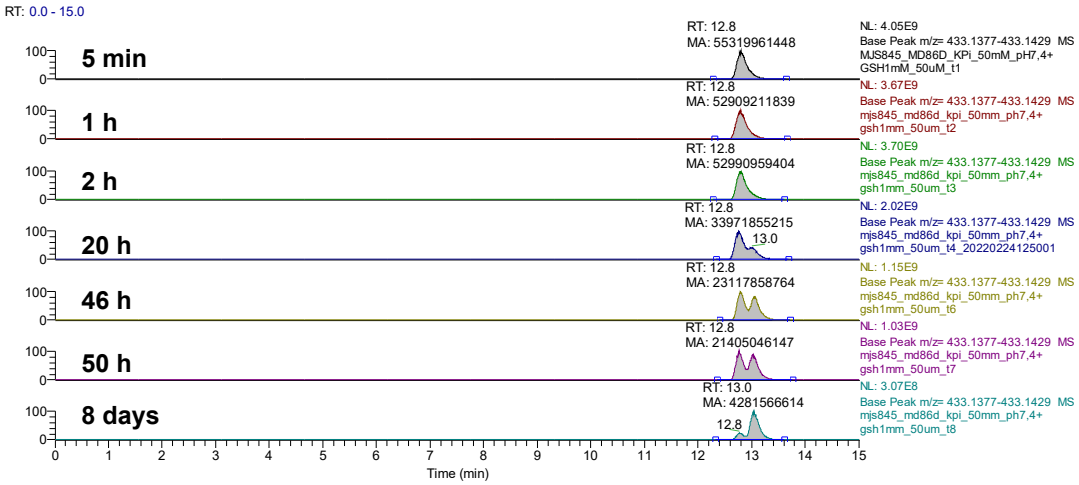

Figure S 10. LC-MS analysis to crude mixture of 1,4-thiazepan-5-one 11.EIC of 1,4-thiazepan-5-one 11-fraction C in 1% ACN/KPi 50 mM, pH 7.4 in presence of GSH (1 mM) over time (base peak *m/z* 433.1403, within 6 ppm range).

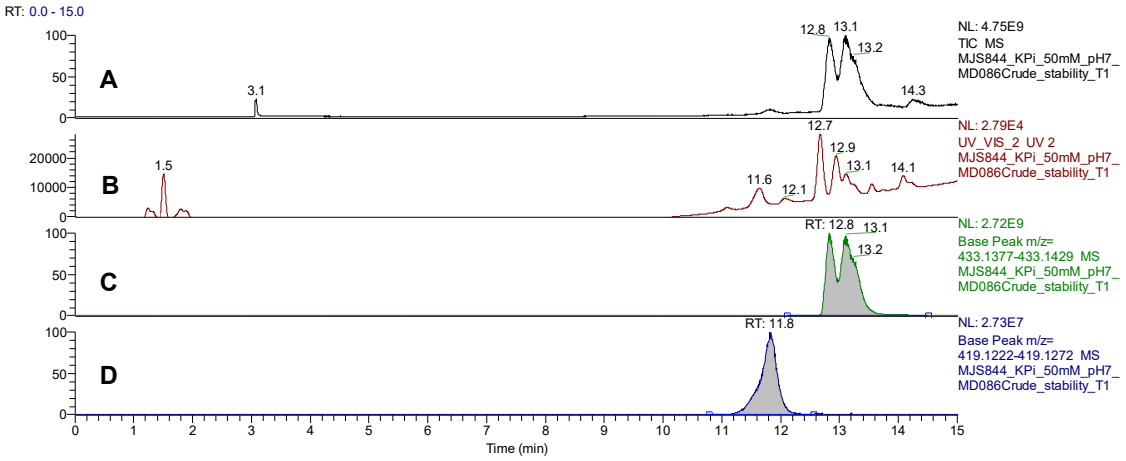

Figure S 11. LC-MS analysis of 1,4-thiazepan-5-one **11** crude mixture. **A)** Total Ion Current (TIC) chromatogram; **B)** Detection at 254 nm chromatogram; **C)** Extracted Ion Chromatogram (EIC) of base of peak at *m/z* 433.1403 $[11+H]^+$; **D)** Extracted Ion Chromatogram (EIC) of base of peak at *m/z* 419.1247 $[\mathbf{S18}+H]^+$.

4. Reaction kinetics for the formation of 1,4-thiazepan-5-one with coumarin NHS-activated acrylate 29

4.1. UV-Vis

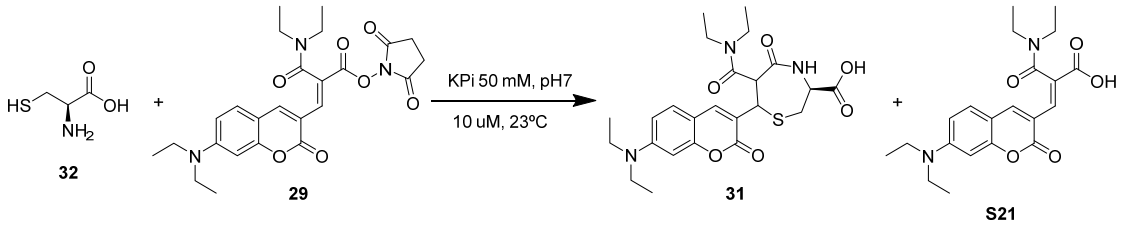

Reactions were performed under second-order conditions in quartz cuvettes (50 mm path length; total volume 3 mL) with solutions pre-equilibrated at room temperature (23 °C). KPi

50 mM, pH 7 (3 mL) was pipetted into the cuvette, followed by *L*-cysteine **32** (30 mM in Milli Q water) (5.0 µL, 0.150 µmol) stock solution. The solution was mixed. The reaction was then initiated by addition of Coumarin NHS-activated acrylate **29** (30 mM in ACN) (5 µL,0.150 µmol). The solution was rapidly homogenized and the reaction was monitored by UV-Vis spectroscopy, fluorescence and LC-MS.

In a control experiment, Coumarin NHS-activated acrylate **29** (30 mM in ACN) (5 µL,0.150 µmol) was added to KPi 50 mM, pH 7 (3 mL), the solution was rapidly homogenized and monitored by UV-Vis for comparison with the reaction's UV-Vis profile.

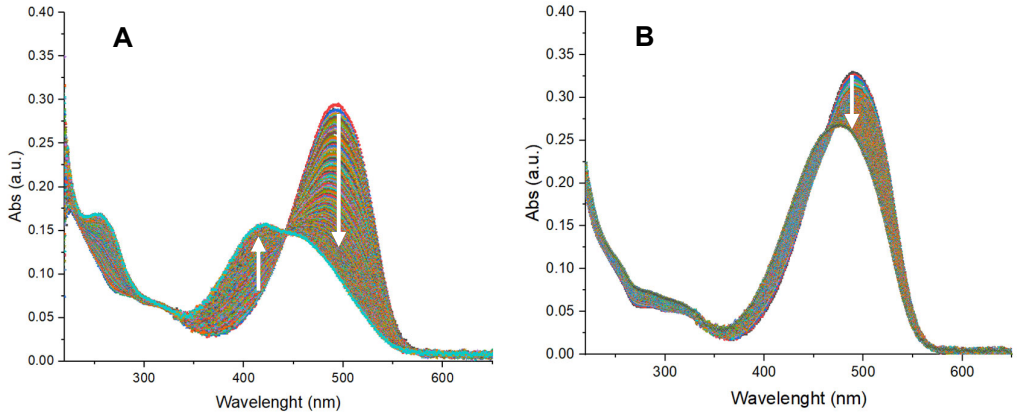

Figure S 12. A) Reaction UV-Vis spectra (220-650 nm) were traced between 30 s and 2 h; **B) 29** hydrolysis UV-Vis spectra (220-650 nm) were traced between 30 s and 6.1 h. λ_{abs} 489 nm.

From this absorbance full scan, the maximum absorbance point (489 nm) of the starting material **29** was selected to monitor the reaction every 30 s.

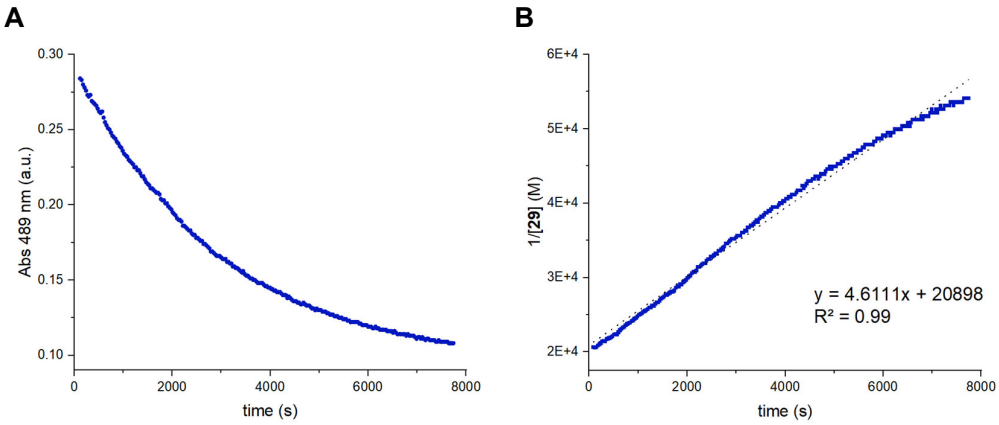

Figure S 13. A) Absorbance intensity at 489 nm in a.u. were traced every 30 s for 124 min. **B)** The plot of 1/[**29**] (M) *vs* time (s) was used to determine the second-order constant (k_2). The concentration of the product was calculated based on the absorvance intensity at 489 nm.

Table S 1. Obtained equations and respective R^2 from the plot 1/[**29**] vs time (s) of the triplicates.

	Equation / R^2	k_2 ($M^{-1}s^{-1}$)
Triplicates	y = 4.6111x + 20898; R² = 0.99	**4.61**
	y = 4.1828x + 22284; R² = 0.98	4.18
	y = 4.7896x + 17955; R² = 0.99	4.79
Average	4.5278	4.53 ± 0.25

4.2. LC-MS

LC-MS were acquired after 120 min of reaction time in positive mode and the HPLC runs were carried out with a gradient of C (Milli Q water containing) and D (acetonitrile, Honeywell HPLC-grade). The mobile phase was t = 0 min, 0% D; t = 25 min, 95% D; t =42 min, 5% D; t = 45 min, stop, at a flow rate of 0.2 mL/min.

From the LC-MS we observed 3 products: The desired **31** (*m/z* =490.2003 $[M+H]^+$), the remaining unreacted **29** (*m/z* =484.2071 $[M+H]^+$) and product **S21** (*m/z* =387.1911 $[M+H]^+$).

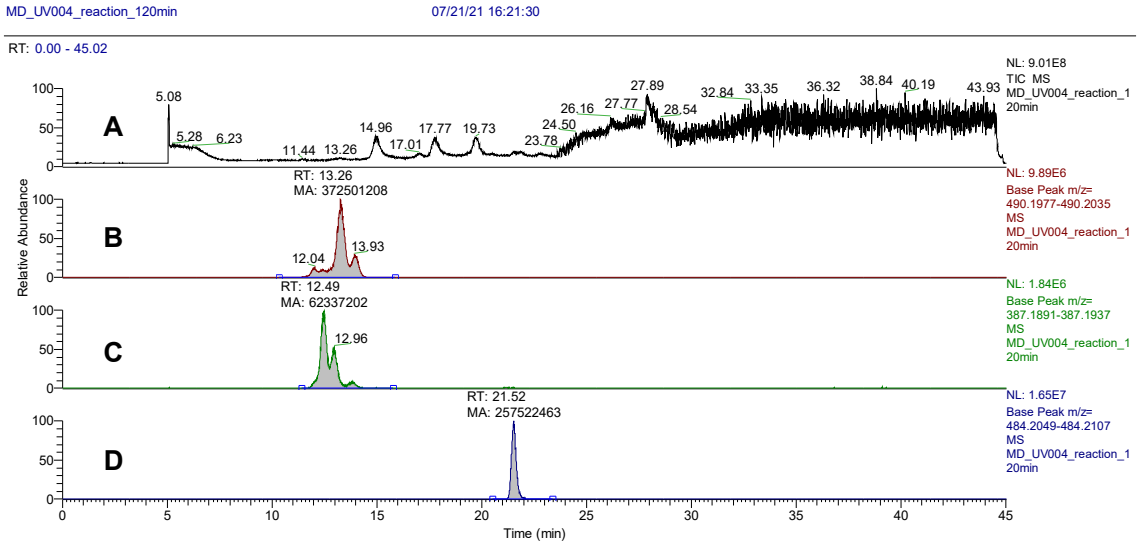

Figure S 14. LC-MS chromatograms of **29** reaction with cysteine in KPi 50mM, pH 7.0 after 120 min: **A)** Total Ion Current (TIC) chromatogram; **B**) Extracted Ion Chromatogram (EIC) of base of peak at m/z 490.2006 [**31**+H]$^+$; **C)** Extracted Ion Chromatogram(EIC) of base of peak at *m/z* 387.1914 [**S21**+H]$^+$. **D) 29** Extracted Ion Chromatogram (EIC) of base of peak at *m/z* 484.2078 [**29**+H]$^+$.

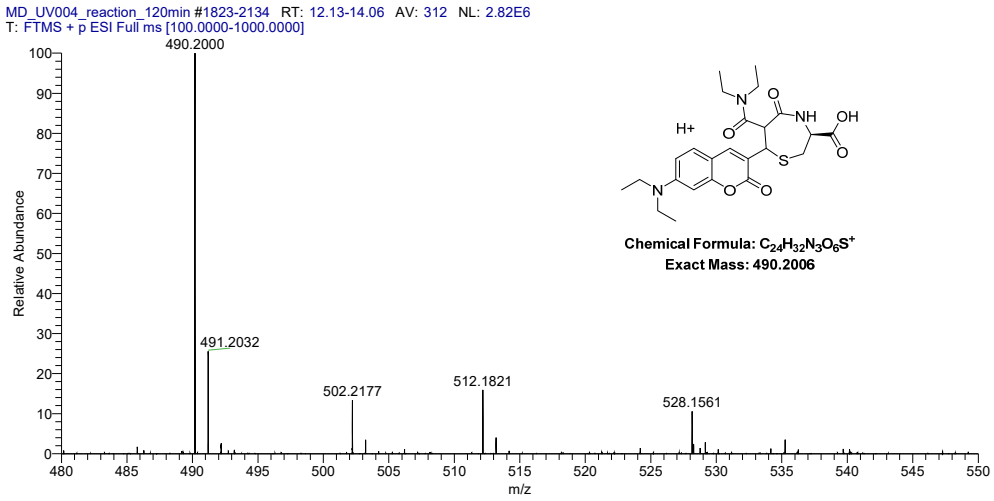

Figure S 15. ESI$^+$-HRMS spectrum of TIC peak at RT 13.26 min and the correspondent product **31**. (Calculated for $C_{24}H_{32}N_3O_6S$ [**31**+H]$^+$: 490.2006, found 490.1998; calculated for $C_{24}H_{32}N_3NaO_6S$ [**31**+Na]$^+$: 512.1826, found 512.1821).

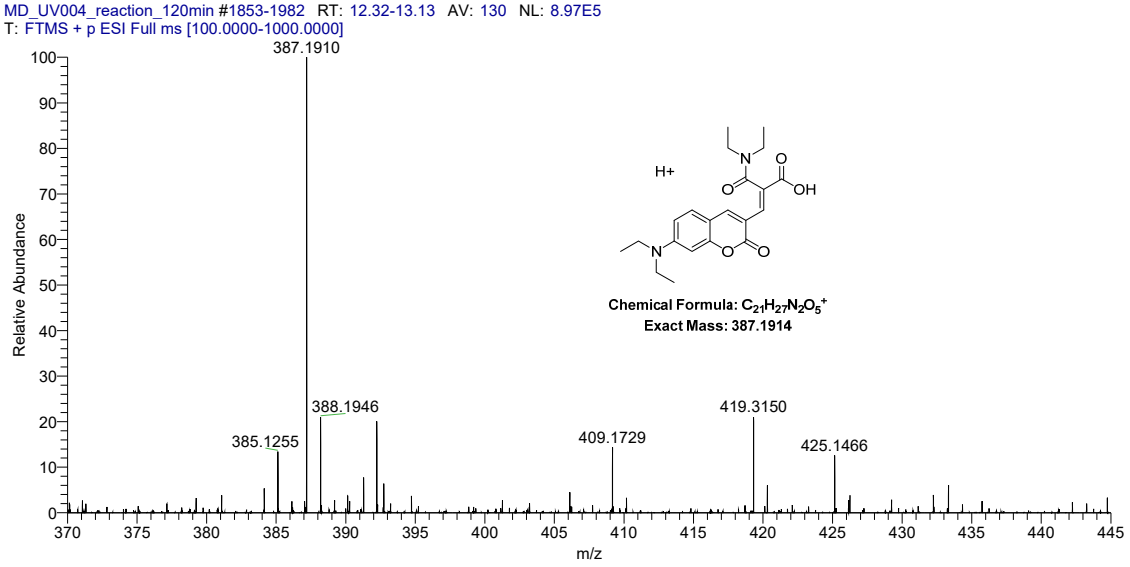

Figure S 16. ESI$^+$-HRMS spectrum of TIC peak at RT 12.49 min and the correspondent hydrolysis product **S21**. (Calculated for $C_{21}H_{27}N_2O_5$ [**S21**+H]$^+$: 387.1914, found 387.1909; calculated for $C_{21}H_{27}N_2NaO_5$ [**S21**+Na]$^+$: 409.1734, found 409.1729).

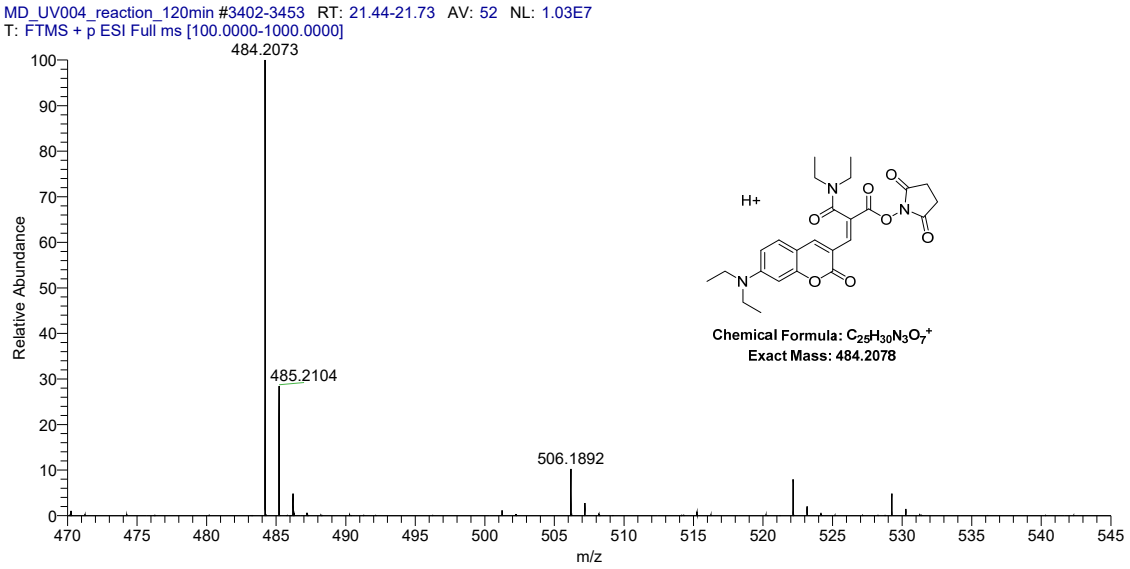

Figure S 17. ESI$^+$-HRMS spectrum of TIC peak at RT 21.52 min and the correspondent **29** structure. (Calculated for $C_{25}H_{30}N_3O_7$ [**29**+H]$^+$: 484.2078, found 484.2071; calculated for $C_{25}H_{30}N_3NaO_7$ [**29**+Na]$^+$: 506.1898 found 506.1892).

5. NHS-activated acrylates stability studies

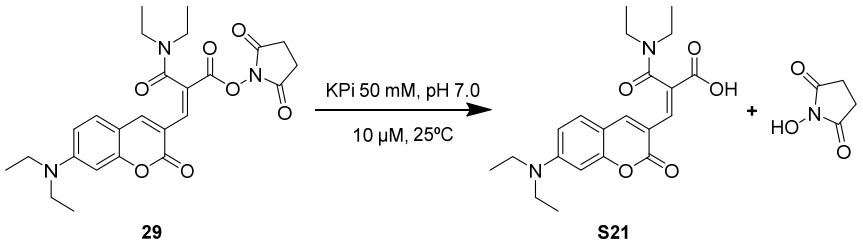

Triplicated solutions of Coumarin NHS-activated acrylate **29** (5.0 µL, 50 nmol) in 1% ACN/KPi 50 mM, pH 7.0 (1.0 mL) were prepared and incubated at 25ºC over 16 h. 20 µL aliquots were taken each hour for LC-MS analysis. The HPLC runs were carried out with a gradient of A (Milli Q water containing 0.1% v/v Formic acid, FA) and B (acetonitrile containing 0.1% v/v FA, Honeywell HPLC-grade). The mobile phase was t = 0 min, 5% B; t = 10 min, 95.5% B; t = 11 min, 95.5% B; t = 12 min, 5% B; t= 15 min, stop at a flow rate of 0.2 mL/min. Coumarin NHS-activated acrylate **29**: RT 13.5 min; hydrolysed coumarin acrylate **S21**: RT 12.4 min, detection at 254 nm, TIC and EIC of both species.

The peak areas of the EIC of Coumarin NHS-activated acrylate **29** over time were converted into remanining concentration based on the following calibration curve.

A

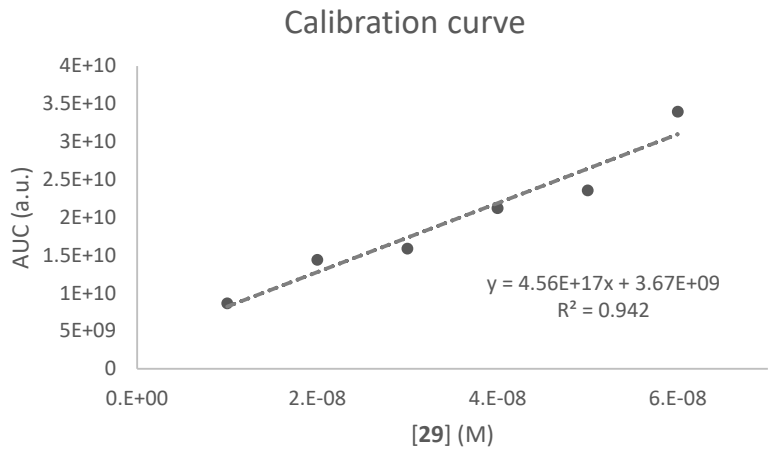

B

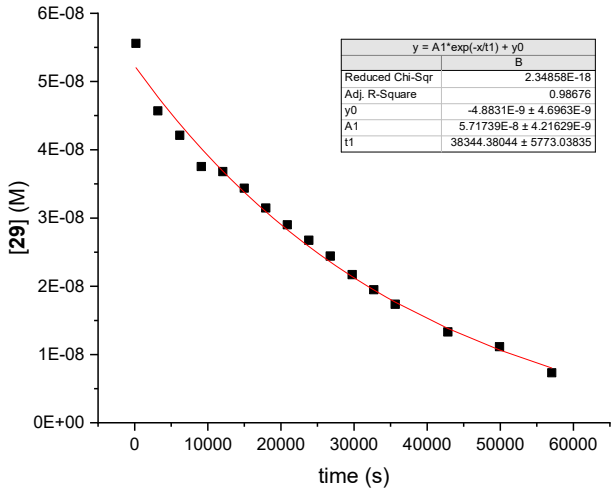

C

Triplicates k_{obs} (s^{-1})	Average k_{obs} (s^{-1})	$t_{1/2}$ (h)
2.61E-05 3.09E-05 2.66E-05	2.78 ± 0.26E-05	6.9

Figure S 18. A) Coumarin NHS-activated acrylate 29 calibration curve of EIC intensity (base peak *m/z* 484.2078, within 6 ppm range) *vs* **29** concentration (M); B) The Coumarin NHS-activated acrylate **29** hydrolysis kinetics was performed in KPi 50mM, pH 7.0 to determine the k_{obs} from the exponential plot of **29** concentration *vs* time (s). The k_{obs} corresponds to the value 1/t1 from the nonlinear fitting equation: $y = A_1 e^{(-x/t1)} + y_0$ and $t_{1/2} = \ln 2 / k_{obs}$; C) Calculated k_{obs} and $t_{1/2}$ from the triplicate analysis.

6. General procedure for the ESI-MS assays with dipeptides and 2,5-dioxopyrrolidin-1-yl-2-(diethylcarbamoyl)-3-(4 (trifluoromethyl)phenyl)acrylate 2

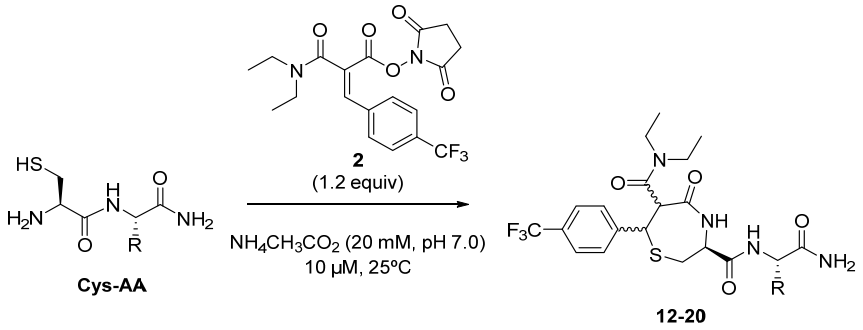

To a fresh solution of dipeptide (**Cys-AA**) (10 mM in water) (4.0 µL, 40 nmol) in ammonium acetate solution 20 mM, pH 7.0 (1.5 mL) was added 2,5-dioxopyrrolidin-1-yl-2-(diethylcarbamoyl)-3-(4-(trifluoromethyl)phenyl)acrylate **2** (10 mM in ACN) (4.8 µL, 48 nmol) and the solution was mixed at 25ºC. The reactions were then monitored in Positive Mode of ESI-MS at 5 min and 24 h and by LC-HRMS in Positive Mode. The HPLC runs were carried out with a gradient of A (Milli Q water containing 0.1% v/v Formic acid, FA) and B (acetonitrile containing 0.1% v/v FA, Honeywell HPLC-grade). The mobile phase was t=0 min, 5% B; t=10 min, 95% B; t=10.1 min, 95.5% B; t=11 min, 95.5% B; t=12 min, 5% B; t=15 min stop, at a flow rate of 0.2 mL/min, detection at 210 nm.

MS/MS fragmentation of the peaks correspondent to the expected products confirmed that the major product formed is the 7 member ring. With dipeptides cysteine-arginine and cysteine-histidine the thioester fragmentation product was observed in negligible amount and, with dipeptide cysteine-lysine the amide fragmentation product was also observed in vestigial amounts.

6.1. Cys-Lys

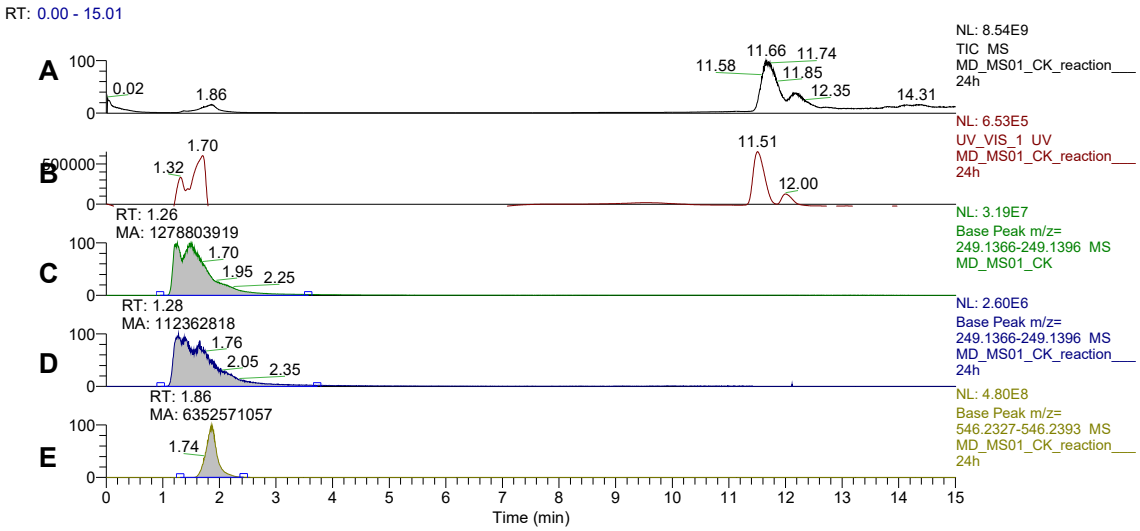

Figure S 19. LC-MS chromatograms of **Cys-Lys** conjugate **12** and **Cys-Lys** dipeptide. **A)** Reaction mixture TIC after 24 h; **B)** Reaction detection at 210 nm, after 24 h; **C)** Reaction t_0 – unreacted **Cys-Lys** EIC (base peak *m/z* 249.1381); **D)** Unreacted **Cys-Lys** EIC after 24 h reaction with 1.2 equiv. of **2**; **E) Cys-Lys** conjugate **12** EIC (base peak *m/z* 546.2360) after 24 h reaction. **Cys-Lys** conversion was calculated based on the EIC intensity (AUC) within δ 6ppm range.

Table S 2. Cys-Lys dipeptide conversion in 24 h reaction with coumarin NHS-activated acrylate **2** according to AUC from EIC chromatograms of base peak *m/z* 249.2381, within δ 6 ppm range.

	t_0	24 h	Conversion
Cys-Lys (AUC a.u.)	1278803919	112362818	91%

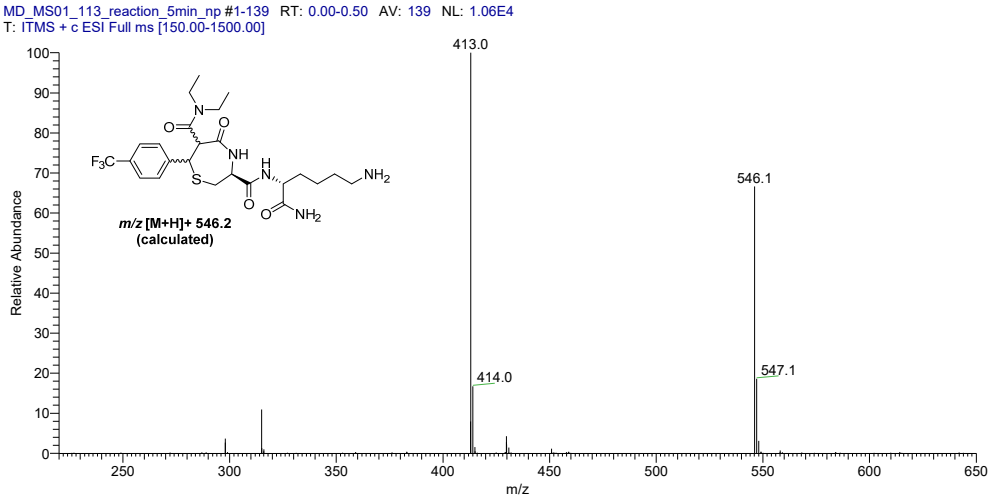

Figure S 20. ESI$^+$-LRMS spectrum of reaction between **Cys-Lys** (calculated $C_9H_{20}N_3O_3S$ *m/z* $[M+H]^+$ 250.1 not found), 2,5-dioxopyrrolidin-1-yl-2-(diethylcarbamoyl)-3-(4-(trifluoromethyl)phenyl)acrylate **2** (calculated *m/z* $C_{19}H_{20}F_3N_2O_5$ [**2**+H]$^+$: 413.1, found 413.0), and the resulting product **12** (calculated for $C_{24}H_{33}F_3N_4O_5S$ [**12**+H]+: 546.2, found 546.1).

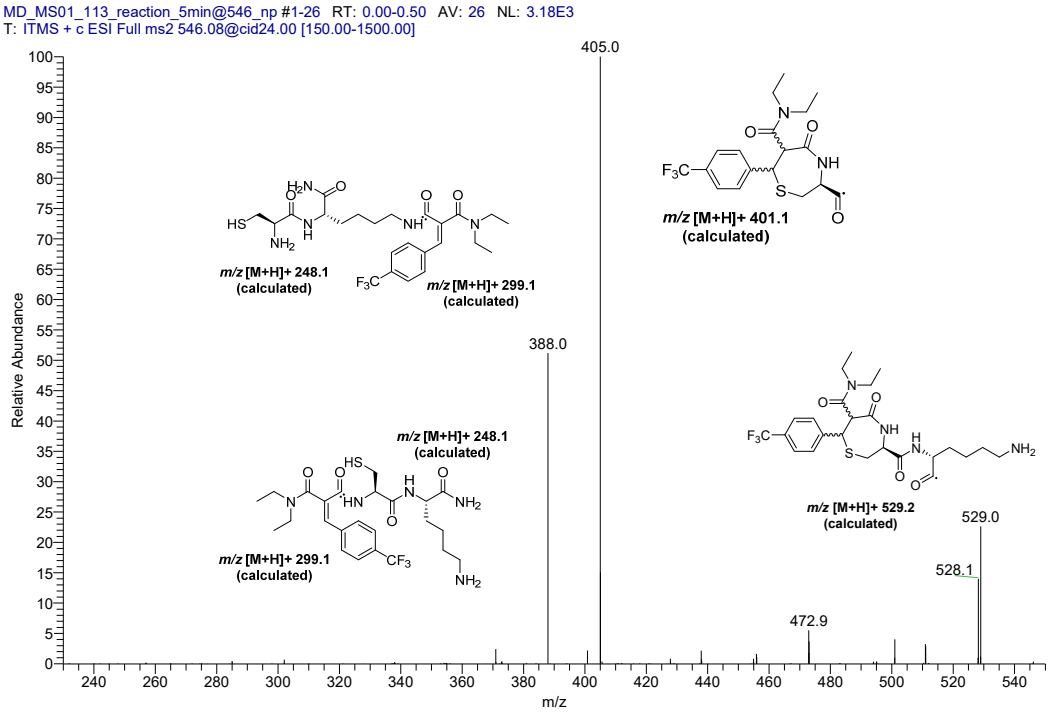

Figure S 21. MS fragmentation analysis of **12** at *m/z* 546.1: *m/z* 529.0 (calculated $C_{24}H_{32}F_3N_4O_4S$ $[M+H]^+$ 529.2) and *m/z* 405.0 (calculated $C_{18}H_{20}F_3N_2O_3S$ $[M+H]^+$ 401.1) indicate 7 member ring product and, *m/z* 247.9 (calculated $C_9H_{18}N_3O_3S$ $[M+H]^+$ 248.1) indicate amide product (traces).

6.2. Cys-His

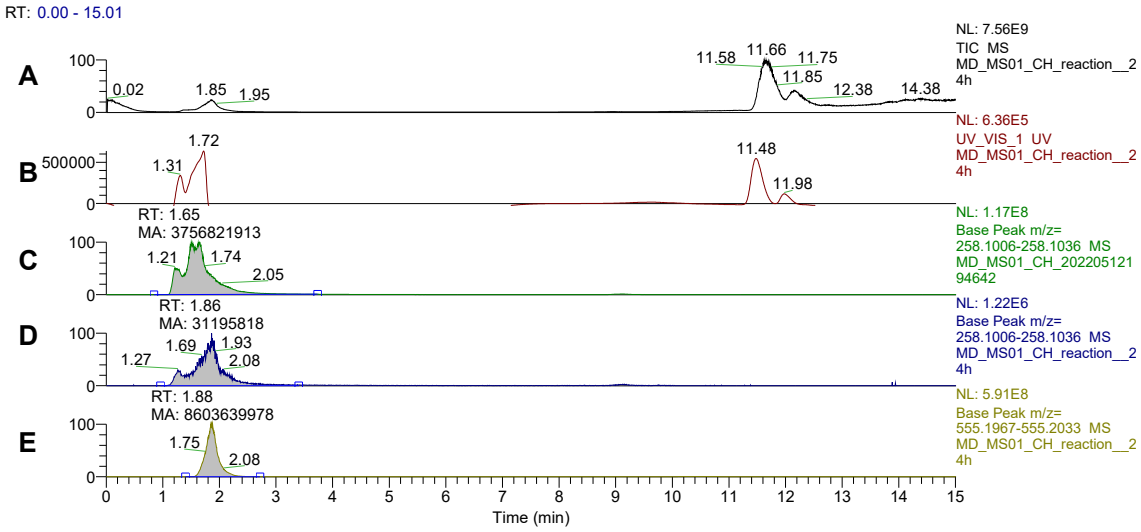

Figure S 22. LC-MS chromatograms of **Cys-His** conjugate **13** and **Cys-His** dipeptide. **A)** Reaction mixture TIC after 24 h; **B)** Reaction detection at 210 nm, after 24 h; **C)** Reaction t_0 – unreacted **Cys-His** EIC (base peak *m/z* 258.1021); **D)** Unreacted **Cys-His** EIC after 24 h reaction with 1.2 equiv. of **2**; **E) Cys-His** conjugate **13** EIC (base peak *m/z* 555.2000) after 24 h reaction. **Cys-His** conversion was calculated based on the EIC intensity (AUC) within δ 6ppm range.

Table S 3. Cys-His dipeptide conversion in 24 h reaction with coumarin NHS-activated acrylate **2** according to AUC from EIC chromatograms of base peak *m/z* 258.1021, within δ 6 ppm range.

	t_0	24 h	Conversion
Cys-His (AUC a.u.)	3756821913	31195817	99%

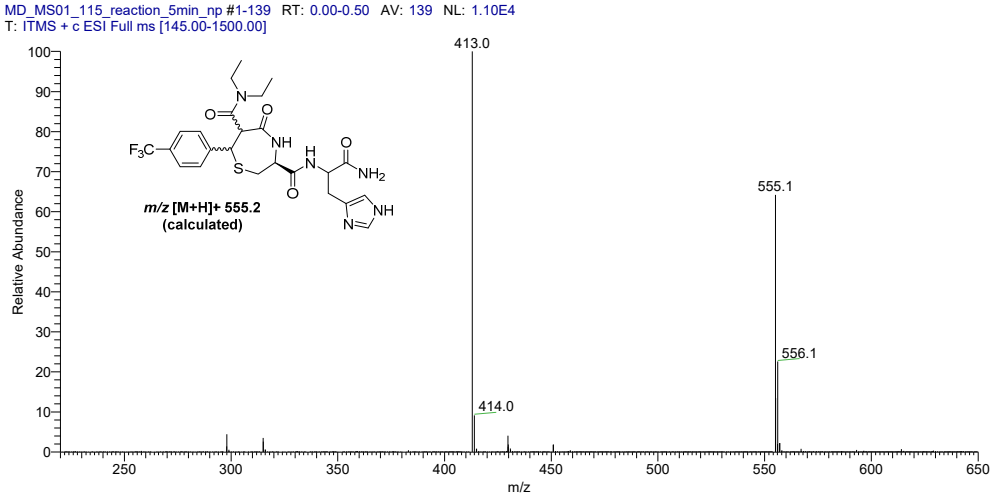

Figure S 23. ESI$^+$-LRMS spectrum of reaction between **Cys-His** (calculated $C_9H_{15}N_4O_3S$ *m/z* $[M+H]^+$ 258.1, found 258.0, as a residual peak), 2,5-dioxopyrrolidin-1-yl-2-(diethylcarbamoyl)-3-(4-(trifluoromethyl)phenyl)acrylate **2** (calculated *m/z* $C_{19}H_{20}F_3N_2O_5$ [**2**+H]$^+$: 413.1, found 413.0), and the resulting product **13** (calculated for $C_{24}H_{28}F_3N_5O_5S$ [**13**+H]+: 555.2, found 555.1).

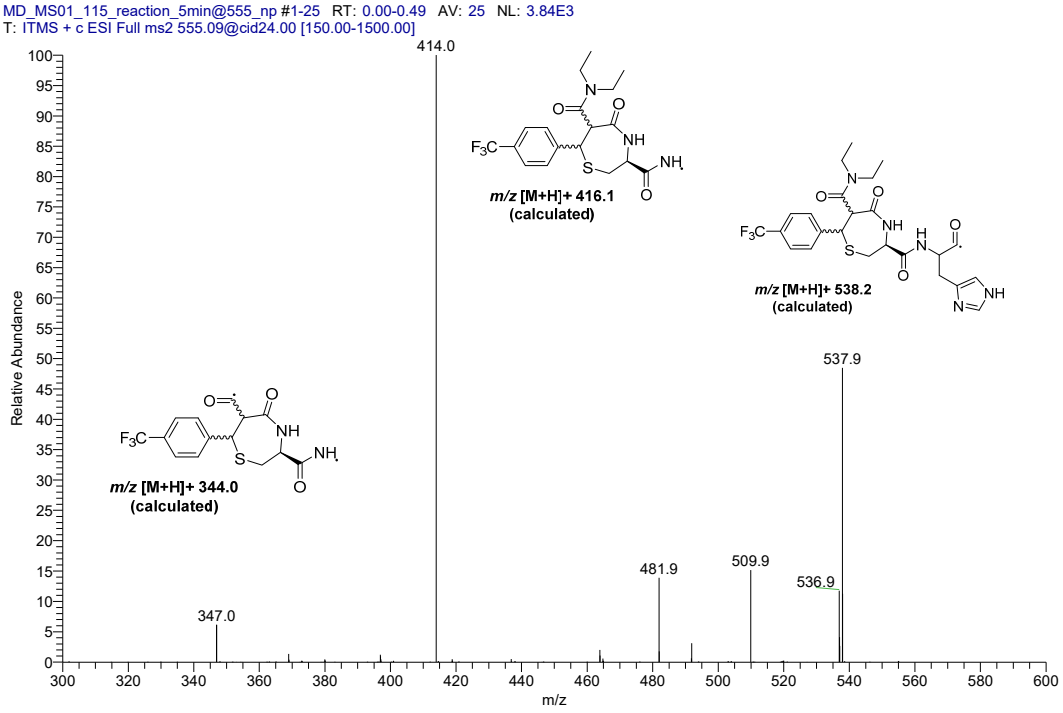

Figure S 24. MS fragmentation analysis of **13** at *m/z* 555.1: *m/z* 537.9 (calculated $C_{24}H_{27}F_3N_5O_4S$ $[M+H]^+$ 538.2), *m/z* 414.0 (calculated $C_{18}H_{21}F_3N_3O_3S$ $[M+H]^+$ 416.1) and, *m/z* 347.0 (calculated $C_{14}H_{11}F_3N_2O_3S$ $[M+H]^+$ 344.0) confirms 7 member ring product. Fragmentations of thioester and amide products were not found.

6.3. Cys-Arg

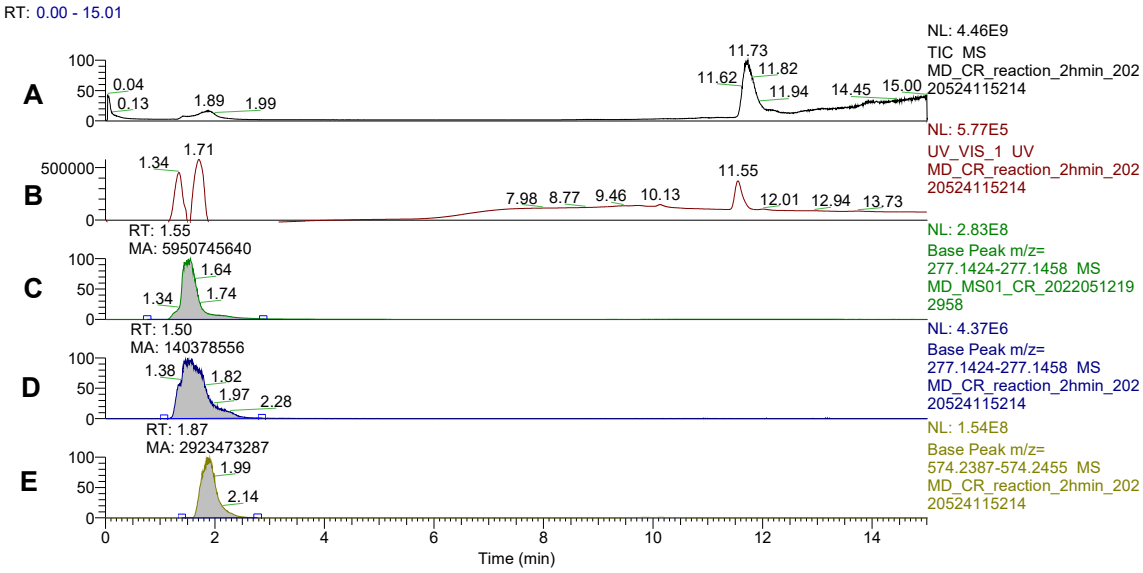

Figure S 25. LC-MS chromatograms of **Cys-Arg** conjugate **14** and **Cys-Arg** dipeptide. **A)** Reaction mixture TIC after 24 h; **B)** Reaction detection at 210 nm, after 24 h; **C)** Reaction t_0 – unreacted **Cys-Arg** EIC (base peak *m/z* 277.1441); **D)** Unreacted **Cys-Arg** EIC after 24 h reaction with 1.2 equiv. of **2**; **E) Cys-Arg** conjugate **14** EIC (base peak *m/z* 574.2421) after 24 h reaction. **Cys-Arg** conversion was calculated based on the EIC intensity (AUC) within δ 6ppm range.

Table S 4. Cys-Arg dipeptide conversion in 24 h reaction with coumarin NHS-activated acrylate **2** according to AUC from EIC chromatograms of base peak m/z 277.1441, within δ 6 ppm range.

	t_0	24 h	Conversion
Cys-Arg (AUC a.u.)	5950745640	140378556	98%

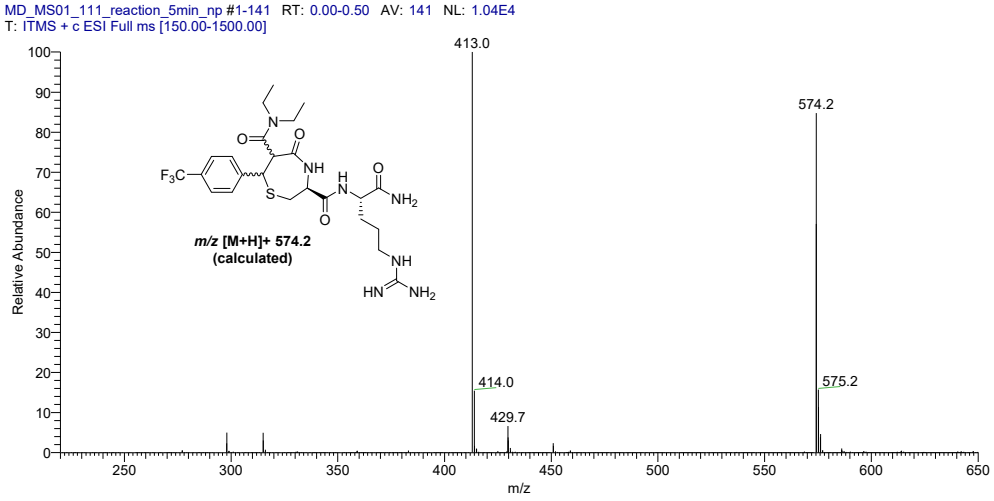

Figure S 26. ESI+-LRMS spectrum of reaction between **Cys-Arg** (calculated *m/z* $C_9H_{20}N_5O_3S$ $[M+H]^+$ 277.1, found 277.1, as a residual peak), 2,5-dioxopyrrolidin-1-yl-2-(diethylcarbamoyl)-3-(4-(trifluoromethyl)phenyl)acrylate **2** (calculated *m/z* $C_{19}H_{20}F_3N_2O_5$ [**2**+H]$^+$: 413.1, found 413.0), and the resulting product **14** (calculated for $C_{24}H_{34}F_3N_6O_5S$ [**14**+H]+: 574.2, found 574.2).

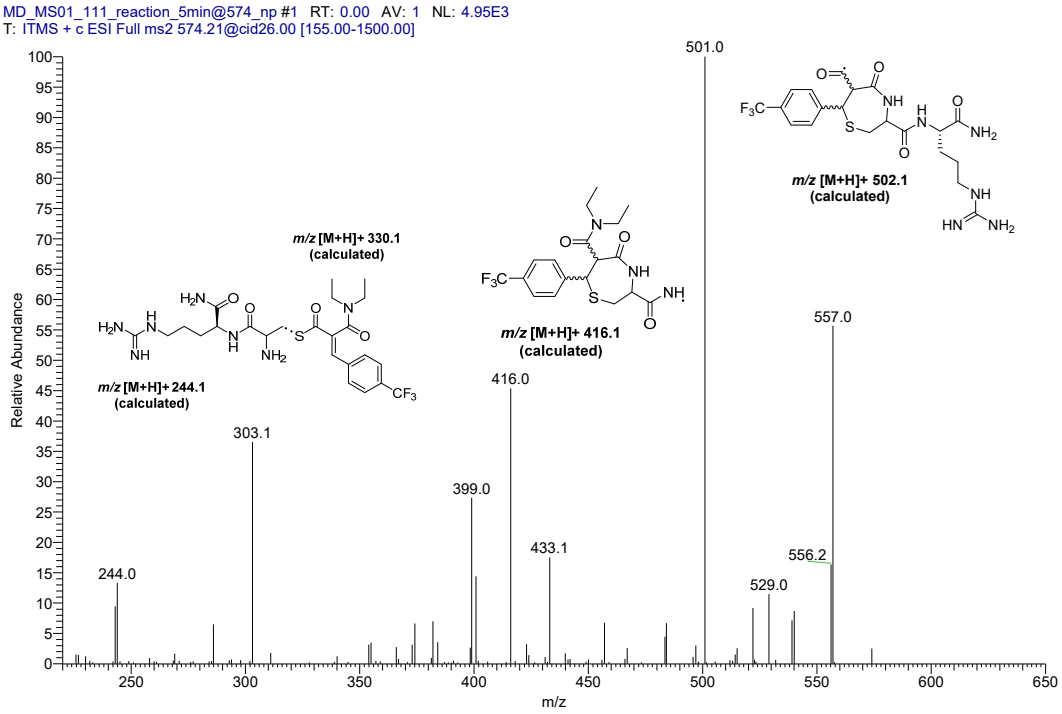

Figure S 27. MS fragmentation analysis of **14** at *m/z* 574.2: *m/z* 501.0 (calculated $C_{20}H_{23}F_3N_5O_5S$ $[M+H]^+$ 502.1) and *m/z* 416.0 (calculated $C_{18}H_{21}F_3N_3O_3S$ $[M+H]^+$ 416.1) confirms 7 member ring product and, *m/z* 244.0 (calculated $C_9H_{18}N_5O_3$ $[M+H]^+$ 244.1) confirms thioester product (very small percentage).

6.4. Cys-Ser

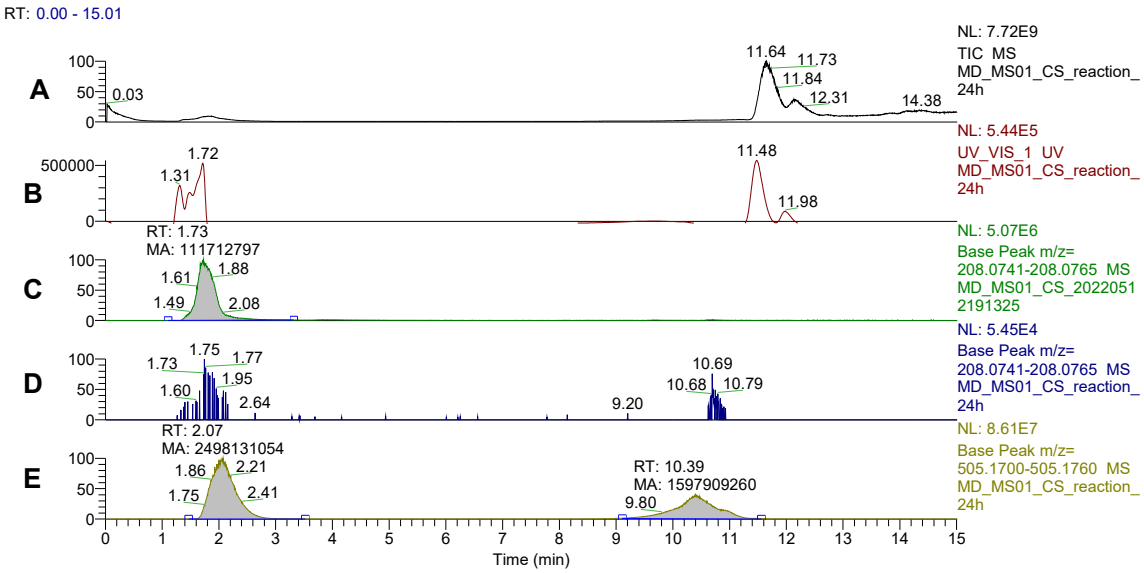

Figure S 28. LC-MS chromatograms of **Cys-Ser** conjugate **15** and **Cys-Ser** dipeptide. **A)** Reaction mixture TIC after 24 h; **B)** Reaction detection at 210 nm, after 24 h; **C)** Reaction t_0 – unreacted **Cys-Ser** EIC (base peak *m/z* 208.0753); **D)** Unreacted **Cys-Ser** EIC after 24 h reaction with 1.2 equiv. of **2**; **E) Cys-Ser** conjugate **15** EIC (base peak *m/z* 505.1730) after 24 h reaction. **Cys-Ser** conversion was calculated based on the EIC intensity (AUC) within δ 6ppm range.

Table S 5. Cys-Ser dipeptide conversion in 24 h reaction with coumarin NHS-activated acrylate **2** according to AUC from EIC chromatograms of base peak m/z 208.0753, within ð 6 ppm range.

	t_0	24 h	Conversion
Cys-Ser (AUC a.u.)	111712796.9	Not detected	>99%

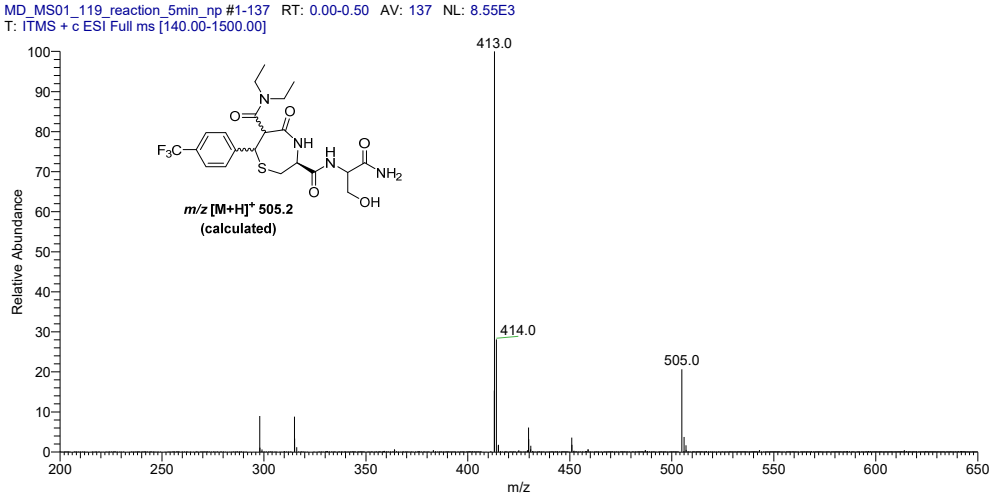

Figure S 29. ESI+-LRMS spectrum of reaction between **Cys-Ser** (calculated $C_6H_{13}N_2O_4S$ *m/z* $[M+H]^+$ 208.1, not found); 2,5-dioxopyrrolidin-1-yl-2-(diethylcarbamoyl)-3-(4-(trifluoromethyl)phenyl)acrylate **2** (calculated *m/z* $C_{19}H_{20}F_3N_2O_5$ [**2**+H]$^+$: 413.1, found 413.0), and the resulting product **15** (calculated for $C_{21}H_{27}F_3N_3O_6S$ [**15**+H]+: 505.2, found 505.0).

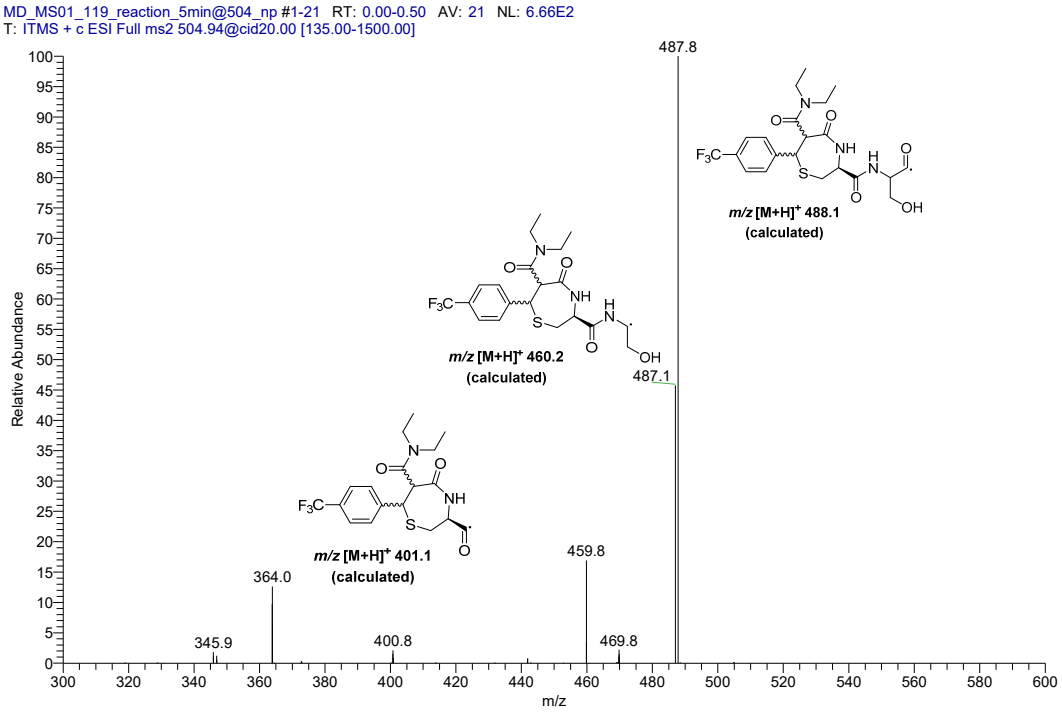

Figure S 30. MS fragmentation analysis of **15** at *m/z* 505.0: *m/z* 487.8 (calculated $C_{21}H_{25}F_3N_3O_5S$ $[M+H]^+$ 488.1), *m/z* 459.8 (calculated $C_{20}H_{25}F_3N_3O_4S$ $[M+H]^+$ 460.2) and, *m/z* 400.8 (calculated $C_{18}H_{20}F_3N_2O_3S$ $[M+H]^+$ 401.1) confirms 7 member ring product. Fragmentations of thioester and amide products were not found.

6.5. Cys-Thr

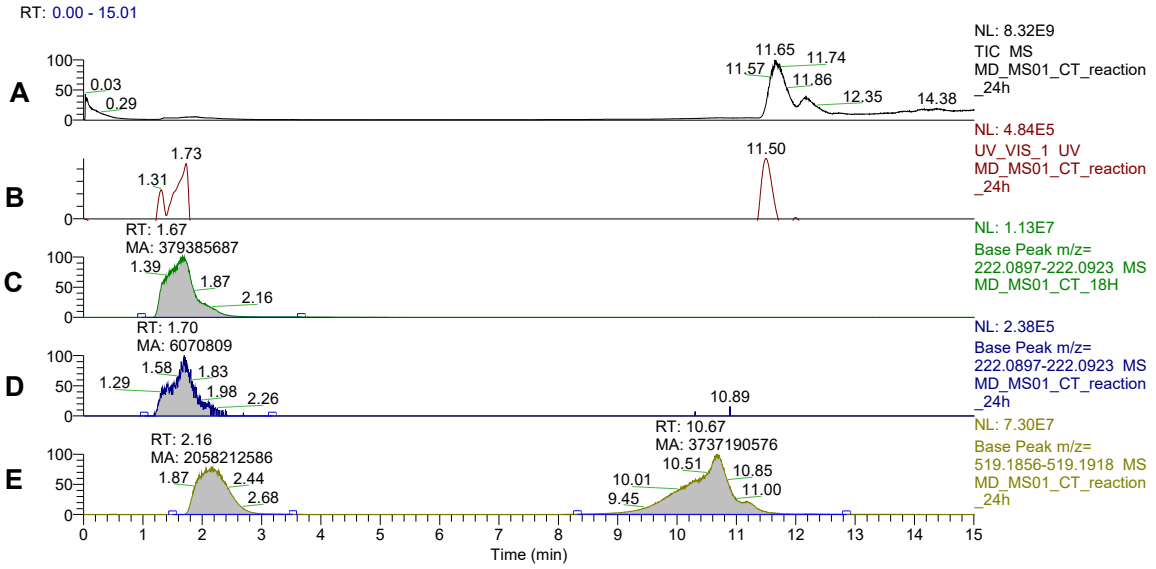

Figure S 31. LC-MS chromatograms of **Cys-Thr** conjugate **16** and **Cys-Thr** dipeptide. **A)** Reaction mixture TIC after 24 h; **B)** Reaction detection at 210 nm, after 24 h; **C)** Reaction t_0 – unreacted **Cys-Thr** EIC (base peak *m/z* 222.0910); **D)** Unreacted **Cys-Thr** EIC after 24 h reaction with 1.2 equiv. of **2**; **E) Cys-Thr** conjugate **16** EIC (base peak *m/z* 519.1887) after 24 h reaction. **Cys-Thr** conversion was calculated based on the EIC intensity (AUC) within δ 6ppm range.

Table S 6. Cys-Thr dipeptide conversion in 24 h reaction with coumarin NHS-activated acrylate **2** according to AUC from EIC chromatograms of base peak m/z 222.0910, within δ 6 ppm range.

	t_0	24 h	Conversion
Cys-Thr (AUC a.u.)	379385687.2	6070809	98%

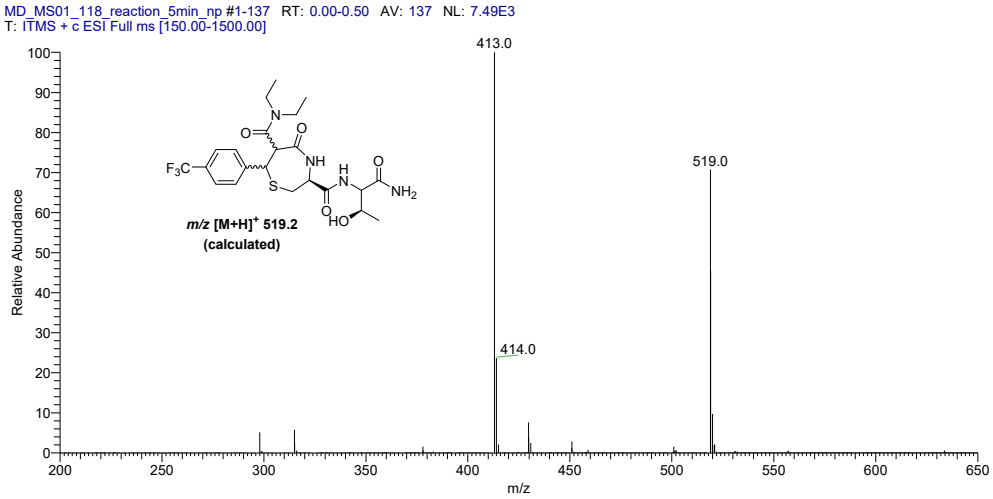

Figure S 32. ESI+-LRMS spectrum of reaction between **Cys-Thr** (calculated $C_7H_{15}N_2O_4S$ *m/z* $[M+H]^+$ 222.1, found 222.0, as a residual peak), 2,5-dioxopyrrolidin-1-yl-2-(diethylcarbamoyl)-3-(4-(trifluoromethyl)phenyl)acrylate **2** (calculated *m/z* $C_{19}H_{20}F_3N_2O_5$ [**2**+H]$^+$: 413.1, found 413.0), and the resulting product **16** (calculated for $C_{22}H_{28}F_3N_3O_6S$ [**16**+H]+: 519.2, found 519.0).

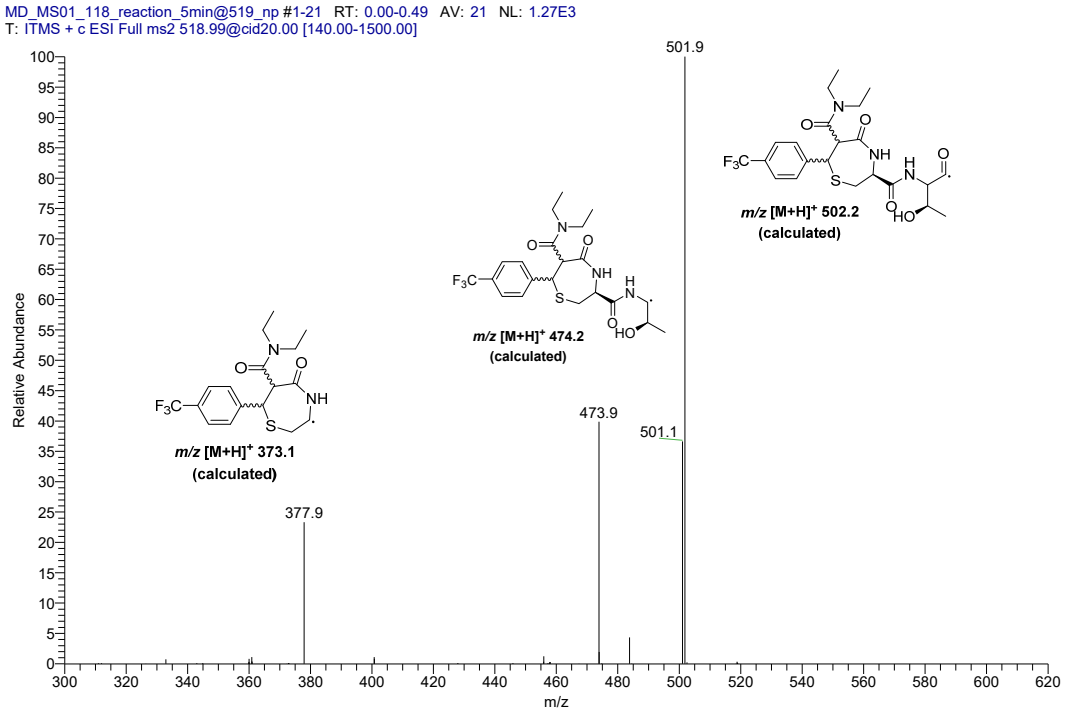

Figure S 33. MS fragmentation analysis of **16** at *m/z* 519.0: *m/z* 501.9 (calculated $C_{22}H_{27}F_3N_3O_5S$ $[M+H]^+$ 502.2), *m/z* 473.9 (calculated $C_{21}H_{27}F_3N_3O_4S$ $[M+H]^+$ 474.2) and, *m/z* 377.9 (calculated $C_{17}H_{20}F_3N_2O_2S$ $[M+H]^+$ 373.1) confirms 7 member ring product. Fragmentations of thioester and amide products were not found.

6.6. Cys-Glu

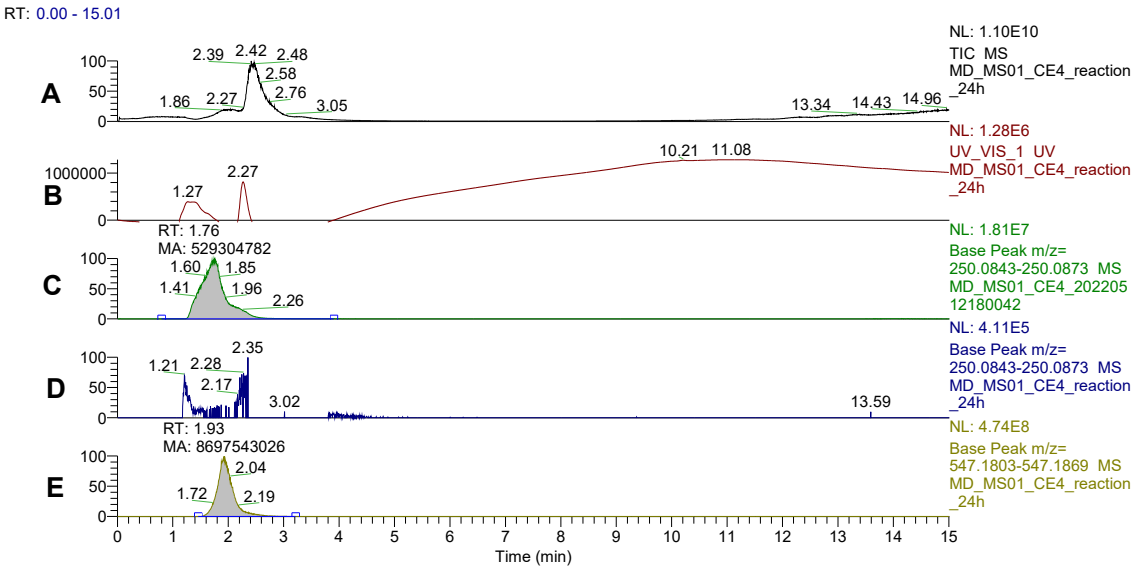

Figure S 34. LC-MS chromatograms of **Cys-Glu** conjugate **17** and **Cys-Glu** dipeptide. **A)** Reaction mixture TIC after 24 h; **B)** Reaction detection at 210 nm, after 24 h; **C)** Reaction t_0 – unreacted **Cys-Glu** EIC (base peak *m/z* 250.0858); **D)** Unreacted **Cys-Glu** EIC after 24 h reaction with 1.2 equiv. of **2**; **E) Cys-Glu** conjugate **17** EIC (base peak *m/z* 547.1836) after 24 h reaction. **Cys-Glu** conversion was calculated based on the EIC intensity (AUC) within δ 6ppm range.

Table S 7. Cys-Glu dipeptide conversion in 24 h reaction with coumarin NHS-activated acrylate **2** according to AUC from EIC chromatograms of base peak m/z 250.0858, within ð 6 ppm range.

	t_0	24 h	Conversion
Cys-Glu (AUC a.u.)	529304781.6	Not detected	>99%

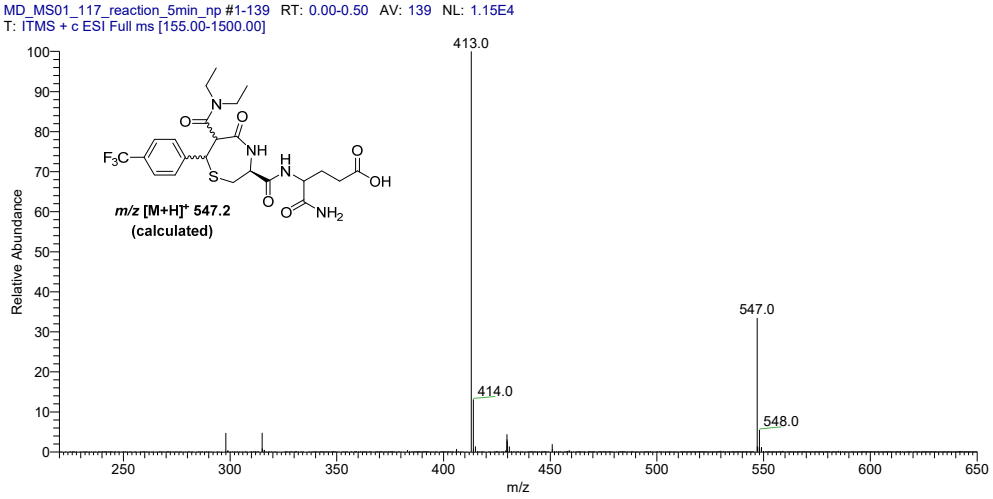

Figure S 35. ESI+-LRMS spectrum of reaction between **Cys-Glu** (calculated $C_8H_{15}N_2O_5S$ *m/z* $[M+H]^+$ 250.1, found 249.9, as a residual peak), 2,5-dioxopyrrolidin-1-yl-2-(diethylcarbamoyl)-3-(4-(trifluoromethyl)phenyl)acrylate **2** (calculated *m/z* $C_{19}H_{20}F_3N_2O_5$ [**2**+H]$^+$: 413.1, found 413.0), and the resulting product **17** (calculated for $C_{23}H_{28}F_3N_3O_7S$ [**17**+H]+: 547.2, found 547.0).

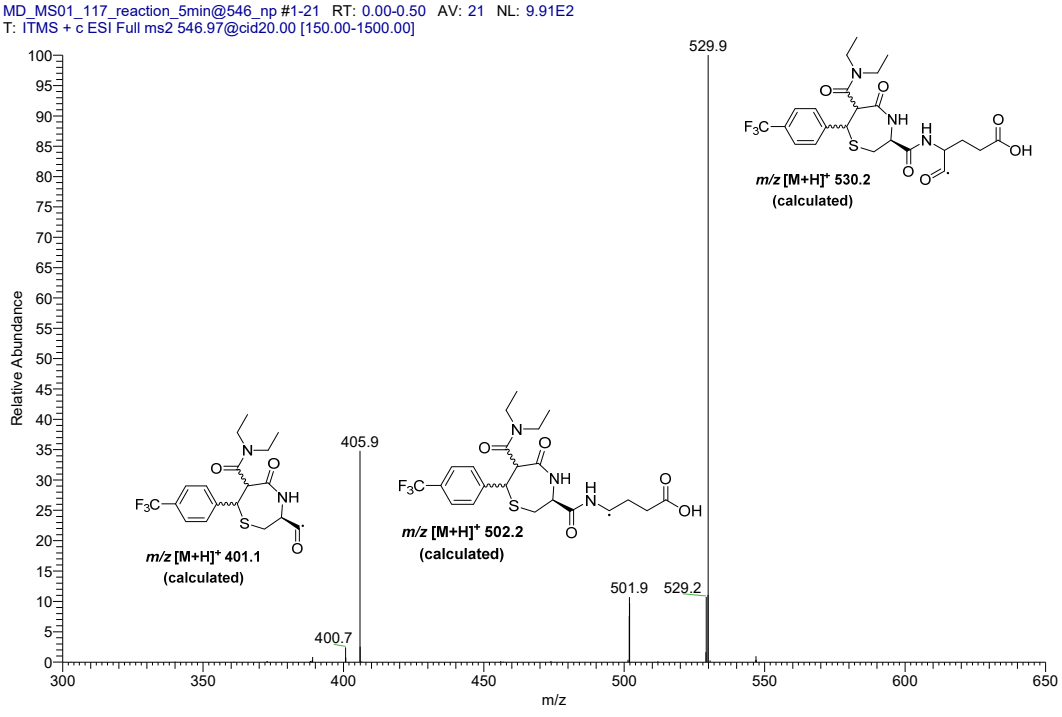

Figure S 36. MS fragmentation analysis of **17** at *m/z* 547.0: *m/z* 529.9 (calculated $C_{23}H_{27}F_3N_3O_6S$ $[M+H]^+$ 530.2), *m/z* 501.9 (calculated $C_{22}H_{27}F_3N_3O_5S$ $[M+H]^+$ 502.2) and, *m/z* 405.9 (calculated $C_{18}H_{20}F_3N_2O_3S$ $[M+H]^+$ 401.1) confirms 7 member ring product. Fragmentations of thioester and amide products were not found.

6.7. Cys-Tyr

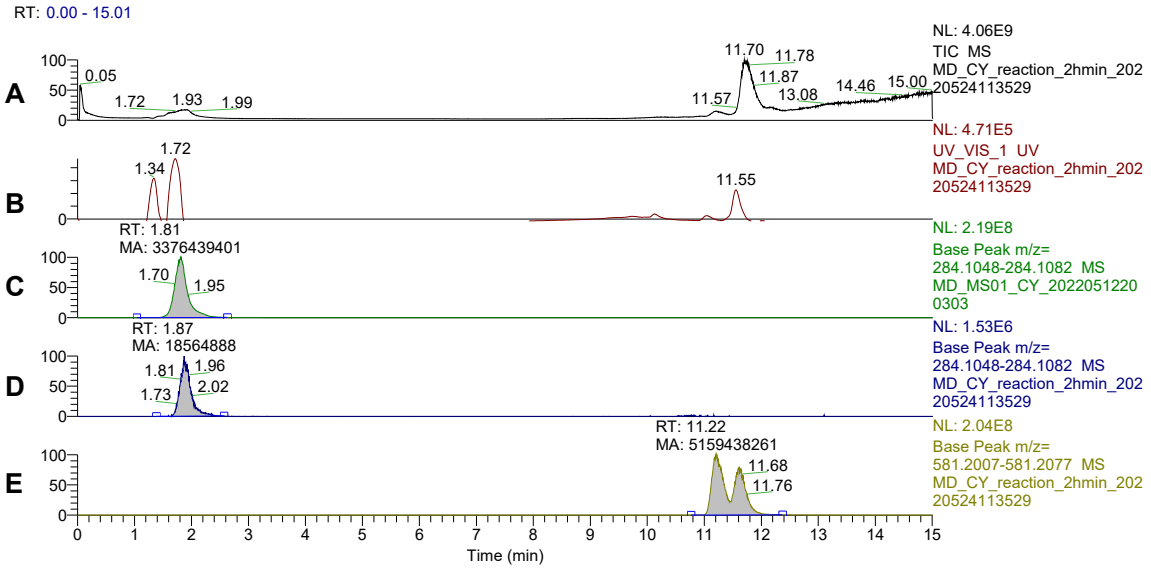

Figure S 37. LC-MS chromatograms of **Cys-Tyr** conjugate **18** and **Cys-Tyr** dipeptide. **A)** Reaction mixture TIC after 24 h; **B)** Reaction detection at 210 nm, after 24 h; **C)** Reaction t_0 – unreacted **Cys-Tyr** EIC (base peak *m/z* 284.1065); **D)** Unreacted **Cys-Tyr** EIC after 24 h reaction with 1.2 equiv. of **2**; **E) Cys-Tyr** conjugate **18** EIC (base peak *m/z* 581.2042) after 24 h reaction. **Cys-Tyr** conversion was calculated based on the EIC intensity (AUC) within δ 6ppm range.

Table S 8. Cys-Tyr dipeptide conversion in 24 h reaction with coumarin NHS-activated acrylate **2** according to AUC from EIC chromatograms of base peak m/z 284.1065, within δ 6 ppm range.

	t_0	24 h	Conversion
Cys-Tyr (AUC a.u.)	3376439401	18564887	>99%

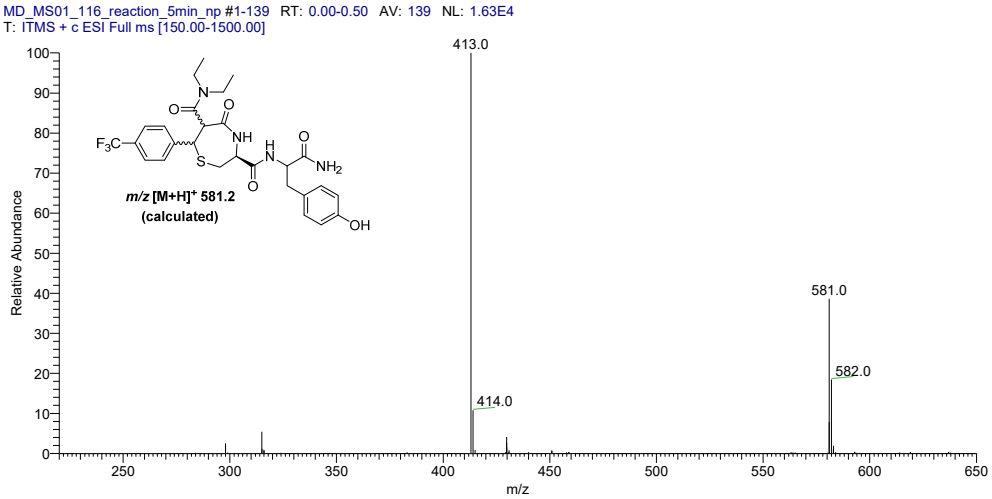

Figure S 38. ESI⁺-LRMS spectrum of reaction between **Cys-Tyr** (calculated $C_{12}H_{17}N_2O_4S$ *m/z* $[M+H]^+$ 284.1, found 284.0, as a residual peak), 2,5-dioxopyrrolidin-1-yl-2-(diethylcarbamoyl)-3-(4-(trifluoromethyl)phenyl)acrylate **2** (calculated *m/z* $C_{19}H_{20}F_3N_2O_5$ [**2**+H]$^+$: 413.1, found 413.0), and the resulting product **18** (calculated for $C_{27}H_{30}F_3N_3O_6S$ [**18**+H]+: 581.2, found 581.0).

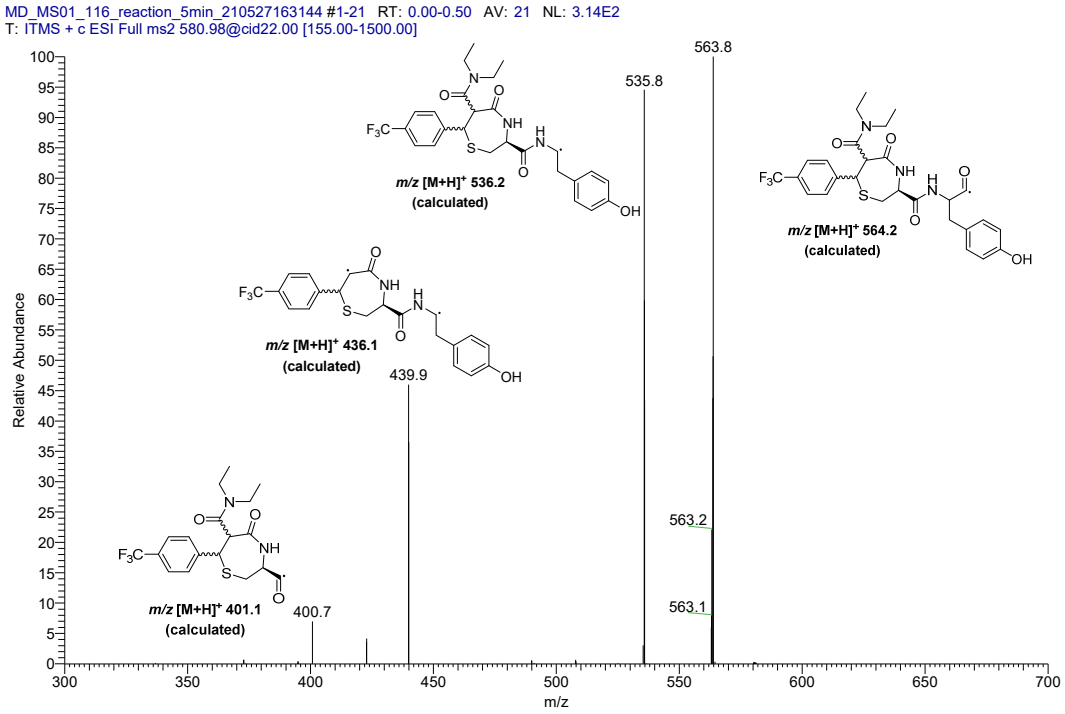

Figure S 39. MS fragmentation analysis of **18** at *m/z* 581.0: *m/z* 563.8 (calculated $C_{27}H_{29}F_3N_3O_4S$ $[M+H]^+$ 564.2), *m/z* 535.8 (calculated $C_{26}H_{29}F_3N_3O_4S$ $[M+H]^+$ 536.2), *m/z* 439.9 (calculated $C_{21}H_{19}F_3N_2O_3S$ $[M+H]^+$ 436.1) and, *m/z* 400.7 (calculated $C_{18}H_{20}F_3N_2O_3S$ $[M+H]^+$ 401.1) confirms 7 member ring product. Fragmentations of thioester and amide products were not found.

6.8. Cys-Ala

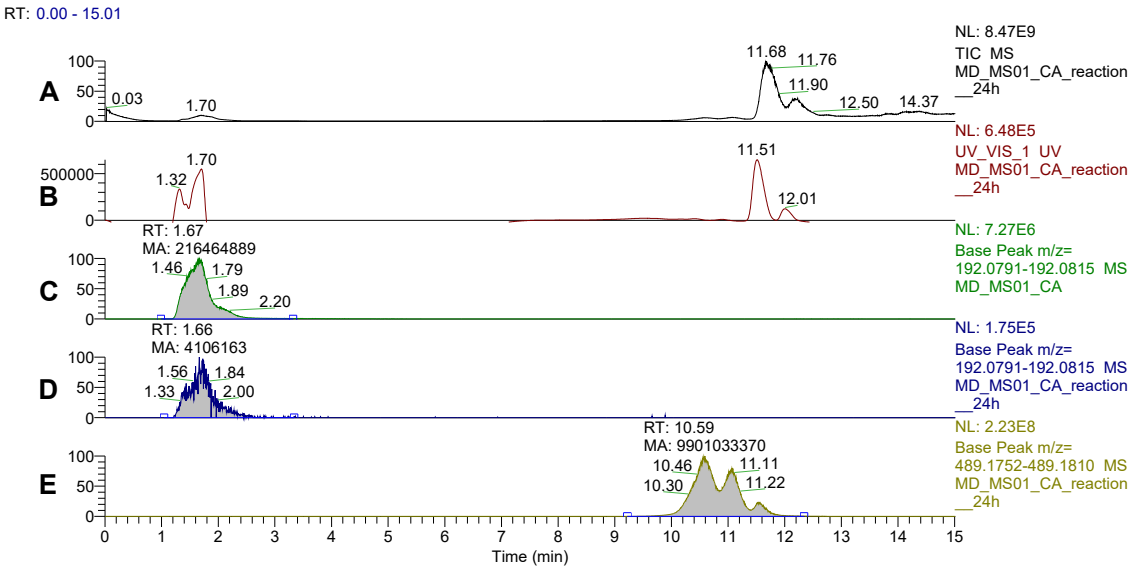

Figure S 40. LC-MS chromatograms of **Cys-Ala** conjugate **19** and **Cys-Ala** dipeptide. **A)** Reaction mixture TIC after 24 h; **B)** Reaction detection at 210 nm, after 24 h; **C)** Reaction t_0 – unreacted **Cys-Ala** EIC (base peak *m/z* 192.0803); **D)** Unreacted **Cys-Ala** EIC after 24 h reaction with 1.2 equiv. of **2**; **E) Cys-Ala** conjugate **19** EIC (base peak *m/z* 489.1781) after 24 h reaction. **Cys-Ala** conversion was calculated based on the EIC intensity (AUC) within δ 6ppm range.

Table S 9. Cys-Ala dipeptide conversion in 24 h reaction with coumarin NHS-activated acrylate **2** according to AUC from EIC chromatograms of base peak m/z 192.0803, within ð 6 ppm range.

	t_0	24 h	Conversion
Cys-Ala (AUC a.u.)	216464889.1	4106163	98%

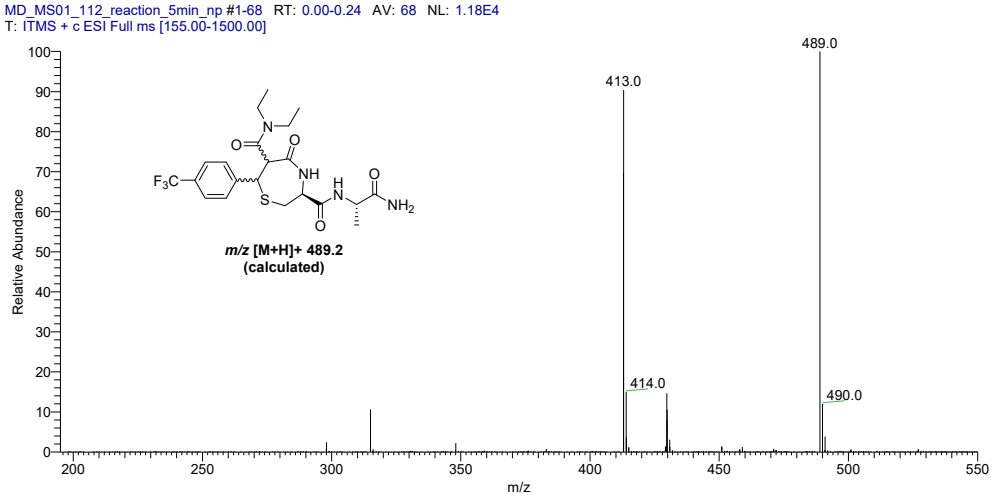

Figure S 41. ESI+-LRMS spectrum of reaction between **Cys-Ala** (calculated *m/z* $[M+H]^+$ 192.1, found 192.0, as a residual peak), 2,5-dioxopyrrolidin-1-yl-2-(diethylcarbamoyl)-3-(4-(trifluoromethyl)phenyl)acrylate **2** (calculated *m/z* $C_{19}H_{20}F_3N_2O_5$ [**2**+H]$^+$: 413.1, found 413.0), and the resulting product **19** (calculated for $C_{21}H_{27}F_3N_4O_4S$ [**19**+H]$^+$: 489.2, found 489.0).

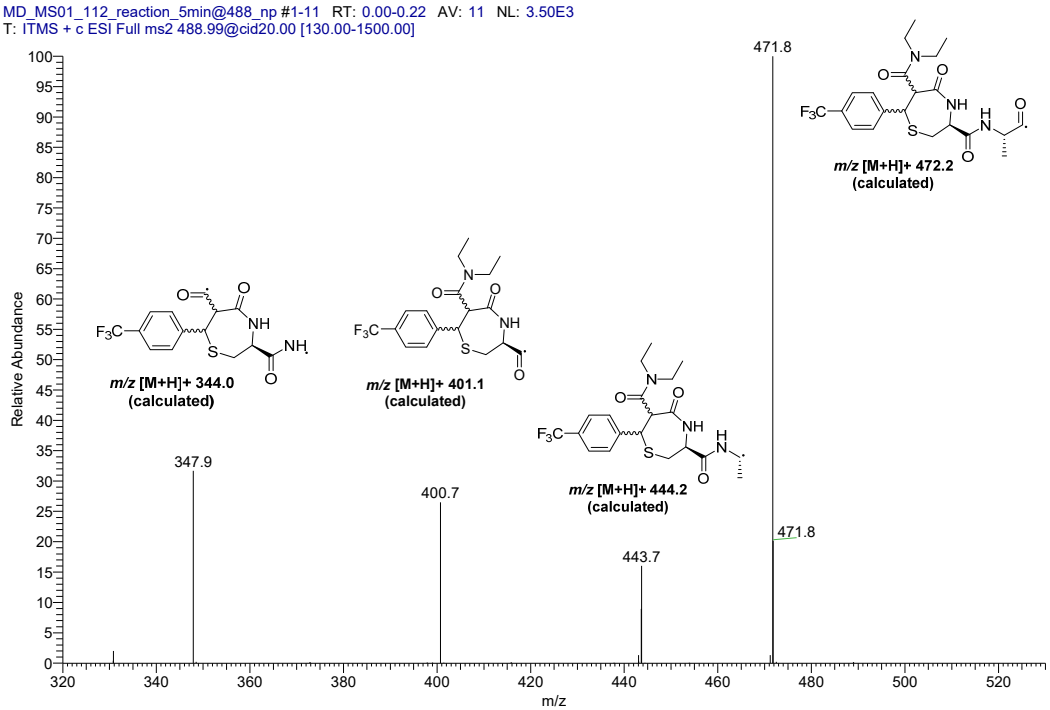

Figure S 42. MS fragmentation analysis of **19** at *m/z* 489.0: *m/z* 471.8 (calculated $C_{21}H_{25}F_3N_3O_4S$ $[M+H]^+$ 472.2), *m/z* 400.7 (calculated $C_{18}H_{20}F_3N_2O_3S$ $[M+H]^+$ 401.1) *m/z* 443.7 (calculated $C_{20}H_{25}F_3N_3O_3S$ $[M+H]^+$ 444.2) and, *m/z*

347.9 (calculated $C_{14}H_{11}F_3N_2O_3S$ $[M+H]^+$ 344.0) confirms 7 member ring product. Fragmentations of thioester and amide products were not found.

6.9. Cys-Leu

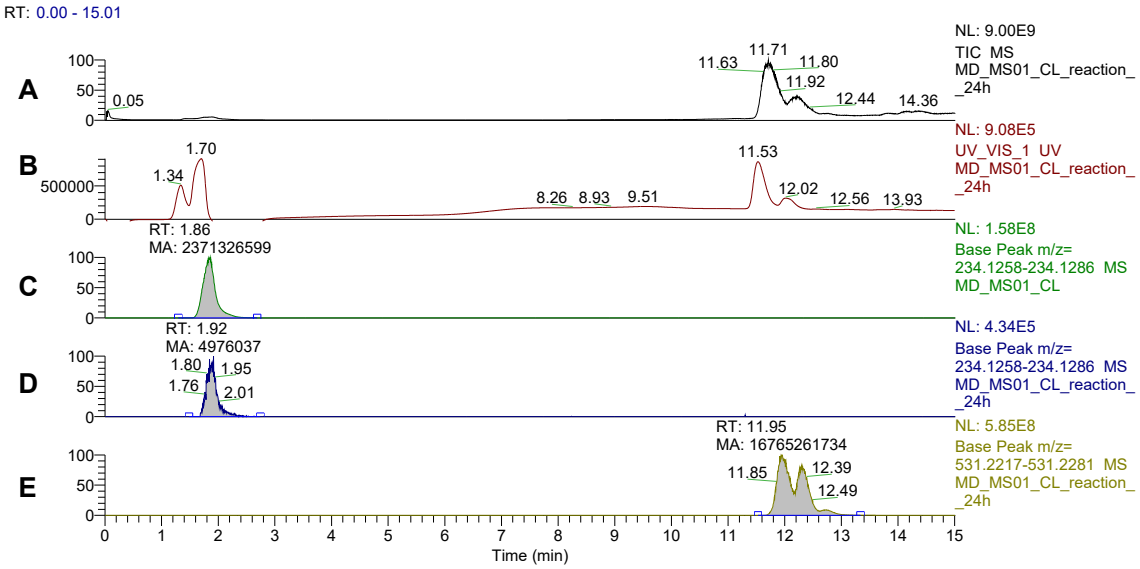

Figure S 43. LC-MS chromatograms of **Cys-Leu** conjugate **20** and **Cys-Leu** dipeptide. **A)** Reaction mixture TIC after 24 h; **B)** Reaction detection at 210 nm, after 24 h; **C)** Reaction t_0 – unreacted **Cys-Leu** EIC (base peak *m/z* 234.1272); **D)** Unreacted **Cys-Leu** EIC after 24 h reaction with 1.2 equiv. of **2**; **E) Cys-Leu** conjugate **20** EIC (base peak *m/z* 531.2249) after 24 h reaction. **Cys-Leu** conversion was calculated based on the EIC intensity (AUC) within δ 6ppm range.

Table S 10. Cys-Leu dipeptide conversion in 24 h reaction with coumarin NHS-activated acrylate **2** according to AUC from EIC chromatograms of base peak m/z 234.1272, within δ 6 ppm range.

	t_0	24 h	Conversion
Cys-Leu (AUC a.u.)	2371326599	4976036	>99%

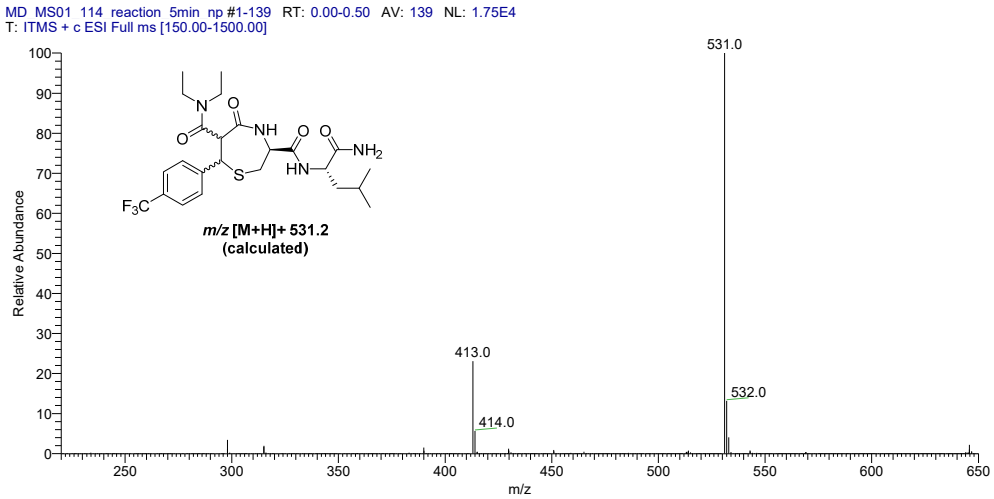

Figure S 44. ESI$^+$-LRMS spectrum of reaction between **Cys-Leu** (calculated $C_9H_{19}N_2O_3S$ *m/z* $[M+H]^+$ 234.1, found 233.9, as a residual peak), 2,5-dioxopyrrolidin-1-yl-2-(diethylcarbamoyl)-3-(4-(trifluoromethyl)phenyl)acrylate **2**

(calculated *m/z* $C_{19}H_{20}F_3N_2O_5$ [**2**+H]$^+$: 413.1, found 413.0), and the resulting product **20** (calculated for $C_{24}H_{32}F_3N_5O_5S$ [**20**+H]+: 531.2, found 531.0).

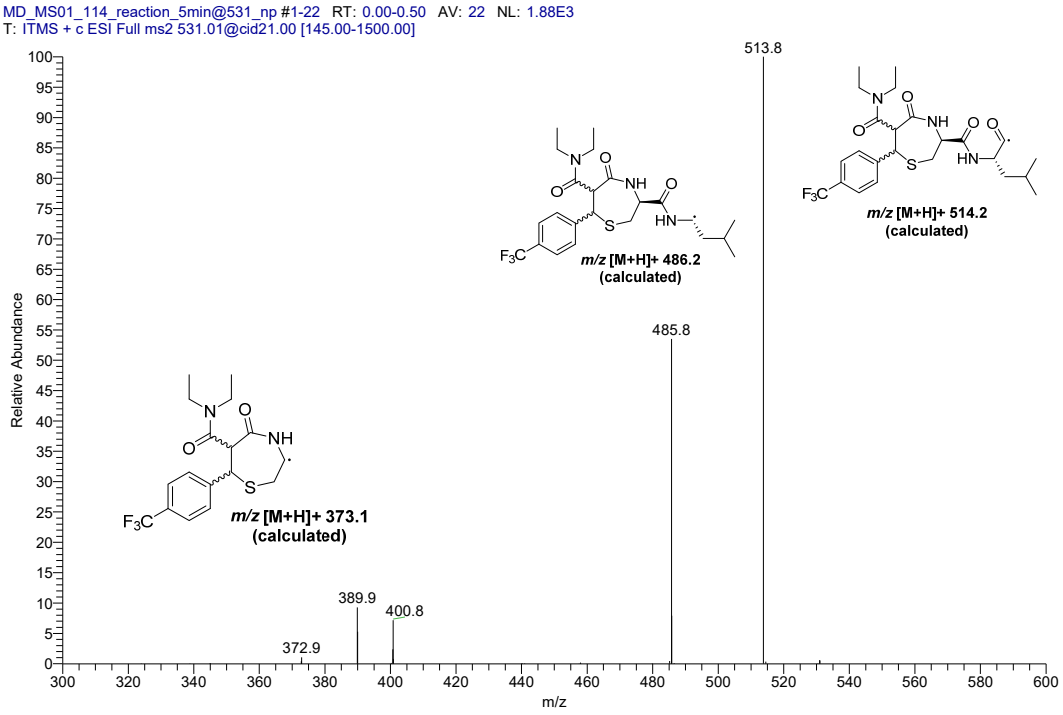

Figure S 45. MS fragmentation analysis of **20** at *m/z* 531.0: *m/z* 513.8 (calculated $C_{24}H_{31}F_3N_3O_4S$ [M+H]$^+$ 514.2), *m/z* 485.8 (calculated $C_{23}H_{31}F_3N_3O_3S$ [M+H]$^+$ 486.2) and, *m/z* 372.9 (calculated $C_{17}H_{20}F_3N_2O_2S$ [M+H]$^+$ 373.1) confirms 7 member ring product. Fragmentations of thioester and amide products were not found.

7. Procedure for the competition assay Cys versus Lys reaction with NHS-activated acrylate 2

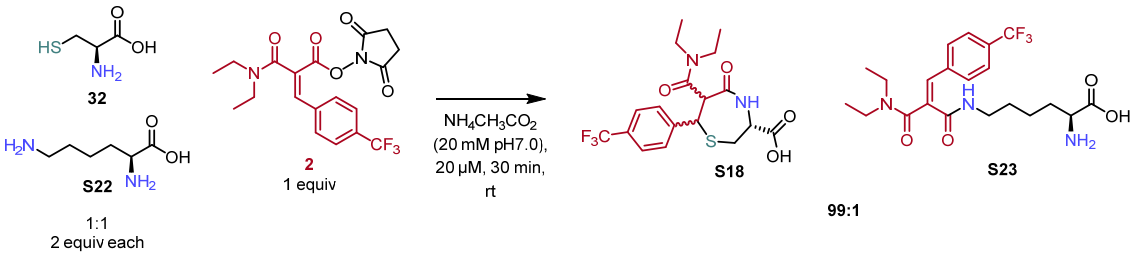

To a solution of *L*-cysteine **32** (10 mM in ammonium acetate 20 mM, pH 7.0) (4 µL, 0.040 µmol) and *L*-lysine hydrate **S22** (10 mM in ammonium acetate 20 mM, pH 7.0) (4 µL, 0.040 µmol) in Ammonium acetate 20 mM, pH 7.0 (1 mL) was added 2,5-dioxopyrrolidin-1-yl-2-(diethylcarbamoyl)-3-(4-(trifluoromethyl)phenyl)acrylate **2** (10 mM in ACN) (2.0 µL, 0.020 µmol). The mass was checked by LC-HRMS after 30 min and 2 h in Positive Mode. The HPLC runs were carried out with a gradient of A (Milli Q water containing 0.1% v/v Formic acid, FA) and B (acetonitrile containing 0.1% v/v FA, Honeywell HPLC-grade). The mobile

phase was t=1 min, 5% B; t=10 min, 95.5% B; t=11 min, 95.5% B; t=12 min, 5% B; t=15 min stop, at a flow rate of 0.2 mL/min, detection at 254 nm.

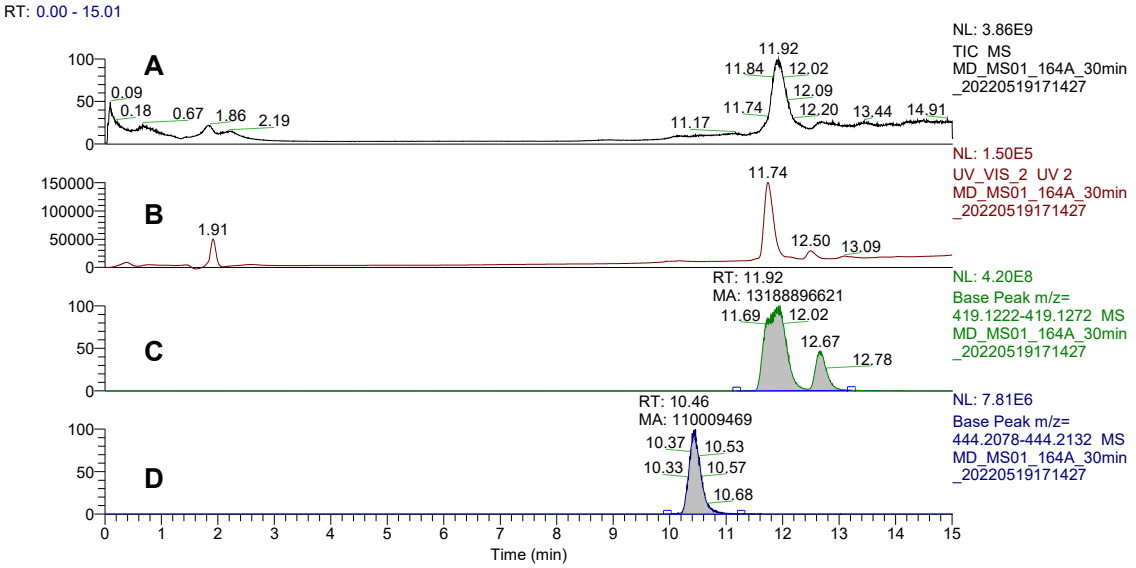

Figure S 46. LC-MS chromatograms of products resulting from competition assays Cys **30** *vs* Lys **S22**. **A)** Reaction mixture TIC after 30 min; **B)** Reaction detection at 254 nm, after 30 min; **C)** 1,4-thiazepan-5-one **S18** base peak *m/z* 419.1242; **D)** Lys amidation product **S23** base peak *m/z* 444.2102. The products ratio was calculated using the EIC integration area of each specie and converted to percentage to afford a 99:1 AUC ratio (1,4-thiazepan-5-one **S18** vs Lys amidation product **S23**).

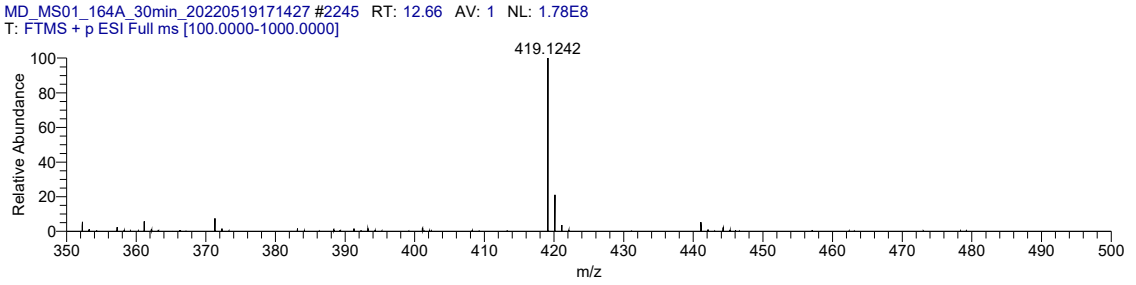

Figure S 47. ESI$^+$-HRMS spectrum of 1,4-thiazepan-5-one **S18** (*m/z* 419.1242 [M+H]$^+$) (from EIC peak at RT 12.66 min).

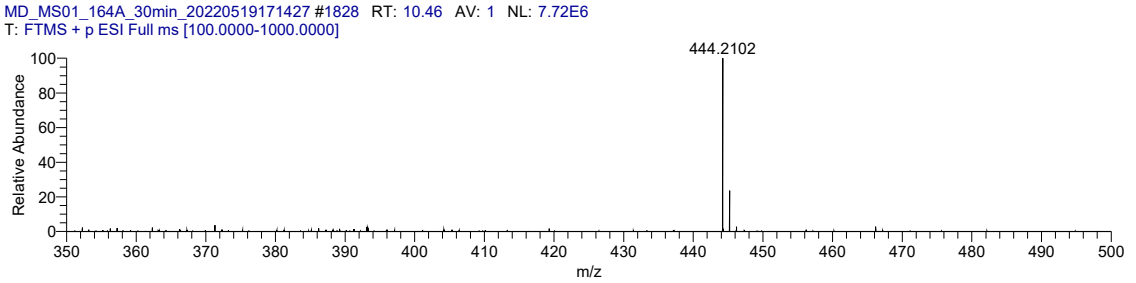

Figure S 48. ESI$^+$-HRMS spectrum of Lys amidation product **S23** (*m/z* 444.2102 [M+H]$^+$) (from EIC peak at RT 10.46 min).

8. General procedure for the ESI-MS assays with Laminin

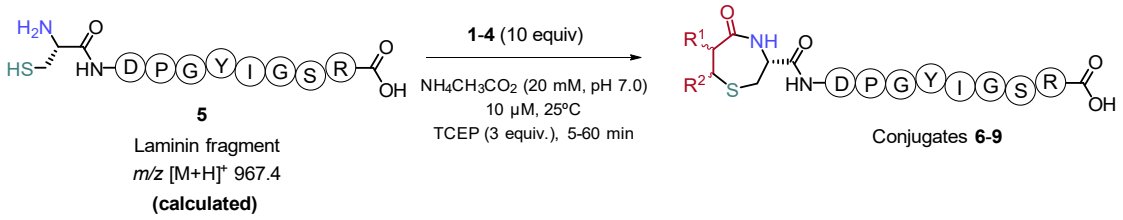

To a solution of Laminin fragment **5** (925-933) (1 mg/mL in water, 0.925 mM) (10 µL, 9.3 nmol) in ammonium acetate 20 mM, pH 7.0 (925 µL) was added 3 equiv. of 3,3',3''-phosphanetriyltripropionic acid hydrochloride (TCEP 1.0 mg/mL in water 3.5 mM) (7.93 µL, 28 nmol) and the mixture was reacted at RT (25ºC) for approximately 1h. Afterwards, 10 equiv. of reagents **1–4** (30 mM in ACN) (3.08 µL, 93 nmol) were added and the reaction was monitored in Positive Mode of ESI-MS after 5 min, 60 min and 1 day. MS fragmentation peaks correspondent to the expected product *m/z* resulted in the same profile to afford a daughter peak of *m/z* 749.2. This fragment confirms that Laminin modification occurs at the *N*-terminal Cys.

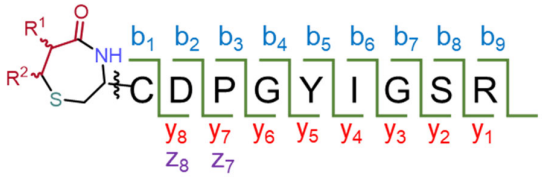

Figure S 49. MS fragmentation of modified laminin **6–9** afforded the fragment in Asp-Pro peptidic bond y_7 as the most intense peak. Fragment z_8 was also observed for conjugates **6–9** and, fragment y_8 was observed for conjugates **6** and **9**, indicating that conjugation was being attained at the *N*-terminal cysteine.

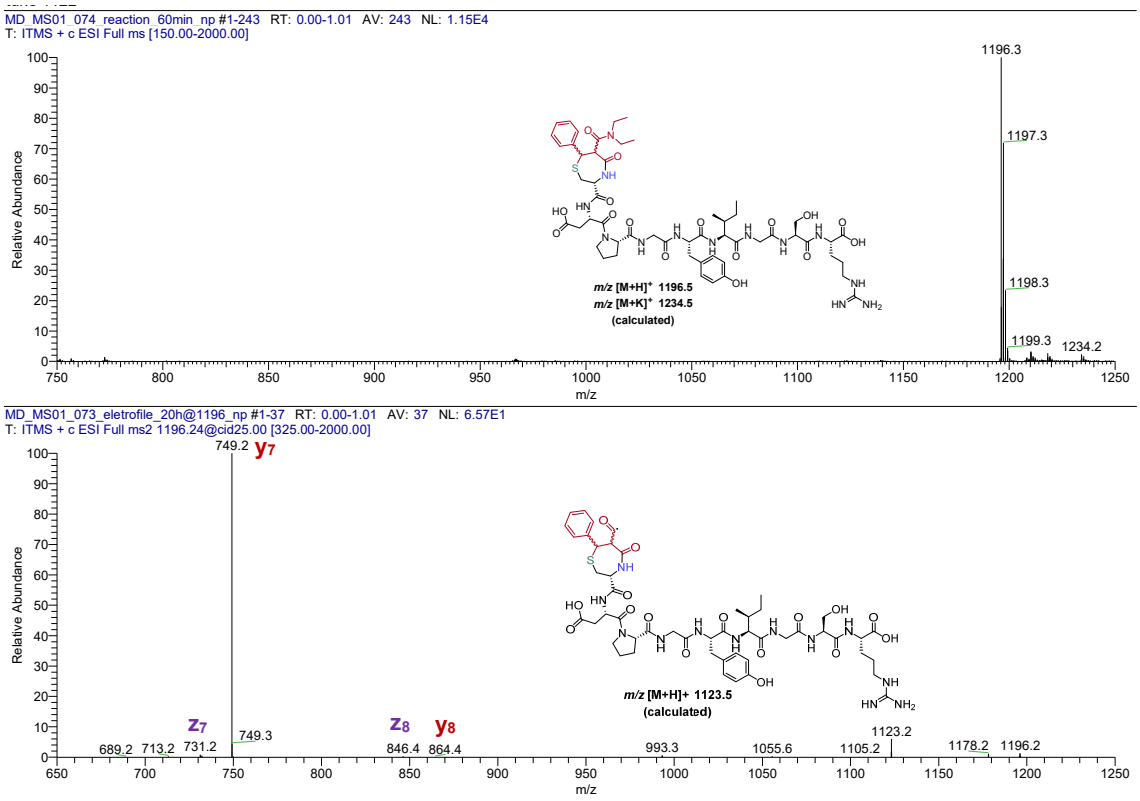

Figure S 50. ESI$^+$-MS spectrum of product **6** obtained from the conjugation of laminin peptide with NHS-activated acrylic derivative **1** with *m/z* [Mconj**6**+H]$^+$ 1196.3, *m/z* [Mconj**6**+K]$^+$ 1234.2 (above); MS fragmentation spectrum of *m/z* [Mconj**6**+H]$^+$ 1196.3 (below), resulting in Asp-Pro fragments *m/z* 731.2 (z_7) and *m/z* 749.2 (y_7), Cys-Asp fragments *m/z* 846.4 (z_8) and *m/z* 864.4 (y_8), *m/z* 1123.2 (calculated $C_{50}H_{67}N_{12}O_{16}S$ [M+H]$^+$ 1123.5) fragment.

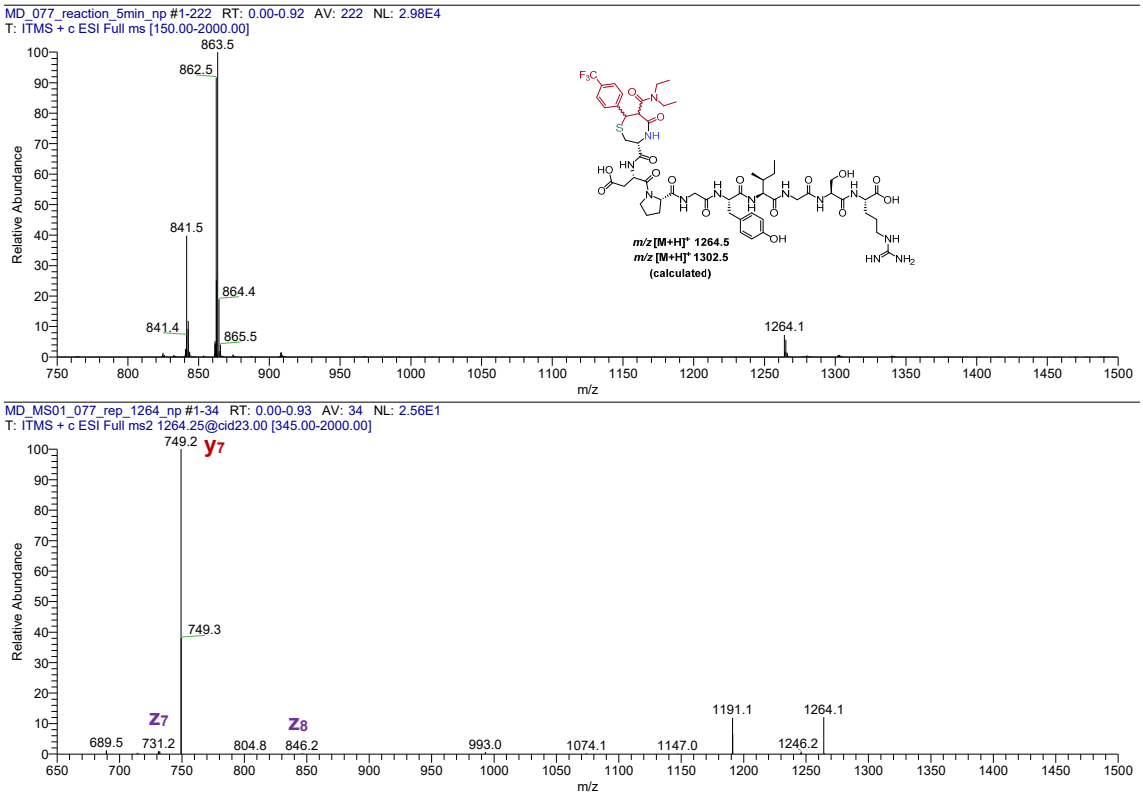

Figure S 51. ESI$^+$-MS spectrum of product **7** obtained from the conjugation of laminin peptide with NHS-activated acrylic derivative **2** with *m/z* [Mconj**7**+H]$^+$ 1264.1, *m/z* [Mconj**7**+K]$^+$ 1302.1 (above); MS fragmentation spectrum of *m/z* [Mconj**7**+H]$^+$ 1264.1 (below), resulting in Asp-Pro fragments *m/z* 731.2 (z_7) and *m/z* 749.2 (y_7), Cys-Asp fragments *m/z* 846.2 (z_8). Note that *m/z* 862.5 corresponds to [2M**2**+K$^+$]$^+$.

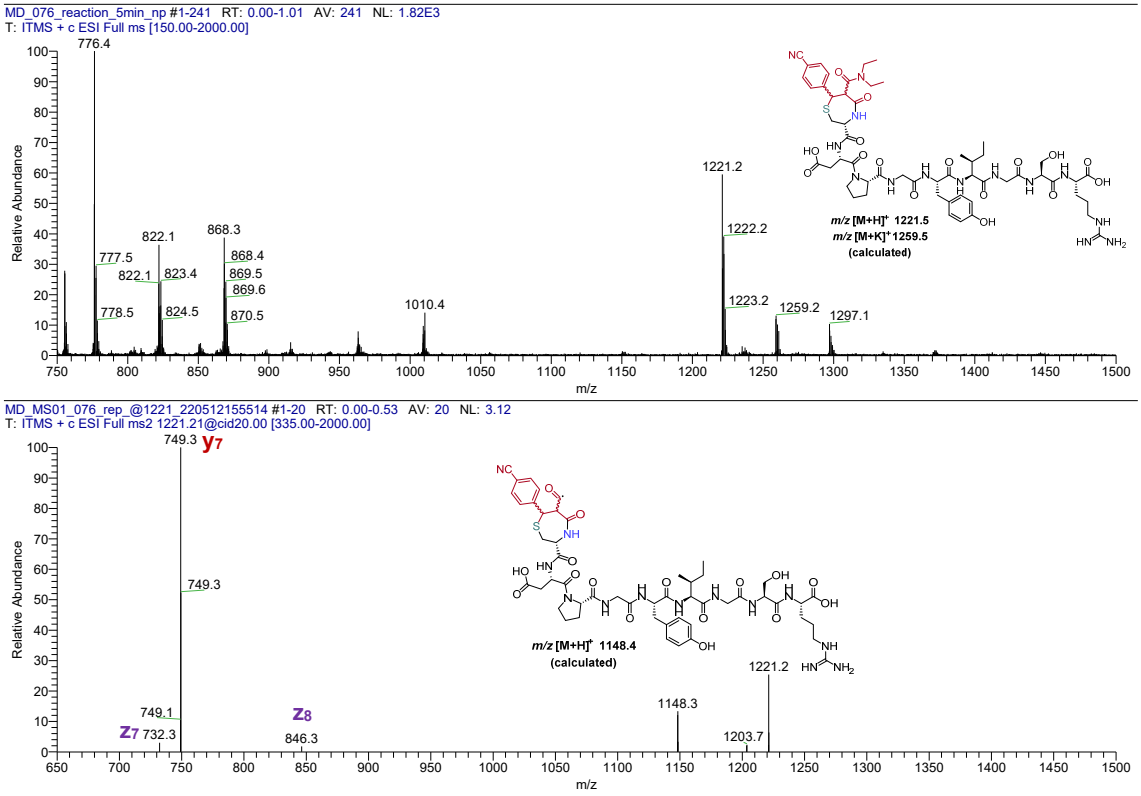

Figure S 52. ESI$^+$-MS spectrum of product **8** obtained from the conjugation of laminin peptide with NHS-activated acrylic derivative **3** with *m/z* [Mconj**8**+H]$^+$ 1221.2, *m/z* [Mconj**8**+K]$^+$ 1259.2 (above); MS fragmentation spectrum of *m/z* [Mconj**8**+H]$^+$ 1221.2 (below), resulting in Asp-Pro fragments *m/z* 732.3 (z_7) and *m/z* 749.3 (y_7), Cys-Asp fragments *m/z* 846.3 (z_8), *m/z* 1148.3 (calculated $C_{51}H_{66}N_{13}O_{16}S$ [M+H]$^+$ 1148.4) fragment. Note that *m/z* 776.4 corresponds to [2M**3**+K$^+$]$^+$.

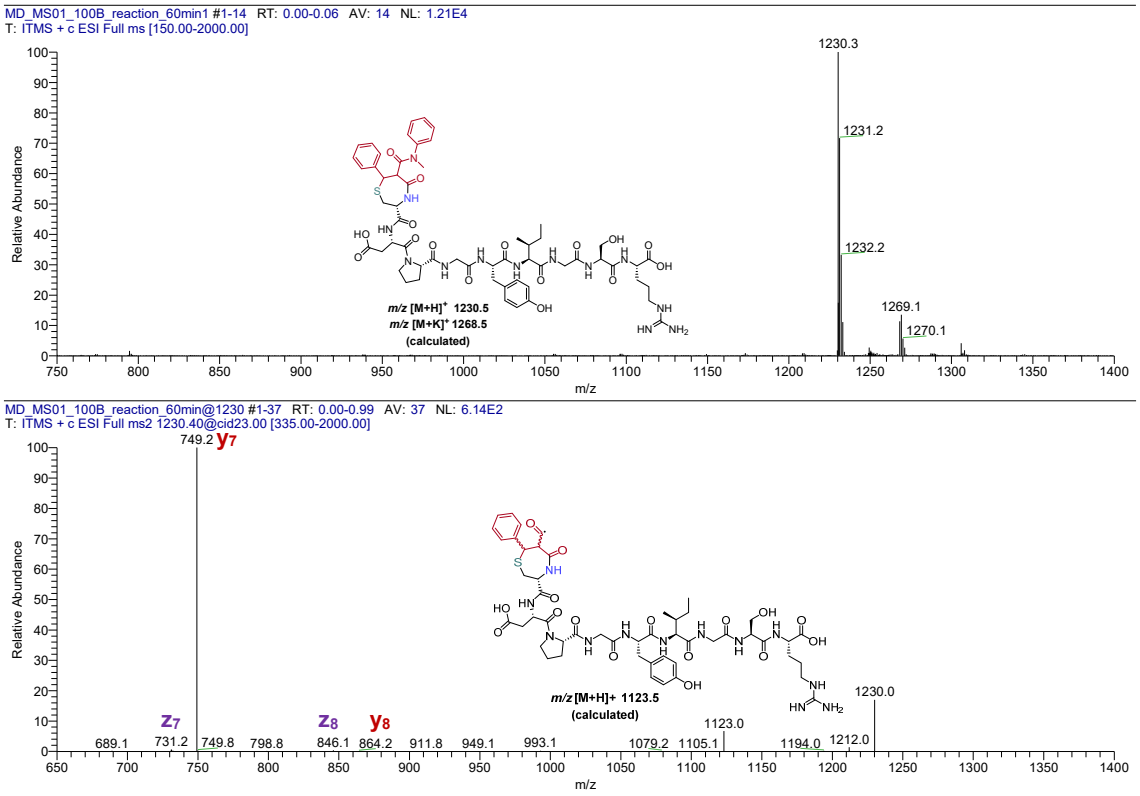

Figure S 53. ESI$^+$-MS spectrum of product **9** obtained from the conjugation of laminin peptide with NHS-activated acrylic derivative **4** with *m/z* [Mconj**9**+H]$^+$ 1230.3, *m/z* [Mconj**9**+K]$^+$ 1269.1 (above); MS fragmentation spectrum of *m/z* [Mconj**9**+H]$^+$ 1230.3 (below) resulting in Asp-Pro fragment *m/z* 731.2 (z_7) and *m/z* 749.2 (y_7), Cys-Asp fragments *m/z* 846.1 (z_8) and *m/z* 864.2 (y_8), *m/z* 1123.1 (calculated $C_{50}H_{67}N_{12}O_{16}S$ [M+H]$^+$ 1123.5) fragment.

9. General procedure for the ESI-MS assays with *C*-Ovalbumin

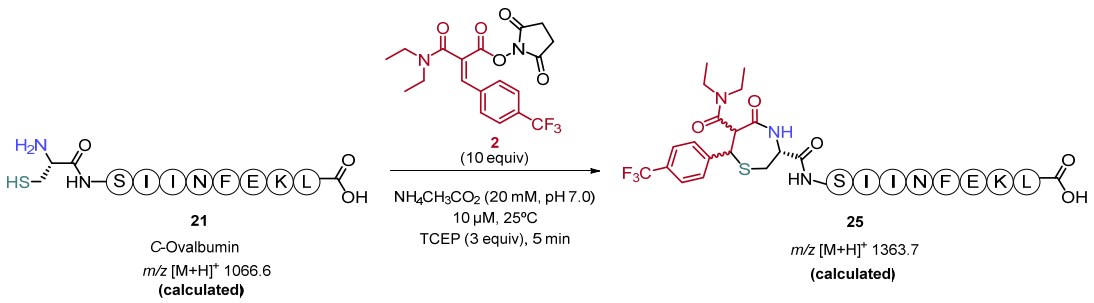

To a solution of *C*-Ovalbumin **21** (1 mg/938 µL in water, 1 mM) (10.0 µL, 10.0 nmol) in ammonium acetate 20 mM, pH 7.0 (1 mL) were added 3 equiv. of 3,3',3''-phosphanetriyltripropionic acid hydrochloride (TCEP 1.0 mg/mL in water 3.5 mM) (8.57 µL, 0.030 µmol) and the mixture was reacted at RT (25ºC) for approximately 1h. Afterwards, 10 equiv. of 2,5-dioxopyrrolidin-1-yl-2-(diethylcarbamoyl)-3-(4-(trifluoromethyl)phenyl)acrylate **2** (30 mM in ACN) (3.33 µL, 0.100 µmol) was added and the reaction was monitored in Positive Mode of ESI-MS at 5 min, 60 min, and 24 h, indicating its stability for at least 1 day.

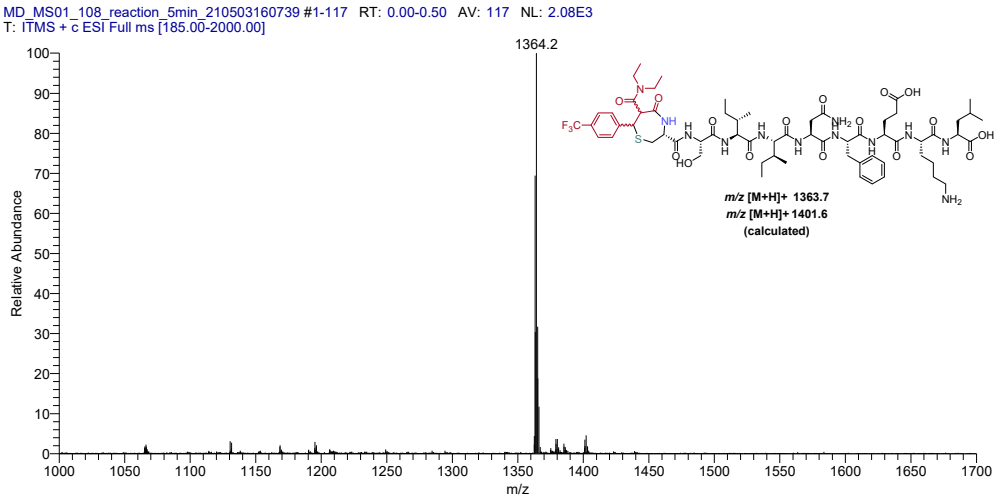

Figure S 54. ESI$^+$-MS spectrum of *C*-Ovalbumin **21** reaction with 10 equiv. of 2,5-dioxopyrrolidin-1-yl-2-(diethylcarbamoyl)-3-(4-(trifluoromethyl)phenyl)acrylate **2** in ammonium acetate 20 mM pH 7.0, at 5 min reaction time. The observed peaks correspond to conjugate **25** *m/z* 1364.2 [Mconj**25**+H]$^+$, *m/z* 1401.1 [Mconj**25**+K]$^+$.

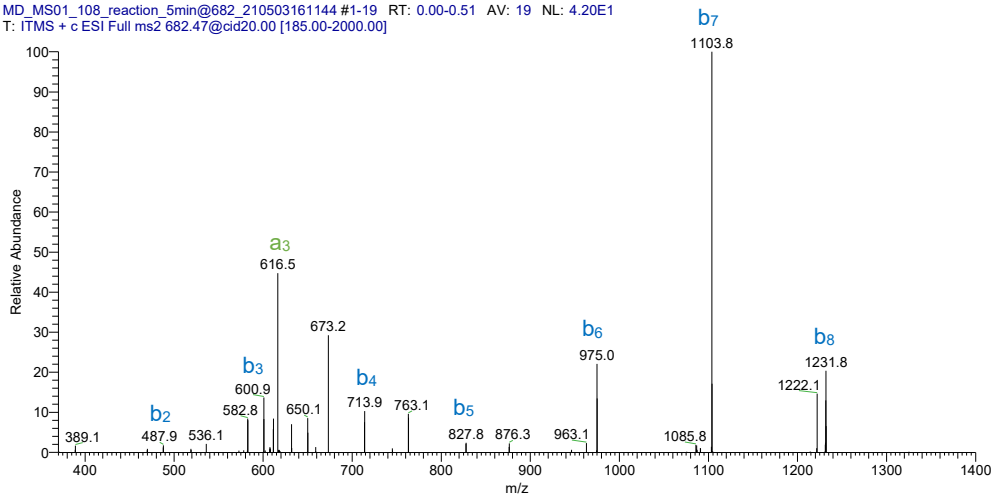

Figure S 55. MS/MS fragmentations of conjugate **25** *m/z* 1364.2 [Mconj**24**+H]$^+$ peak. Reaction conditions: *C*-ovalbumin **21** (10.0 nmol) in ammonium acetate 20 mM, pH 7.0, 10 equiv. of 2,5-dioxopyrrolidin-1-yl-2-(diethylcarbamoyl)-3-(4-(trifluoromethyl)phenyl)acrylate **2** after 5 min reaction.

Table S 11. List of fragments from MS/MS fragmentations of conjugate **25** *m/z* 1364.2 peak.

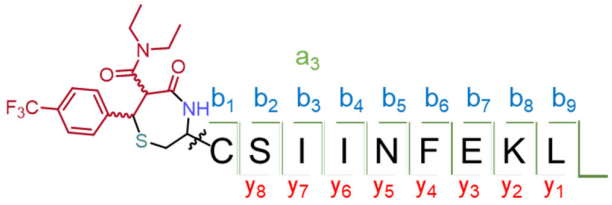

Fragment	Calculated *m/z*	Found *m/z*
[M-(Leu)]$^+$ (**b$_8$**)	1232.6	1231.8
[M-(Lys-Leu)]$^+$ (**b$_7$**)	1104.5	1103.8
[M-(Glu-Lys-Leu)]$^+$ (**b$_6$**)	975.4	975.0
[M-(Phe-Glu-Lys-Leu)]$^+$ (**b$_5$**)	828.4	827.8
[M-(Asn-Phe-Glu-Lys-Leu)]$^+$ (**b$_4$**)	714.3	713.9
[M-(Ile-Asn-Phe-Glu-Lys-Leu)]$^+$ (**a$_3$**)	616.2	616.5
[M-(Ile-Asn-Phe-Glu-Lys-Leu)]$^+$ (**b$_3$**)	601.2	600.9
[M-(Ile-Ile-Asn-Phe-Glu-Lys-Leu)]$^+$ (**b$_2$**)	488.1	487.9

The fragments observed by AIF fragmentation confirm that modification is achieved in the *N*-terminal Cys and not at the Lys residue.

10. General procedure for the ESI-MS assays with Cys-Bombesin

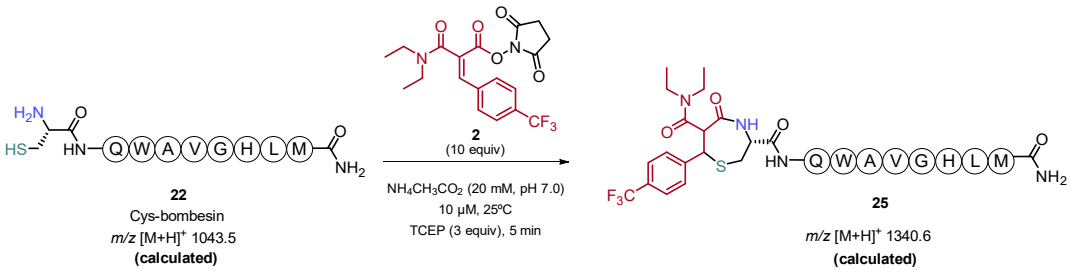

To a solution of Cys-Bombesin **22** (1 mg/959 µL in water, 1 mM) (10 µL, 10.0 nmol) in ammonium acetate 20 mM, pH 7.0 (1 mL) was added 3 equiv of 3,3',3''-phosphanetriyltripropionic acid hydrochloride (TCEP 1.0 mg/mL in water 3.5 mM) (8.57 µL, 0.030 µmol) and the mixture was reacted at RT (25ºC) for approximately 1h. Afterwards, 10 equiv of 2,5-dioxopyrrolidin-1-yl-2-(diethylcarbamoyl)-3-(4-(trifluoromethyl)phenyl)acrylate **2** (30 mM in ACN) (3.33 µL, 0.100 µmol) was added and the reaction was monitored in Positive Mode of ESI-MS at 5 min and 24h, indicating its stability for at least 1 day.

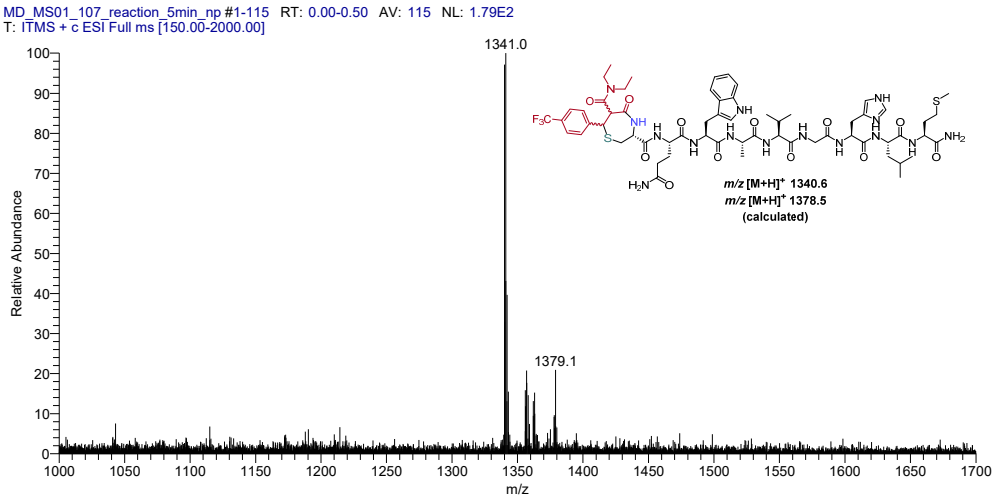

Figure S 56. ESI$^+$-MS spectra of Cys-Bombesin **22** reactions with 10 equiv of 2,5-dioxopyrrolidin-1-yl-2-(diethylcarbamoyl)-3-(4-(trifluoromethyl)phenyl)acrylate **2** in ammonium acetate 20 mM pH 7.0, at 5 min reaction time. The observed peaks correspond to conjugate **25** *m/z* 1341.0 [Mconj**25**+H]$^+$, *m/z* 1379.1 [Mconj**25**+K]$^+$.

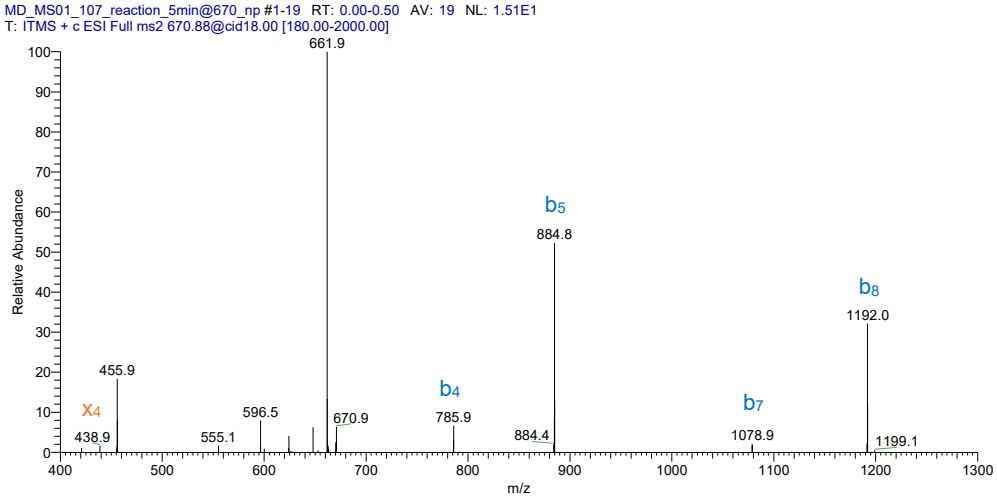

Figure S 57. MS/MS fragmentations of conjugate **25** *m/z* 1341.0 [Mconj**25**+H]$^+$ peak. Reaction conditions: Cys-Bombesin **22** (10.0 nmol) in ammonium acetate 20 mM, pH 7.0, 10 equiv. of 2,5-dioxopyrrolidin-1-yl-2-(diethylcarbamoyl)-3-(4-(trifluoromethyl)phenyl)acrylate **2** after 5 min reaction.

Table S 12. List of fragments from MS/MS fragmentations of conjugate **25** *m/z* 1341.0 peak.

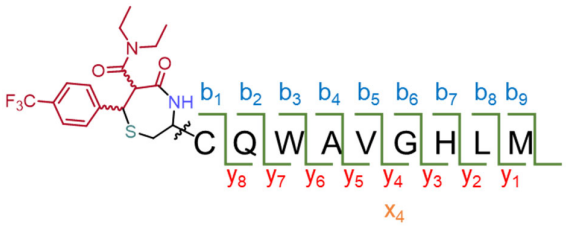

Fragment	Calculated *m/z*	Found *m/z*
[M-Met]$^+$ (**b$_8$**)	1192.5	1192.0
[M-(Leu-Met)]$^+$ (**b$_7$**)	1079.4	1078.9
[M-(Gly-His-Leu-Met)]$^+$ (**b$_5$**)	885.4	884.2
[M-(Val-Gly-His-Leu-Met)]$^+$ (**b$_4$**)	786.3	785.9
[M-(Cys-Gln-Trp-Ala-Val)]$^+$ (**x$_4$**)	439.2	438.9

The fragments observed by AIF fragmentation confirm that modification is achieved in the *N*-terminal Cys. No further key fragmentations were observed.

11. General procedure for the ESI-MS assays with Cys-Cys-Bombesin

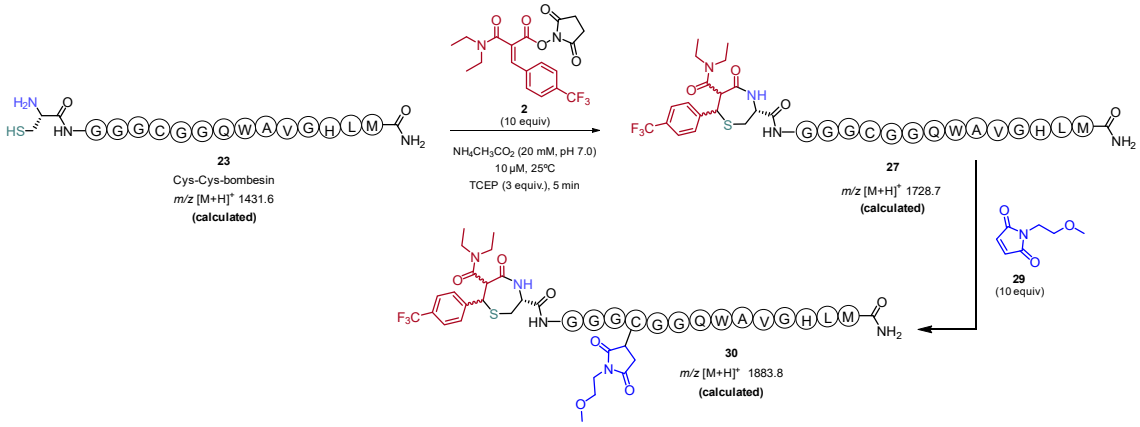

To a solution of Cys-Cys-Bombesin **23** (1 mg/698 µL in water, 1 mM) (10.0 µL, 10.0 nmol) in ammonium acetate 20 mM, pH 7.0 (1 mL) was added 3 equiv. of 3,3',3''-phosphanetriyltripropionic acid hydrochloride (TCEP 1.0 mg/mL in water 3.5 mM) (8.57 µL, 0.030 µmol) and the mixture was reacted at RT (25ºC) for approximately 1h. Afterwards, 10 equiv of reagent **2** (30 mM in ACN) (3.33 µL, 0.100 µmol) was added and the reaction was monitored in Positive Mode of ESI-MS and LC-HRMS Positive Mode at 5 min. After 30 min of the first step reaction, maleimide **29** (30 mM in ACN) (3.33 µL, 0.100 µmol) was added and the reaction was again monitored in Positive Mode of ESI-MS and LC-HRMS

in Positive Mode at 15 min, 90 min and 24 h, indicating stability of the conjugate for at least 1 day. The HPLC runs were carried out with a gradient of A (Milli Q water containing 0.1% v/v Formic acid, FA) and B (acetonitrile containing 0.1% v/v FA, Honeywell HPLC-grade). The mobile phase was t=3 min, 5% B; t=20 min, 95% B; t=21 min, 95% B; t=22 min, 5% B; t=25 min stop, at a flow rate of 0.2 mL/min, detection at 210 nm. MS fragmentations were conducted in Positive Mode of ESI-MS.

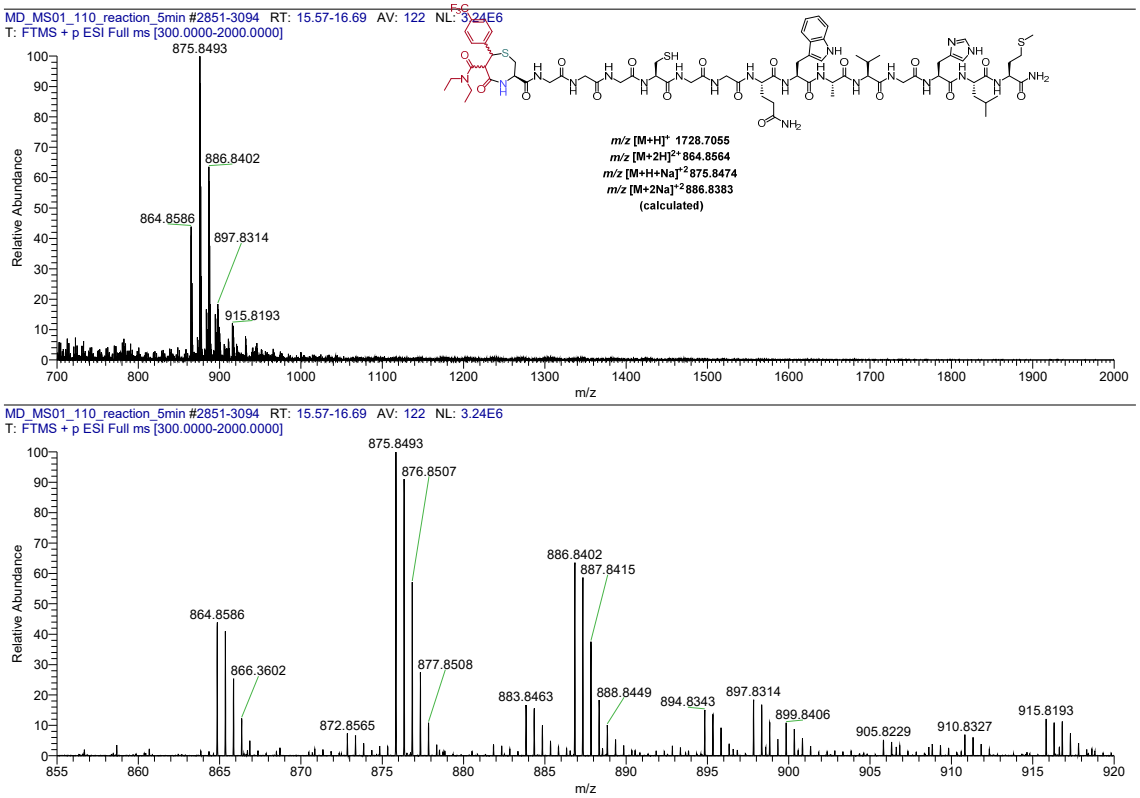

Figure S 58. Full ESI$^+$-HRMS spectra of Cys-Cys-Bombesin **23** reaction with 10 equiv of 2,5-dioxopyrrolidin-1-yl-2-(diethylcarbamoyl)-3-(4-(trifluoromethyl)phenyl)acrylate **2** in ammonium acetate 20 mM pH 7.0, at 5 min reaction time. The observed peaks correspond to conjugate **27** *m/z* 864.8586 [Mconj**27**+2H]$^{2+}$, *m/z* 875.8493 [Mconj**27**+H+Na]$^{2+}$, *m/z* 886.8402 [Mconj**27**+2Na]$^{2+}$.

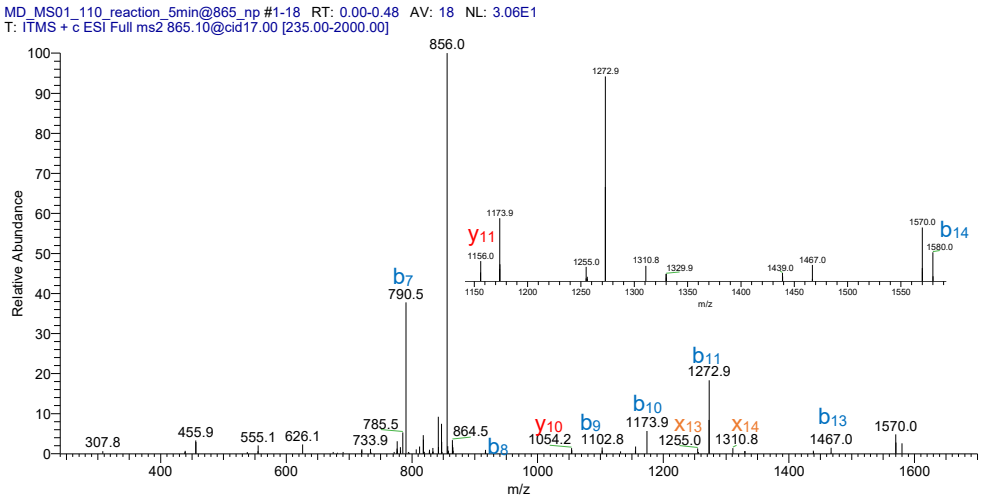

Figure S 59. MS/MS fragmentations of conjugate **27** *m/z* 1729.1 [Mconj**26**+H]$^+$ peak. Reaction conditions: Cys-Cys Bombesin **23** (10.0 nmol) in ammonium acetate 20 mM, pH 7.0, 10 equiv. of 2,5-dioxopyrrolidin-1-yl-2-(diethylcarbamoyl)-3-(4-(trifluoromethyl)phenyl)acrylate **2** after 5 min reaction.

Table S 13. List of fragments from MS/MS fragmentations of X conjugate *m/z* 1729.1 peak.

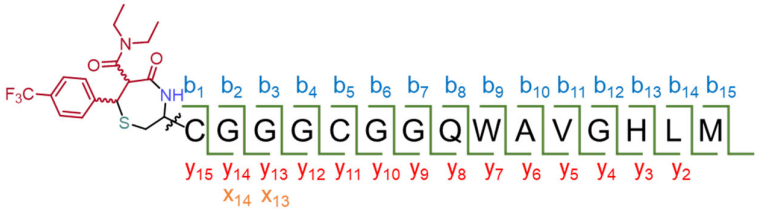

Fragment	Calculated *m/z*	Found *m/z*
[M-Met]$^+$ (**b$_{14}$**)	1580.6	1580.0
[M-Gly]$^+$ (**x$_{14}$**)	1311.6	1310.8
[M-(Leu-Met)]$^+$ (**b$_{13}$**)	1467.6	1467.0
[M-(Cys-Gly)]$^+$ (**x$_{13}$**)	1254.6	1255.0
[M-(Gly-His-Leu-Met)]$^+$ (**b$_{11}$**)	1273.5	1272.9
[M-(Val-Gly-His-Leu-Met)]$^+$ (**b$_{10}$**)	1174.4	1173.9
[M-(Cys-Gly-Gly-Gly-)]$^+$ (**y$_{11}$**)	1155.5	1156.0
[M-(Cys-Gly-Gly-Gly-Cys)]$^+$ (**y$_{10}$**)	1052.5	1054.2
[M-(Ala-Val-Gly-His-Leu-Met)]$^+$ (**b$_9$**)	1103.4	1102.8
[M-(Trp-Ala-Val-Gly-His-Leu-Met)]$^+$ (**b$_8$**)	917.3	917.0
[M-(Gln-Trp-Ala-Val-Gly-His-Leu-Met)]$^+$ (**b$_7$**)	789.2	790.5
[M-(Gly-Gln-Trp-Ala-Val-Gly-His-Leu-Met)]$^+$ (**b$_6$**)	732.2	733.9

The fragments observed by AIF fragmentation confirm that modification is achieved in the *N*-terminal Cys. No further key fragmentations were observed.

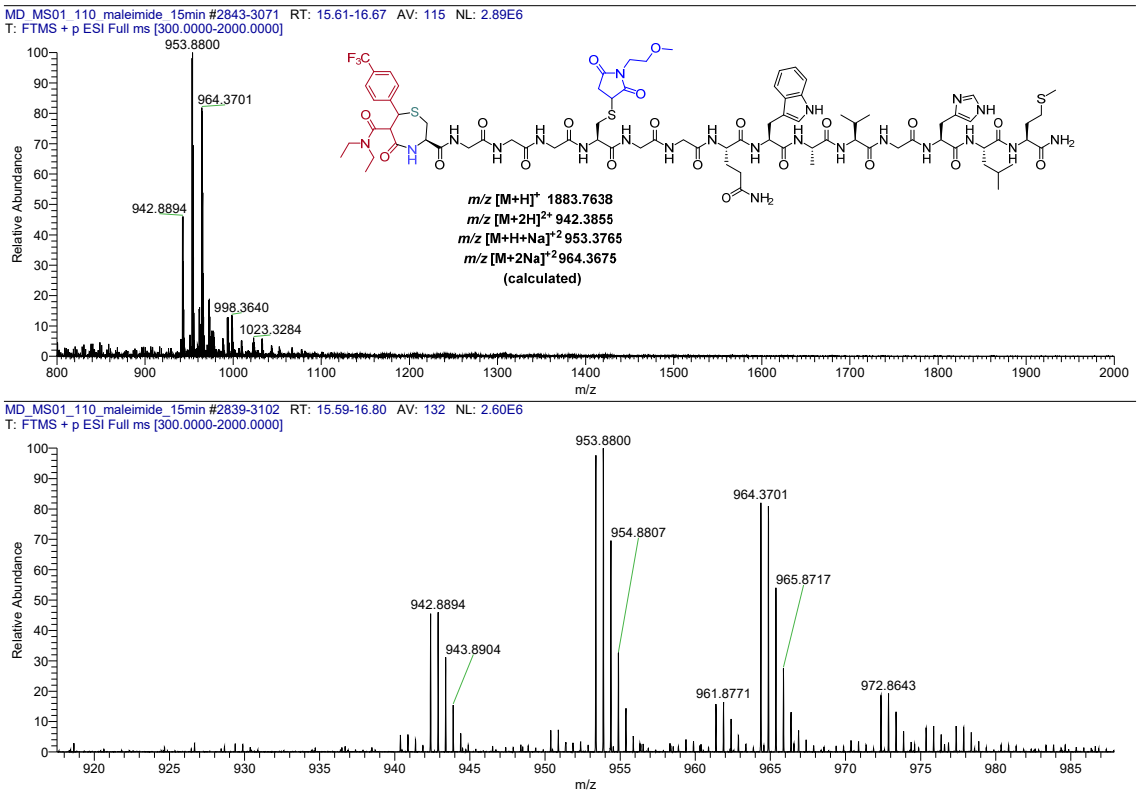

Figure S 60. Full ESI$^+$-HRMS spectra of Cys-Cys-Bombesin **23** reaction with 10 equiv of 2,5-dioxopyrrolidin-1-yl-2-(diethylcarbamoyl)-3-(4-(trifluoromethyl)phenyl)acrylate **2** and 10 equiv of maleimide **29** in ammonium acetate 20 mM pH 7.0, at 15 min reaction time. The observed peaks correspond to conjugate **30** *m/z* 942.8894 [Mconj**30**+2H]$^{2+}$, *m/z* 953.8800 [Mconj**30**+H+Na]$^{2+}$, *m/z* 964.3701 [Mconj**30**+2Na]$^{2+}$. Maleimide **29** was only added after 30 min first step reaction.

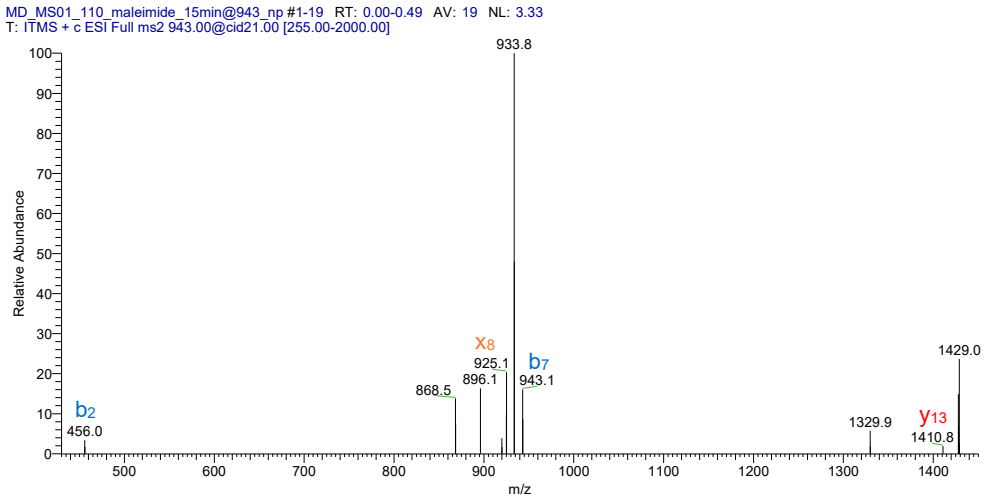

Figure S 61. MS/MS fragmentations of conjugate **30** *m/z* 1884.0 [Mconj**30**+H]$^+$ peak. Reaction conditions: Cys-Cys-Bombesin **23** (10.0 nmol) in ammonium acetate 20 mM, pH 7.0, 10 equiv of 2,5-dioxopyrrolidin-1-yl-2-(diethylcarbamoyl)-3-(4-(trifluoromethyl)phenyl)acrylate **2**, 10 equiv. of maleimide **29**, after 15 min reaction.

Table S 14. List of fragments from MS/MS fragmentations of **30** conjugate *m/z* 1884.0 peak.

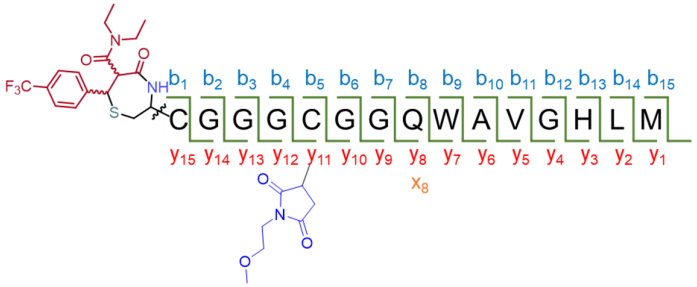

Fragment	Calculated *m/z*	Found *m/z*
[M-(Cys-Gly)]$^+$ (**y_{13}**)	1409.6	1410.8
[M-(Cys-Gly-Gly-Gly-Cys-Gly-Gly)]$^+$ (**x_8**)	923.5	925.0
[M-(Gln-Trp-Ala-Val-Gly-His-Leu-Met)]$^+$ (**b_7**)	944.3	943.1
[M-(Gly-Gly-Cys-Gly-Gly-Gln-Trp-Ala-Val-Gly-His-Leu-Met)]$^+$ (**b_2**)	458.1	456.0

The fragments observed by AIF fragmentation confirm that modification with NHS-activated acrylate **2** is achieved in the *N*-terminal Cys and fragment **y13** indicates that maleimide **27** was installed at the in chain cysteine residue.

12. General Procedure for the ESI-MS assay with Calcitonin Salmon

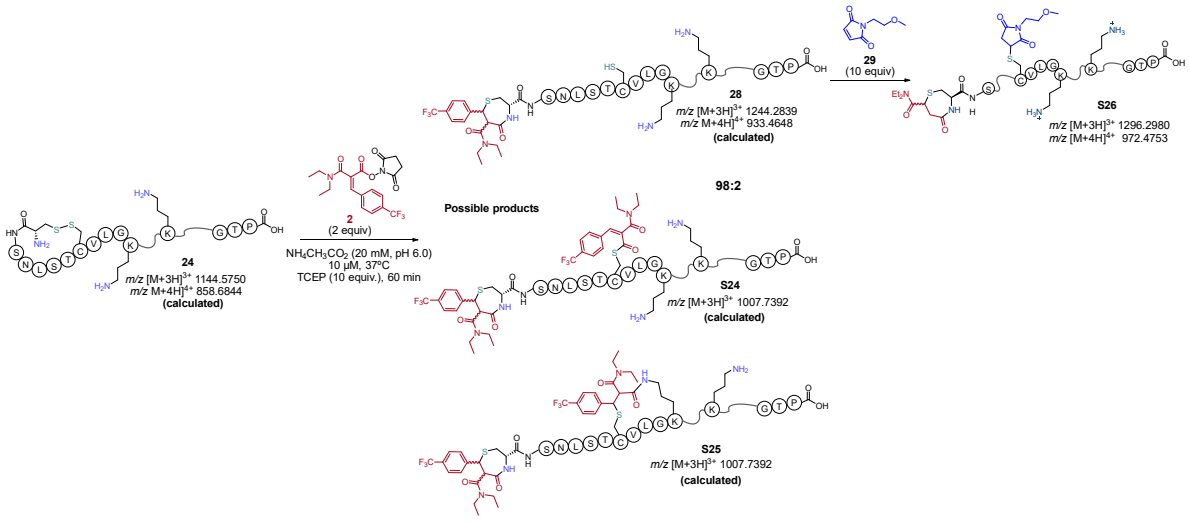

To a solution of Calcitonin Salmon **24** (1 mg/291 µL in water, 1 mM) (10.0 µL, 10.0 nmol) in ammonium acetate 20 mM, pH 6.0 (1 mL) was added 10 equiv of 3,3',3''-phosphanetriyltripropionic acid hydrochloride (TCEP 1.0 mg/mL in water 3.5 mM) (28.6 µL, 0.100 µmol) and the mixture was reacted at 37ºC for approximately 1h. Afterwards, 2 equiv of reagent **2** (30 mM in ACN) (0.67 µL, 0.020 µmol) was added and the reaction was

monitored in Positive Mode of ESI-MS and LC-HRMS Positive Mode at 5 min, 60 min and 2 h. After 2 h of the first step reaction, maleimide **29** (30 mM in ACN) (3.33 µL, 0.100 µmol) was added and the reaction was again monitored in Positive Mode of ESI-MS and LC-HRMS in Positive Mode at 15 min, and 60 min. The HPLC runs were carried out with a gradient of A (Milli Q water containing 0.1% v/v Formic acid, FA) and B (acetonitrile containing 0.1% v/v FA, Honeywell HPLC-grade). The mobile phase was t=1 min, 5% B; t=10 min, 95% B; t=11 min, 95% B; t=12 min, 5% B; t=15 min stop, at a flow rate of 0.3 mL/min, detection at 254 nm. MS fragmentations were conducted in Positive Mode of ESI-MS.

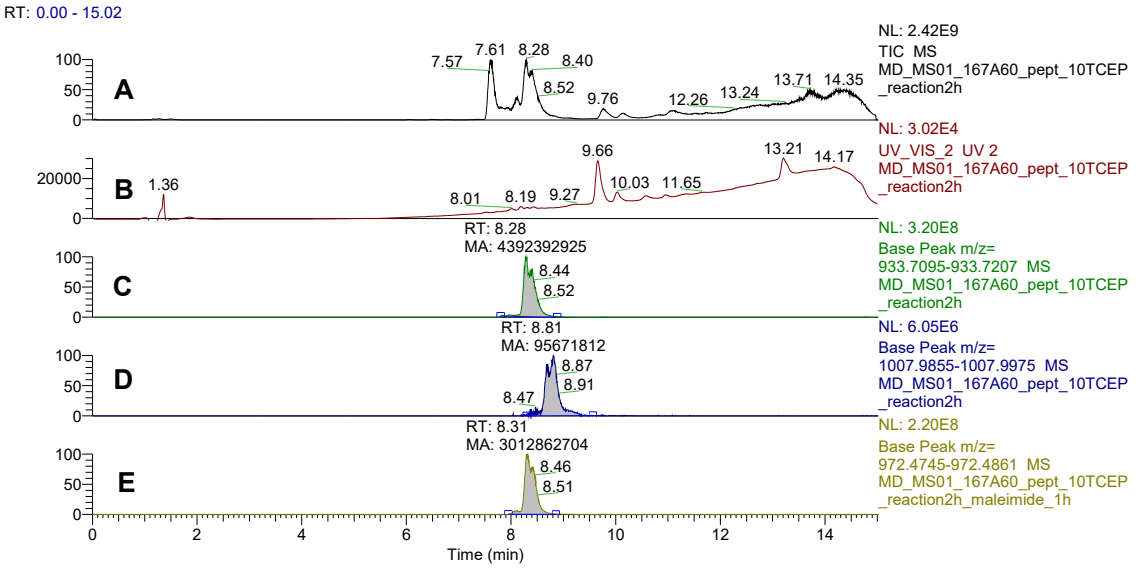

Figure S 62: LC-MS chromatograms of Calcitonin Salmon conjugates **28** and **S24–25**. **A)** First step reaction mixture TIC after 2h; **B)** Reaction detection at 254 nm, after 2 h; **C)** Calcitonin-conjugate **28** EIC (base peak *m/z* 933.7148) after 2 h reaction; **D)** Calcitonin di-modified conjugate **S24–25** EIC (base peak *m/z* 1007.9915) after 2 h reaction; **E)** Calcitonin dual conjugate **S26** EIC (base peak *m/z* 972.4803); after 60 min reaction. The products ratio was calculated using the EIC integration area of each specie and converted to percentage to afford a 98:2 AUC ratio (conjugate **28** *vs* Conjugates **S24–25**).

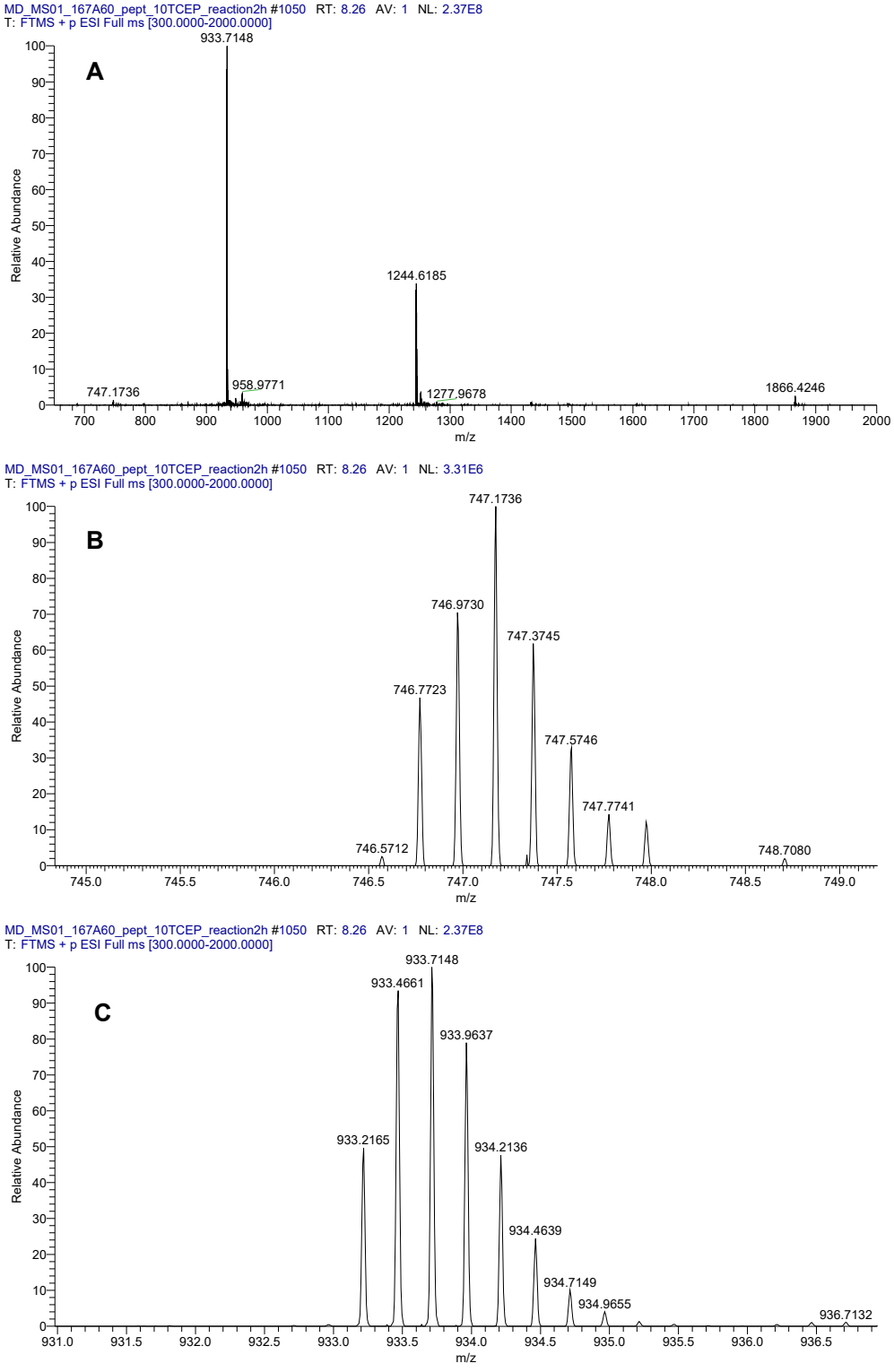
MD_MS01_167A60_pept_10TCEP_reaction2h #1050 RT: 8.26 AV: 1 NL: 2.37E8
T: FTMS + p ESI Full ms [300.0000-2000.0000]
A
933.7148
1244.6185
747.1736
958.9771
1277.9678
1866.4246
Relative Abundance
m/z
MD_MS01_167A60_pept_10TCEP_reaction2h #1050 RT: 8.26 AV: 1 NL: 3.31E6
T: FTMS + p ESI Full ms [300.0000-2000.0000]
B
747.1736
746.9730
747.3745
746.7723
747.5746
747.7741
746.5712
748.7080
Relative Abundance
m/z
MD_MS01_167A60_pept_10TCEP_reaction2h #1050 RT: 8.26 AV: 1 NL: 2.37E8
T: FTMS + p ESI Full ms [300.0000-2000.0000]
C
933.7148
933.4661
933.9637
933.2165
934.2136
934.4639
934.7149
934.9655
936.7132
Relative Abundance
m/z

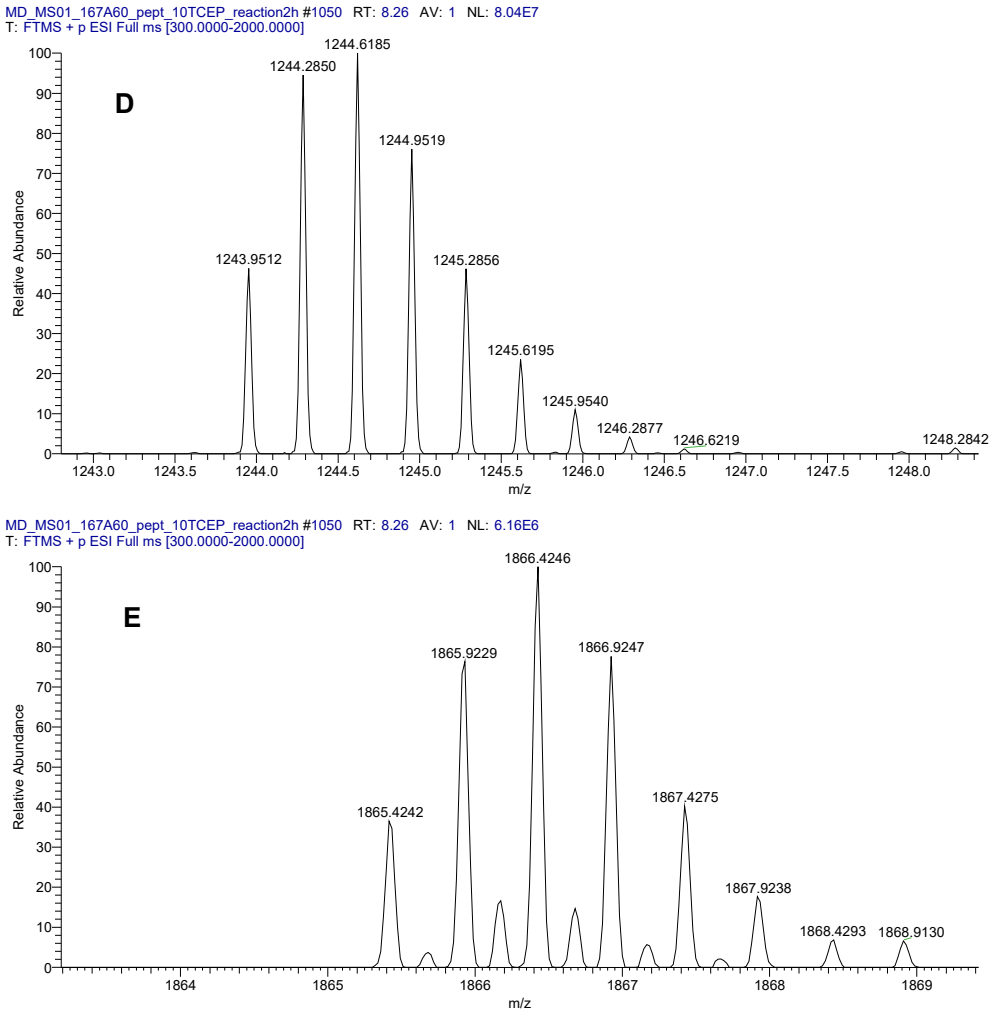

Figure S 63. A) Full ESI^{+}-HRMS spectrum of Calcitonin conjugate **28** ($C_{160}H_{261}F_3N_{45}O_{50}S_2$ $[M+5H]^{5+}$ calculated: 746.9733, found *m/z* 747.1736; $C_{160}H_{260}F_3N_{45}O_{50}S_2$ $[M+4H]^{4+}$ calculated: 933.4648, found *m/z* 933.4661; $C_{160}H_{259}F_3N_{45}O_{50}S_2$ $[M+3H]^{3+}$ calculated: 1244.2839, found *m/z* 1244.6185; $C_{160}H_{258}F_3N_{45}O_{50}S_2$ $[M+2H]^{2+}$ calculated: 1865,9223, found *m/z* 1866.4246, from TIC peak at RT 8.26 min); **B)** zoom-in of quintuple charged Calcitonin conjugate **28**; **C)** zoom-in on quadruple charged Calcitonin conjugate **28**; **D)** zoom-in of triple charged Calcitonin conjugate **28, E)** zoom-in of double charged Calcitonin conjugate **28**.

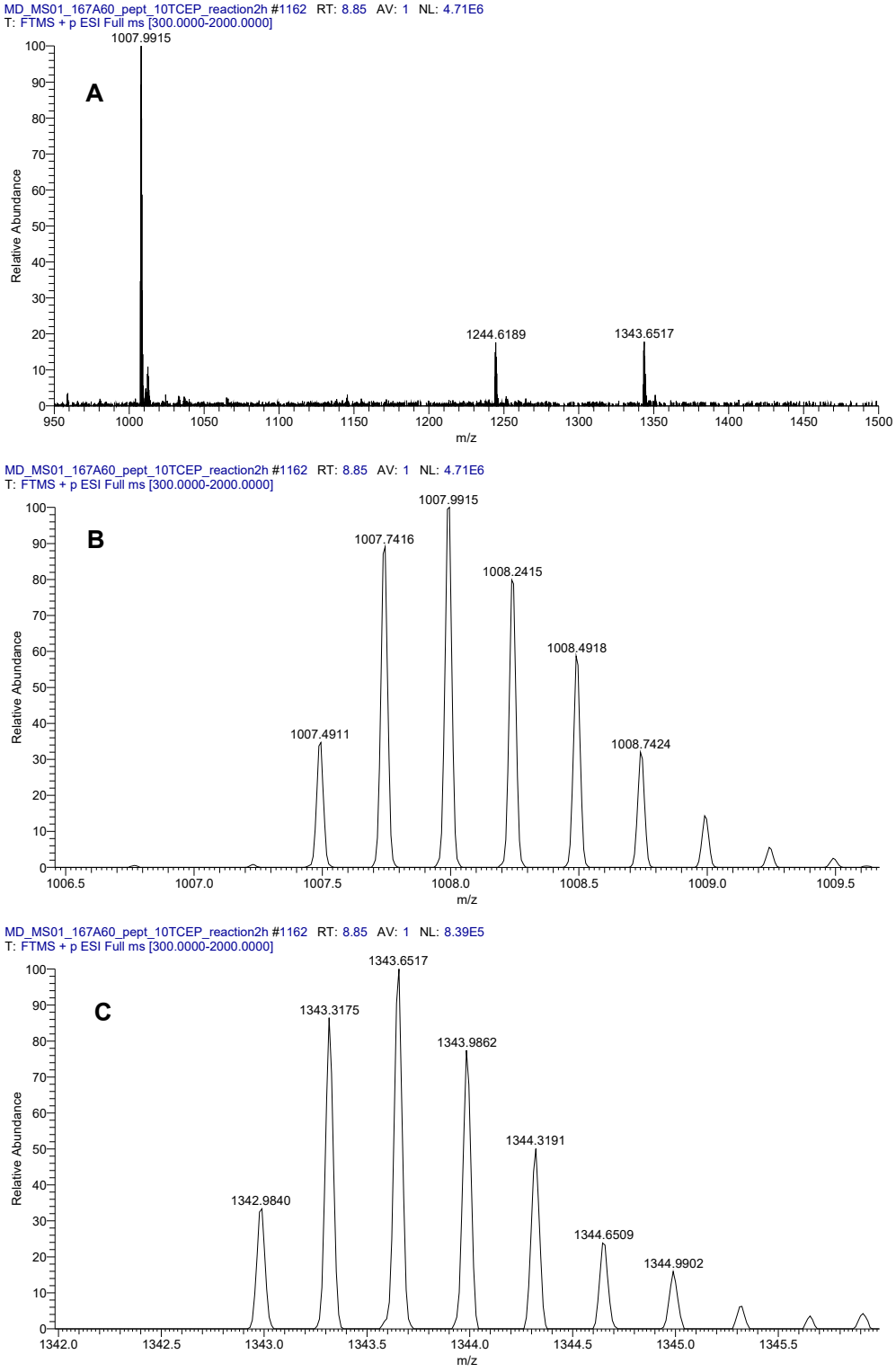

Figure S 64. A) Full ESI^{+}-HRMS spectrum of Calcitonin conjugates **S24–25** ($C_{175}H_{274}F_6N_{46}O_{52}S_2$ $[M+4H]^{4+}$ calculated: 1007.7392, found *m/z* 1007.9915; $C_{175}H_{273}F_6N_{46}O_{52}S_2$ $[M+3H]^{3+}$ calculated: 1343.3165, found *m/z* 1343.6517; from TIC peak at RT 8.85 min); **B)** zoom-in of quadruple charged Calcitonin conjugate **S24–25**; **C)** zoom-in on triple charged Calcitonin conjugate **S24–25**.

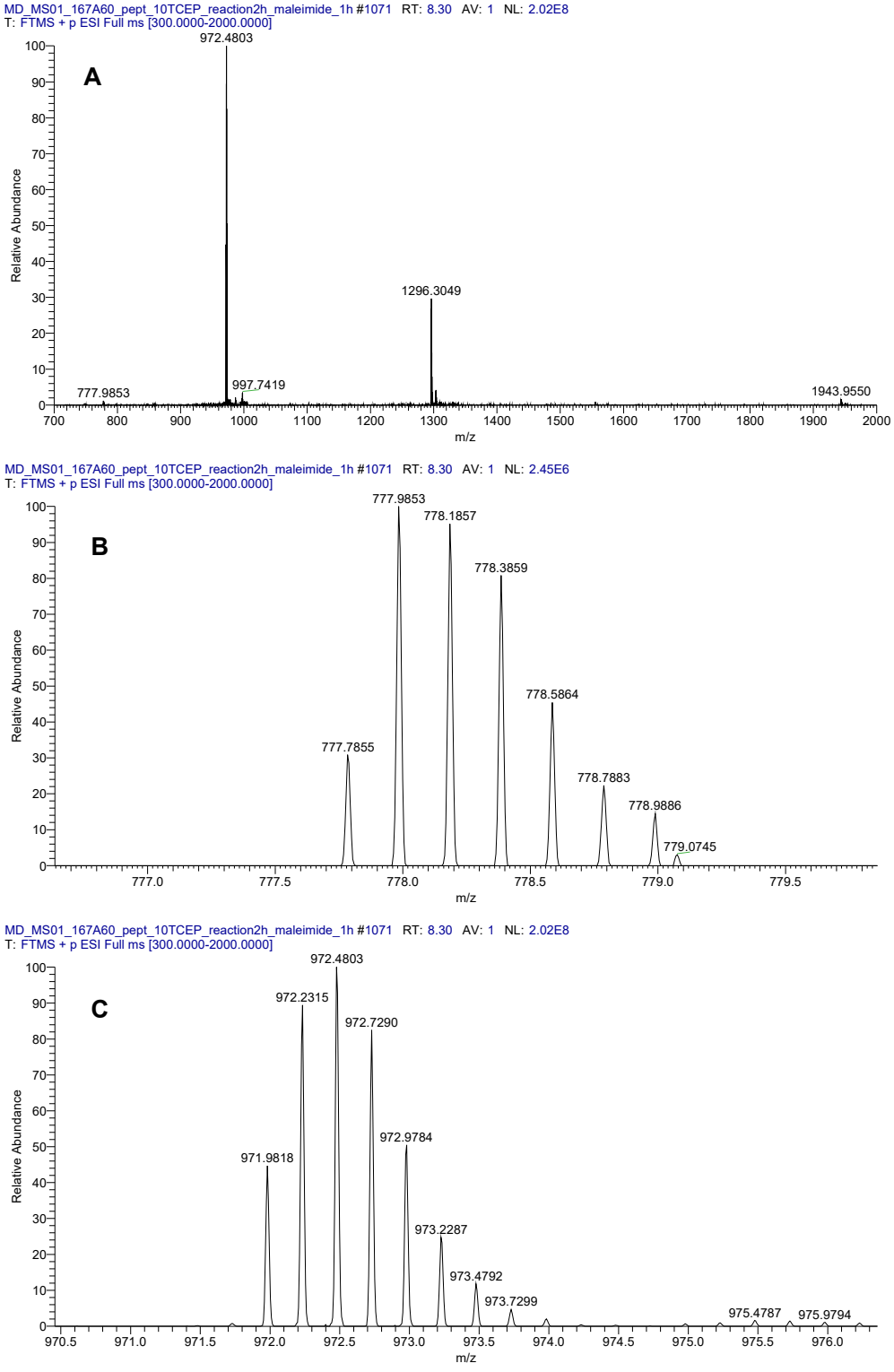
MD_MS01_167A60_pept_10TCEP_reaction2h_maleimide_1h #1071 RT: 8.30 AV: 1 NL: 2.02E8
T: FTMS + p ESI Full ms [300.0000-2000.0000]
A
Relative Abundance
m/z
972.4803
1296.3049
997.7419
777.9853
1943.9550
MD_MS01_167A60_pept_10TCEP_reaction2h_maleimide_1h #1071 RT: 8.30 AV: 1 NL: 2.45E6
T: FTMS + p ESI Full ms [300.0000-2000.0000]
B
Relative Abundance
m/z
777.9853
778.1857
778.3859
778.5864
777.7855
778.7883
778.9886
779.0745
MD_MS01_167A60_pept_10TCEP_reaction2h_maleimide_1h #1071 RT: 8.30 AV: 1 NL: 2.02E8
T: FTMS + p ESI Full ms [300.0000-2000.0000]
C
Relative Abundance
m/z
972.4803
972.2315
972.7290
972.9784
971.9818
973.2287
973.4792
973.7299
975.4787
975.9794

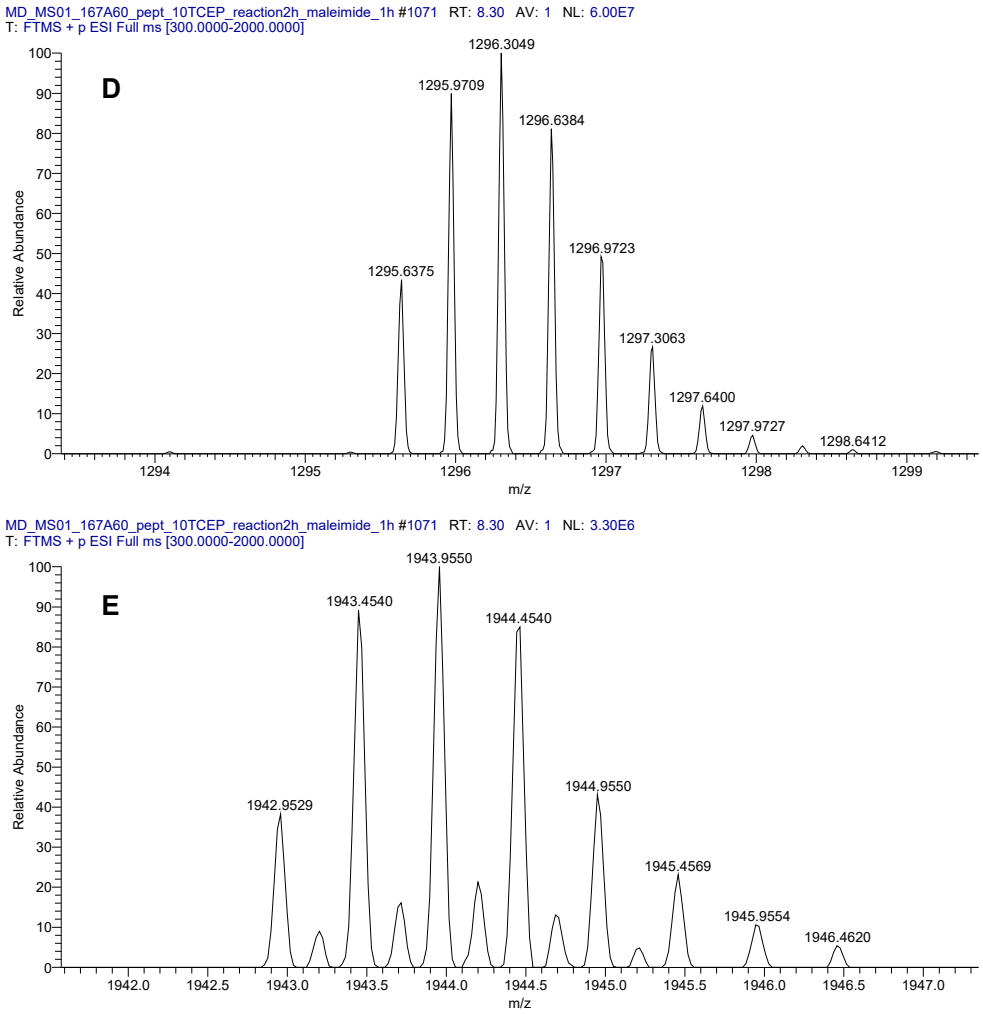

Figure S 65. A) Full ESI^{+}-HRMS spectrum of Calcitonin dual conjugate **S26** ($C_{167}H_{269}F_3N_{45}O_{54}S_2$ $[M+5H]^{5+}$ calculated: 778.1817, found *m/z* 777.9853; $C_{167}H_{268}F_3N_{45}O_{54}S_2$ $[M+4H]^{4+}$ calculated: 972.4753, found *m/z* 972.4803; $C_{160}H_{267}F_3N_{45}O_{50}S_2$ $[M+3H]^{3+}$ calculated: 1296.2980, found *m/z* 1296.3049; $C_{160}H_{266}F_3N_{45}O_{50}S_2$ $[M+2H]^{2+}$ calculated 1943.9434, found *m/z* 1943.9550, from TIC peak at RT 8.30 min); **B)** zoom-in of quintuple charged Calcitonin conjugate **S26**; **C)** zoom-in on quadruple charged Calcitonin conjugate **S26**; **D)** zoom-in of triple charged Calcitonin conjugate **S26, E)** zoom-in of double charged Calcitonin conjugate **S26**.

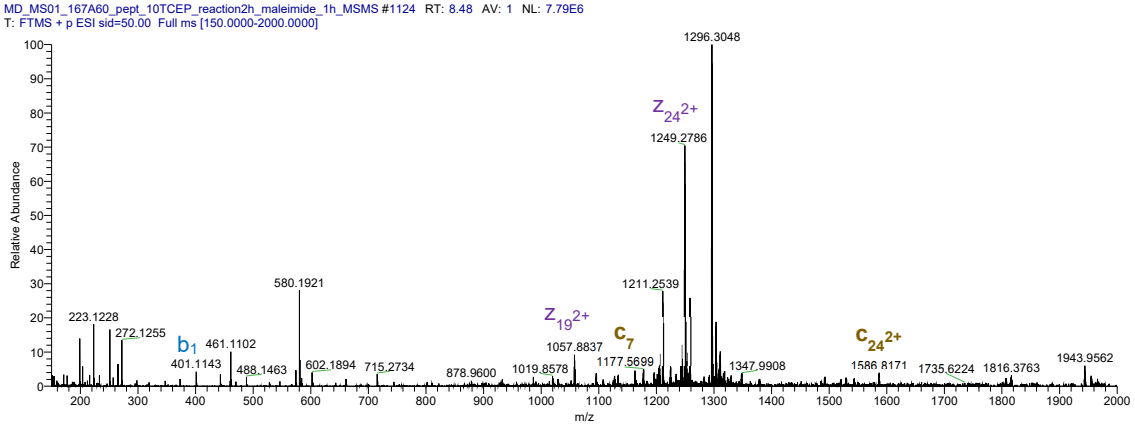

Figure S 66. MS fragmentation of conjugate **S26** – AIF with 50 ev of the peak at 8.30 min (150-2000 *m/z*).

Table S 15. List of fragments from MS/MS fragmentations of **S26** conjugate *m/z* 972.4753 peak.

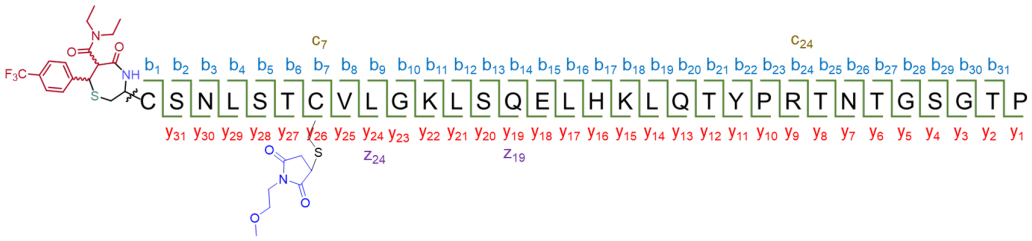

Fragment	Calculated *m/z*	Found *m/z*
[M-(CSNLSTCV)]$^{2+}$ (**z_{24}**)	1249.6463	1249.2786
[M-(TNTGSGTP)]$^{2+}$ (**c_{24}**)	1585.2856	1586.8171
[M-(CSNLSTCVLGKLS)]$^{2+}$ (**z_{19}**)	1057.0300	1057.8837
[M-(VLGKLSQELHKLQTYPRTNTGSGTP)]$^{+}$ (**c_7**)	1177.4396	1177.5699
[M-(CSNLSTCVLGKLSQELHKLQTYPRTNTGSGTP)]$^{+}$ (**b_1**)	401.1147	401.1143

The fragments observed by AIF fragmentation confirm that modification is achieved in the *N*-terminal Cys and maleimide **29** is added to the in-chain cysteine. Additionally, Lys residues were not modified. No further key fragmentations were observed.

12.1. Trypsin digestion

To confirm the exact structure of the double modification, trypsin digestion was performed considering that trypsin will cut the peptide at Lys (K) and Arg (R) residues. Therefore, ammonium bicarbonate (1.6 mg, 0.020 mmol) is added to an aliquot of the reaction mixture (100 µL), then a trypsin solution (2.0 µL, 0.1 µg/µL in ammonium bicarbonate (16 mg/mL)) is added and incubated for 24 h at 37ºC, the reaction was monitored by LC-HRMS in Positive Mode. The HPLC runs were carried out with a gradient of A (Milli Q water containing 0.1% v/v Formic acid, FA) and B (acetonitrile containing 0.1% v/v FA, Honeywell HPLC-grade). The mobile phase was t=5 min, 3% B; t=75 min, 95% B; t=85 min, 95% B; t=88 min, 3% B; t=90 min stop, at a flow rate of 0.2 mL/min.

The Extracted Ion chromatogram (EIC) within a 6 ppm range charged by 2 H^+ was searched for **S26 fragment 1**:

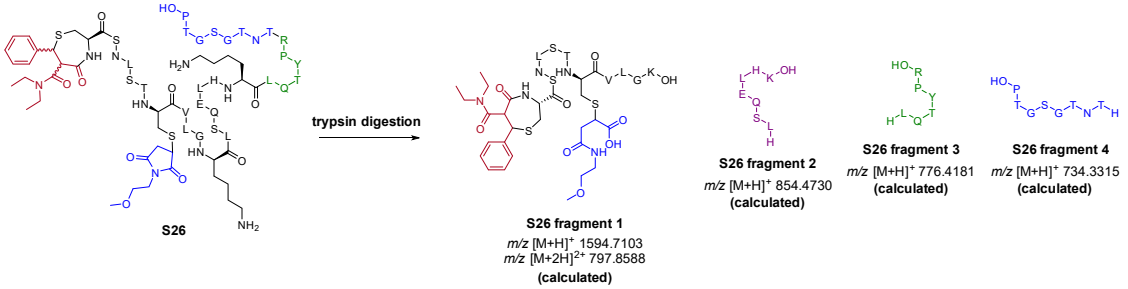

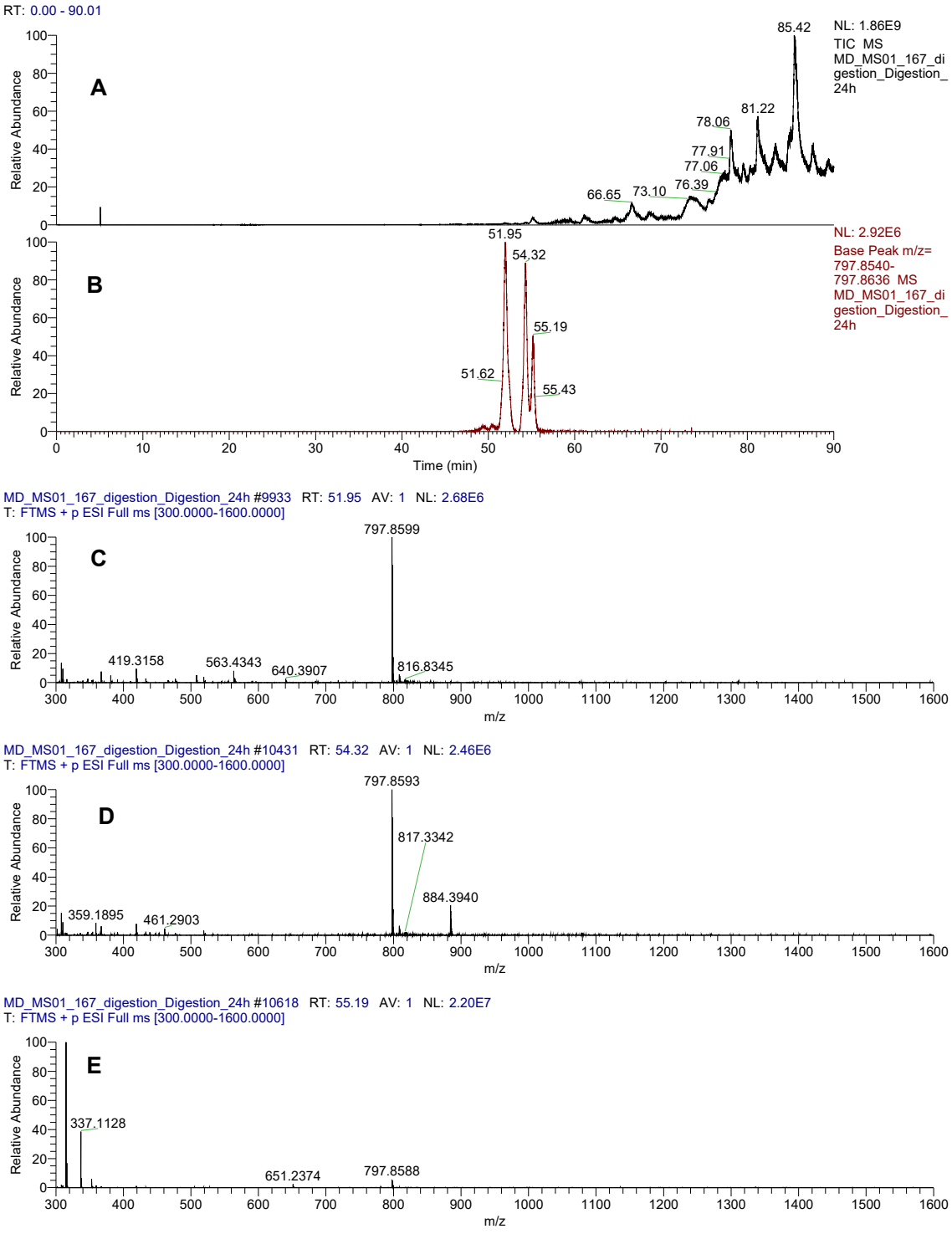

Figure S 67. A) Full ESI^{+}-HRMS spectrum of Calcitonin Salmon conjugate **S26** digestion with trypsin after 24 h; **B)** EIC spectrum of *m/z* 797.8588 [**S26 - fragment 1**+2H]$^{2+}$ (δ 6 ppm). **C)** spectrum of peak at 51.95 min. **D)** spectrum of peak at 54.32 min; **E)** spectrum of peak at 55.19 min.

13. Procedure for the bioconjugation reactions with coumarin-NHS activated acrylate derivates

13.1. General procedure for peptide bioconjugation with 2,5-dioxopyrrolidin-1-yl-3-(7-(diethylamino)-2-oxo-2H-chromen-3-yl)-2 (diethylcarbamoyl)acrylate 29

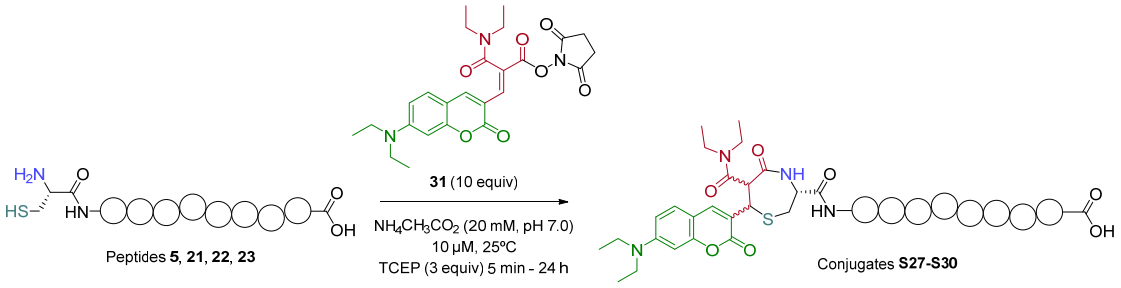

To a solution of peptide (1 mM in water) (10 µL, 0.0100 µmol) in ammonium acetate 20 mM, pH 7.0 (1 mL) was added 3 equiv of 3,3',3''-phosphanetriyltripropionic acid hydrochloride (TCEP 1.0 mg/mL in water 3.5 mM) (8.57 µL, 0.030 µmol) and the mixture was reacted at 25ºC (RT) for approximately 1h. Afterwards, 10 equiv of 2,5-dioxopyrrolidin-1-yl-3-(7 (diethylamino)-2-oxo-2H-chromen-3-yl)-2 (diethylcarbamoyl)acrylate **31** (30 mM in ACN) (3.33 µL, 0.100 µmol) was added and the reaction progression was monitored by LC-HRMS in Positive Mode. The HPLC runs were carried out with a gradient of A (Milli Q water containing 0.1% v/v Formic acid, FA) and B (acetonitrile containing 0.1% v/v FA, Honeywell HPLC-grade). The mobile phase was t=0 min, 1% B; t=10 min, 75% B; t=10.1 min, 95% B; t=12 min, 95% B; t=12.5 min, 1% B; t=15 min stop, at a flow rate of 0.3 mL/min, detection at 254 nm.

13.2. Conjugation with laminin fragment 5

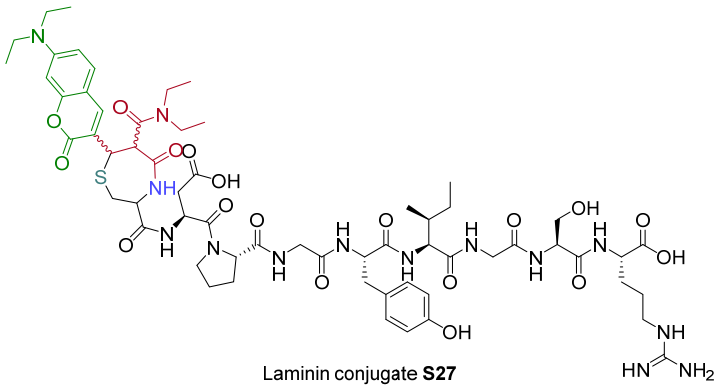

Laminin conjugate **S27**

m/z $[M+H]^+$ 1335.6038
m/z $[M+2H]^{2+}$ 668.3055
m/z $[M+3H]^{3+}$ 445.8728
(calculated)

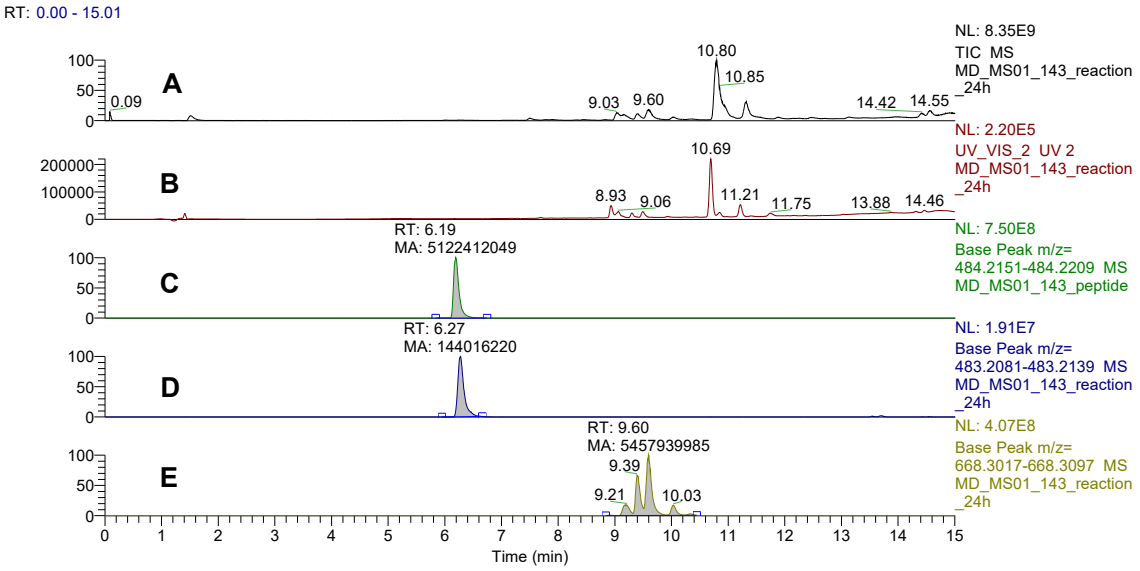

Figure S 68. LC-MS chromatograms of Laminin conjugate **S27** and Laminin fragment. **A)** Reaction mixture TIC after 24 h; **B)** Reaction detection at 254 nm, after 24 h; **C)** Reaction t_0 – unreacted laminin **5** EIC (base peak *m/z* 484.2180); **D)** Unreacted laminin **5** EIC after 24 h reaction with 10 equiv of **31**; **E)** Laminin conjugate **S27** EIC (base peak *m/z* 668.3057) after 24 h reaction. Laminin conversion was calculated based on the EIC intensity (AUC) within δ 6 ppm range.

Table S 16. Laminin peptide **5** conversion in 24 h reaction with coumarin NHS-activated acrylate **31** according to AUC from EIC chromatograms of base peak *m/z* 484.2180, within δ 6 ppm range.

	t_0	24 h	Conversion
Laminin (AUC a.u.)	5122412049	144016220	97%

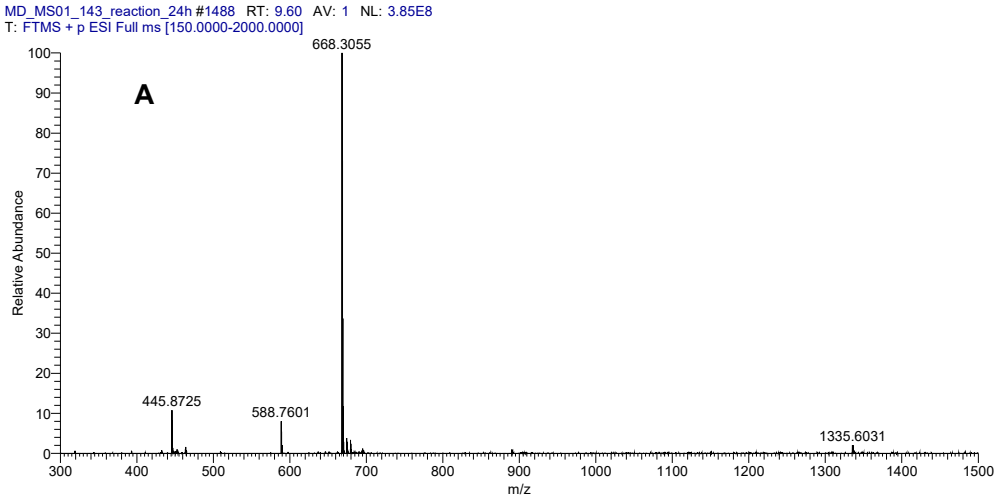

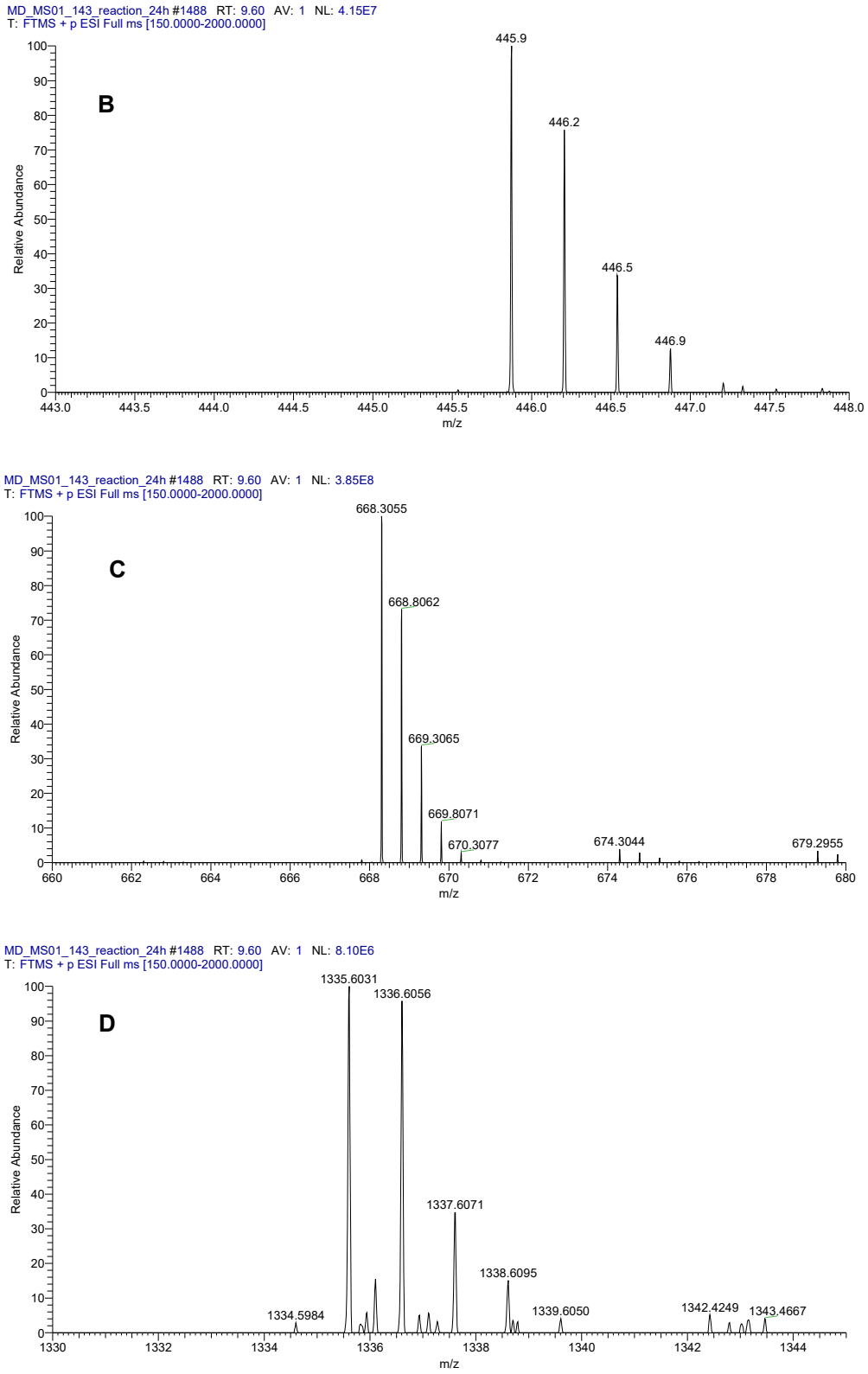

Figure S 69. A) Full ESI^{+}-HRMS spectrum of Laminin conjugate **S27** ($C_{61}H_{89}N_{14}O_{18}S$ $[M+3H]^{3+}$ calculated: 445.8728, found *m/z* 445.8725; $C_{61}H_{88}N_{14}O_{18}S$ $[M+2H]^{2+}$ calculated: 668.3055, found *m/z* 668.3055; $C_{61}H_{87}N_{14}O_{18}S$ $[M+H]^{+}$ calculated: 1335.6038, found *m/z* 1335.6031, from TIC peak at RT 9.6 min); **B)** zoom-in of triple charged Laminin conjugate **S27**; **C)** zoom-in on double charged laminin conjugate **S27**; **D)** zoom-in of mono charged Laminin conjugate **S27**.

13.3. Conjugation with *C*-Ovalbumin 21

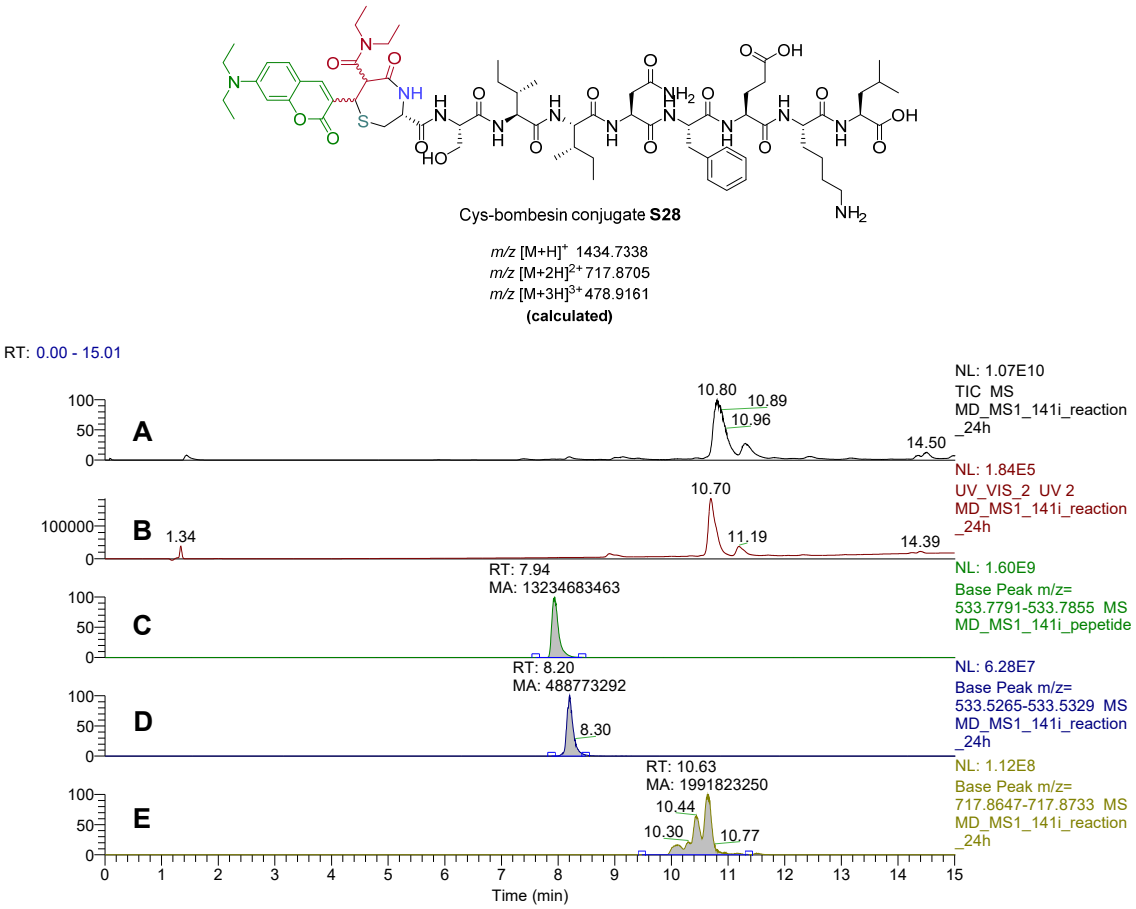

Figure S 70. LC-MS chromatograms of *C*-Ovalbumin conjugate **S28** and *C*-Ovalbumin peptide **21**. **A)** Reaction mixture TIC after 24 h; **B)** Reaction detection at 254 nm, after 24 h; **C)** Reaction t_0 – unreacted *C*-Ovalbumin **21** EIC (base peak *m/z* 533.7823); **D)** Unreacted *C*-Ovalbumin **21** EIC after 24 h reaction with 10 equiv of **31**; **E)** *C*-Ovalbumin conjugate **S28** EIC (base peak *m/z* 717.8690) after 24 h reaction. *C*-Ovalbumin conversion was calculated based on the EIC intensity (AUC) within δ 6ppm range.

Table S 17. *C*-Ovalbumin peptide **21** conversion in 24 h reaction with coumarin NHS-activated acrylate **31** according to AUC from EIC chromatograms of base peak *m/z* 533.7823, within δ 6 ppm range.

	t_0	24 h	Conversion
***C*-Ovalbumin (AUC a.u.)**	13234683463	488773292	96%

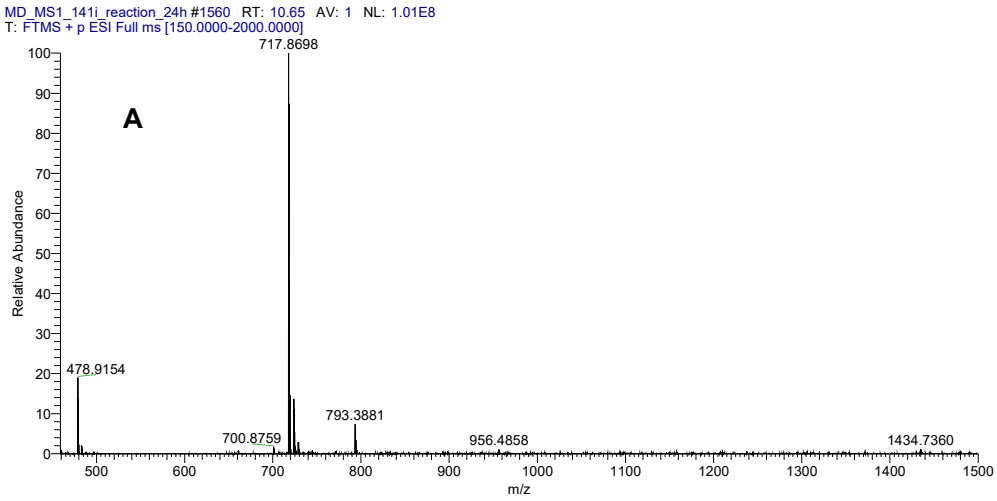
MD_MS1_141i_reaction_24h #1560 RT: 10.65 AV: 1 NL: 1.01E8
T: FTMS + p ESI Full ms [150.0000-2000.0000]
A
Relative Abundance
m/z
717.8698
478.9154
793.3881
700.8759
956.4858
1434.7360

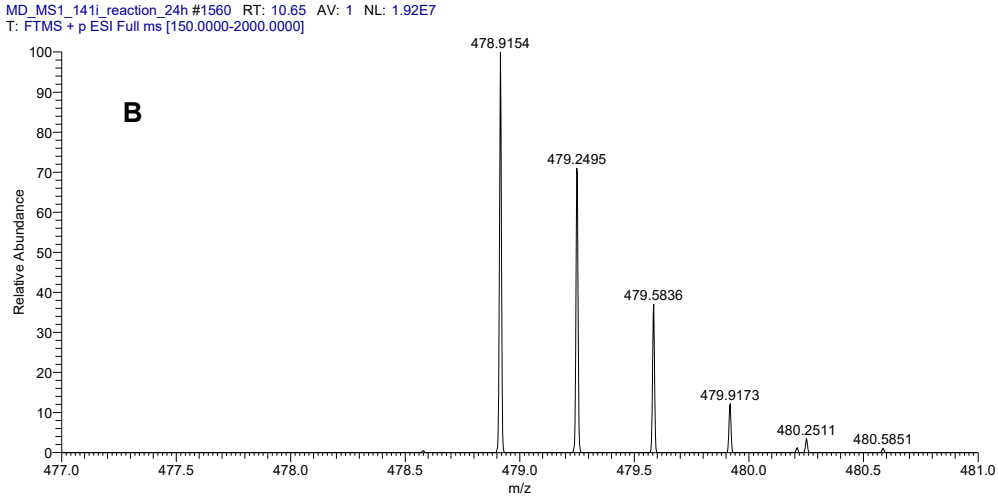
MD_MS1_141i_reaction_24h #1560 RT: 10.65 AV: 1 NL: 1.92E7
T: FTMS + p ESI Full ms [150.0000-2000.0000]
B
Relative Abundance
m/z
478.9154
479.2495
479.5836
479.9173
480.2511
480.5851

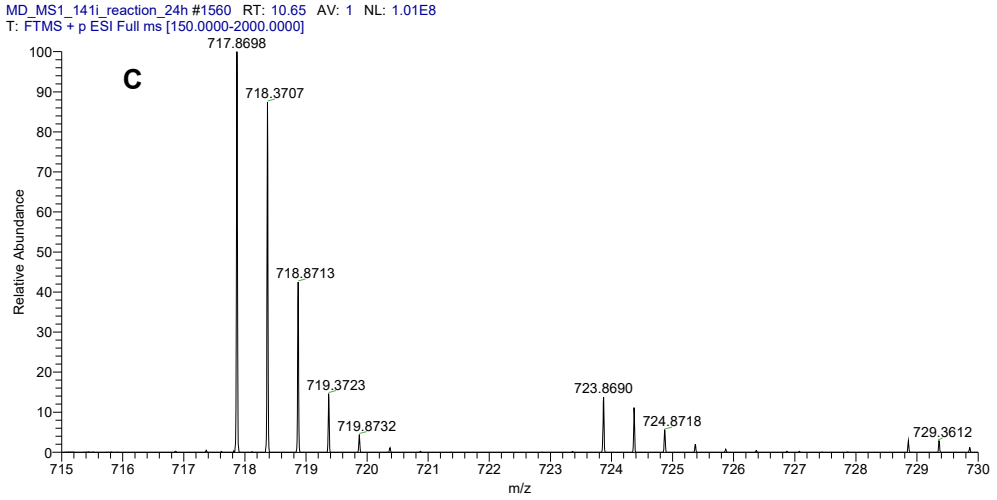
MD_MS1_141i_reaction_24h #1560 RT: 10.65 AV: 1 NL: 1.01E8
T: FTMS + p ESI Full ms [150.0000-2000.0000]
C
Relative Abundance
m/z
717.8698
718.3707
718.8713
719.3723
719.8732
723.8690
724.8718
729.3612

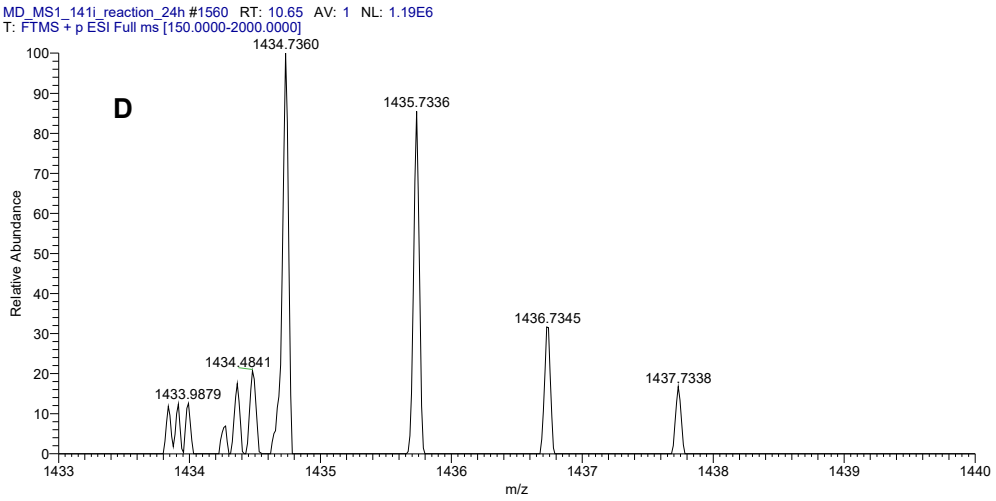

Figure S 71. A) Full ESI⁺-HRMS spectrum of *C*-Ovalbumin conjugate **S28** ($C_{69}H_{106}N_{13}O_{18}S$ $[M+3H]^{3+}$ calculated: 478.9161, found *m/z* 478.9154; $C_{69}H_{105}N_{13}O_{18}S$ $[M+2H]^{2+}$ calculated: 717.8705, found *m/z* 717.8698; $C_{69}H_{104}N_{13}O_{18}S$ $[M+H]^{+}$ calculated: 1434.7338, found *m/z* 1434.7360, from TIC peak at RT 10.65 min); **B)** zoom-in of triple charged *C*-Ovalbumin conjugate **S28**; **C)** zoom-in on double charged *C*-Ovalbumin conjugate **S28**; **D)** zoom-in of mono charged *C*-Ovalbumin conjugate **S28**.

13.4. Conjugation with Cys-Bombesin 22

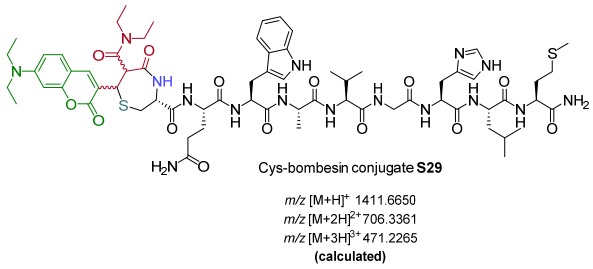

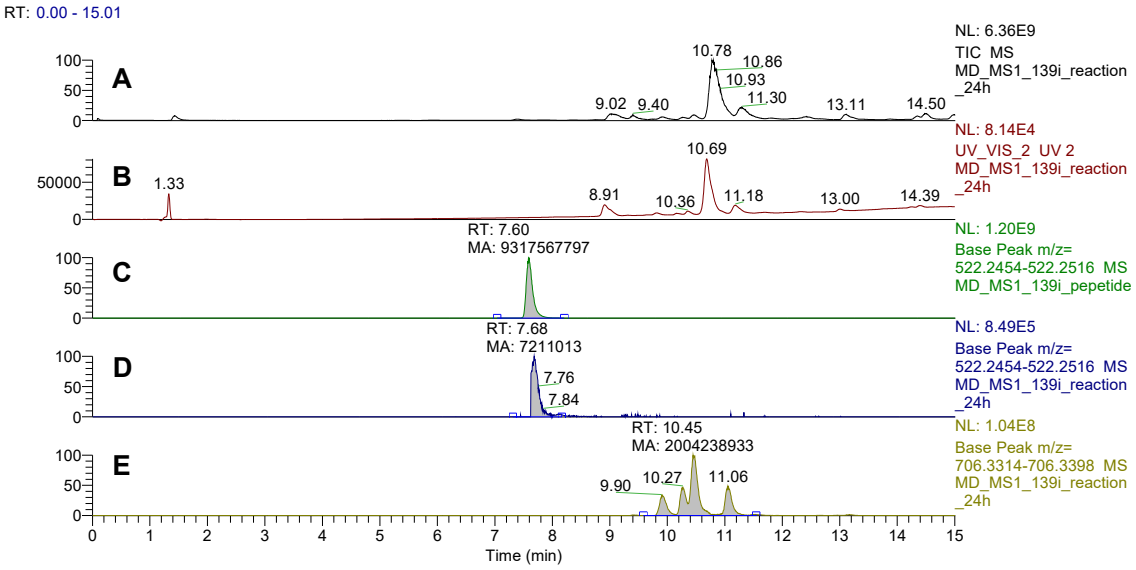

Figure S 72. LC-MS chromatograms of Cys-Bombesin conjugate **S29** and Cys-Bombesin peptide. **A)** Reaction mixture TIC after 24 h; **B)** Reaction detection at 254 nm, after 24 h; **C)** Reaction t_0 – unreacted Cys-Bombesin **22** EIC (base peak *m/z* 522.2485); **D)** Unreacted Cys-Bombesin **22** EIC after 24 h reaction with 10 equiv of **S29**; **E)** Cys-Bombesin conjugate **S29** EIC (base peak *m/z* 706.3356) after 24 h reaction. Cys-Bombesin conversion was calculated based on the EIC intensity (AUC) within δ 6 ppm range.

Table S 18. Cys-Bombesin peptide **22** conversion in 24 h reaction with coumarin NHS-activated acrylate **31** according to AUC from EIC chromatograms of base peak *m/z* 522.2485, within ð 6 ppm range.

	t_0	24 h	Conversion
Cys-Bombesin (AUC a.u.)	9317567797	7211013	>99%

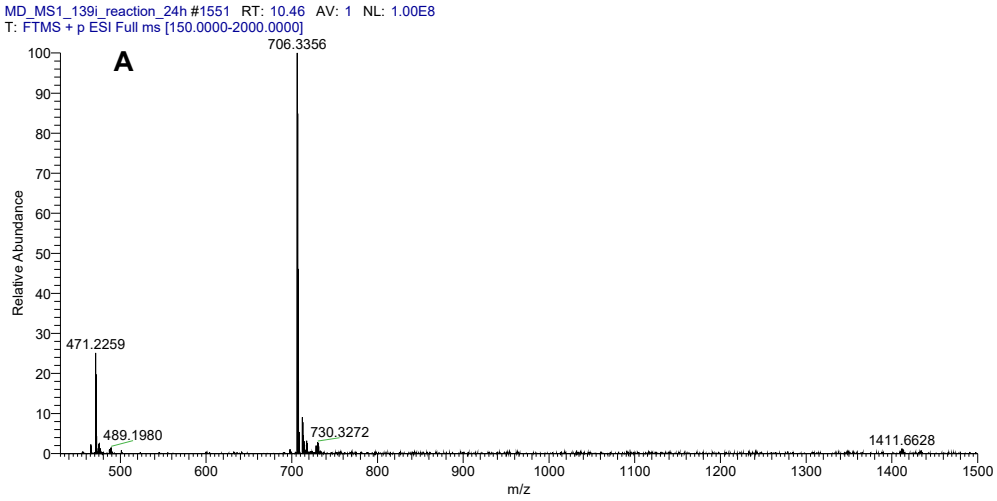

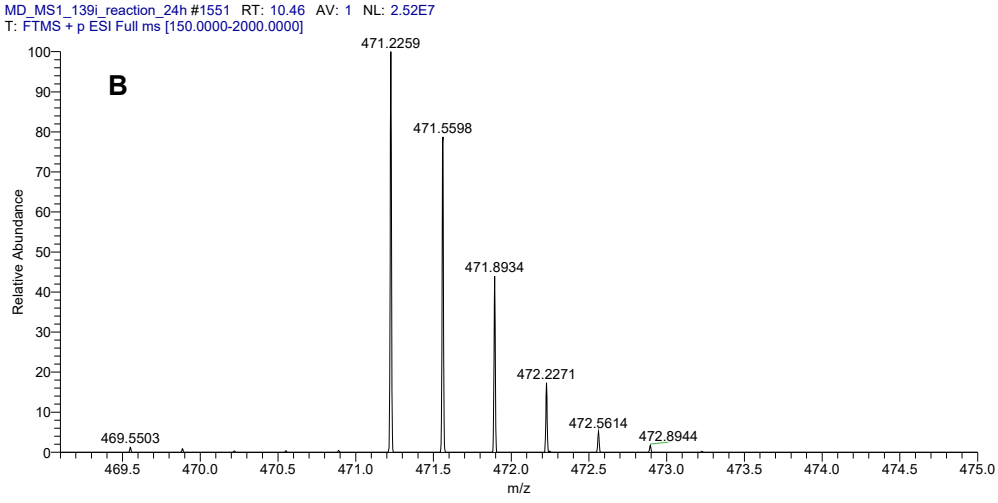

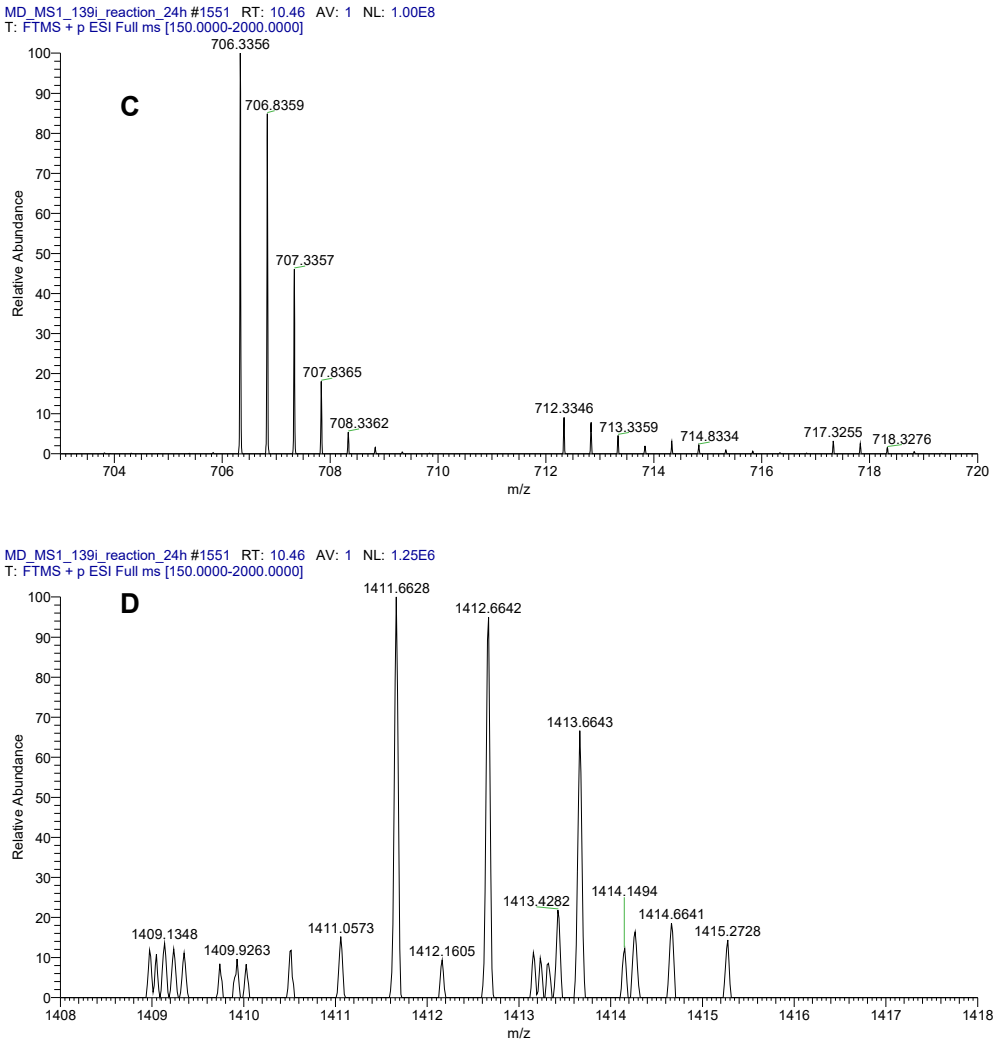

Figure S 73. A) Full ESI^{+}-HRMS spectrum of Cys-Bombesin conjugate **S29** ($C_{67}H_{97}N_{16}O_{14}S_2$ $[M+3H]^{3+}$ calculated: 471.2265, found *m/z* 471.2259; $C_{67}H_{96}N_{16}O_{14}S_2$ $[M+2H]^{2+}$ calculated: 706.3361, found *m/z* 706.3356; $C_{67}H_{95}N_{16}O_{14}S_2$ $[M+H]^{+}$ calculated: 1411.6650, found *m/z* 1411.6628, from TIC peak at RT 10.46 min); **B)** zoom-in of triple charged Cys-Bombesin in conjugate **S29**; **C)** zoom-in on double charged Cys-Bombesin conjugate **S29**; **D)** zoom-in of mono charged Cys-Bombesin conjugate **S29**.

13.5. Conjugation with Cys-Cys-Bombesin 23

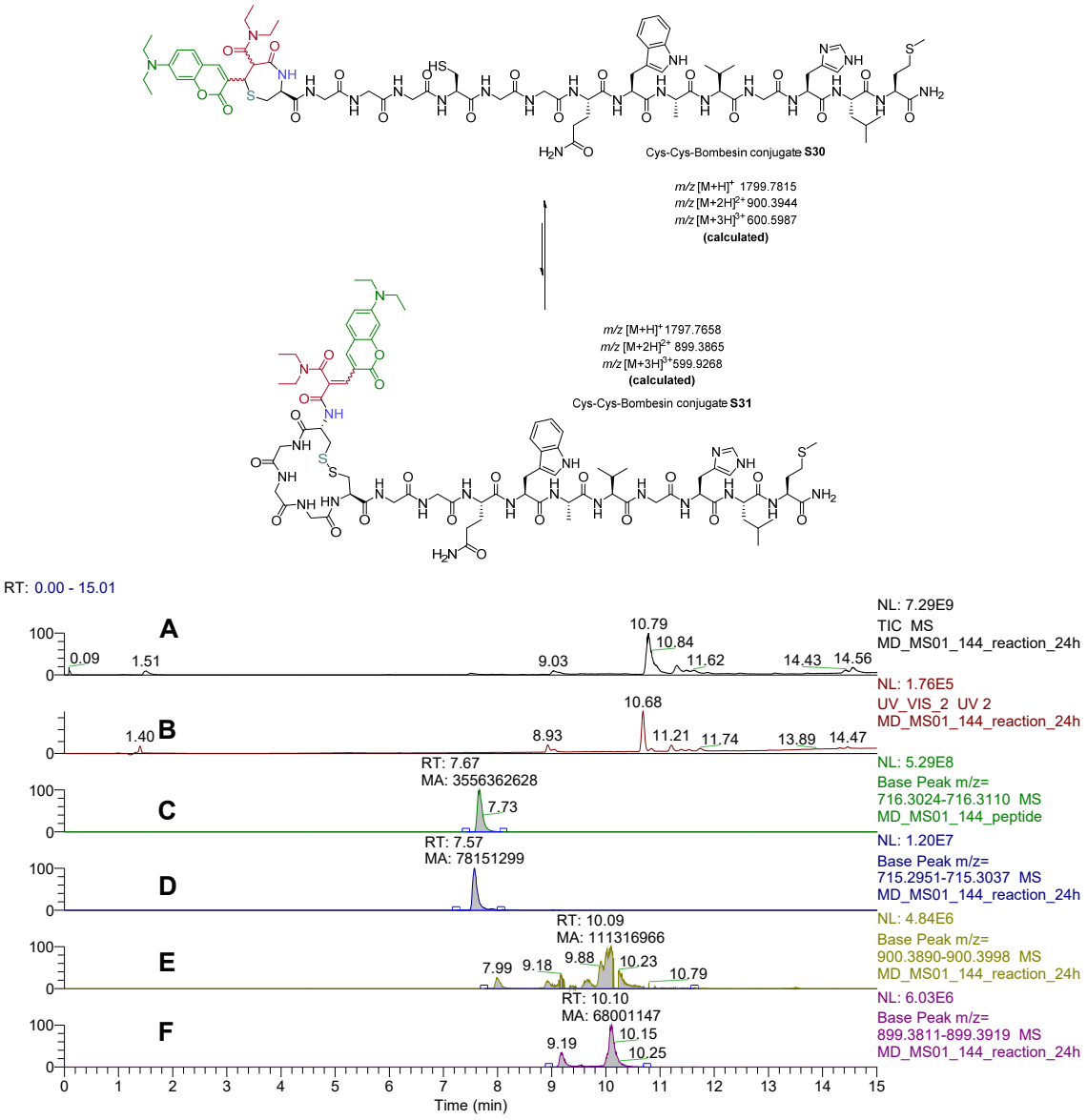

Figure S 74. LC-MS chromatograms of Cys-Cys-Bombesin conjugates **S30** and **S31** and Cys-Cys-Bombesin peptide **23**. **A)** Reaction mixture TIC after 24 h; **B)** Reaction detection at 254 nm, after 24 h; **C)** Reaction t_0 – unreacted Cys-Cys-Bombesin **23** EIC (base peak *m/z* 716.3067); **D)** Unreacted Cys-Cys-Bombesin **23** EIC after 24 h reaction with 10 equiv of **31**; **E)** Cys-Cys-Bombesin conjugate **S30** EIC (base peak *m/z* 900.3944) after 24 h reaction. **F)** Cys-Cys-Bombesin conjugate **S31** EIC (base peak *m/z* 899.3865) after 24 h reaction. Cys-Cys-Bombesin **23** conversion was calculated based on the EIC intensity (AUC) within δ 6 ppm range.

Table S 19. Cys-Cys-Bombesin peptide **23** conversion in 24 h reaction with coumarin NHS-activated acrylate **31** according to AUC from EIC chromatograms of base peak *m/z* 716.3067, within δ 6 ppm range.

	t_0	24 h	Conversion
Cys-Cys-Bombesin (AUC a.u.)	3556362628	78151299	98%

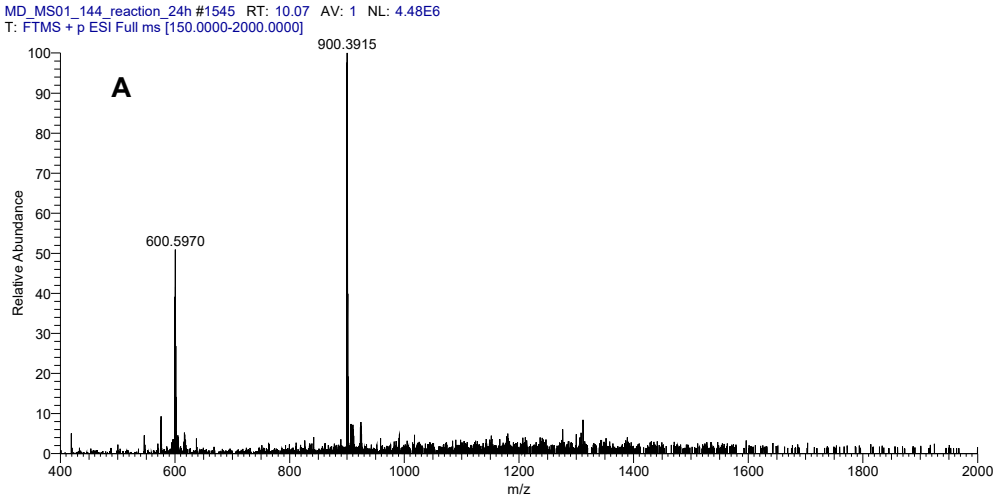

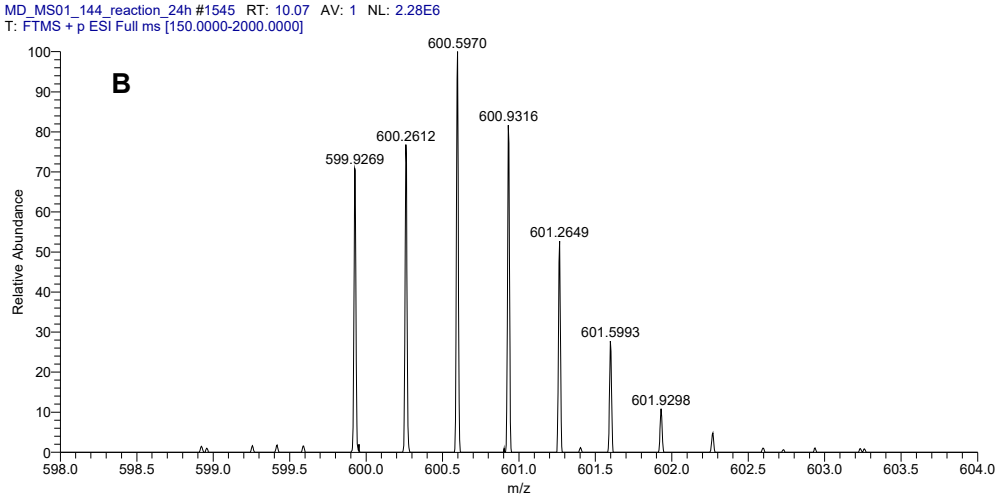

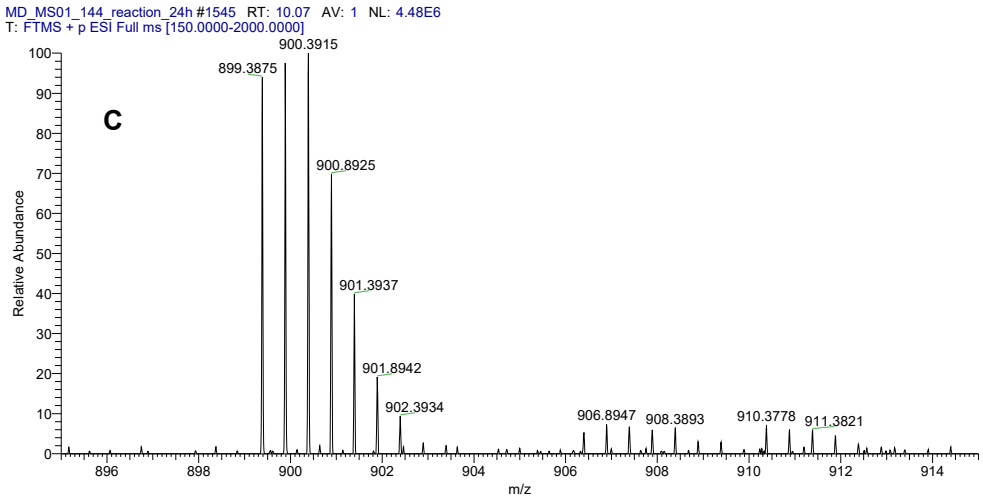

Figure S 75. A) Full ESI^{+}-HRMS spectrum of Cys-Cys-Bombesin conjugate **S30** ($C_{80}H_{117}N_{22}O_{20}S_3$ $[M+3H]^{3+}$ calculated: 600.5987, found *m/z* 600.5970; $C_{80}H_{116}N_{22}O_{20}S_3$ $[M+2H]^{2+}$ calculated: 900.3944, found *m/z* 900.3915; $C_{80}H_{115}N_{22}O_{20}S_3$ $[M+H]^{+}$ calculated: 1799.7815, not found, from TIC peak at RT 10.07 min); **B)** zoom-in of triple charged Cys-Cys-Bombesin in conjugate **S30**; **C)** zoom-in on double charged Cys-Cys-Bombesin conjugate **S30**.

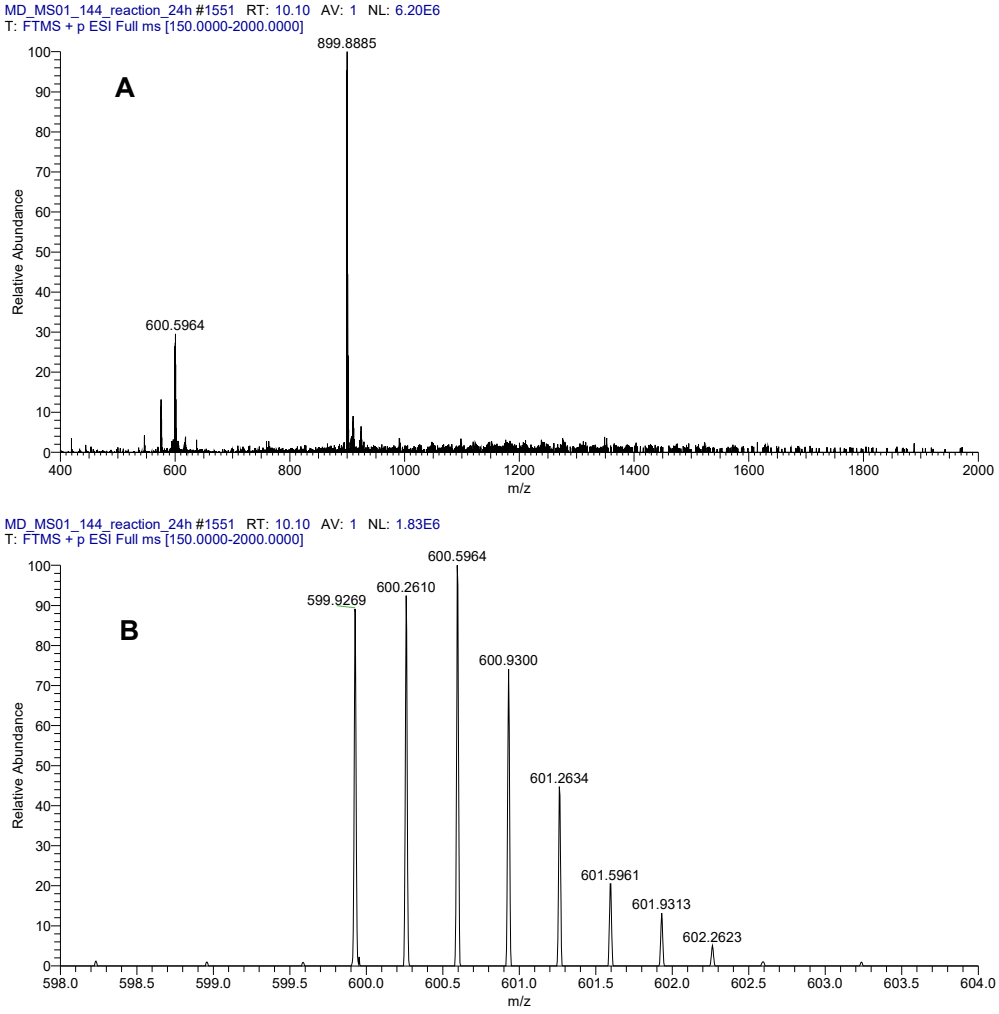

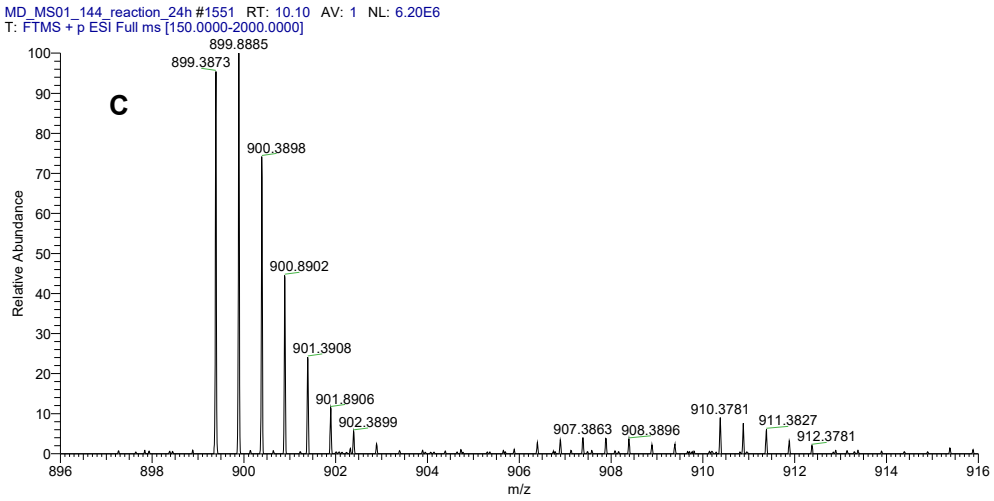

Figure S 76. A) Full ESI$^+$-HRMS spectrum of Cys-Cys-Bombesin conjugate **S30** ($C_{81}H_{116}N_{21}O_{20}S_3$ $[M+3H]^{3+}$ calculated: 599.9268, found *m/z* 599.9269; $C_{81}H_{115}N_{21}O_{20}S_3$ $[M+2H]^{2+}$ calculated: 899.3865, found *m/z* 899.8885; $C_{81}H_{114}N_{21}O_{20}S_3$ $[M+H]^+$ calculated: 1797.7658, not found, from TIC peak at RT 10.1 min); **B)** zoom-in of triple charged Cys-Cys-Bombesin in conjugate **S30**; **C)** zoom-in on double charged Cys-Cys-Bombesin conjugate **S30**.

13.6. Procedure for the peptide conjugation with 2,5-dioxopyrrolidin-1-yl-13-((7-(diethylamino)-2-oxo-2H-chromen-3 yl)methylene)-11-methyl-12-oxo-2,5,8-trioxa-11-azatetradecan-14-oate 34

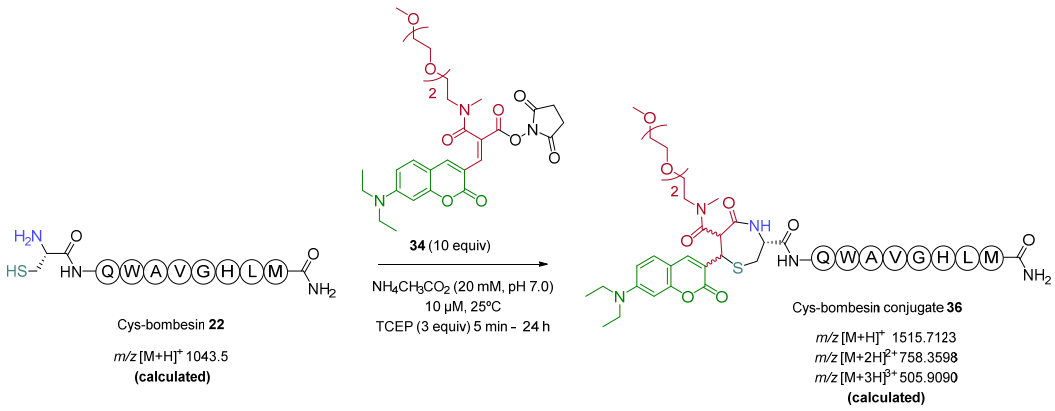

To a solution of Cys-bombesin **22** (1 mM in water) (10 µL, 10.0 nmol) in ammonium acetate 20 mM, pH 7.0 (1.0 mL) was added 3 equiv of 3,3',3"-phosphanetriyltripropionic acid hydrochloride (TCEP 1.0 mg/mL in water 3.5 mM) (8.57 µL, 30.0 nmol) and the mixture was reacted at 25ºC (RT) for approximately 1 h. Afterwards, 10 equiv of 2,5-dioxopyrrolidin-1-yl-13-((7-(diethylamino)-2-oxo-2H-chromen-3 yl)methylene)-11-methyl-12-oxo-2,5,8-trioxa-11-azatetradecan-14-oate **34** (30 mM in ACN) (3.33 µL, 0.100 µmol) was added and the reaction progression was monitored by LC-HRMS in Positive Mode. The HPLC runs were carried out with a gradient of A (Milli Q water containing 0.1% v/v Formic acid, FA) and B (acetonitrile containing 0.1% v/v FA, Honeywell HPLC-grade). The mobile phase was t = 0 min, 1% B;

t = 10 min, 75% B; t = 10.1 min, 95% B; t = 12 min, 95% B; t = 12.5 min, 1% B; t = 15 min stop, at a flow rate of 0.3 mL/min, detection at 254 nm.

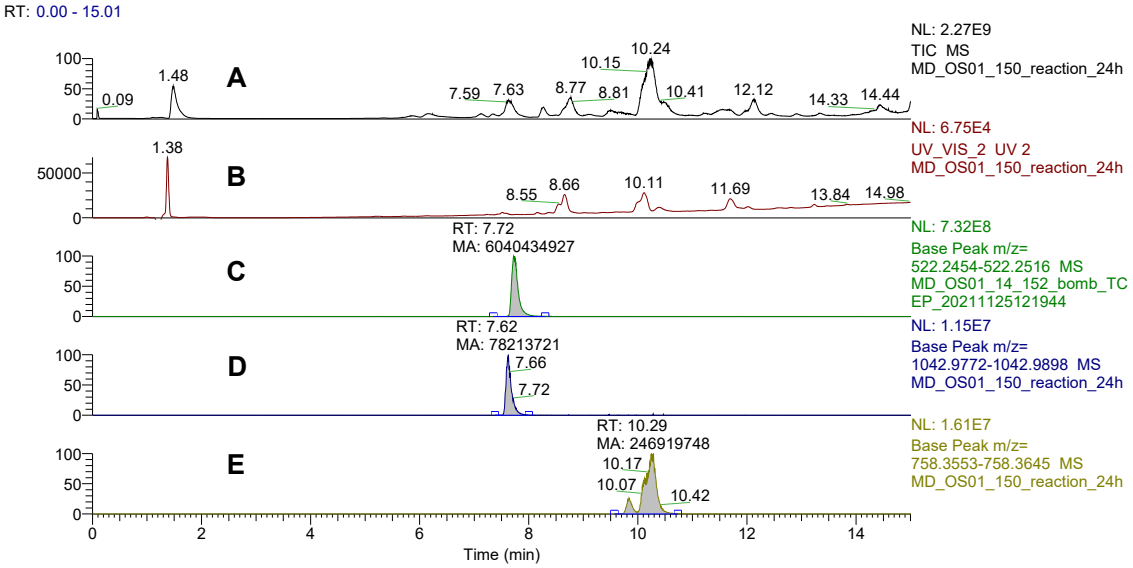

Figure S 77. HPLC chromatograms of Cys-Bombesin conjugate **36** and Cys-Bombesin peptide **22**. **A)** Reaction mixture TIC after 24 h; **B)** Reaction detection at 254 nm, after 24 h; **C)** Reaction t_0 – unreacted Cys-Bombesin EIC (base peak *m/z* 522.2485); **D)** Unreacted Cys-Bombesin EIC after 24 h reaction with 10 equiv of **34**; **E)** Cys-Bombesin conjugate **36** EIC (base peak *m/z* 758.3599) after 24 h reaction. Cys-Bombesin conversion was calculated based on the EIC intensity (AUC) within δ 6 ppm range.

Table S 20. Cys-Bombesin peptide conversion in 24 h reaction with coumarin NHS-activated acrylate **34** according to AUC from EIC chromatograms of base peak *m/z* 522.2485, within δ 6 ppm range.

	t_0	24 h	Conversion
Cys-Bombesin (AUC a.u.)	6040434927	78213720	99%

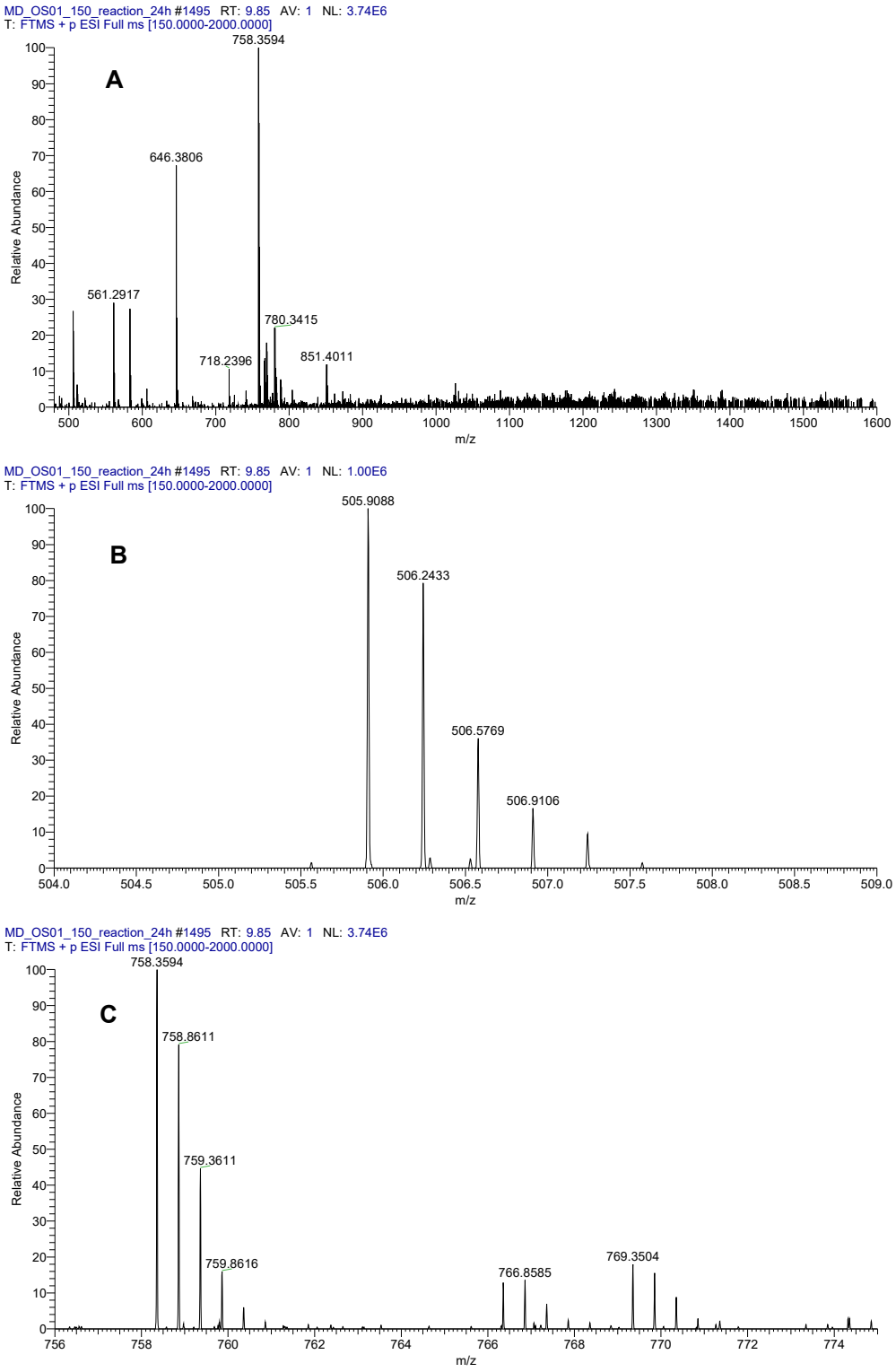

Figure S 78. A) Full ESI$^+$-HRMS spectrum of Cys-Bombesin conjugate **36** ($C_{71}H_{105}N_{16}O_{17}S_2$ $[M+3H]^{3+}$ calculated: 505.9090, found *m/z* 505.9088; $C_{71}H_{104}N_{16}O_{17}S_2$ $[M+2H]^{2+}$ calculated: 758.3598, found *m/z* 758.3594; $C_{71}H_{103}N_{16}O_{17}S_2$ $[M+H]^+$ calculated: 1515.7123, not found, from TIC peak at RT 9.85 min); **B)** zoom-in of triple charged Cys-Bombesin in conjugate **36**; **C)** zoom-in on double charged Cys-Bombesin conjugate **36**.

14. Isolation of bioconjugates

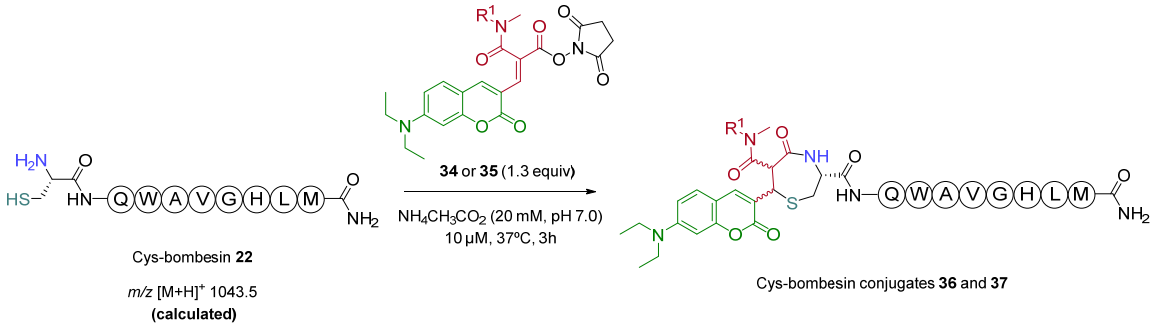

To a solution of Cys-bombesin **22** (20 mM, 2.86 µmol) in ammonium acetate 20 mM, pH 7.0 (143 µL) was added 1.3 equiv. of reagent **34** – **35** (20 mM, 3.72 µmol in DMF) (186 µL) at 37ºC.The reaction progression was monitored by LC-HRMS in Positive Mode. The HPLC runs were carried out with a gradient of A (Milli Q water containing 0.1% v/v Formic acid, FA) and B (acetonitrile containing 0.1% v/v FA, Honeywell HPLC-grade). The mobile phase was t = 0 min, 5% B; t = 4 min, 5% B; t = 15 min, 95% B; t = 16 min, 95% B; t = 17min, 5% B; t = 20 min stop, at a flow rate of 0.3 mL/min, detection at 254 nm and 365 nm.

Bioconjugates were purified by reverse phase preparative HPLC carried out with a gradient of gradient of A (Milli Q water containing 0.1% v/v Formic acid, FA) and B (acetonitrile containing 0.1% v/v FA, Honeywell HPLC-grade). The mobile phase was t = 0 min, 5% B; t = 4 min, 5% B; t = 15 min, 95% B; t = 16 min, 95% B; t = 17min, 5% B; t = 18 min stop, at a flow rate of 5 mL/min, detection at 365 nm.

14.1. Cys-Bombesin conjugate 36

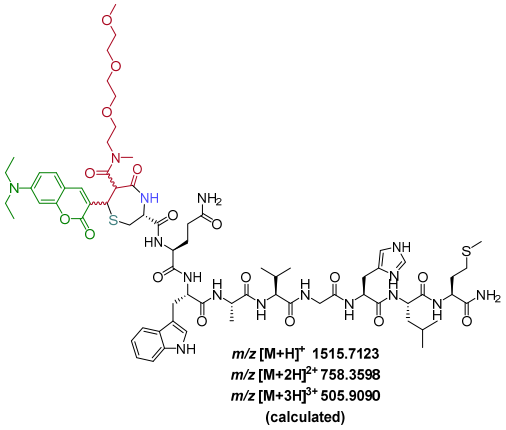

Cys-bombesin conjugate **36** was attained with 8.6% isolated yield.

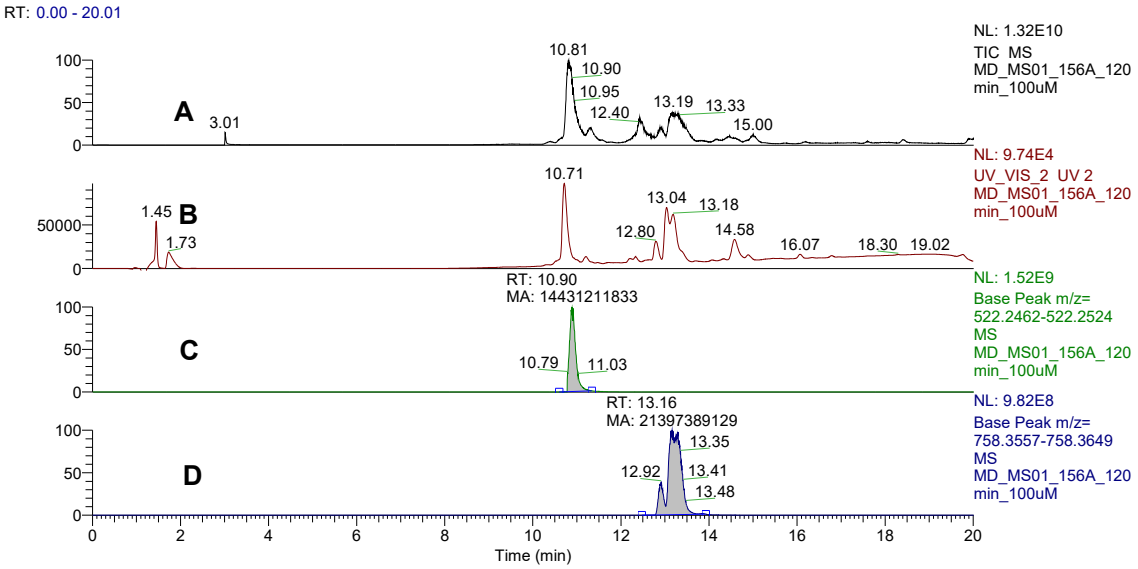

Figure S 79. HPLC chromatograms of Cys-Bombesin **22** reaction with **34** conjugate after 2h. **A)** TIC; **B)** Full spectrum UV detection at 254 nm; **C)** Cys-bombesin **22** EIC (base peak *m/z* 522.2493); **D)** Conjugate **36** EIC (base peak *m/z* 758.3603).

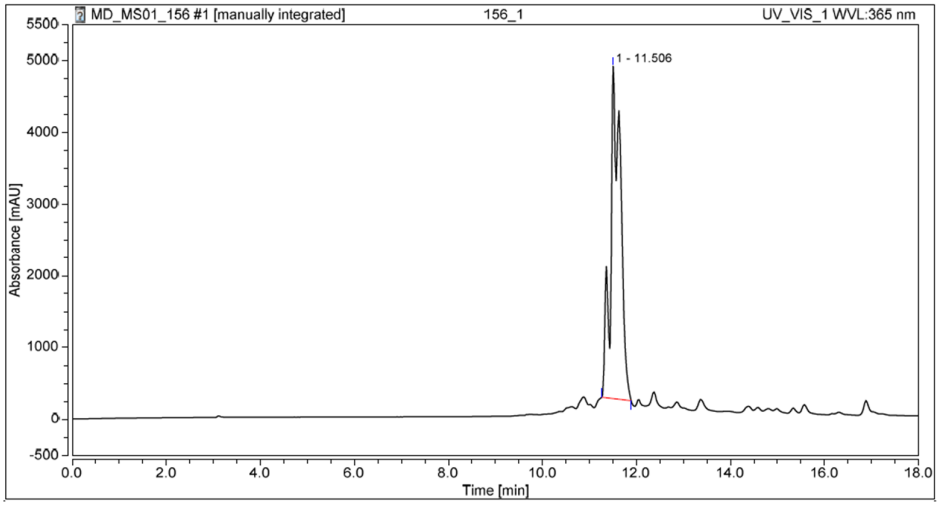

Figure S 80. Semi preparative RP-HPLC chromatogram monitored at 365 nm. The desired product **36** was isolated at 11.5 min.

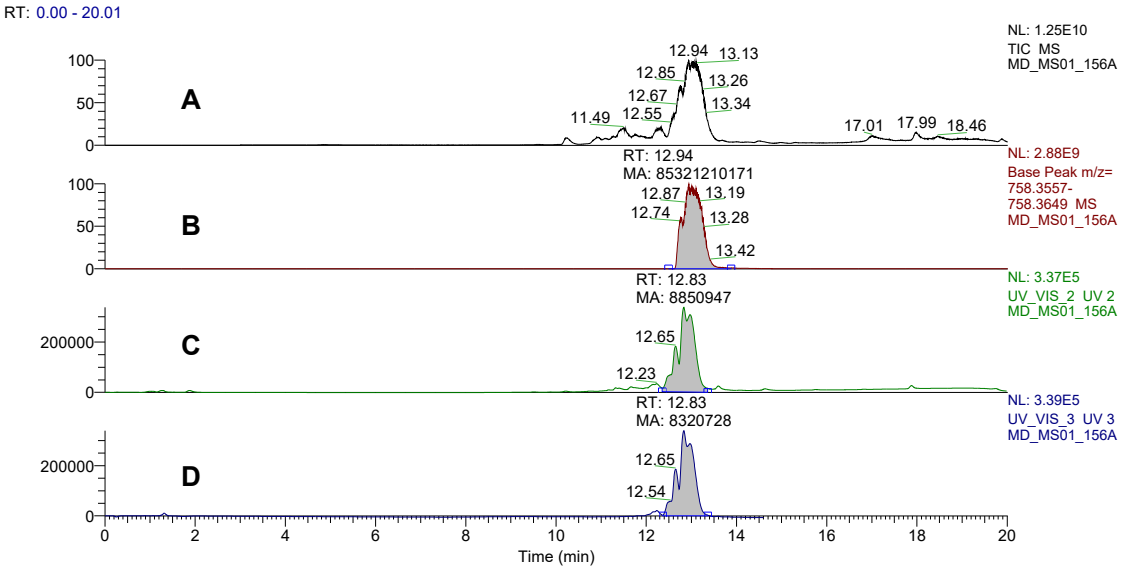

Figure S 81. HPLC chromatograms of Cys-Bombesin conjugate **36** after purification with preparative reverse phase HPLC: **A)** TIC; **B)** Cys-Bombesin conjugate **36** EIC (base peak *m/z* 758.3603); **C)** Conjugate **36** detection at 254 nm; **D)** Conjugate **36** detection at 365 nm.

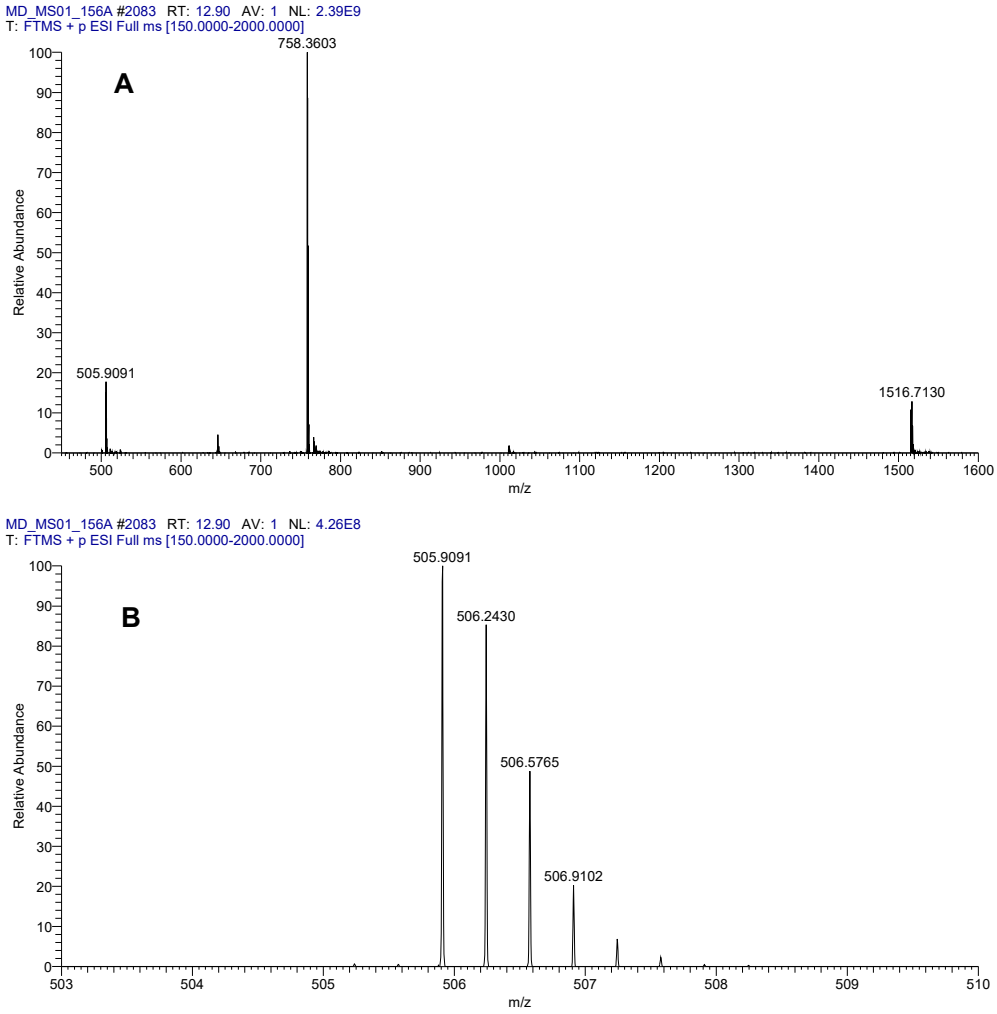

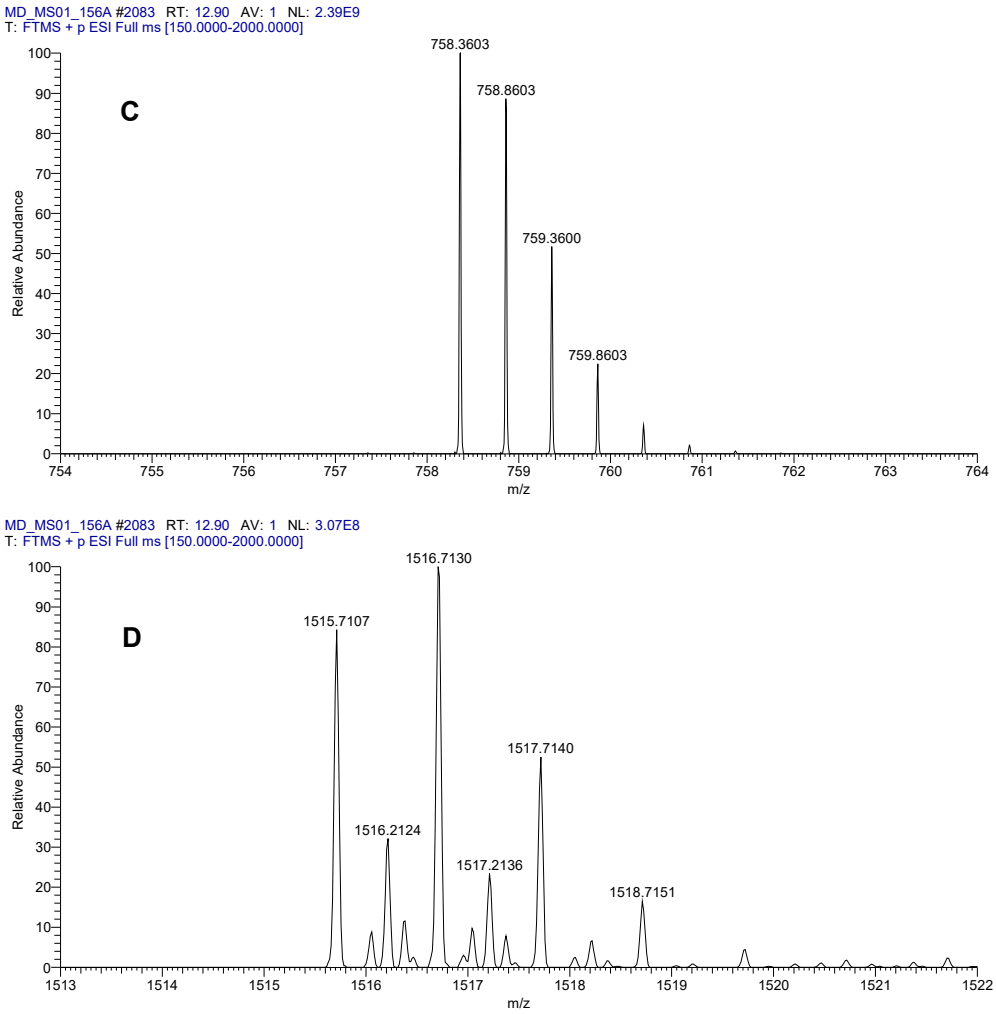

Figure S 82. A) Full ESI^{+}-HRMS spectrum of Cys-Bombesin conjugate **36** ($C_{71}H_{105}N_{16}O_{17}S_2$ $[M+3H]^{3+}$ calculated: 505.9090, found *m/z* 505.9091; $C_{71}H_{104}N_{16}O_{17}S_2$ $[M+2H]^{2+}$ calculated: 758.3598, found *m/z* 758.3603; $C_{71}H_{103}N_{16}O_{17}S_2$ $[M+H]^{+}$ calculated: 1515.7123, found *m/z* 1515.7107, from TIC peak at RT 12.9 min); **B)** zoom-in of triple charged Cys-Bombesin in conjugate **36**; **C)** zoom-in on double charged Cys-Bombesin conjugate **36**; **D)** zoom-in on mono charged Cys-Bombesin conjugate **36**.

14.2. Cys-Bombesin conjugate 37

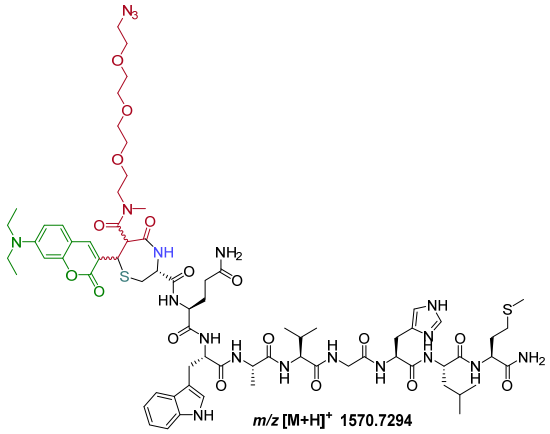

Cys-bombesin conjugate **37** was attained with 13.9% isolated yield.

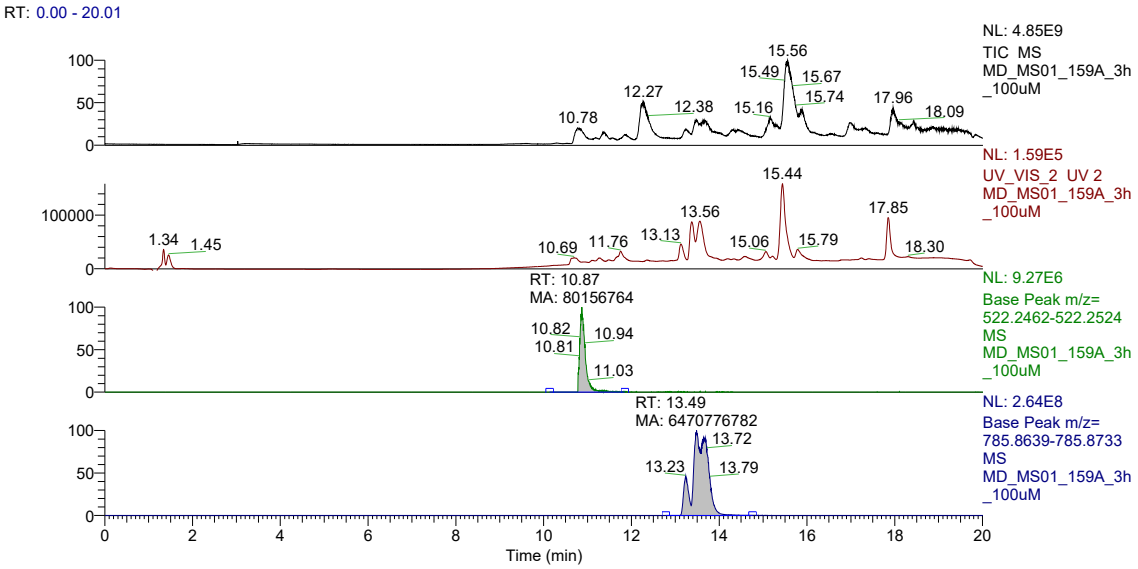

Figure S 83. HPLC chromatograms of Cys-Bombesin **22** reaction with **35** conjugate after 3h. **A)** TIC; **B)** Full spectrum UV detection at 254 nm; **C)** Cys-bombesin **22** EIC (base peak *m/z* 522.2493); **D)** Conjugate **37** EIC (base peak *m/z* 785.8686).

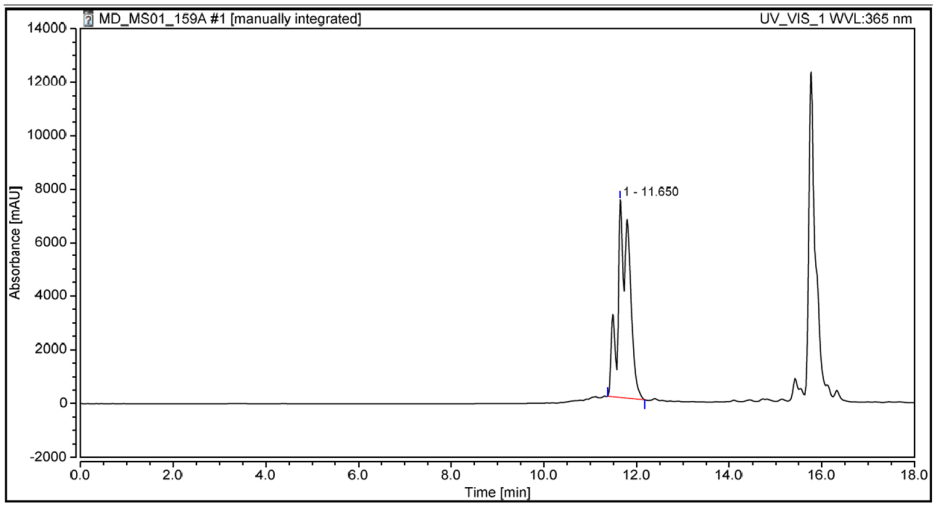

Figure S 84. Semi preparative RP-HPLC chromatogram monitored at 365 nm. The desired product **37** was isolated at 11.7 min.

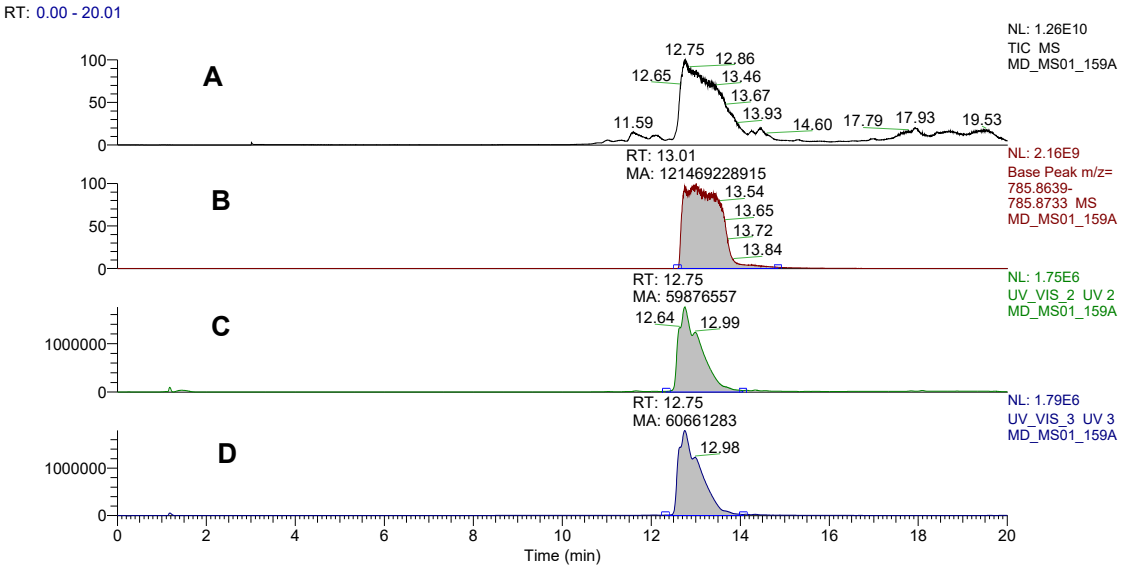

Figure S 85. HPLC chromatograms of Cys-Bombesin conjugate **37** after purification with preparative reverse phase HPLC: **A)** TIC; **B)** Cys-Bombesin conjugate **37** EIC (base peak *m/z* 785.8686); **C)** Conjugate **37** detection at 254 nm; **D)** Conjugate **37** detection at 365 nm.

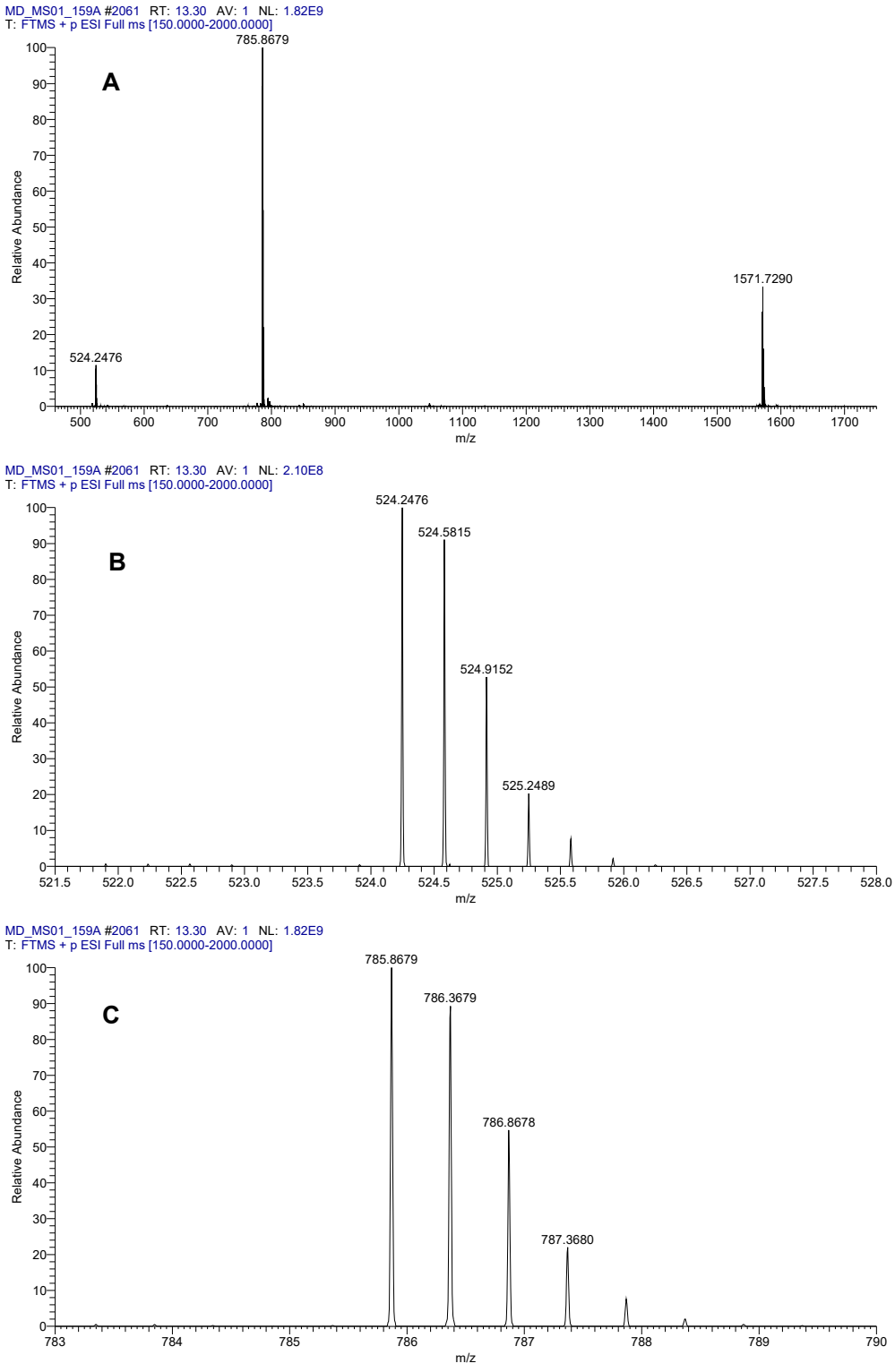
MD_MS01_159A #2061 RT: 13.30 AV: 1 NL: 1.82E9
T: FTMS + p ESI Full ms [150.0000-2000.0000]
A
785.8679
1571.7290
524.2476
Relative Abundance
m/z
MD_MS01_159A #2061 RT: 13.30 AV: 1 NL: 2.10E8
T: FTMS + p ESI Full ms [150.0000-2000.0000]
B
524.2476
524.5815
524.9152
525.2489
Relative Abundance
m/z
MD_MS01_159A #2061 RT: 13.30 AV: 1 NL: 1.82E9
T: FTMS + p ESI Full ms [150.0000-2000.0000]
C
785.8679
786.3679
786.8678
787.3680
Relative Abundance
m/z

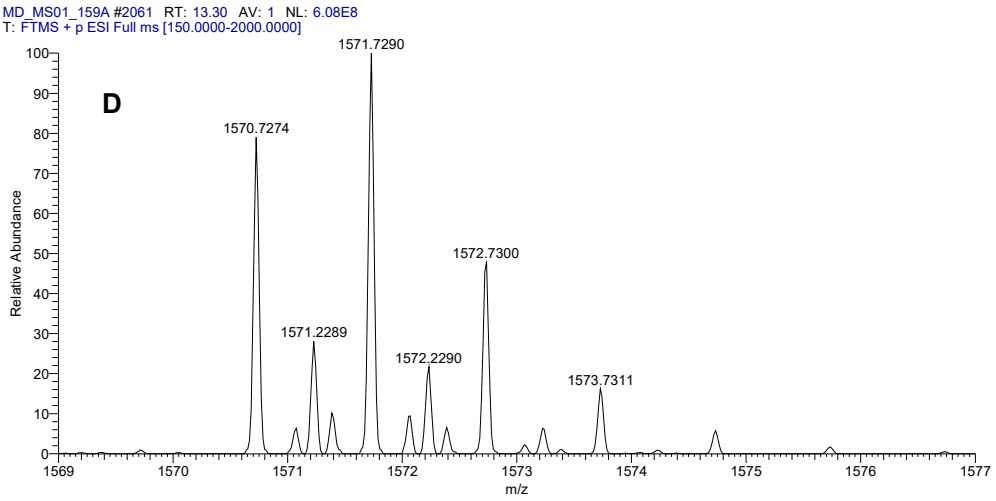

Figure S 86. A) Full ESI$^+$-HRMS spectrum of Cys-Bombesin conjugate **37** ($C_{72}H_{106}N_{19}O_{17}S_2$ $[M+3H]^{3+}$ calculated: 524.2480, found *m/z* 524.2476; C $C_{72}H_{105}N_{19}O_{17}S_2$ $[M+2H]^{2+}$ calculated: 785.8683, found *m/z* 785.8679; $C_{72}H_{104}N_{19}O_{17}S_2$ $[M+H]^+$ calculated: 1570.7294, found *m/z* 1570.7274, from TIC peak at RT 13.3 min); **B)** zoom-in of triple charged Cys-Bombesin in conjugate **37**; **C)** zoom-in on double charged Cys-Bombesin conjugate **37**; **D)** zoom-in on mono charged Cys-Bombesin conjugate **37**.

15. Synthesis of Cys-bombesin conjugate 38

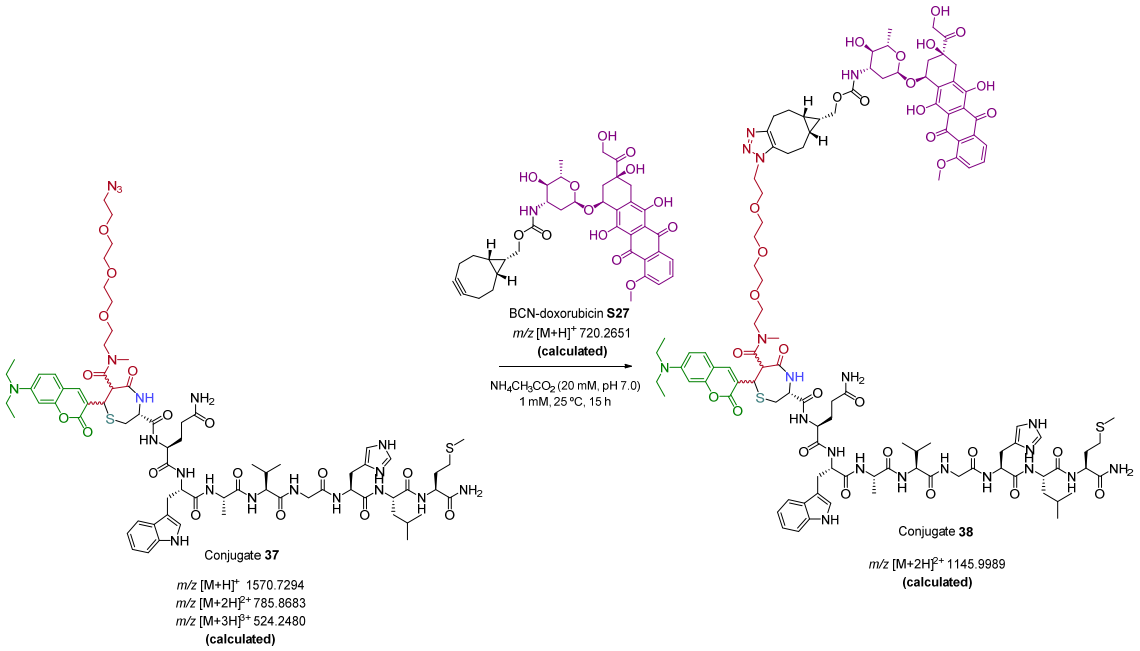

To a solution of Cys-Bombesin-Coumarin-PEG-azide conjugate **37** (10 mM in 50% ACN:KPi 50 mM, pH 7.0) (10.0 µL, 0.100 µmol) in 50% ACN:Ammonium acetate 20 mM, pH 7.0 (100 µL) was added a solution of BCN-Doxorubicin **S27** (1 mM in ACN) (10.0 µL, 0.100 µmol). The reaction was monitored by LC-MS with UV detection at 480 nm after 15–18 h, showing complete conversion into the desired conjugate **38**.

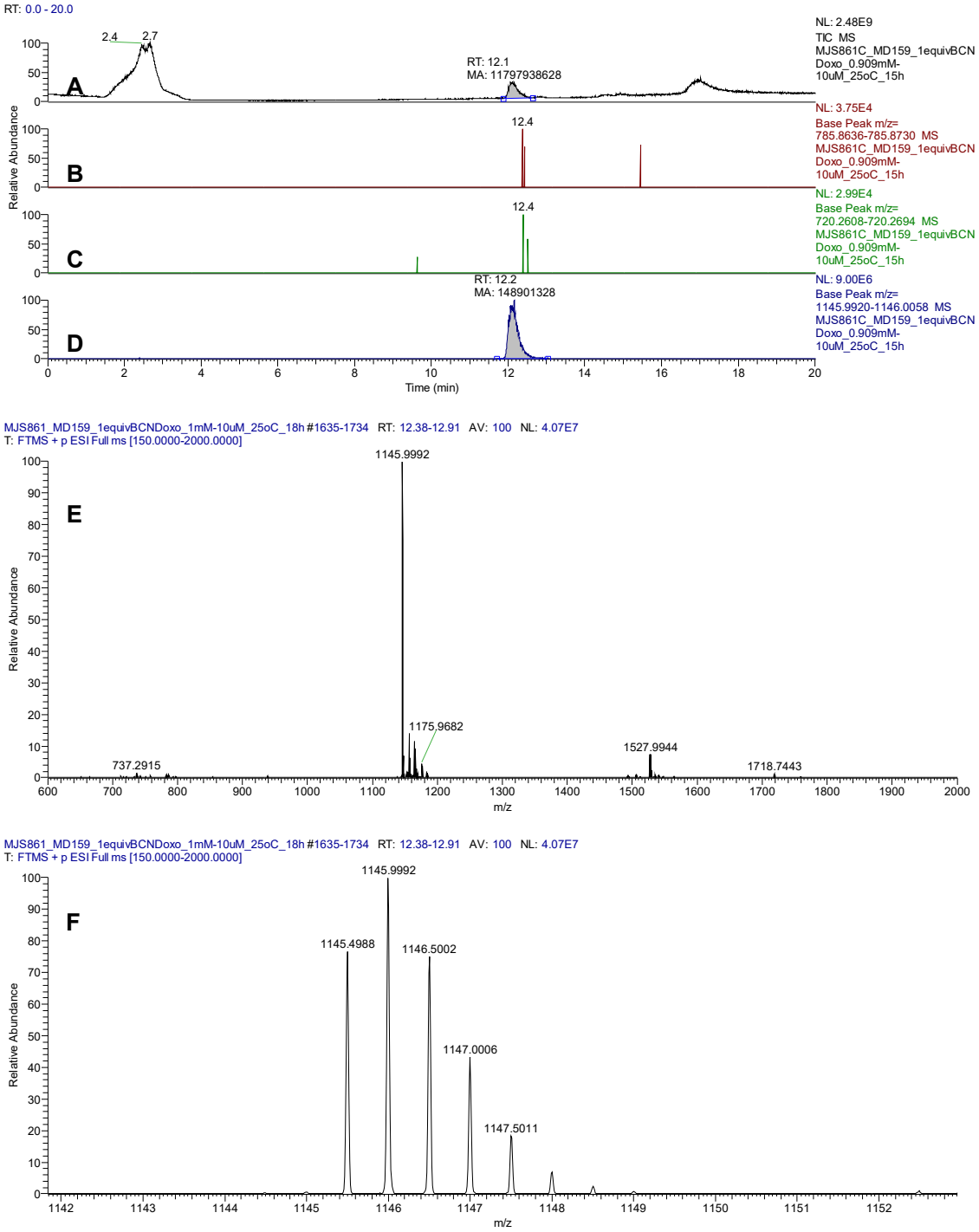

Figure S 87. LC-MS chromatograms of Cys-bombesin conjugate **37** after click reaction with BCN-doxorubicin **S27**: **A)** TIC; **B)** Cys-bombesin conjugate **37** EIC (base peak *m/z* 785.8683); **C)** BCN-doxorubicin **S27** EIC (base peak *m/z* 720.2651); **D)** Cys-bombesin conjugate **38** EIC (base peak *m/z* 1145.9989). **E)** ESI^{+}-HRMS spectrum of Cys-Bombesin conjugate **38** ($C_{110}H_{146}N_{20}O_{30}S_{22}$ $[M+2H]^{2+}$ calculated: 1145.9989, found *m/z* 1145.9992); **F)** zoom-in of double charged Cys-Bombesin in conjugate **38**.

16. Cell culture and staining procedures

Cell culture and maintenance

HeLa and HEK 293T cells used in this work were purchased from ECACC (European Collection of Authenticated Cell Cultures). The cells were cultured in Dulbecco's Modified Eagle Medium, DMEM (GIBCO™), supplemented with 10% fetal bovine serum (FBS, GIBCO™) and 1% penicillin/streptomycin (GIBCO™) and maintained in a humidified atmosphere with 5% CO_2 at 37 °C. This cell culture line was maintained with routinely subcultures (using TrypLE Express without phenol red, GIBCO™, for chemical detaching) and counted with a Neubauer chamber.

Confocal and multiphoton laser-scanning microscopy

All measurements were performed on a Leica TCS SP5 (Leica Microsystems CMS GmbH, Manheim, Germany) inverted confocal microscope (DMI6000). Images were collected at 514×514 resolution.

Excitation was provided by an Argon laser, He-Ne laser lines and Ti: sapphire laser (Spectra-Physics Mai Tai BB, 710-990 nm, 100 fs, 82 MHz) that were focused into the sample by an apochromatic water immersion objective (63x, NA 1.2; Zeiss, Jena Germany). A 111.4 μm diameter pinhole positioned in front of the image plane blocked out-of-focus signals.

HeLa and HEK 293T cells were co-incubated with 30 μM of conjugate **36** (excitation at 488 nm) and with commercially dye WGA-Alexa 633 (excitation at 633 nm) or Hoechst 33342 (Ti: sapphire laser) were incubated for 15 minutes according to the instructions of the supplier (Thermo Fisher Scientific). After completing the labeling protocol the unbounded dyes were removed by washing the cells with DPBS. A blank control with untreated cells maintained in either DPBS (for shorter incubation times) or cell culture medium (for longer incubation times) was added to the assay.

The cells were imaged according with the above descriptions and analyzed using ImageJ.

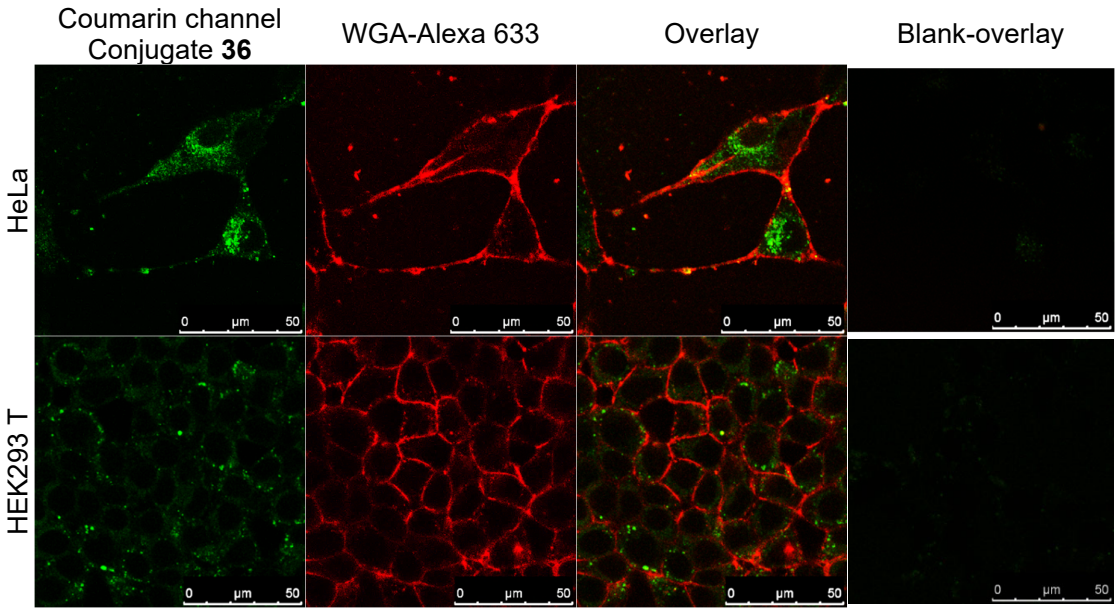

Figure S 88. Confocal microscopy imaging to HeLa and HEK293-T cells after 15 min incubation with conjugate **36** (30 µM) and WGA-Alexa 633.

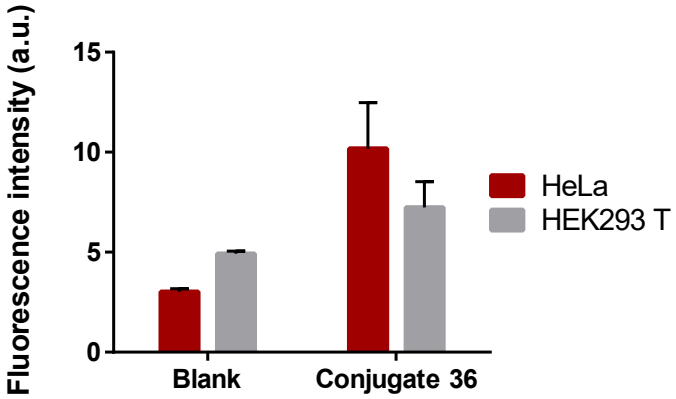

Figure S 89. Fluorescence intensity quantification of blank-overlay *vs* Conjugate **36**.

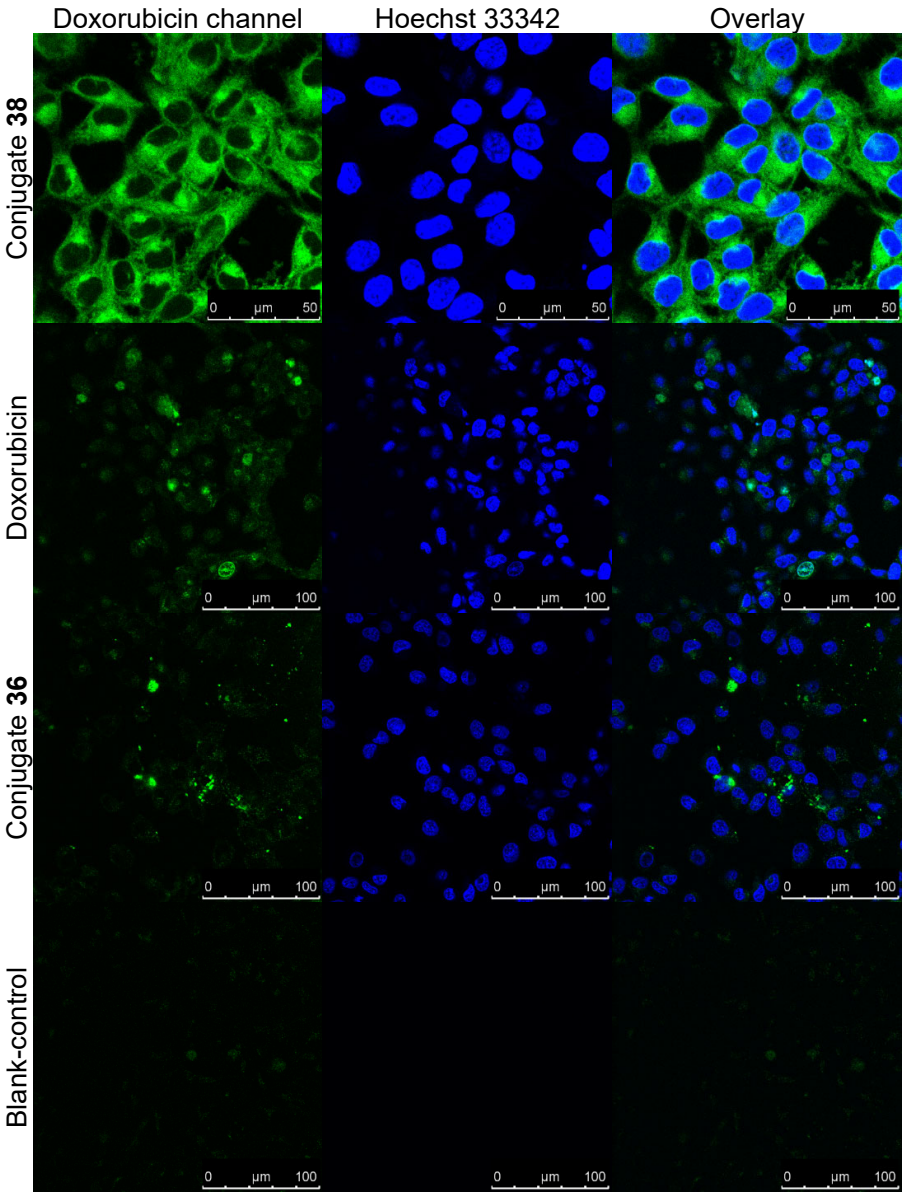

Figure S 90. Confocal microscopy imaging to HeLa cells after 15 min incubation with conjugates **36** and **38** (30 µM) and Hoechst 33342 probe for nucleus staining.

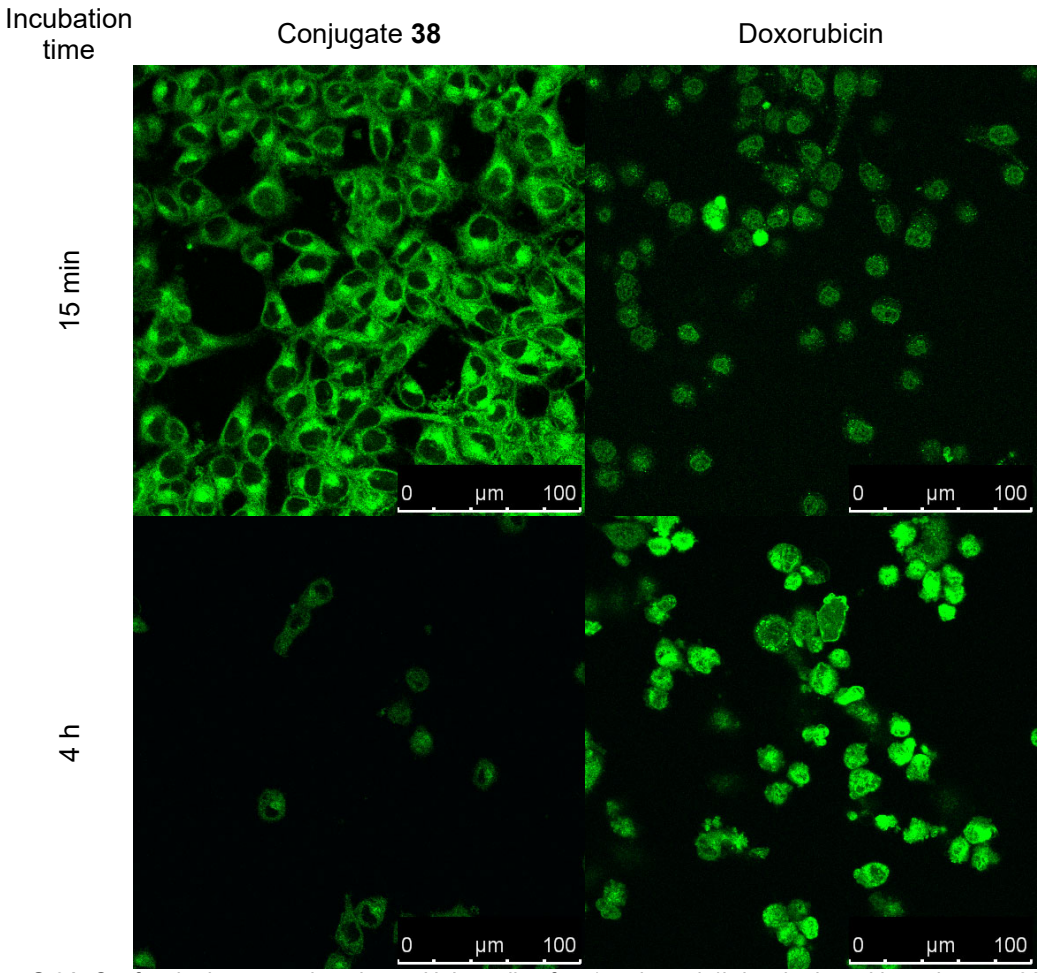

Figure S 91. Confocal microscopy imaging to HeLa cells after 15 min and 4h incubation with conjugates **36** and **38** (30 µM) with no Hoechst 33342 probe.

Wide-field fluorescence microscopy

HeLa cells were incubated with 30 μM of each compound for 15 min. A blank control with untreated cells maintained in either DPBS (for shorter incubation times) or cell culture medium (for longer incubation times) was added to the assay.

Bright field and fluorescence images were taken with an Olympus IX83 inverted microscope equipped with Digital Hamamatsu CMOS camera (C11440-36U) and Imaging Workstation (HP Z2 SFF G4). An UPLXAPO60X NA1.40 objective lens was used. Fluorescence images were acquired with: 1) Exciter filter: 340-390 nm, beam splitter: 410 nm, barrier filter: 420 nm; 2) Exciter filter: 470-495 nm, beam splitter: 505 nm, barrier filter: 510 nm; 3) Exciter filter: 530-550 nm, beam splitter: 570 nm, barrier filter: 575-625 nm.

The cells were imaged and analyzed using cellSens dimension and ImageJ software.

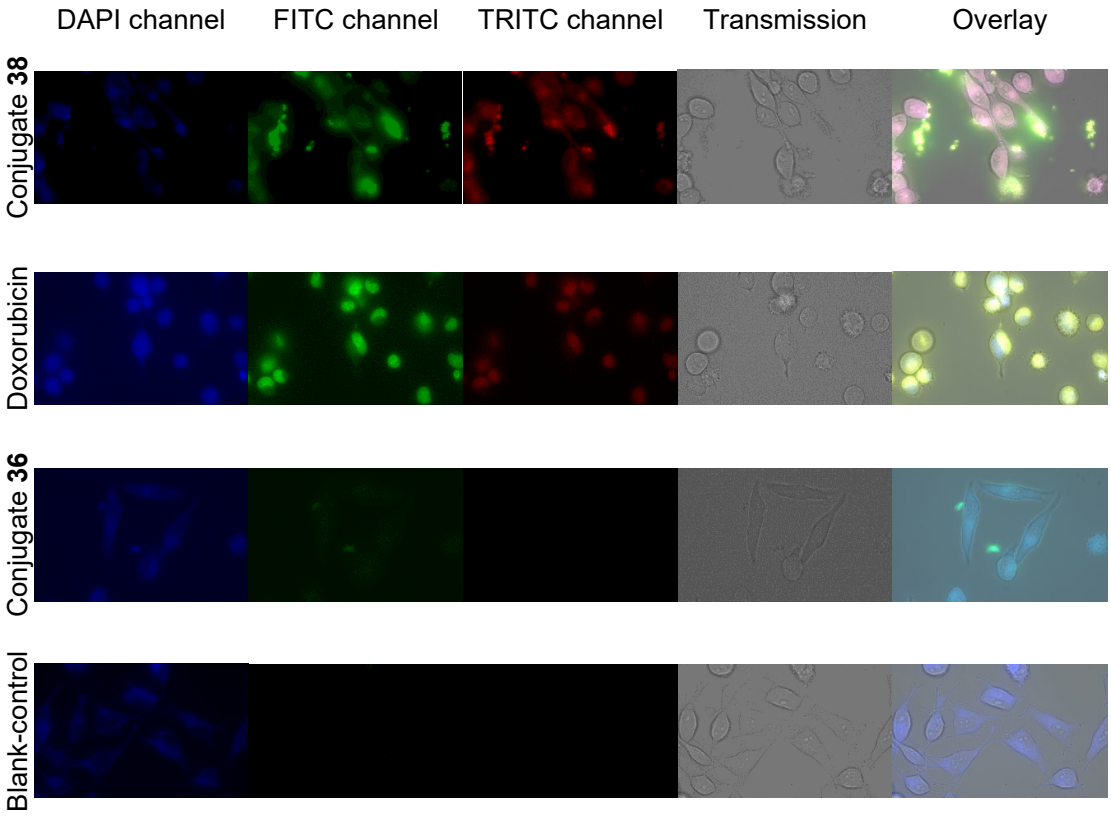

Figure S 92. Confocal and multiphoton laser-scanning and Wide-field fluorescence imaging to HeLa cells after 15 min incubation with conjugates **36** and **38** (30 μM) with DAPI channel overlay.

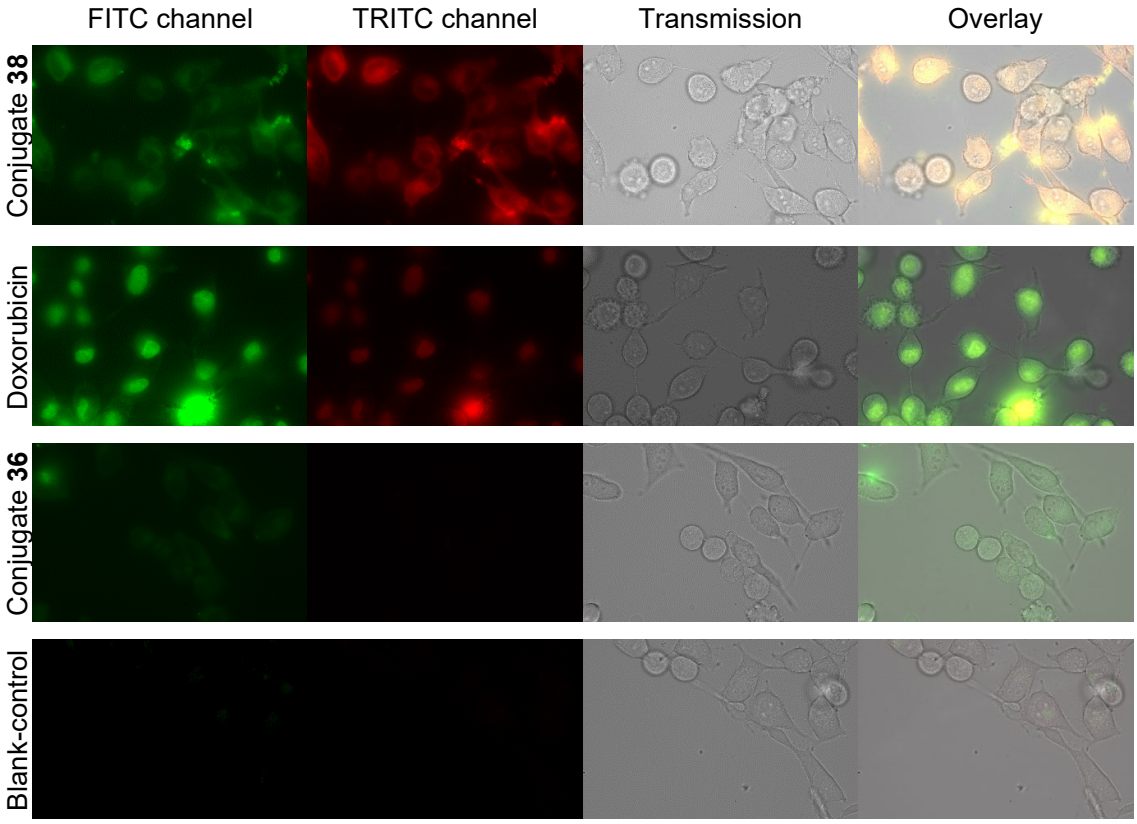

Figure S 93. Confocal and multiphoton laser-scanning and Wide-field fluorescence imaging to HeLa cells after 15 min incubation with conjugates **36** and **38** (30 μM).

17. Cytotoxicity assay

The toxicity effect of each compound was evaluated by resazurin based assay using PrestoBlue™, PB (Invitrogen, Carlsbad, CA, USA) reagent. Briefly, HeLa cell line were seeded in 96-well tissue cultured plates (Orange) at initial density of $1x10^4$-$2x10^4$ cells per well and left during 24h in CO_2 incubator (5%) at 37 °C. Then, complete cell medium (DMEM supplemented with 10% FBS and 1% penicillin-streptomycin) was discarded and replaced with solution of different compound doses previously prepared in complete cell culture medium. HeLa cells were incubated for additional 24h. Finally, the PB viability assay was performed accordingly with PrestoBlue ™ reagent kit protocol. The resazurin conversion into resorufin was monitored by measuring fluorescence intensity (excitation 530 nm, emission 590 nm) in a microplate reader (BMG Labtech, Polar Star Optima) at 37 ºC.

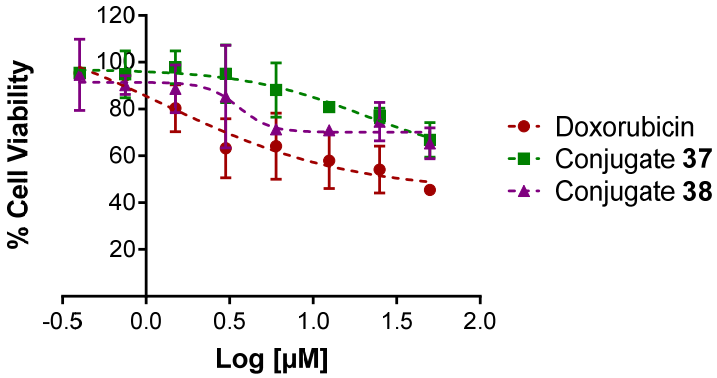

Figure S 94. Fluorometric cell viability assays in HeLa cells with doxorubicin positive control, conjugate **37** negative control and conjugate **38**.

18. NMR Spectra

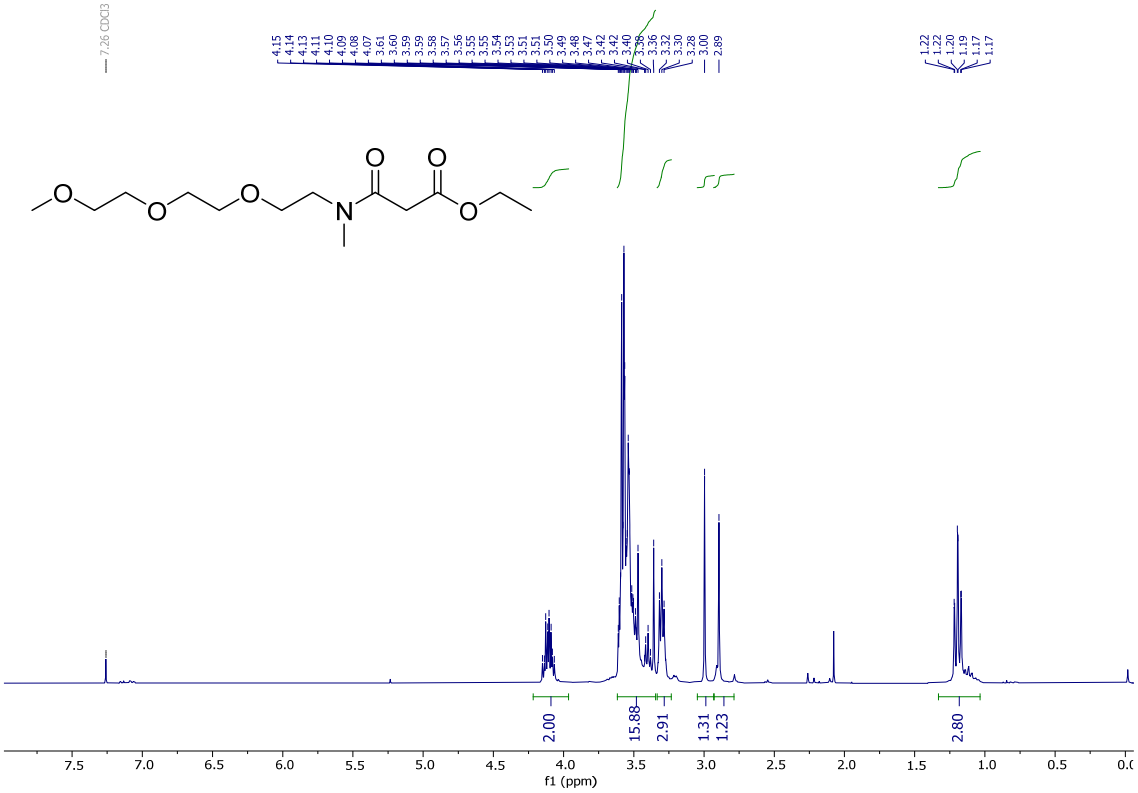

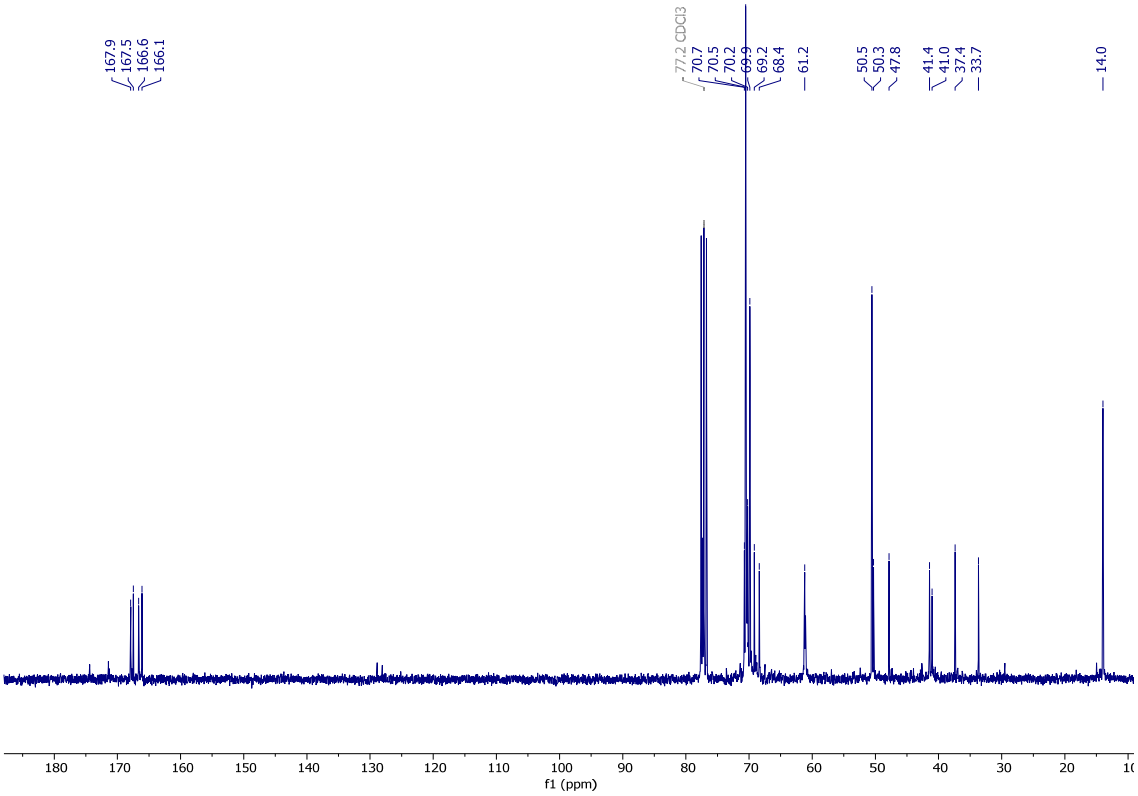

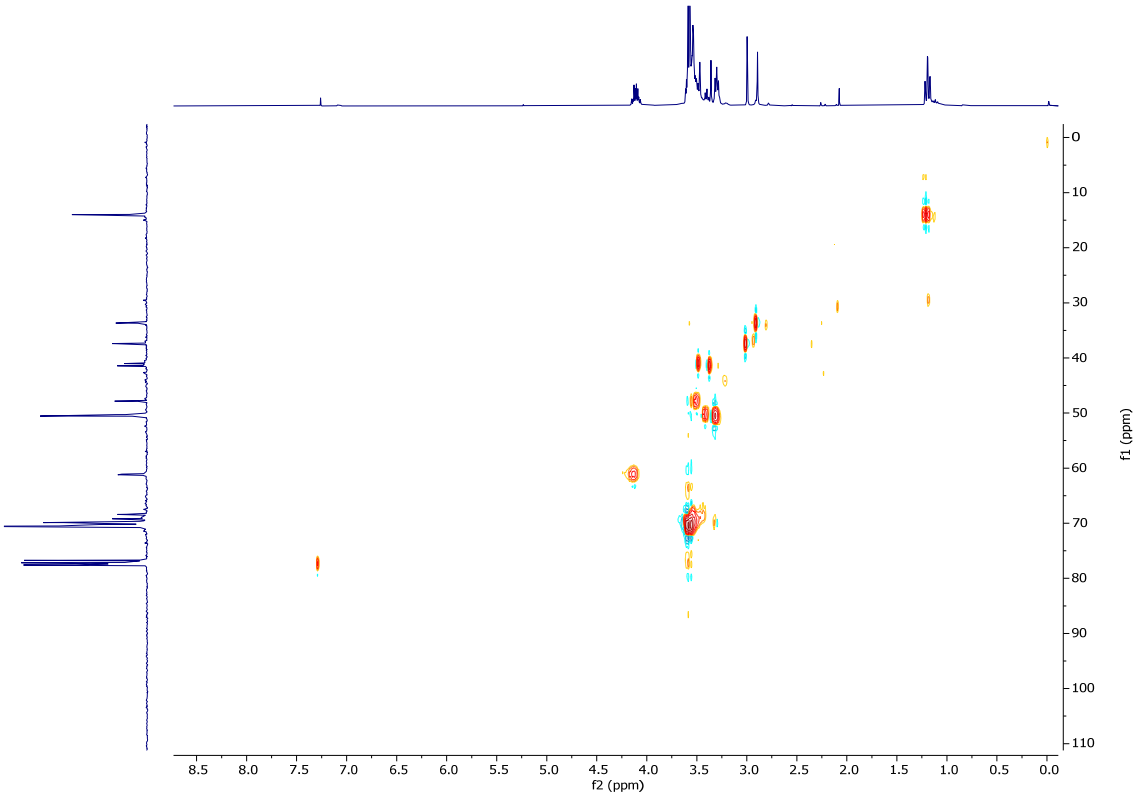

Figure S 95. ^{1}H-NMR, ^{13}C-NMR and HSQC of compound **S1** in $CDCl_3$.

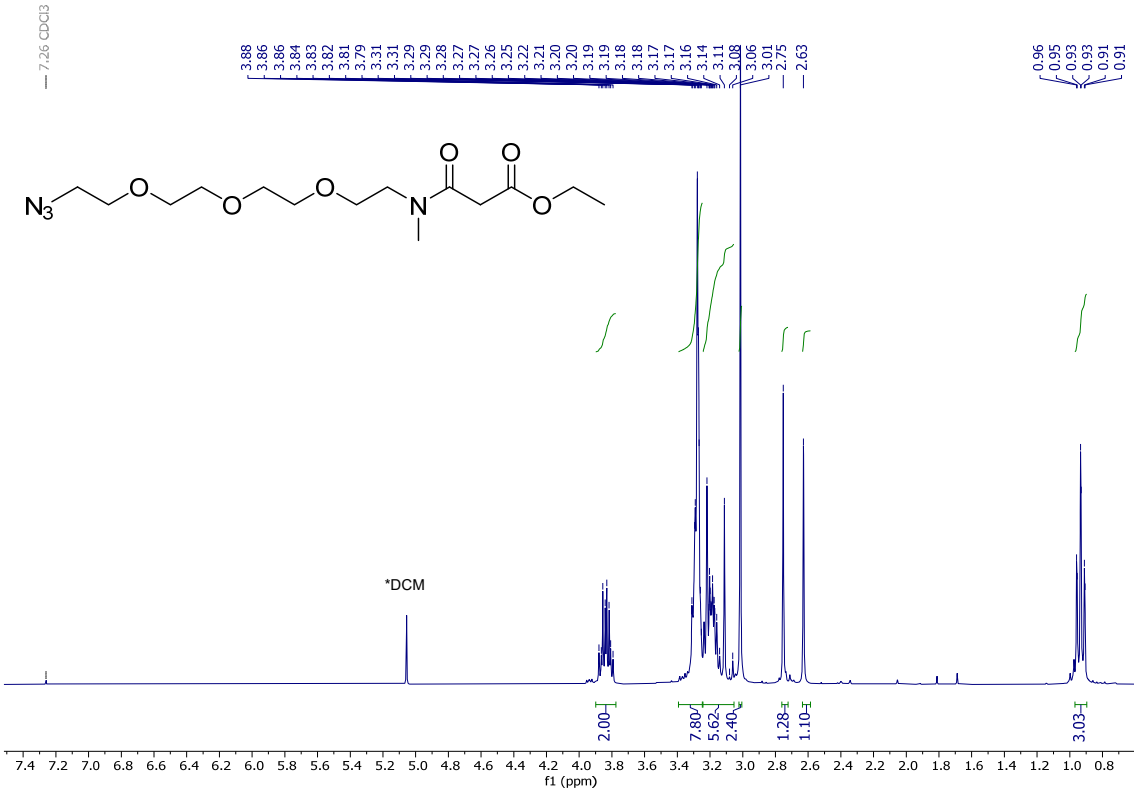

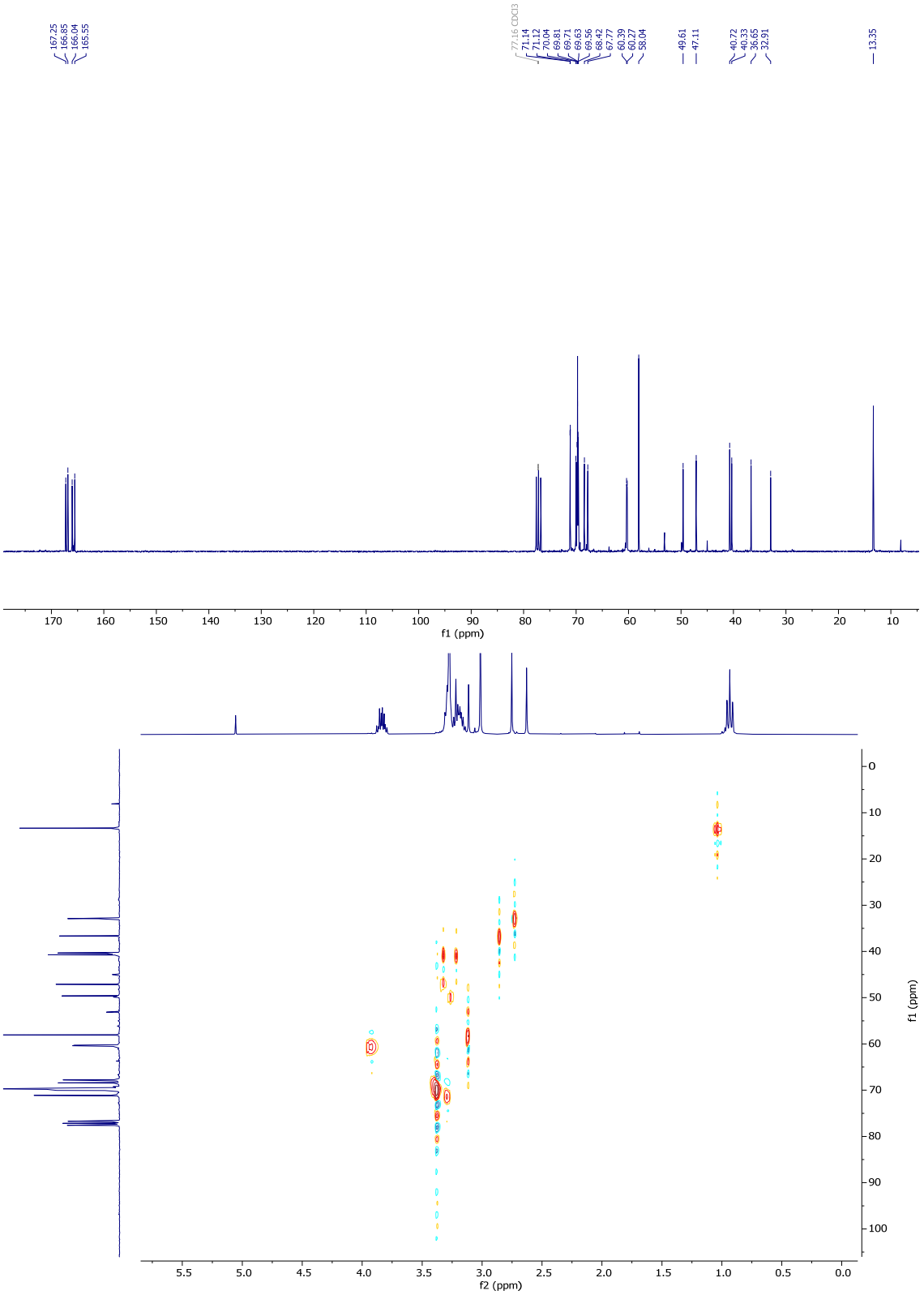

Figure S 96. ^{1}H-NMR, ^{13}C-NMR and HSQC of compound **S2** in $CDCl_3$.

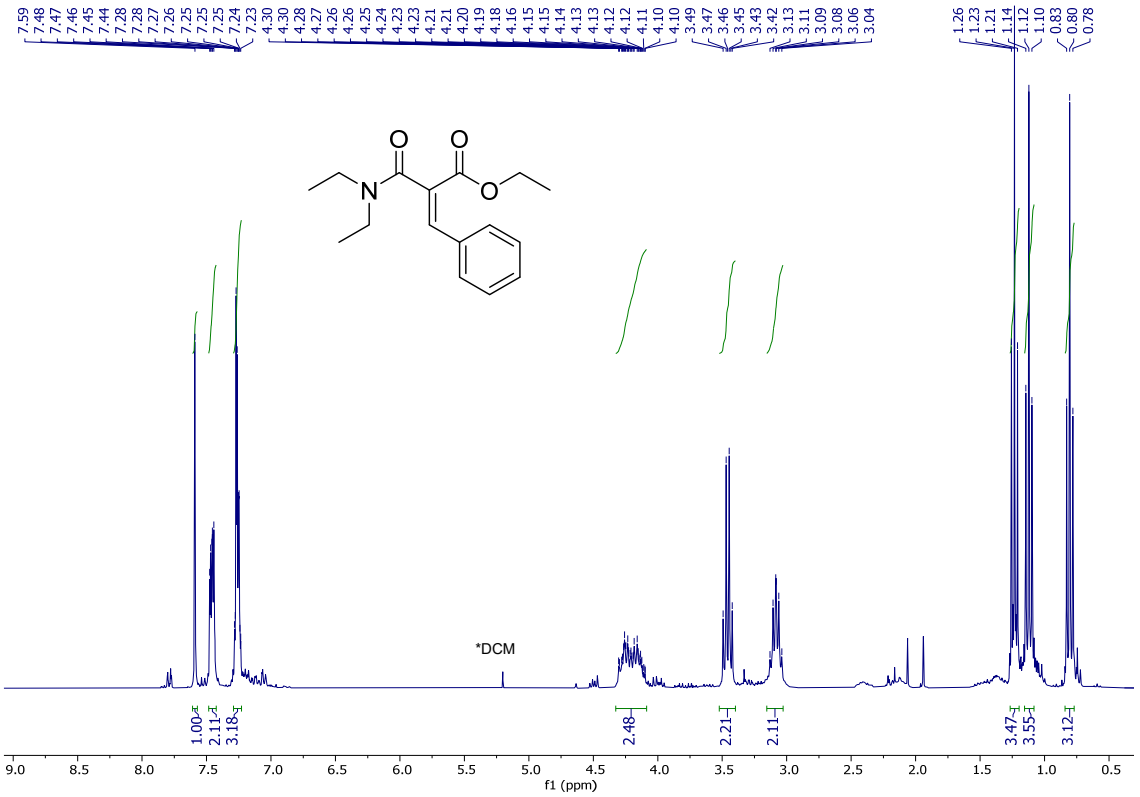
*DCM
f1 (ppm)

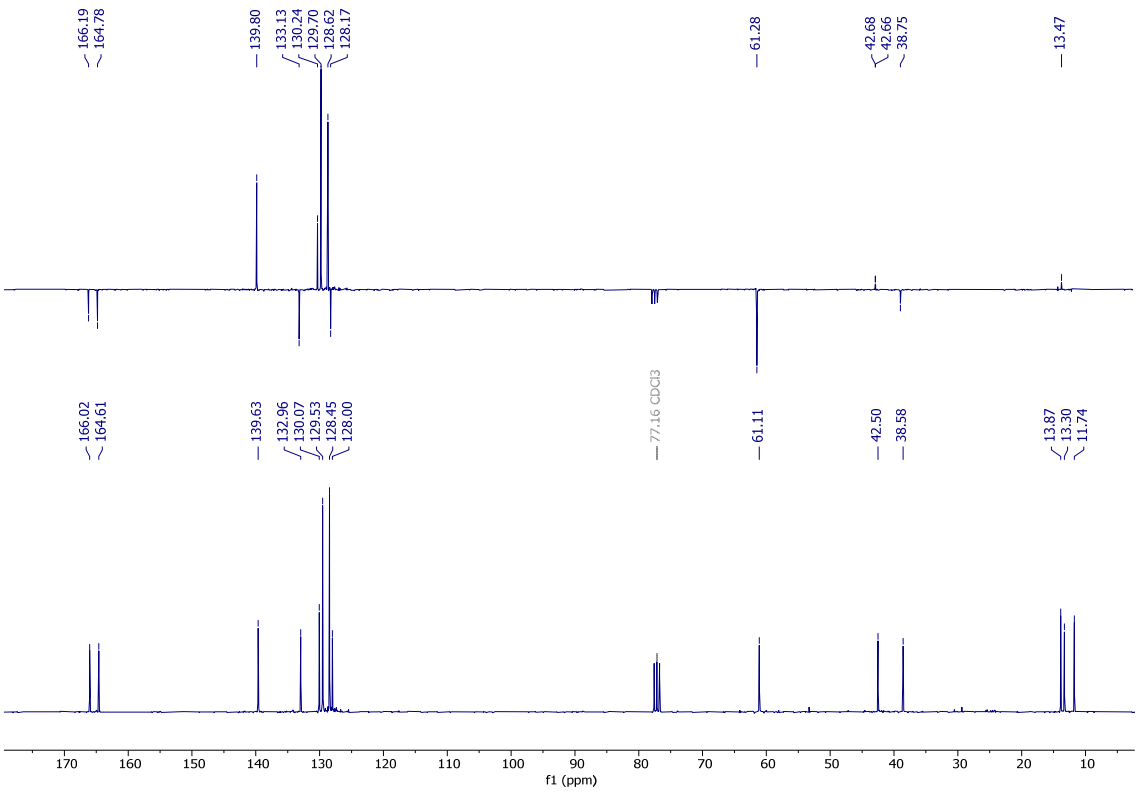
77.16 CDCl3
f1 (ppm)

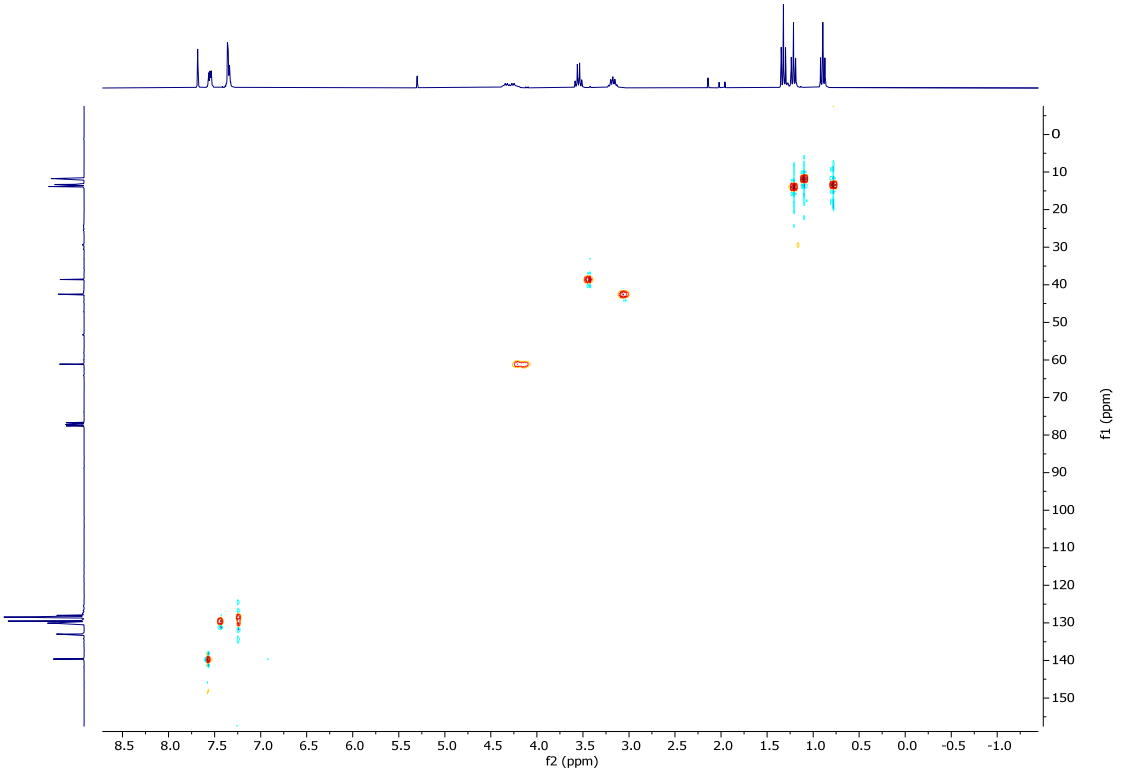

Figure S 97. ^{1}H-NMR, APT, ^{13}C-NMR and HSQC of compound **S3** in $CDCl_3$.

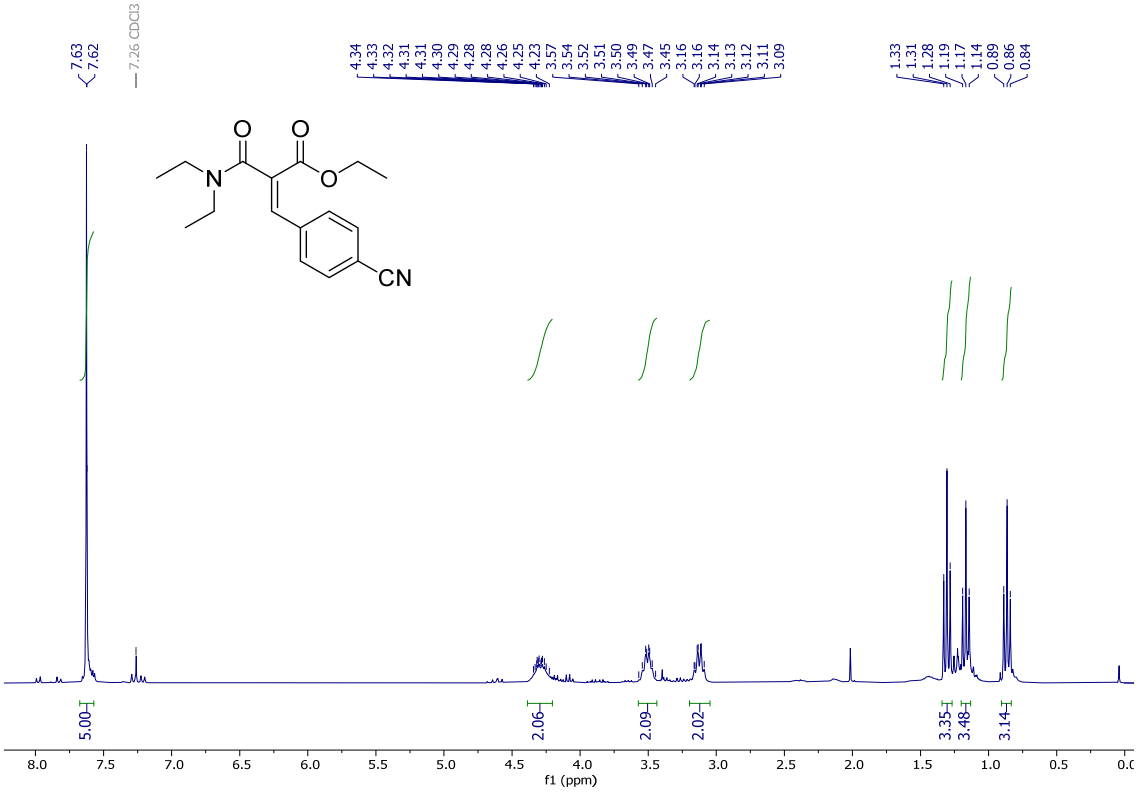

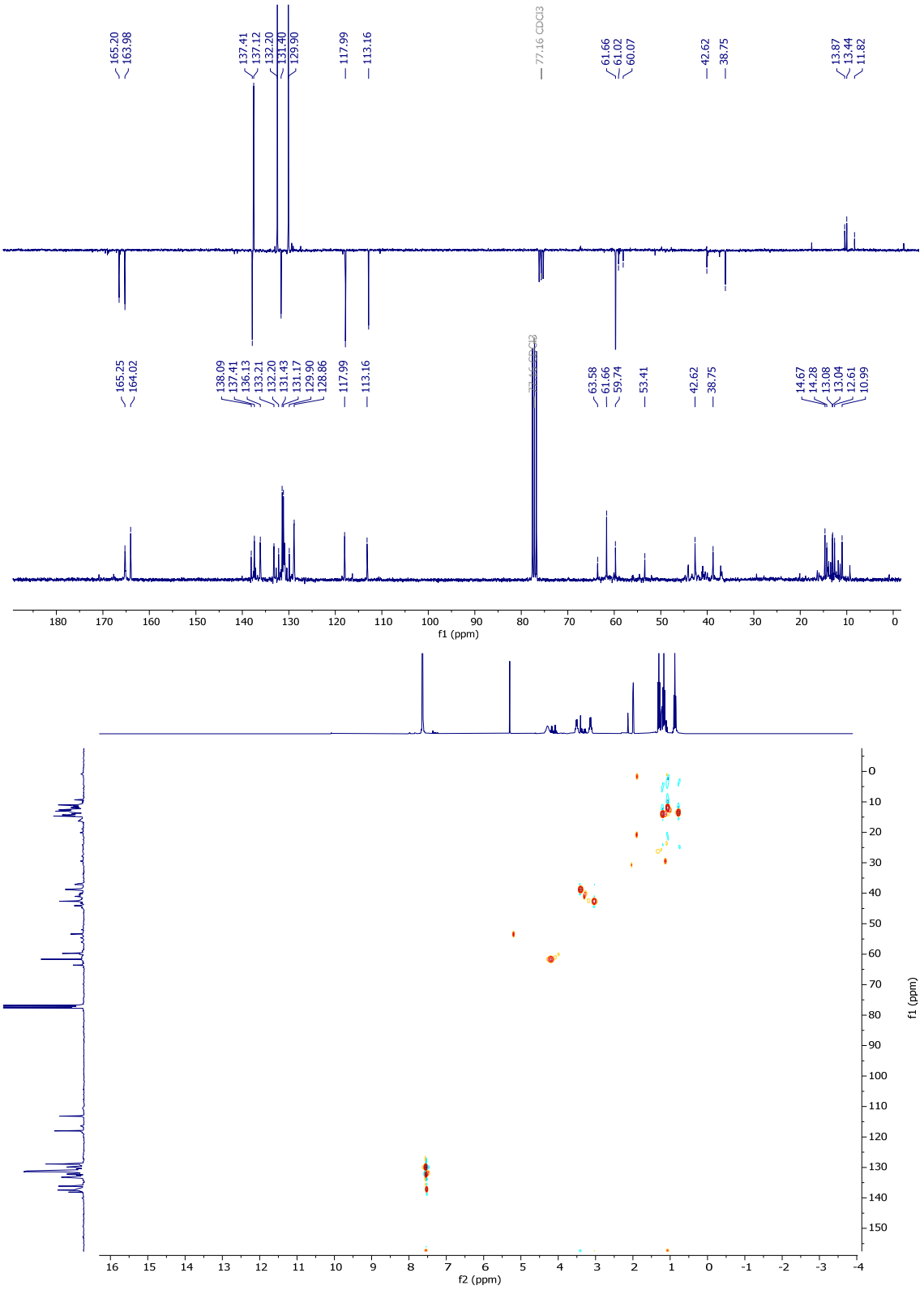

Figure S 98. ^{1}H-NMR, APT, ^{13}C-NMR and HSQC of compound **S4** in $CDCl_3$.

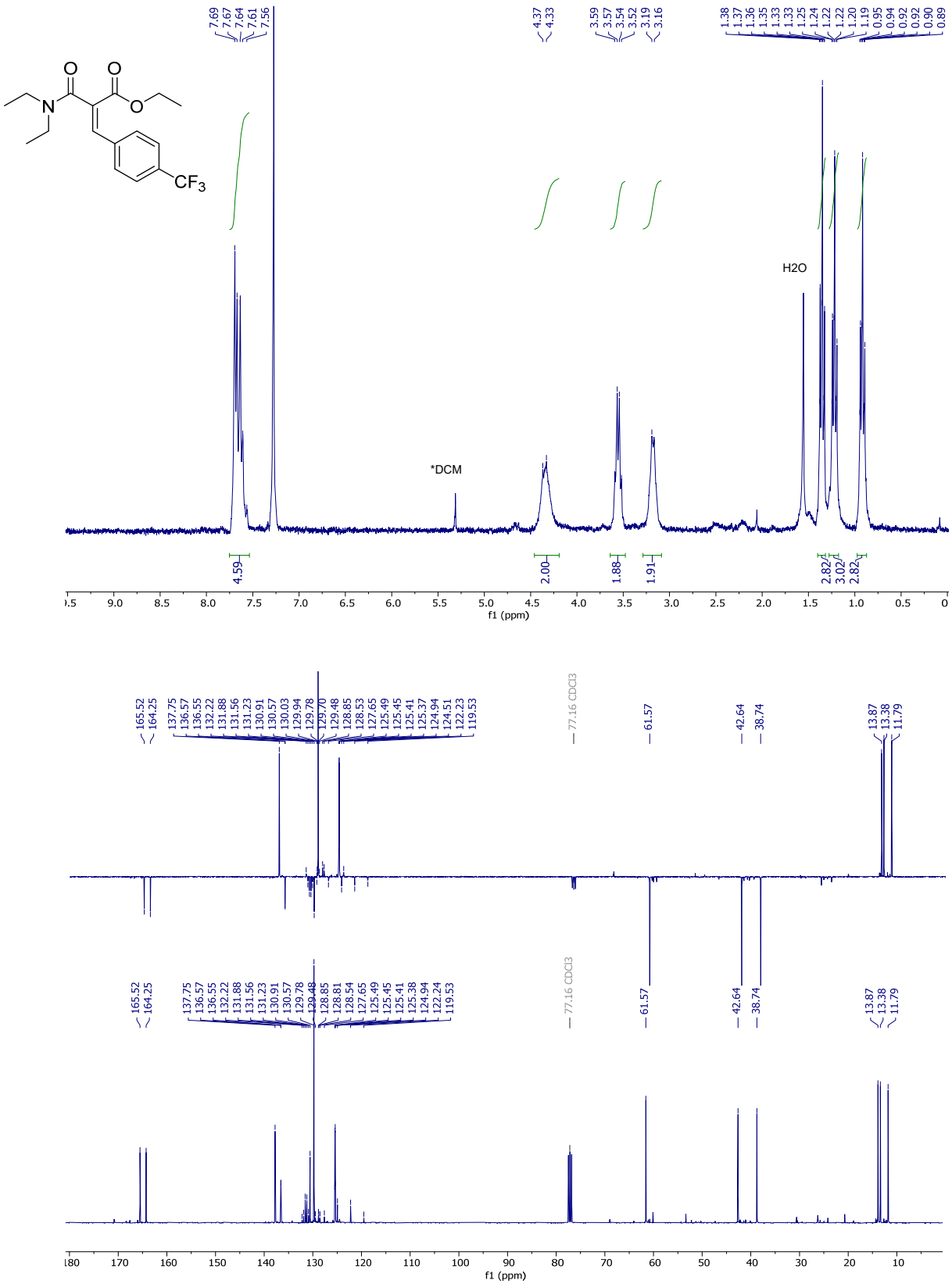
7.69
7.67
7.64
7.61
7.56
4.37
4.33
3.59
3.57
3.54
3.52
3.19
3.16
1.38
1.37
1.36
1.35
1.33
1.33
1.25
1.24
1.22
1.22
1.20
1.19
0.95
0.94
0.92
0.92
0.90
0.89
H2O
*DCM
4.59
2.00
1.88
1.91
2.82
3.02
2.82
f1 (ppm)
165.52
164.25
137.75
136.57
136.55
132.22
131.88
131.56
131.23
130.91
130.57
130.03
129.94
129.78
129.70
129.48
128.85
128.53
127.65
125.49
125.45
125.41
125.37
124.94
124.51
122.23
119.53
77.16 CDCl3
61.57
42.64
38.74
13.87
13.38
11.79
f1 (ppm)

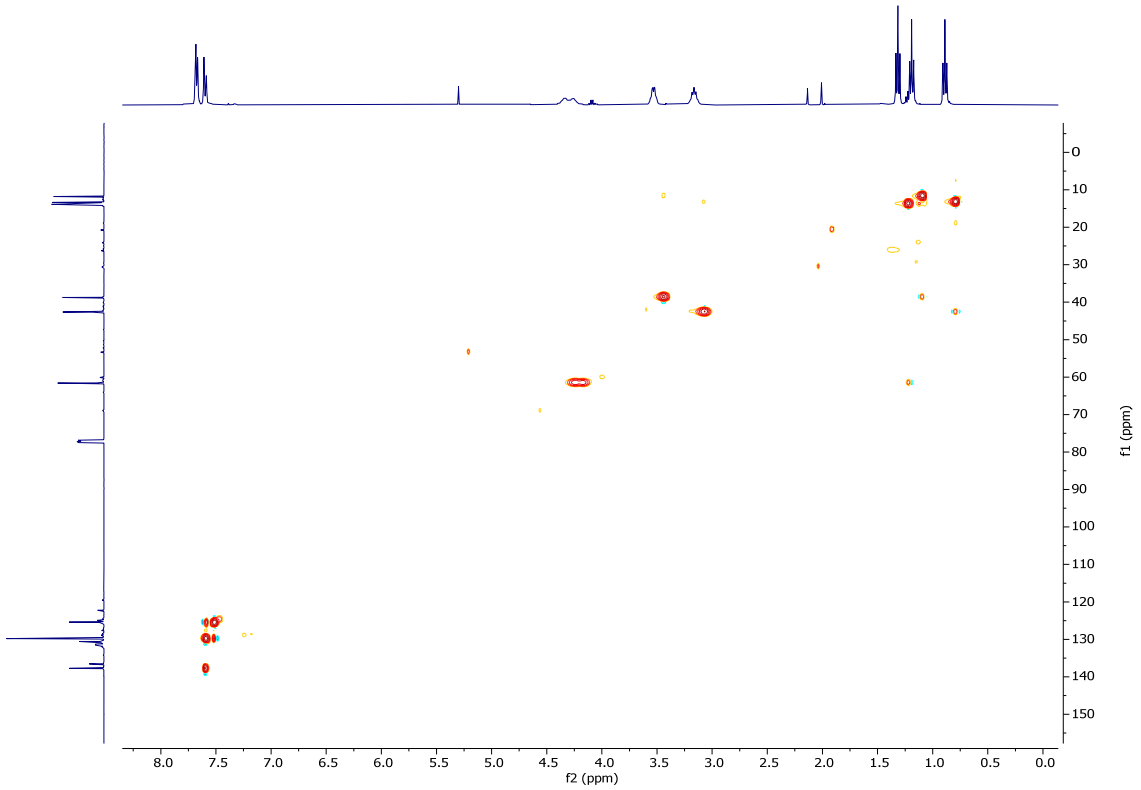

Figure S 99. ^{1}H-NMR, APT, ^{13}C-NMR and HSQC of compound **S5** in $CDCl_3$.

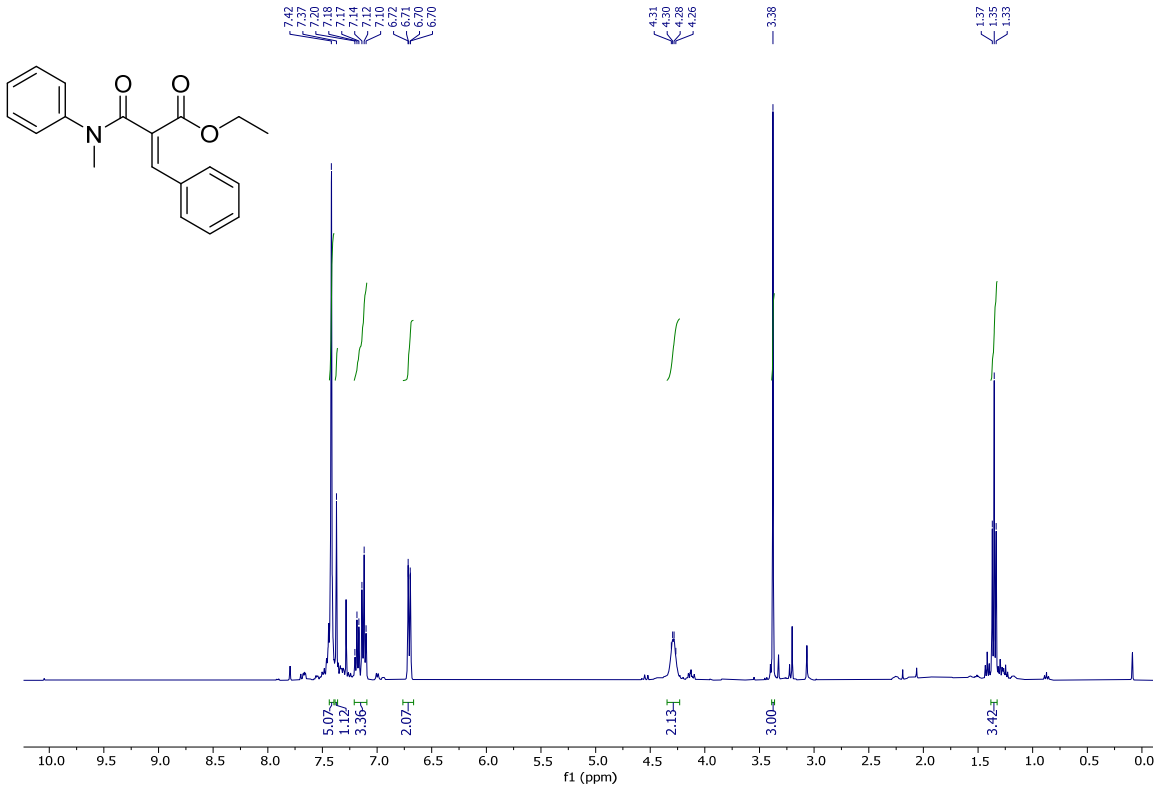

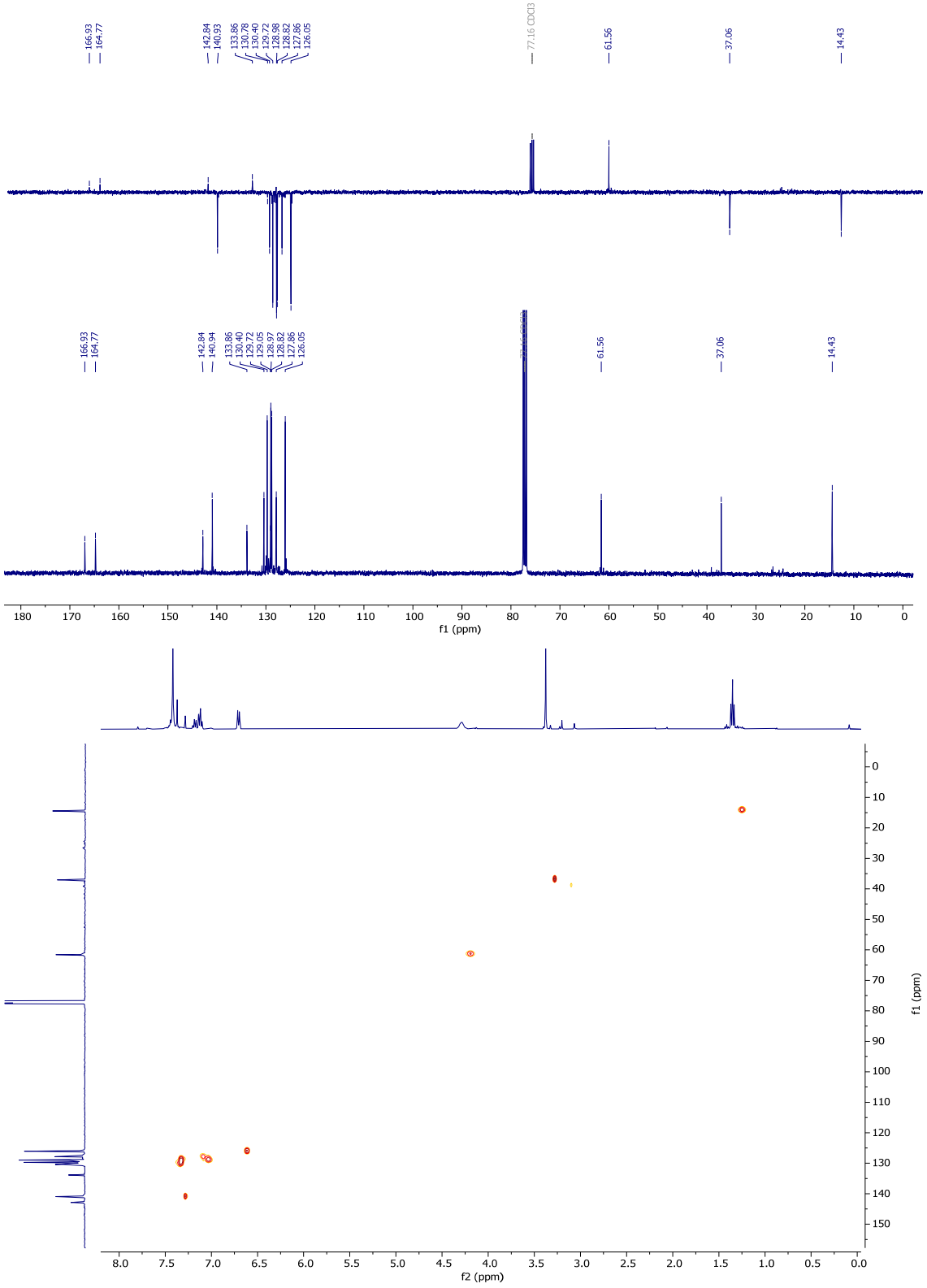

Figure S 100. ^{1}H-NMR, APT, ^{13}C-NMR and HMQC of compound **S6** in $CDCl_3$.

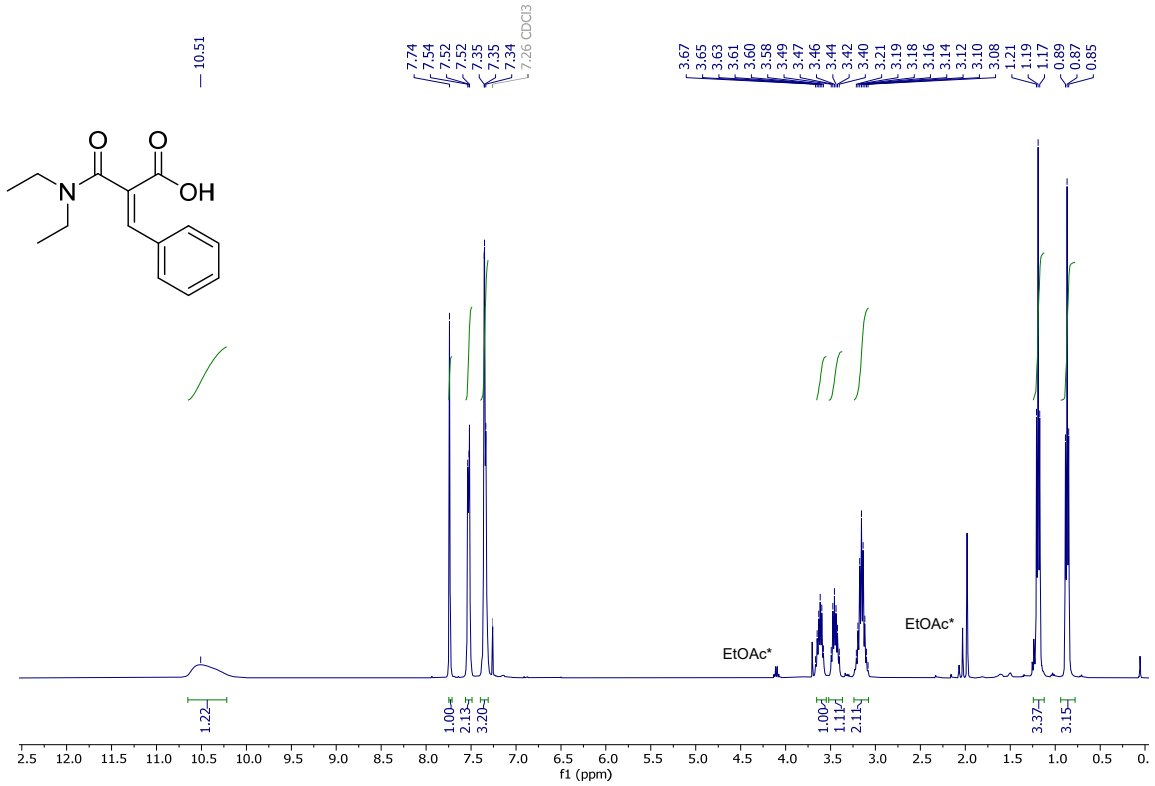
10.51
7.74
7.54
7.52
7.52
7.35
7.35
7.34
7.26 CDCl3
3.67
3.65
3.63
3.61
3.60
3.58
3.49
3.47
3.46
3.44
3.42
3.40
3.21
3.19
3.18
3.16
3.14
3.12
3.10
3.08
1.21
1.19
1.17
0.89
0.87
0.85
O
O
N
OH
EtOAc*
EtOAc*
1.22
1.00
2.13
3.20
1.00
1.11
2.11
3.37
3.15
f1 (ppm)

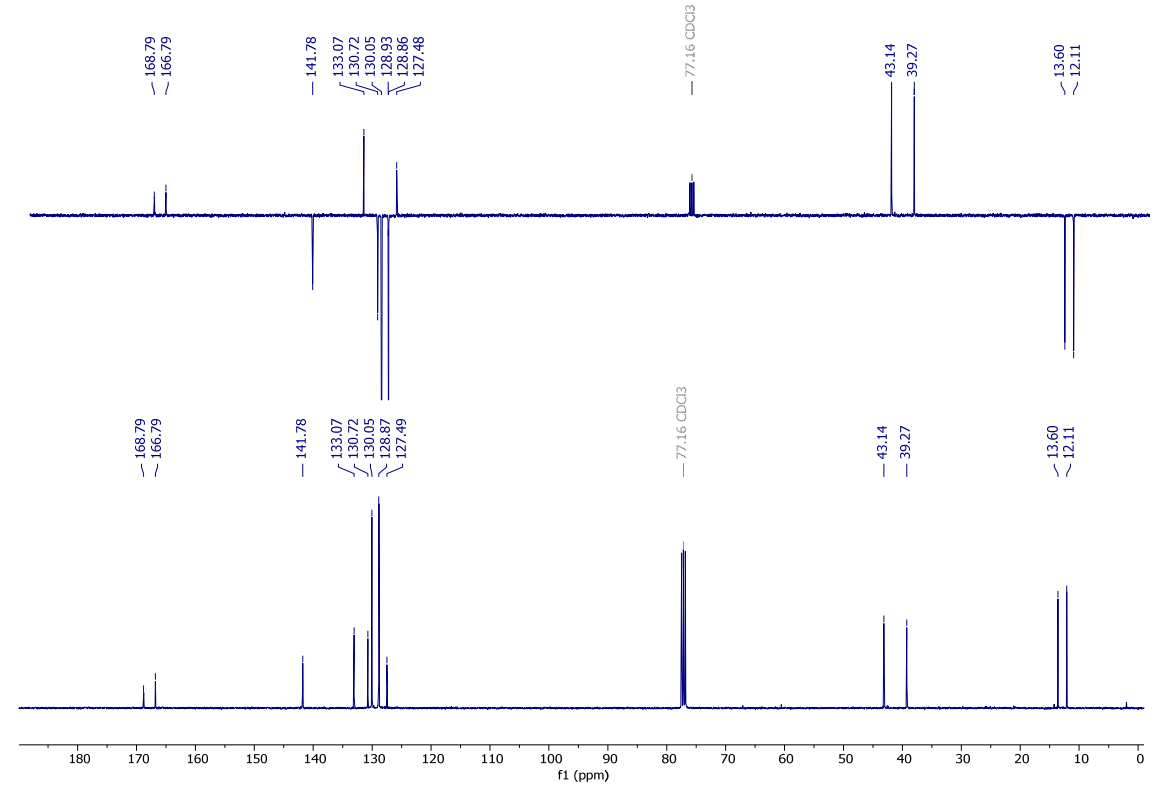
168.79
166.79
141.78
133.07
130.72
130.05
128.93
128.86
127.48
77.16 CDCl3
43.14
39.27
13.60
12.11
168.79
166.79
141.78
133.07
130.72
130.05
128.87
127.49
77.16 CDCl3
43.14
39.27
13.60
12.11
f1 (ppm)

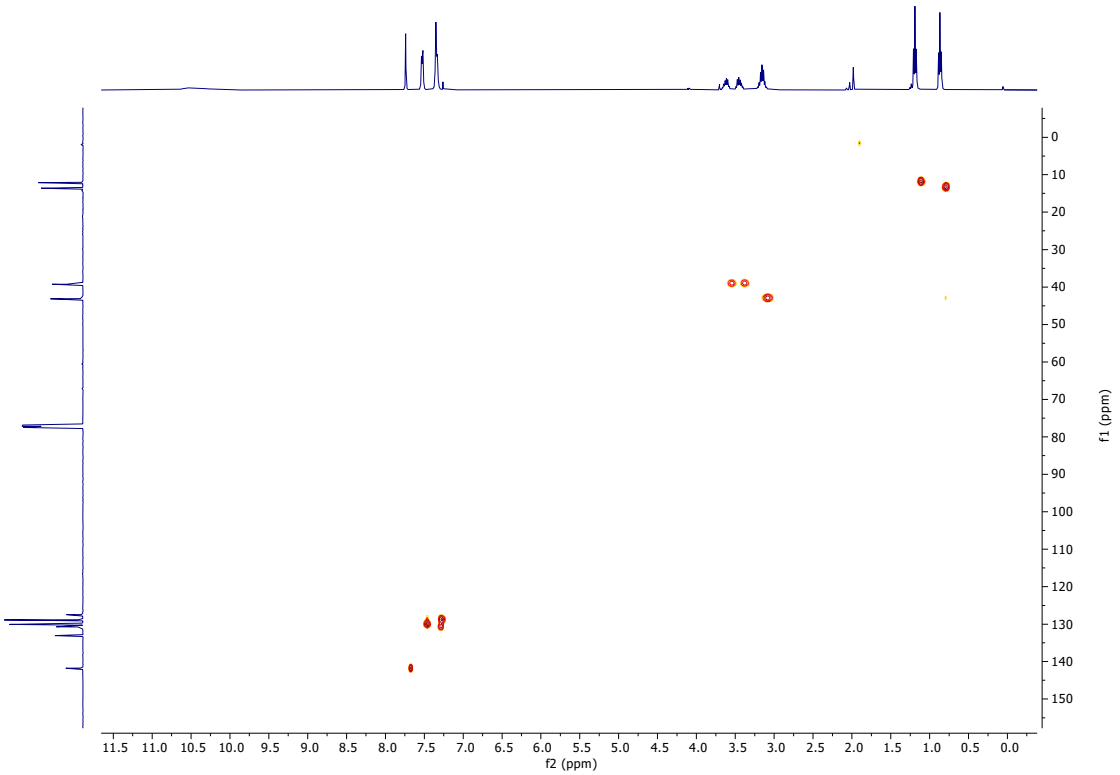

Figure S 101. ^{1}H-NMR, APT, ^{13}C-NMR and HMQC of compound **S7** in $CDCl_3$.

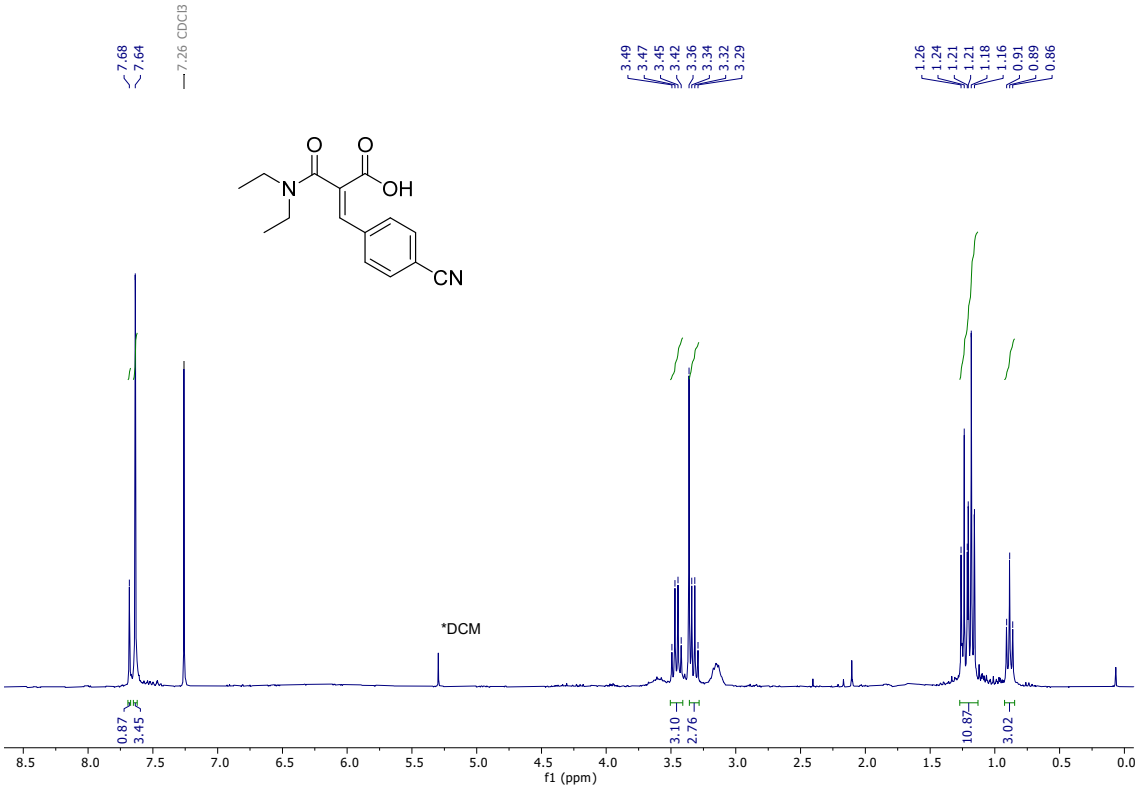

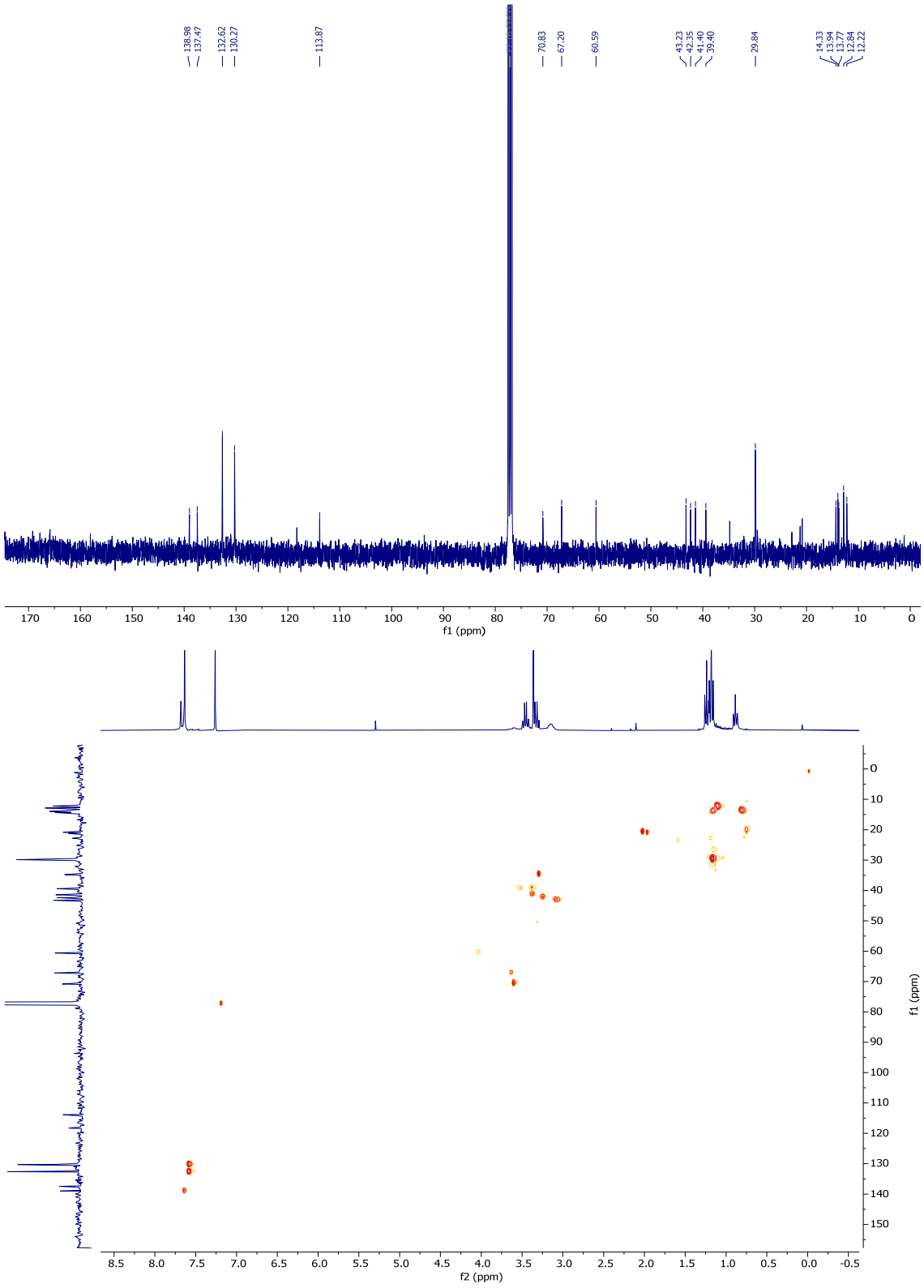

Figure S 102. ^{1}H-NMR, ^{13}C-NMR and HMQC of compound **S8** in $CDCl_3$.

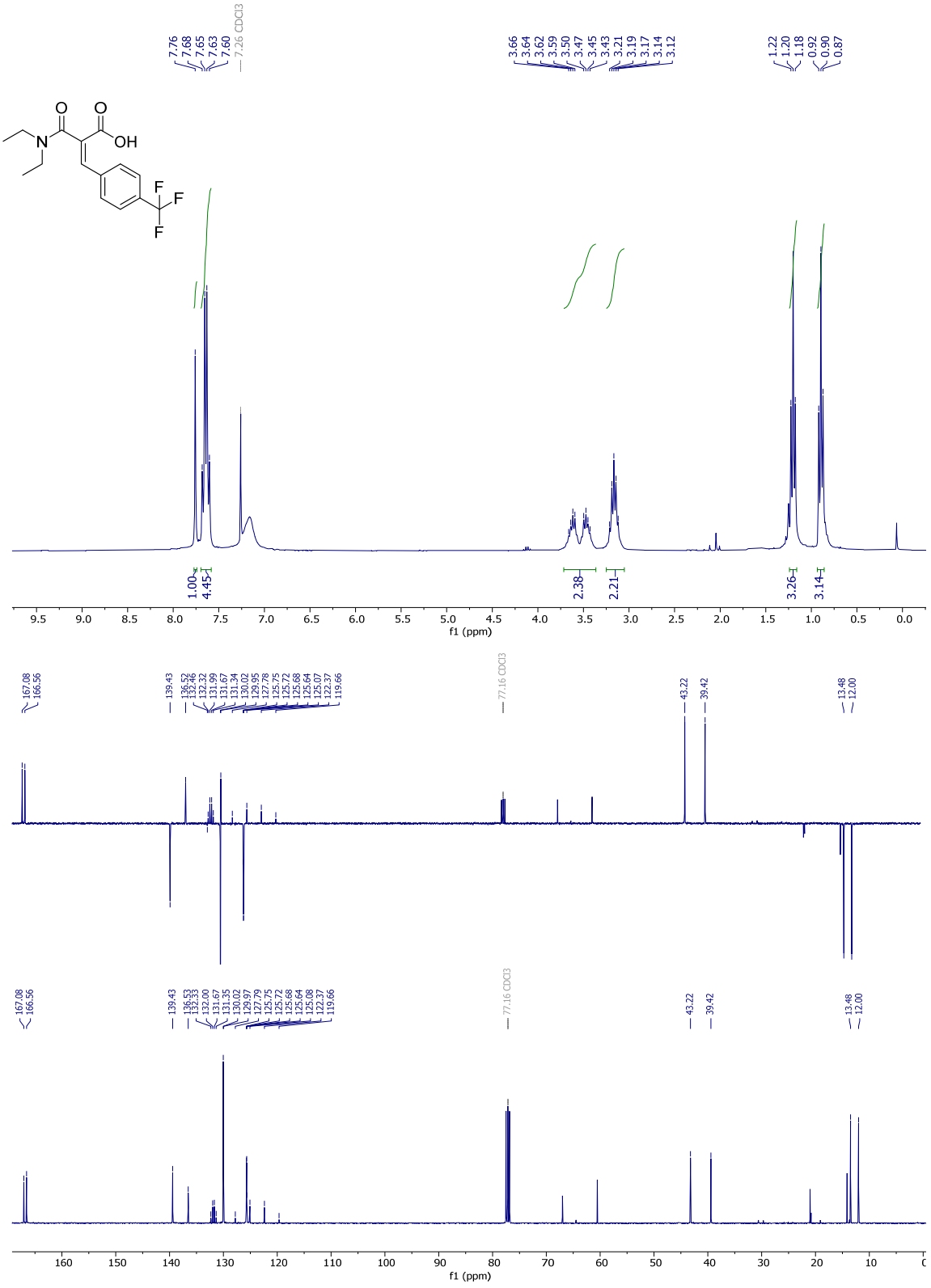
7.76
7.68
7.65
7.63
7.60
7.26 CDCl3
3.66
3.64
3.62
3.59
3.50
3.47
3.45
3.43
3.21
3.19
3.17
3.14
3.12
1.22
1.20
1.18
0.92
0.90
0.87
O
O
N
OH
F
F
F
1.00
4.45
2.38
2.21
3.26
3.14
f1 (ppm)
167.08
166.56
139.43
136.53
132.32
131.99
131.67
131.34
130.02
129.95
127.78
125.75
125.72
125.68
125.64
125.07
122.37
119.66
77.16 CDCl3
43.22
39.42
13.48
12.00
f1 (ppm)

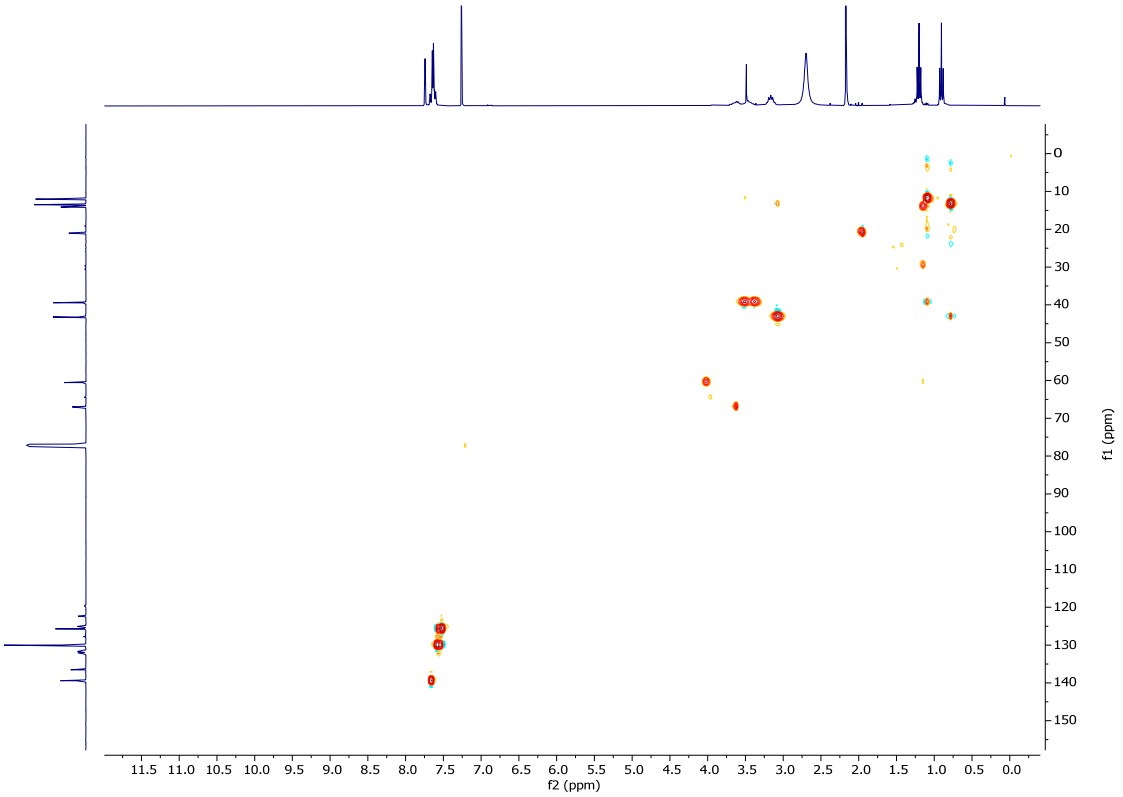

Figure S 103. ^{1}H-NMR, ^{13}C-NMR and HSQC of compound **S9** in $CDCl_3$.

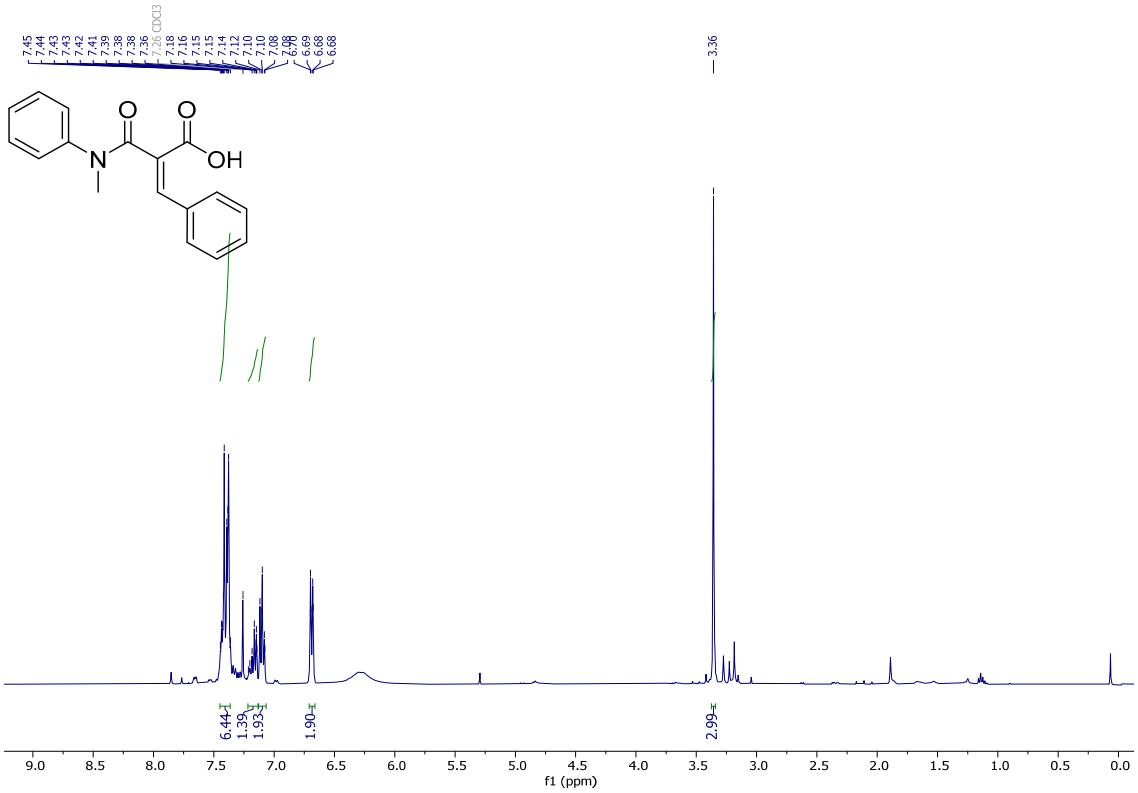

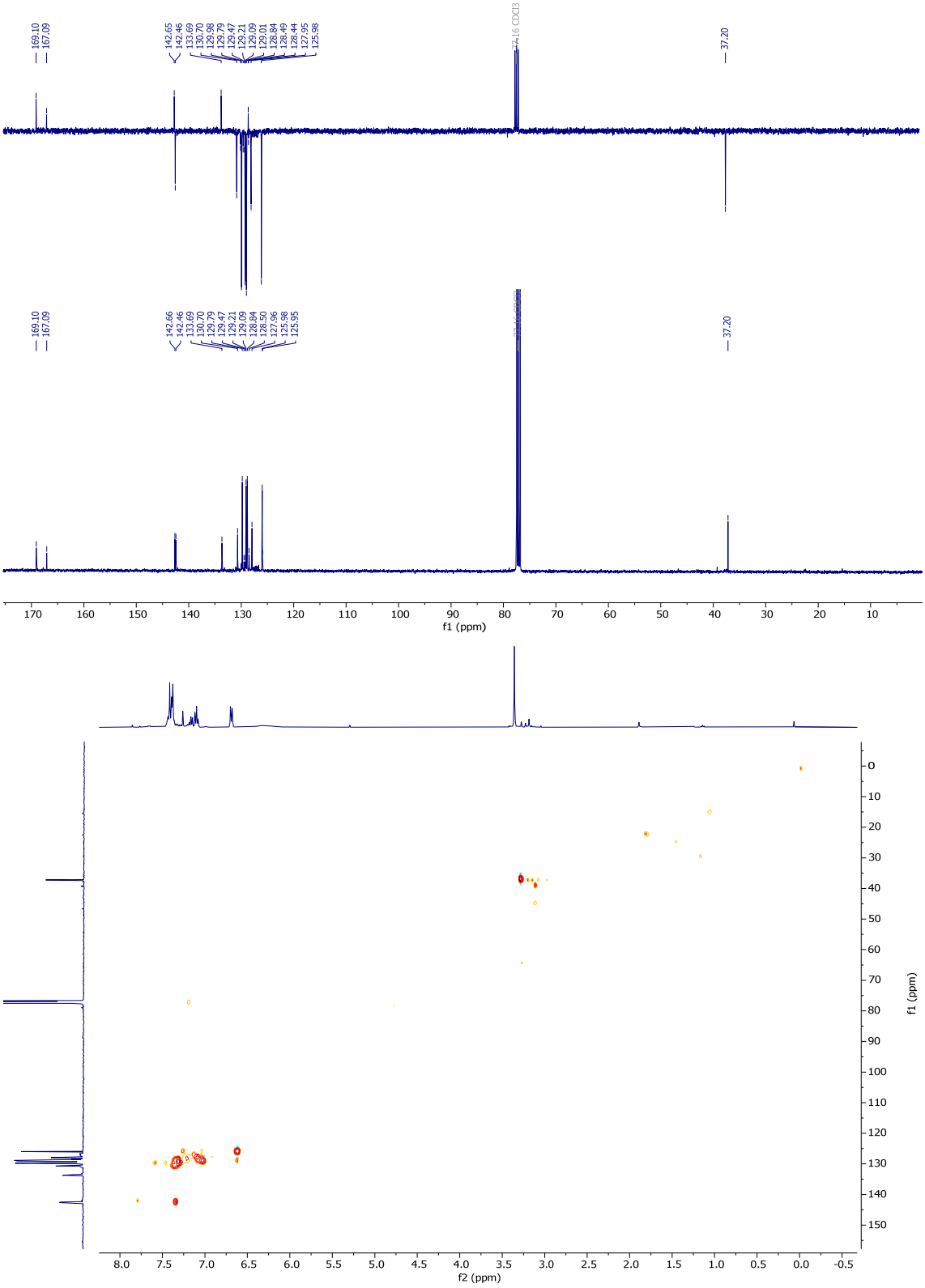

Figure S 104. ^{1}H-NMR, ^{13}C-NMR and HSQC of compound **S10** in $CDCl_3$.

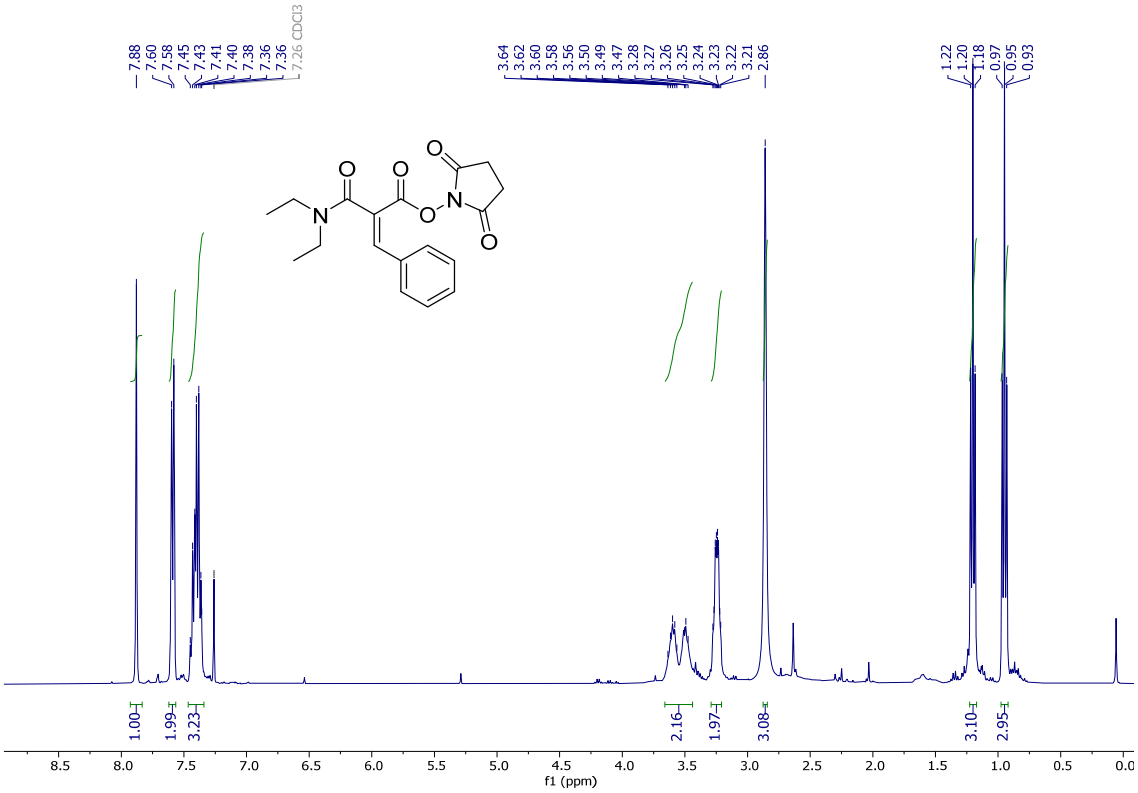
7.88
7.60
7.58
7.45
7.43
7.41
7.40
7.38
7.36
7.36
7.26 CDCl3
3.64
3.62
3.60
3.58
3.56
3.50
3.49
3.47
3.28
3.27
3.26
3.25
3.24
3.23
3.22
3.21
2.86
1.22
1.20
1.18
0.97
0.95
0.93
1.00
1.99
3.23
2.16
1.97
3.08
3.10
2.95
f1 (ppm)

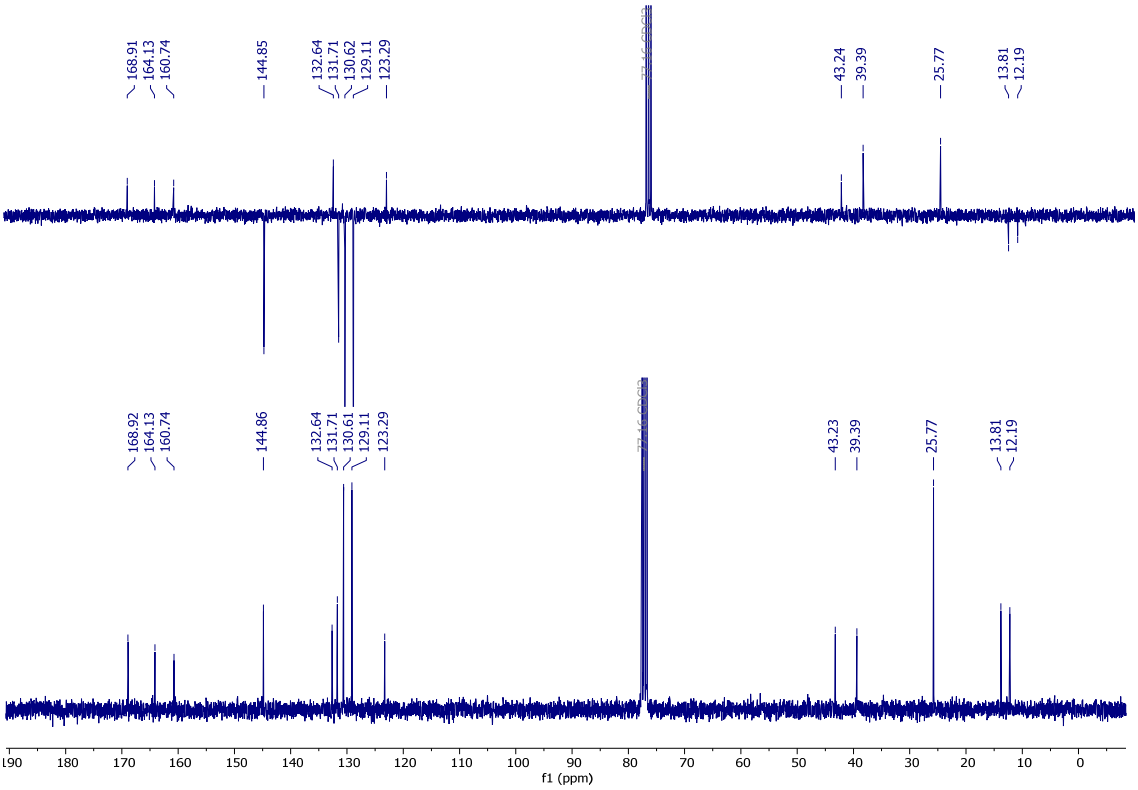
168.91
164.13
160.74
144.85
132.64
131.71
130.62
129.11
123.29
77.16 CDCl3
43.24
39.39
25.77
13.81
12.19
168.92
164.13
160.74
144.86
132.64
131.71
130.61
129.11
123.29
77.16 CDCl3
43.23
39.39
25.77
13.81
12.19
f1 (ppm)

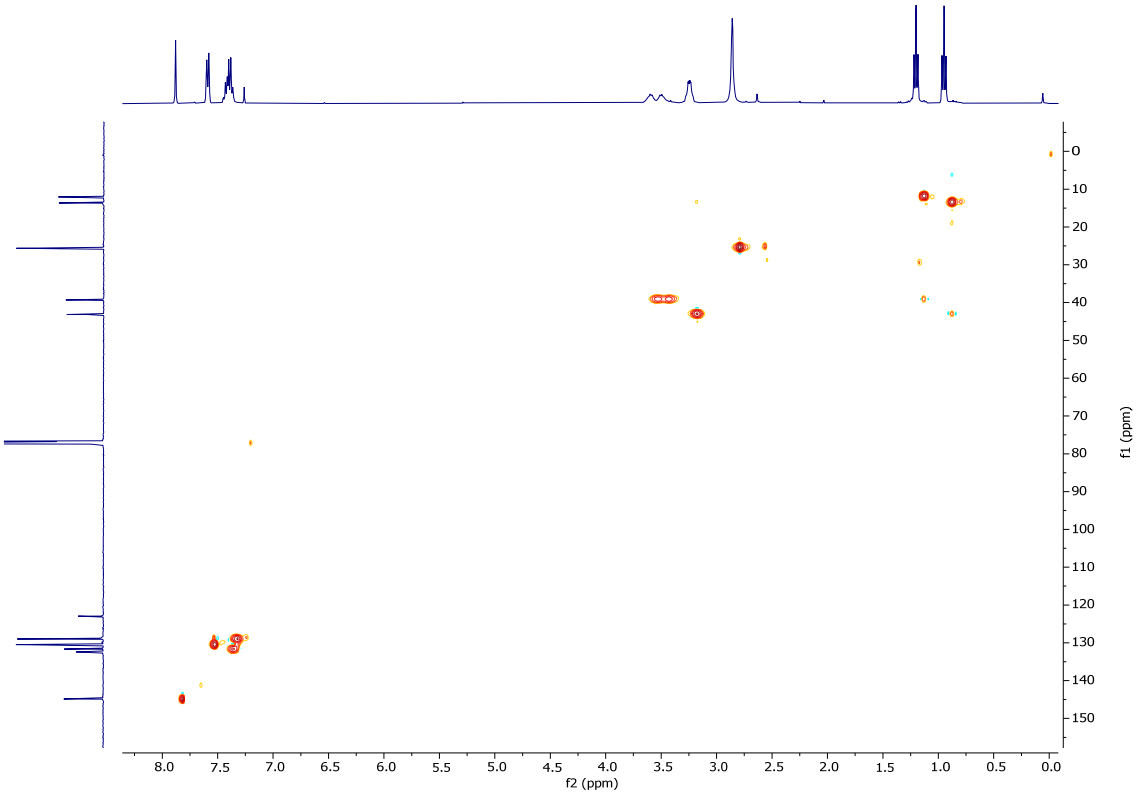

Figure S 105. ^{1}H-NMR, APT, ^{13}C-NMR and HMQC of compound **1** in $CDCl_3$.

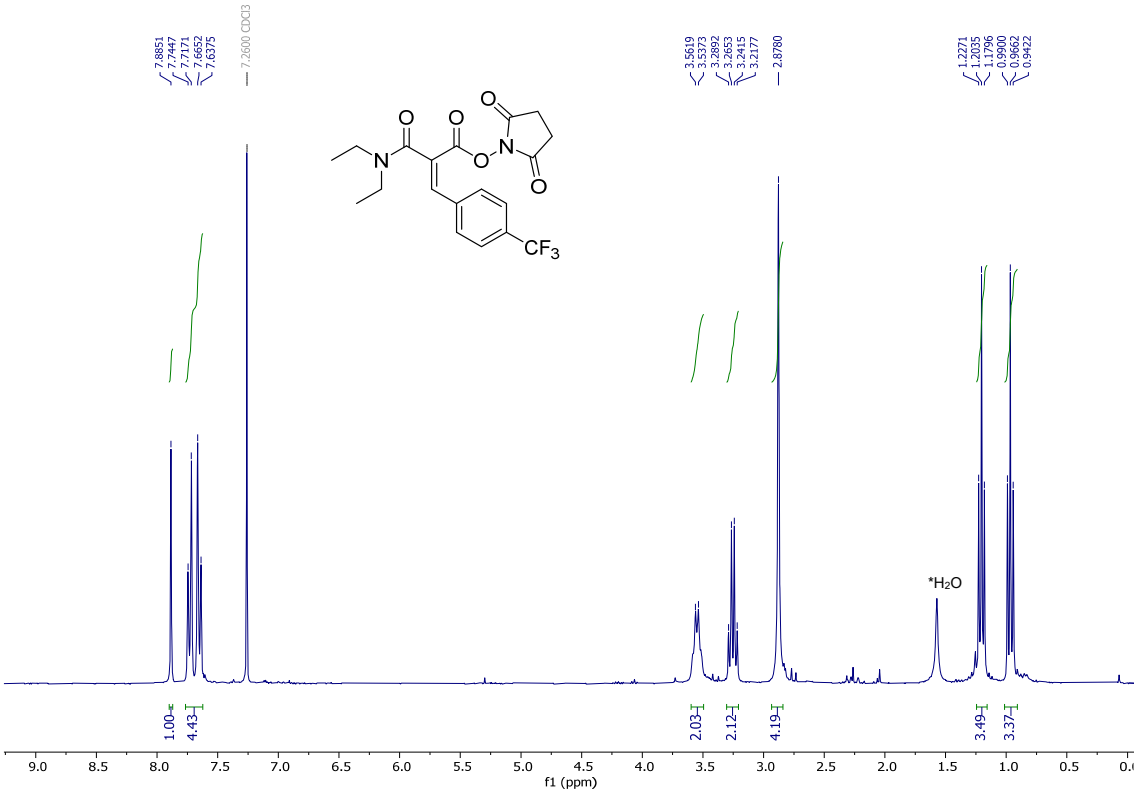

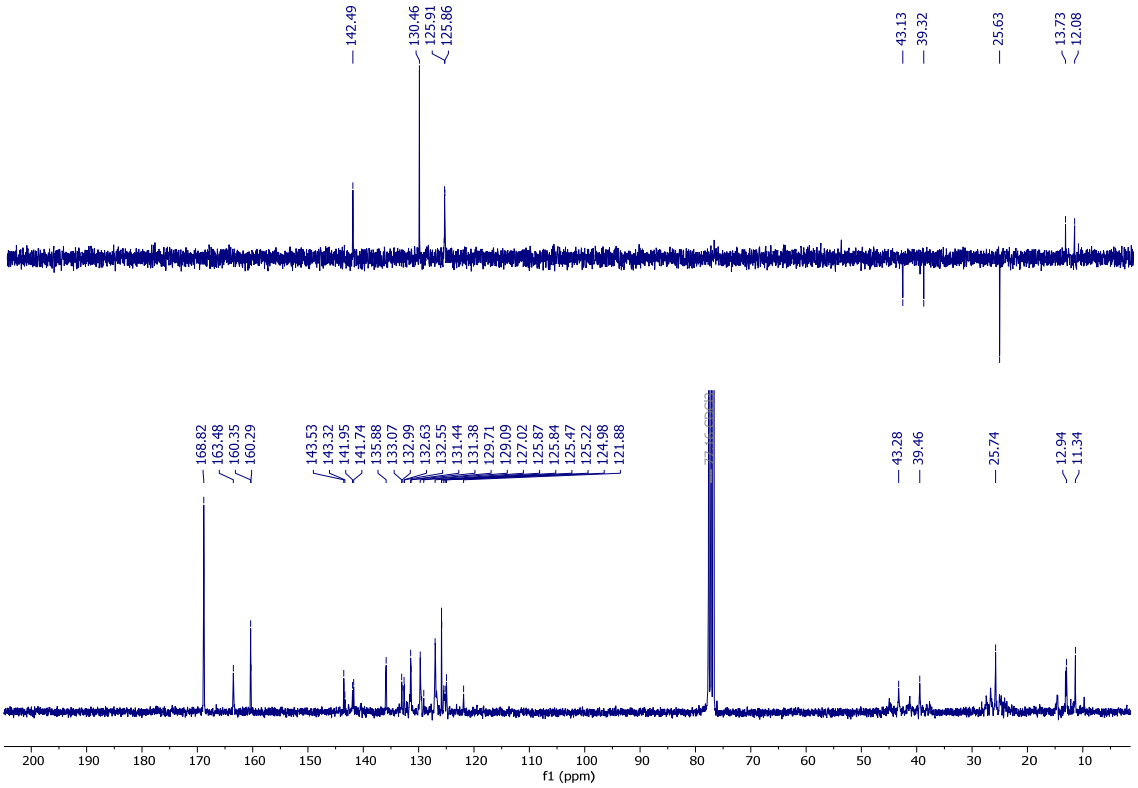

Figure S 106. ^{1}H-NMR, DEPT-135 and ^{13}C-NMR of compound **2** in $CDCl_3$.

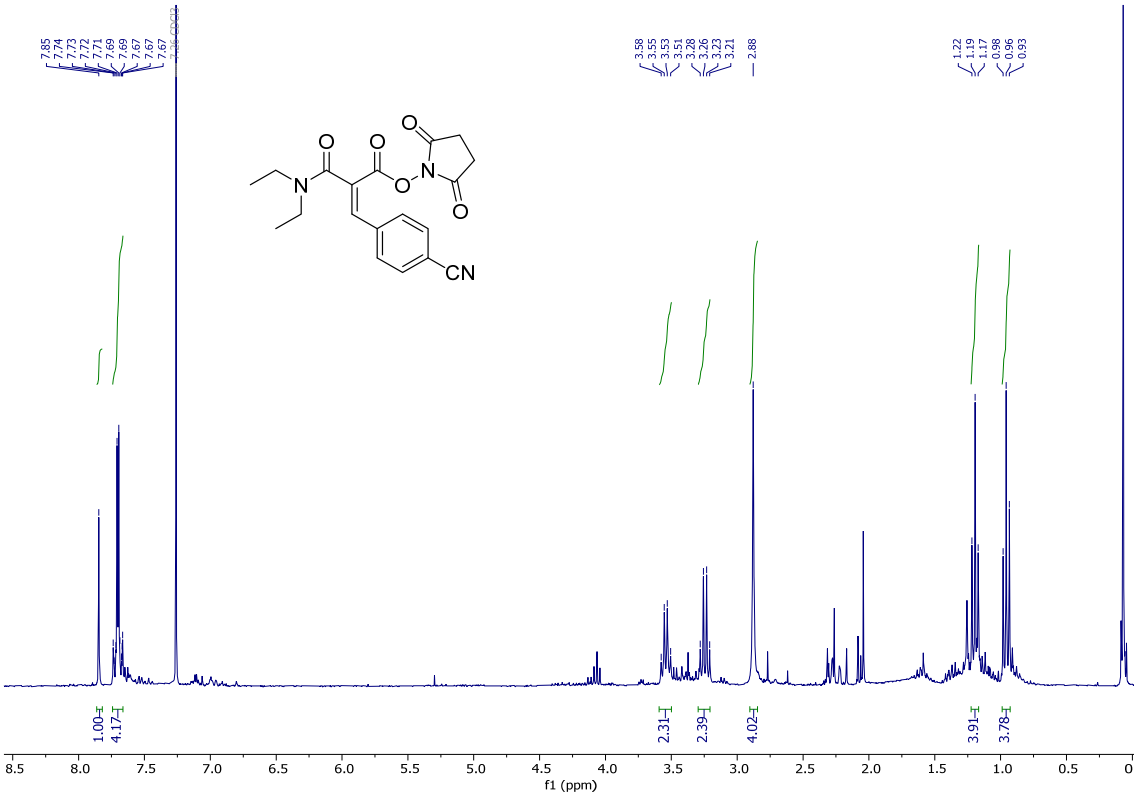

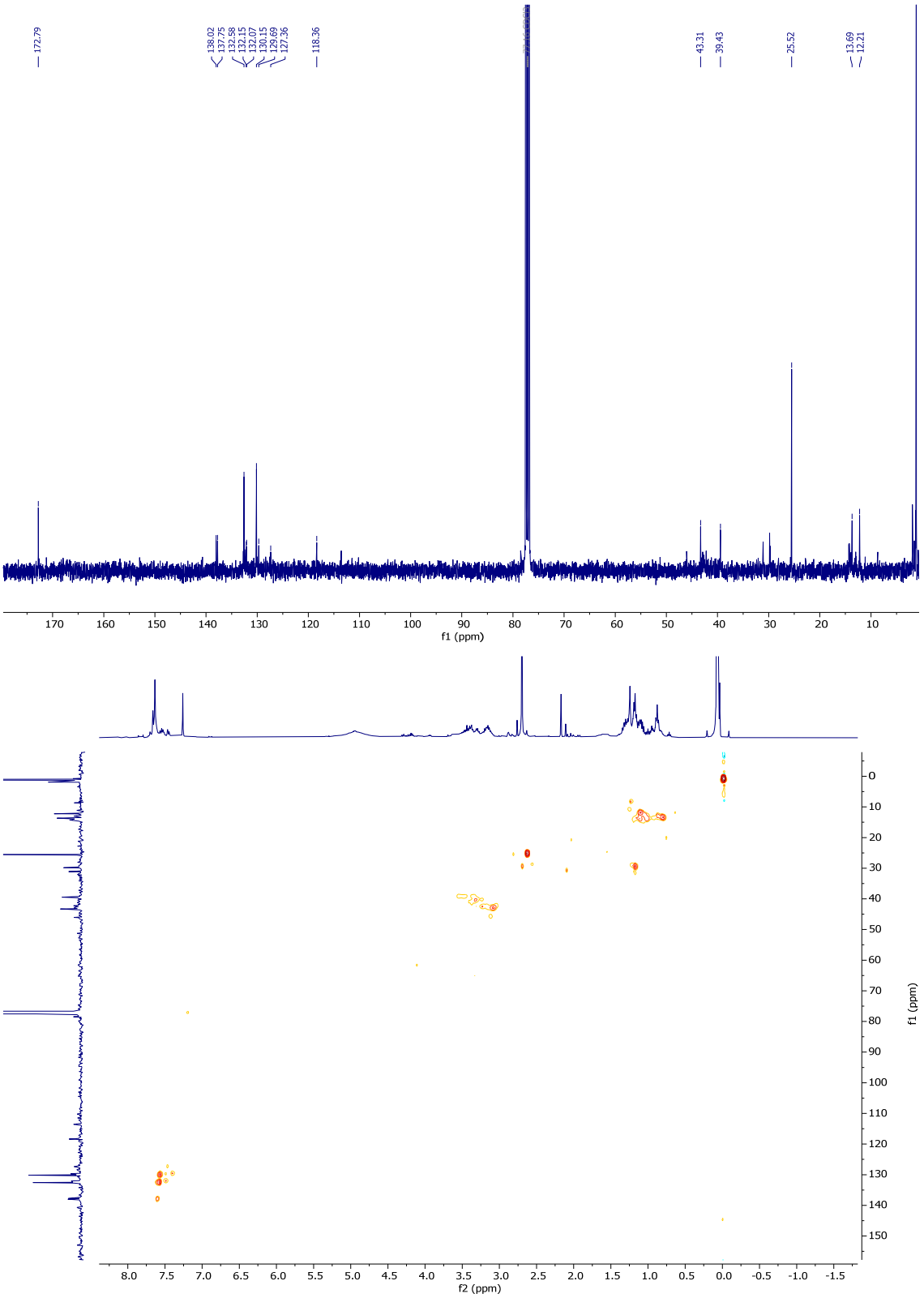

Figure S 107. ^{1}H-NMR, APT, ^{13}C-NMR and HMQC of compound **3** in $CDCl_3$.

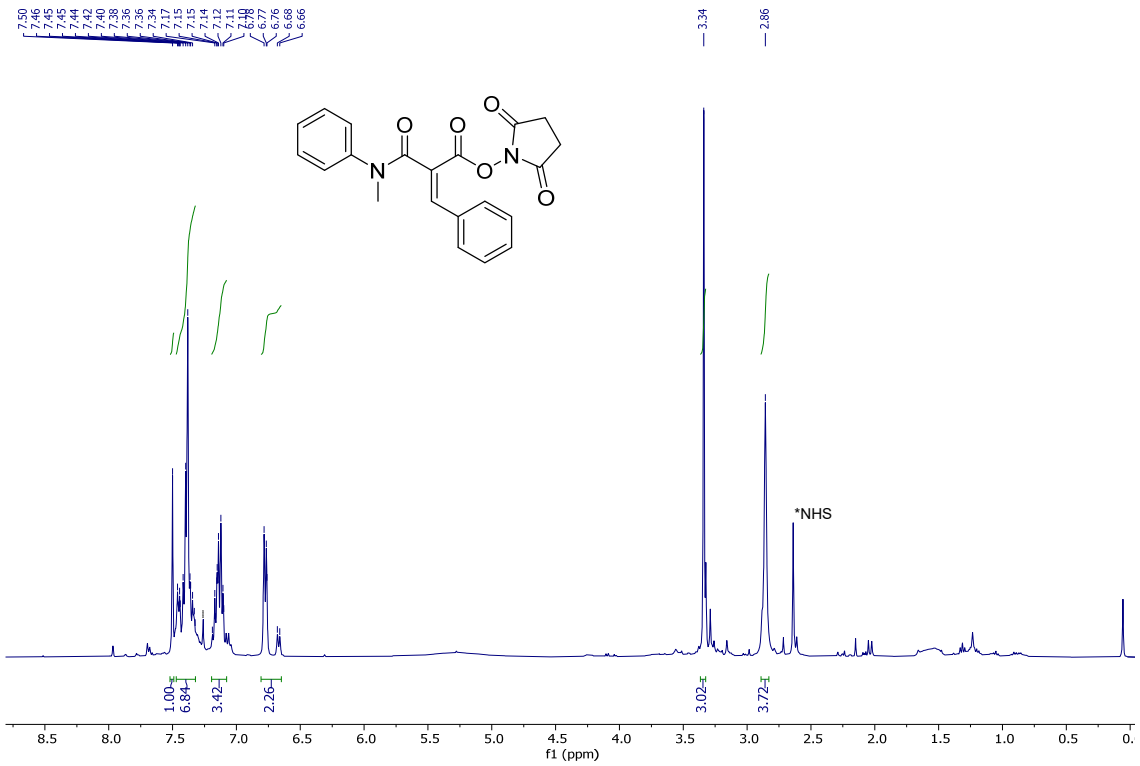
7.50
7.46
7.45
7.45
7.44
7.42
7.40
7.38
7.36
7.36
7.34
7.17
7.15
7.15
7.14
7.12
7.11
7.10
6.78
6.77
6.76
6.68
6.66
3.34
2.86
*NHS
1.00
6.84
3.42
2.26
3.02
3.72
f1 (ppm)

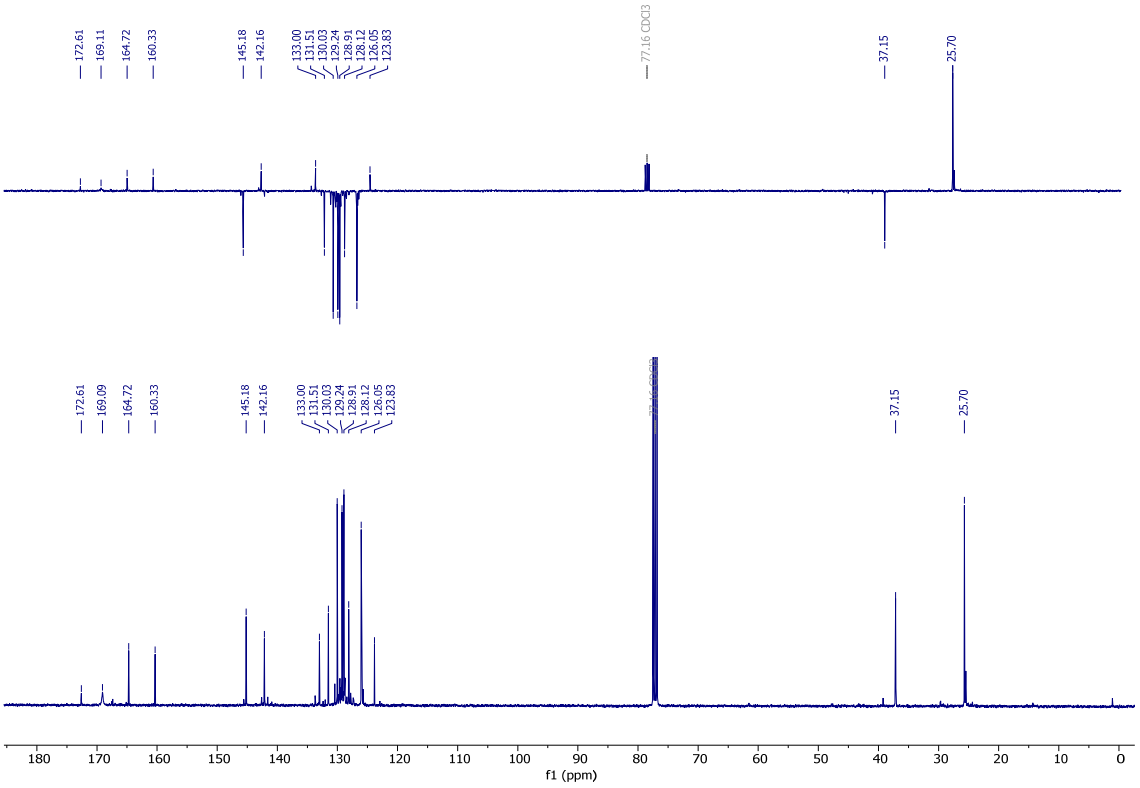
172.61
169.11
164.72
160.33
145.18
142.16
133.00
131.51
130.03
129.24
128.91
128.12
126.05
123.83
77.16 CDCl3
37.15
25.70
172.61
169.09
164.72
160.33
145.18
142.16
133.00
131.51
130.03
129.24
128.91
128.12
126.05
123.83
37.15
25.70
f1 (ppm)

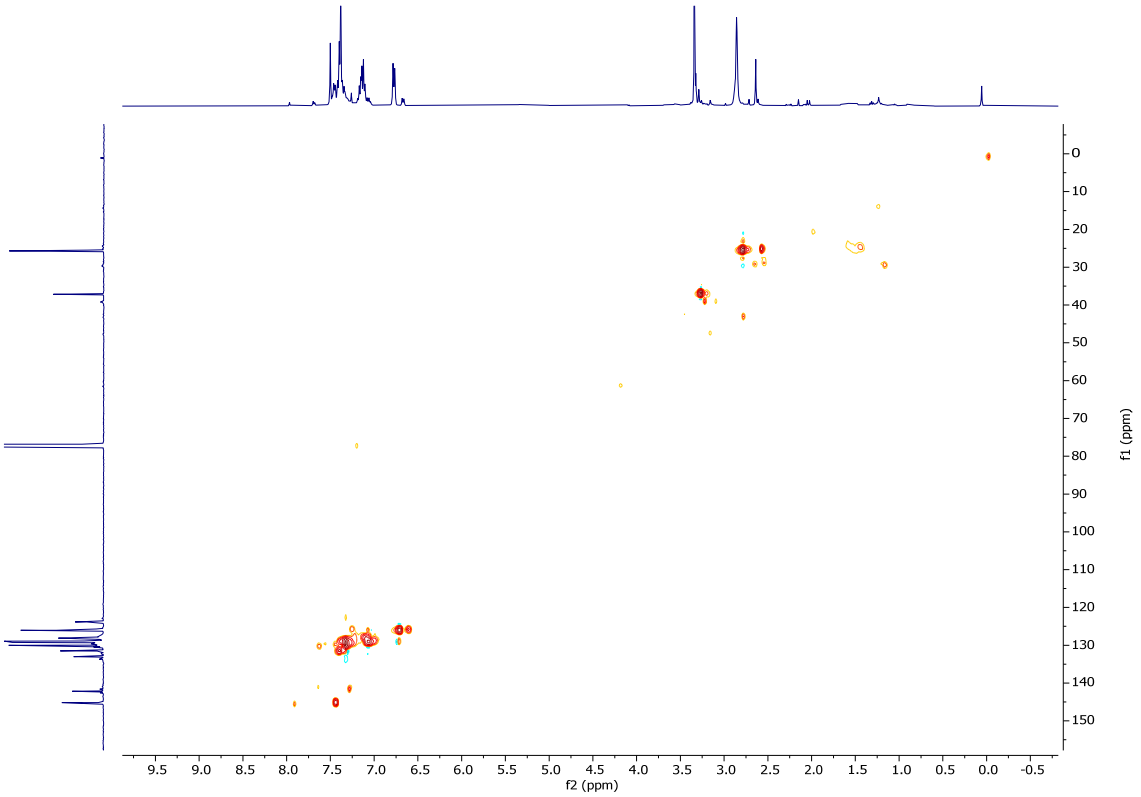

Figure S 108. ^{1}H-NMR, APT, ^{13}C-NMR and HSQC of compound **4** in $CDCl_3$.

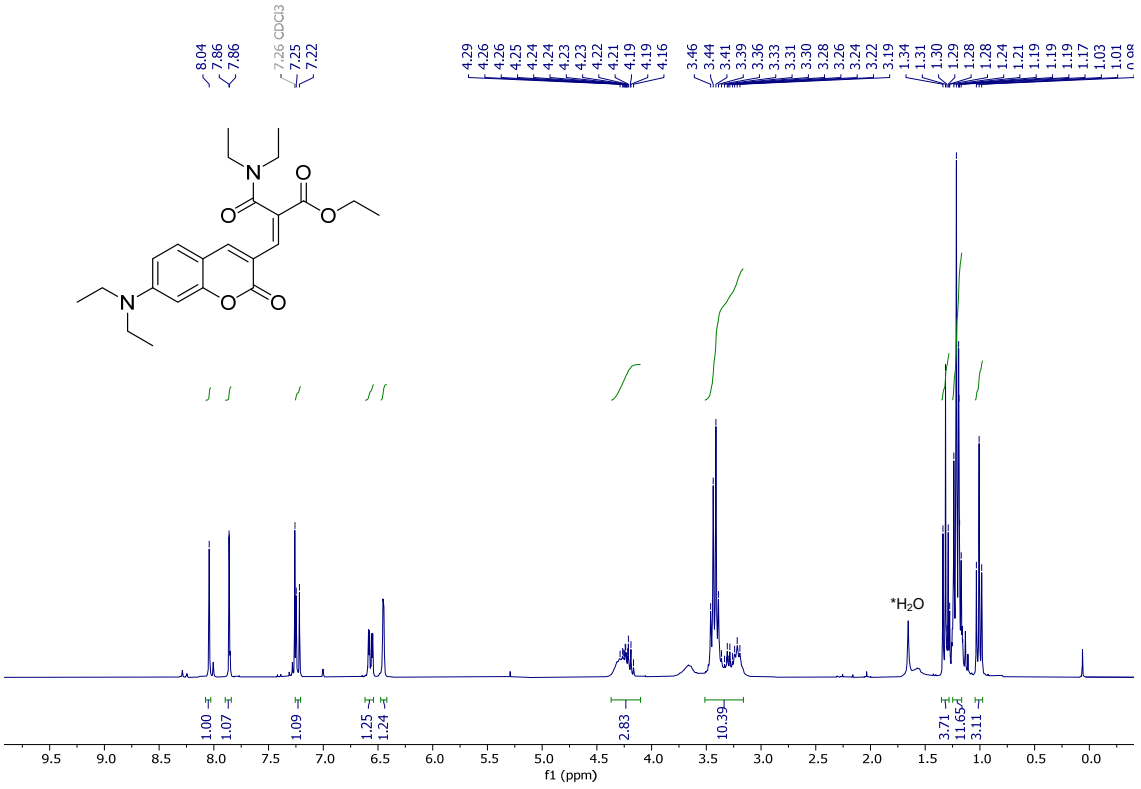

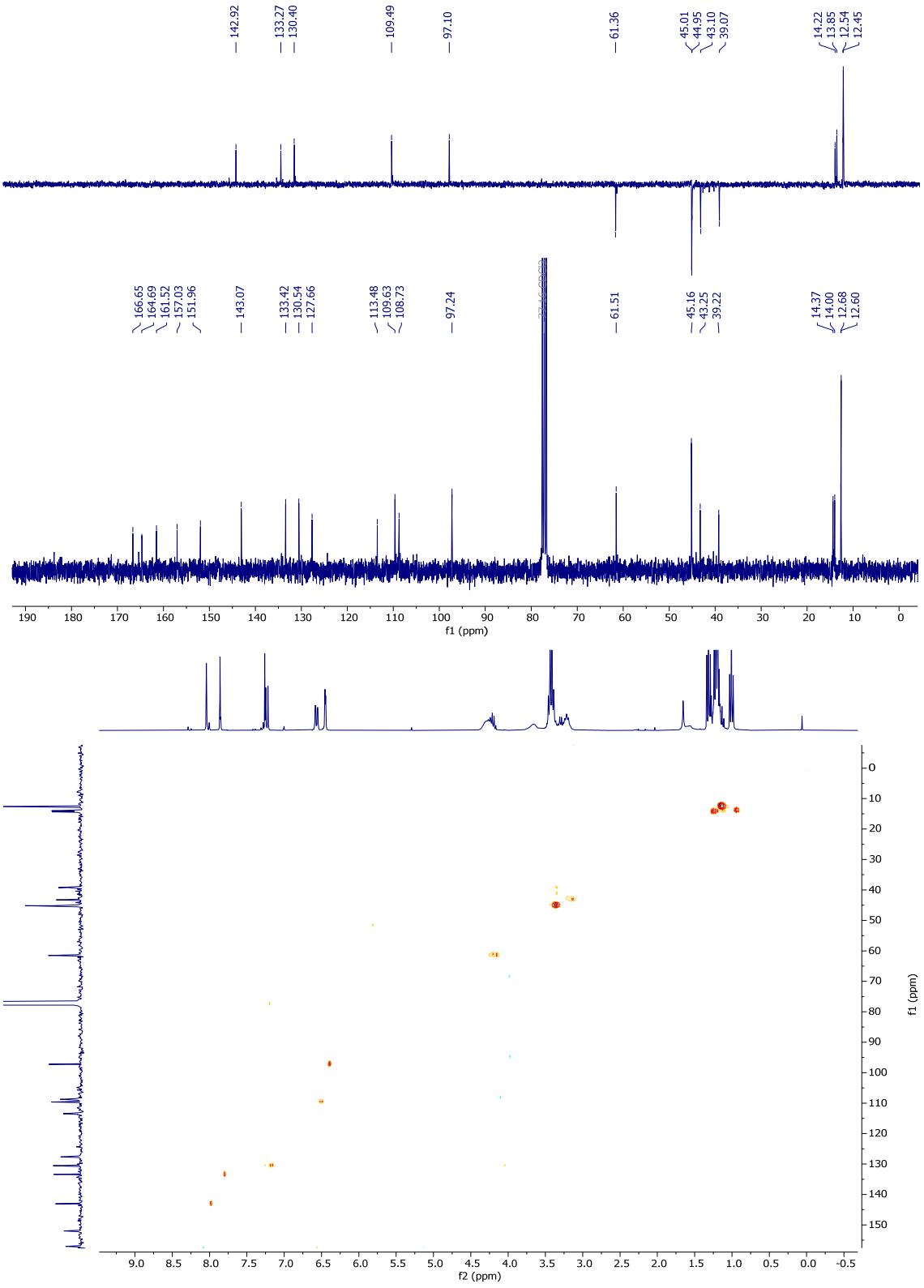

Figure S 109. ^{1}H-NMR, APT, ^{13}C-NMR and HMQC of compound **S11** in $CDCl_3$.

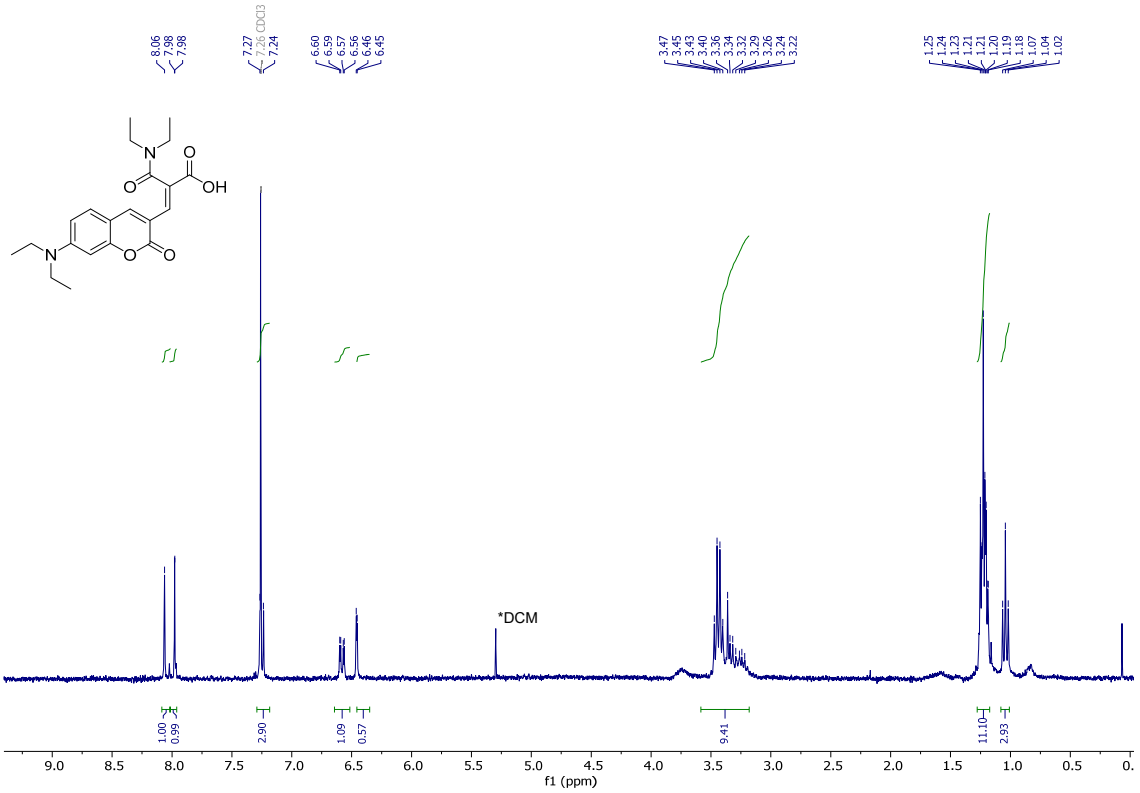
8.06
7.98
7.98
7.27
7.26 CDCl3
7.24
6.60
6.59
6.57
6.56
6.46
6.45
3.47
3.45
3.43
3.40
3.36
3.34
3.32
3.29
3.26
3.24
3.22
1.25
1.24
1.23
1.21
1.21
1.20
1.19
1.18
1.07
1.04
1.02
O
O
OH
N
O
O
N
*DCM
1.00
0.99
2.90
1.09
0.57
9.41
11.10
2.93
f1 (ppm)

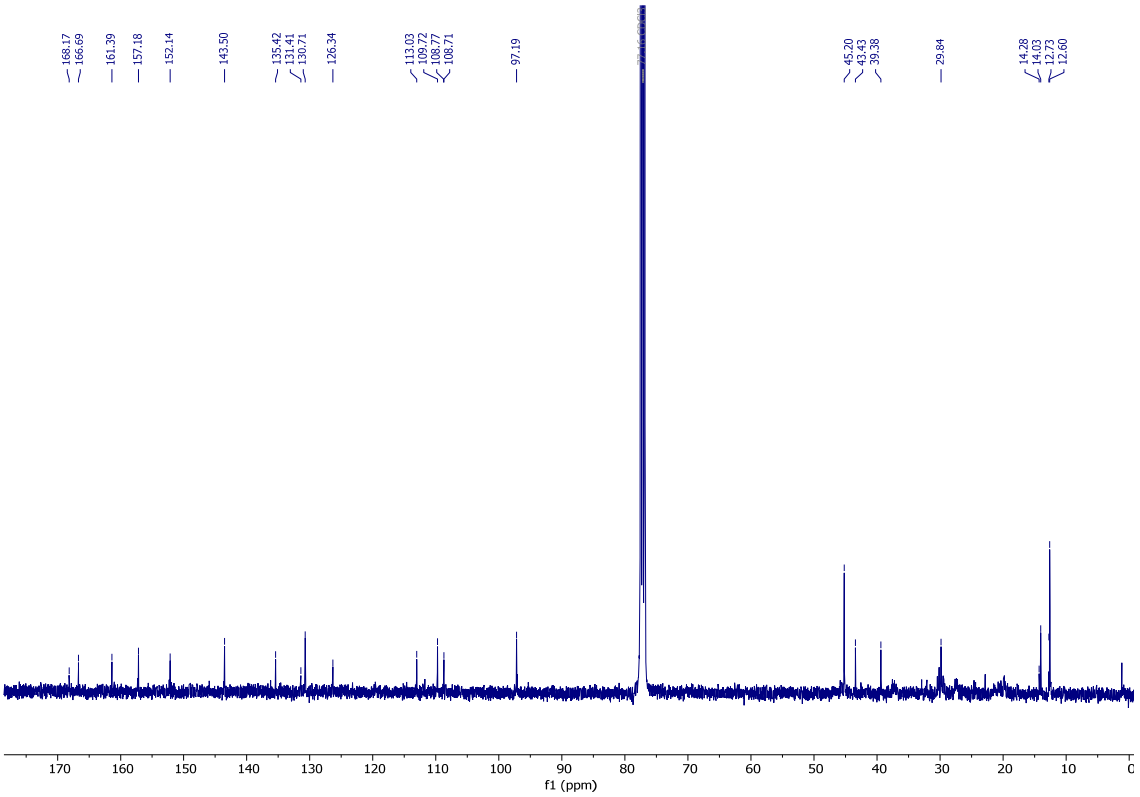
168.17
166.69
161.39
157.18
152.14
143.50
135.42
131.41
130.71
126.34
113.03
109.72
108.77
108.71
97.19
45.20
43.43
39.38
29.84
14.28
14.03
12.73
12.60
f1 (ppm)

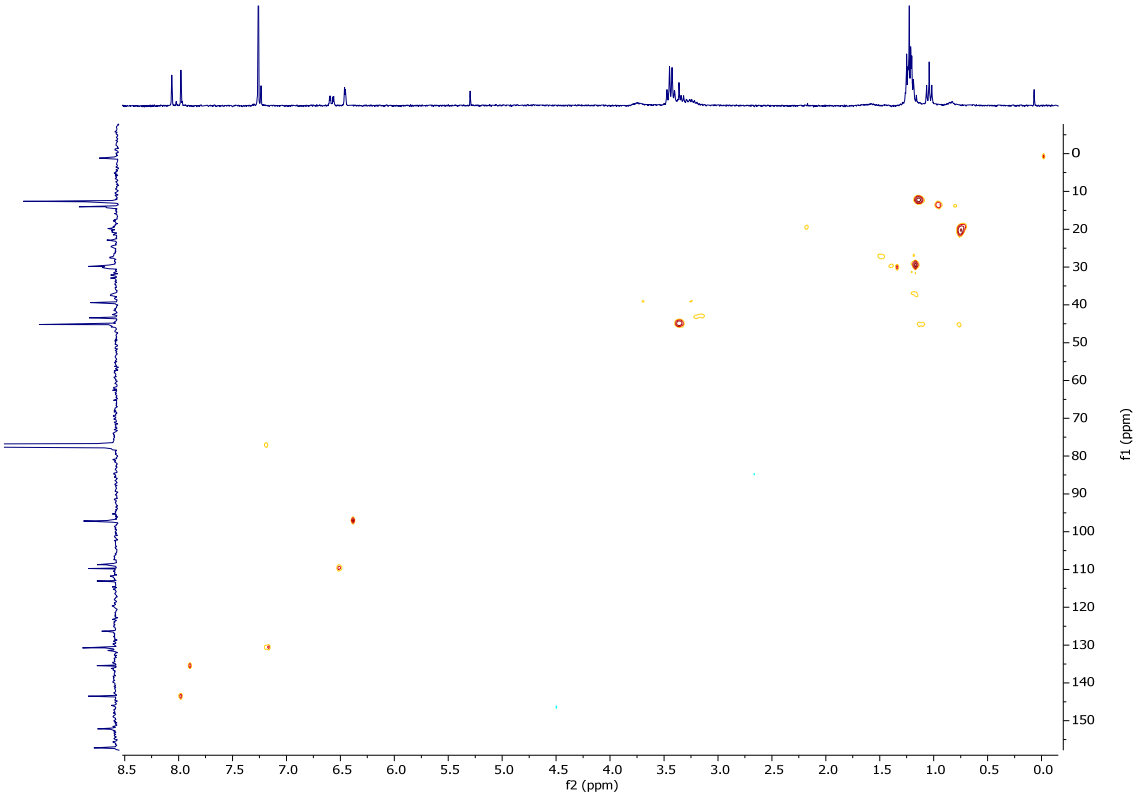

Figure S 110. ^{1}H-NMR, ^{13}C-NMR and HMQC of compound **S14** in $CDCl_3$.

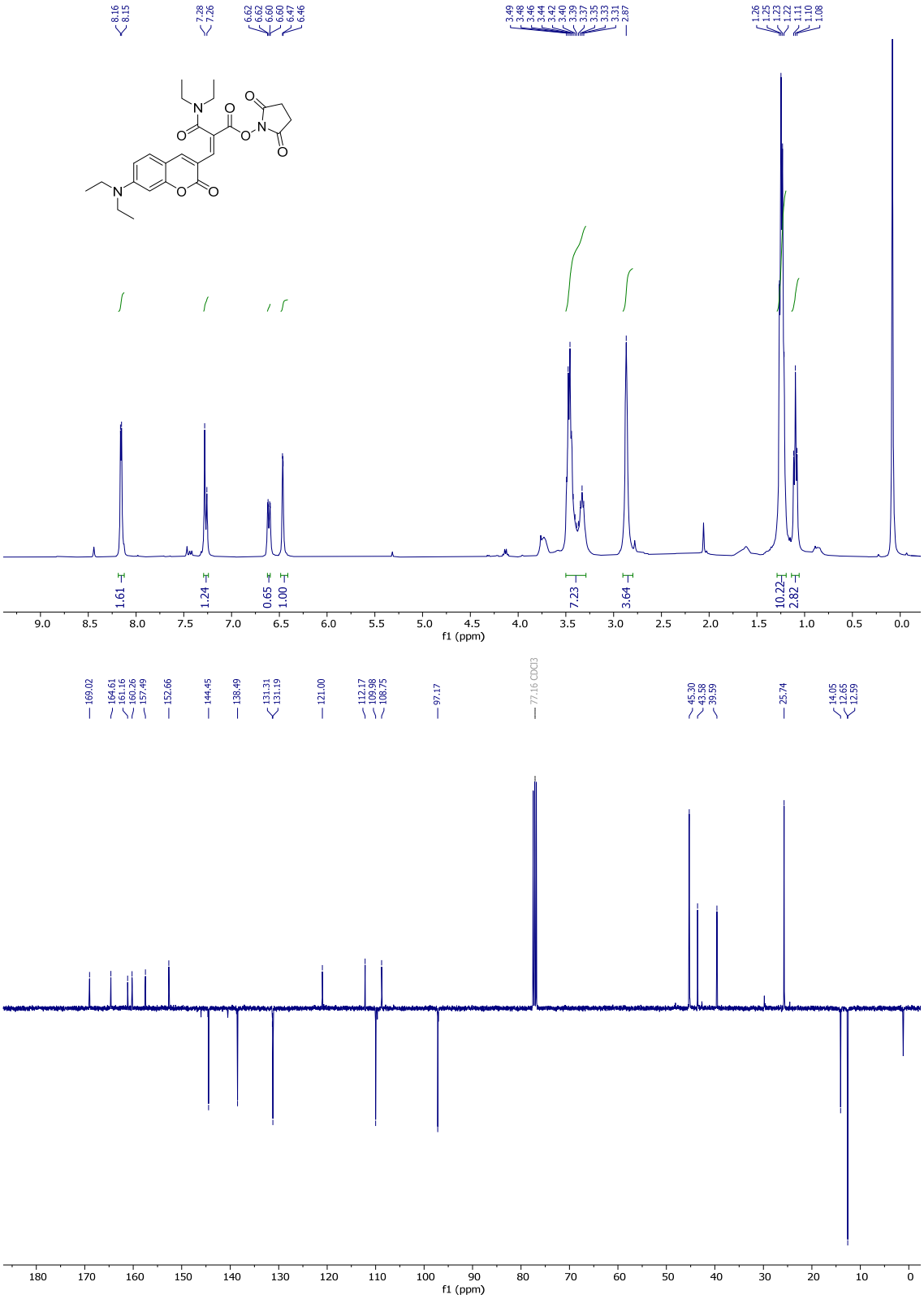

Figure S 111. ^{1}H-NMR and APT of compound **29** in $CDCl_3$.

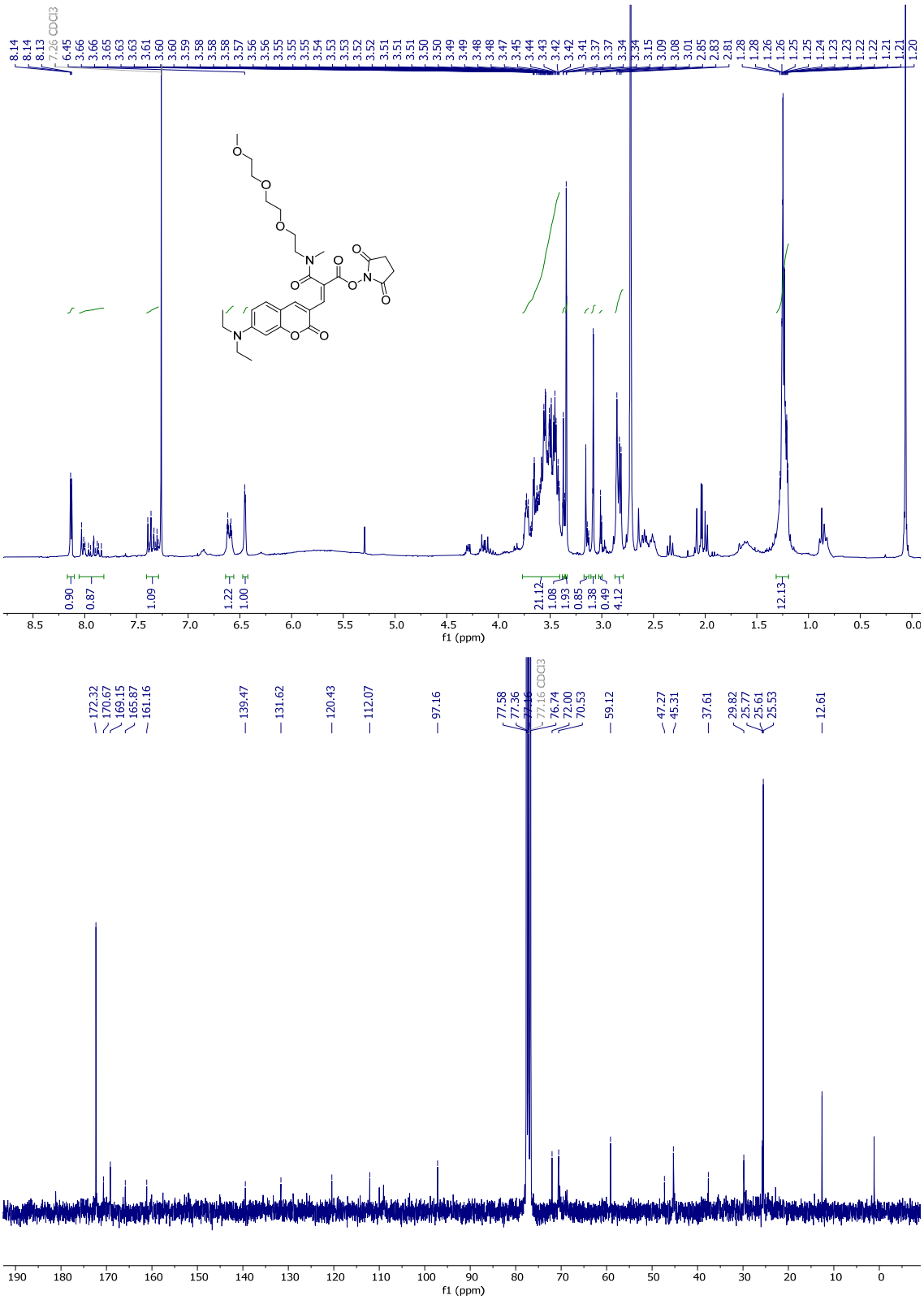

Figure S 112. ^{1}H-NMR and ^{13}C-NMR of compound **32** in $CDCl_3$.

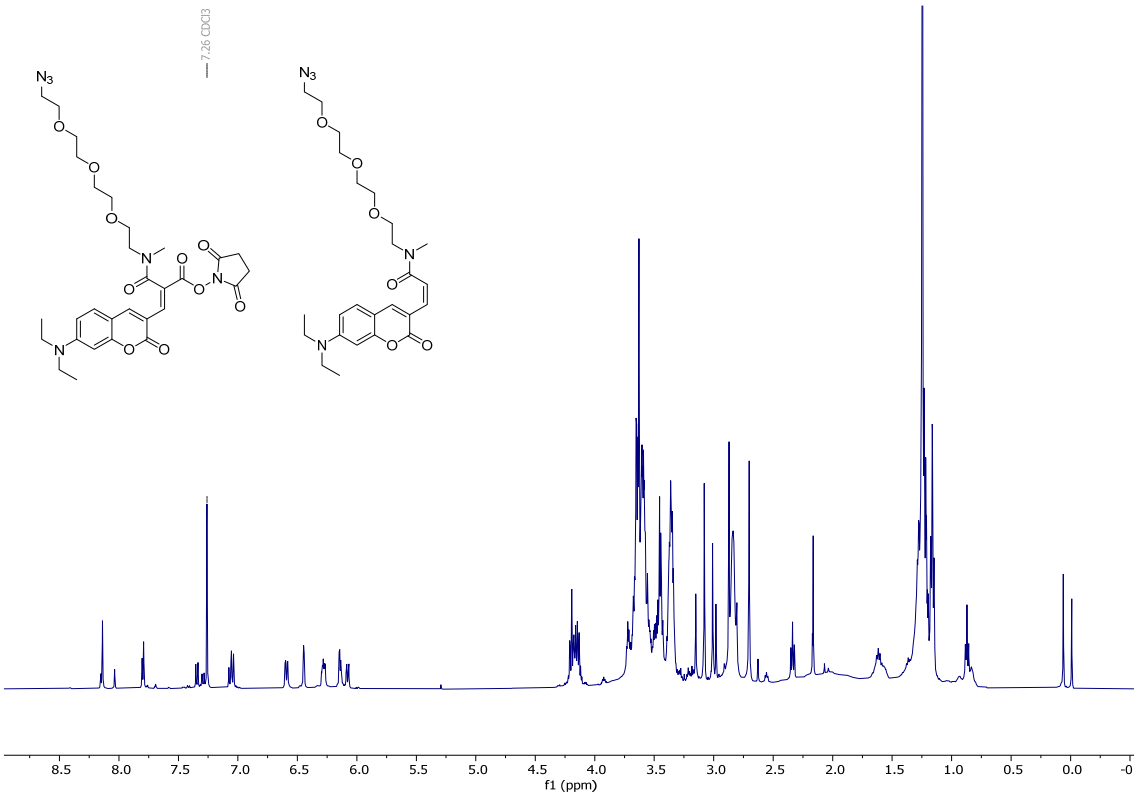

Figure S 113. ^{1}H-NMR, in $CDCl_3$, of **33** that coeluted with **S17** during the isolation step.

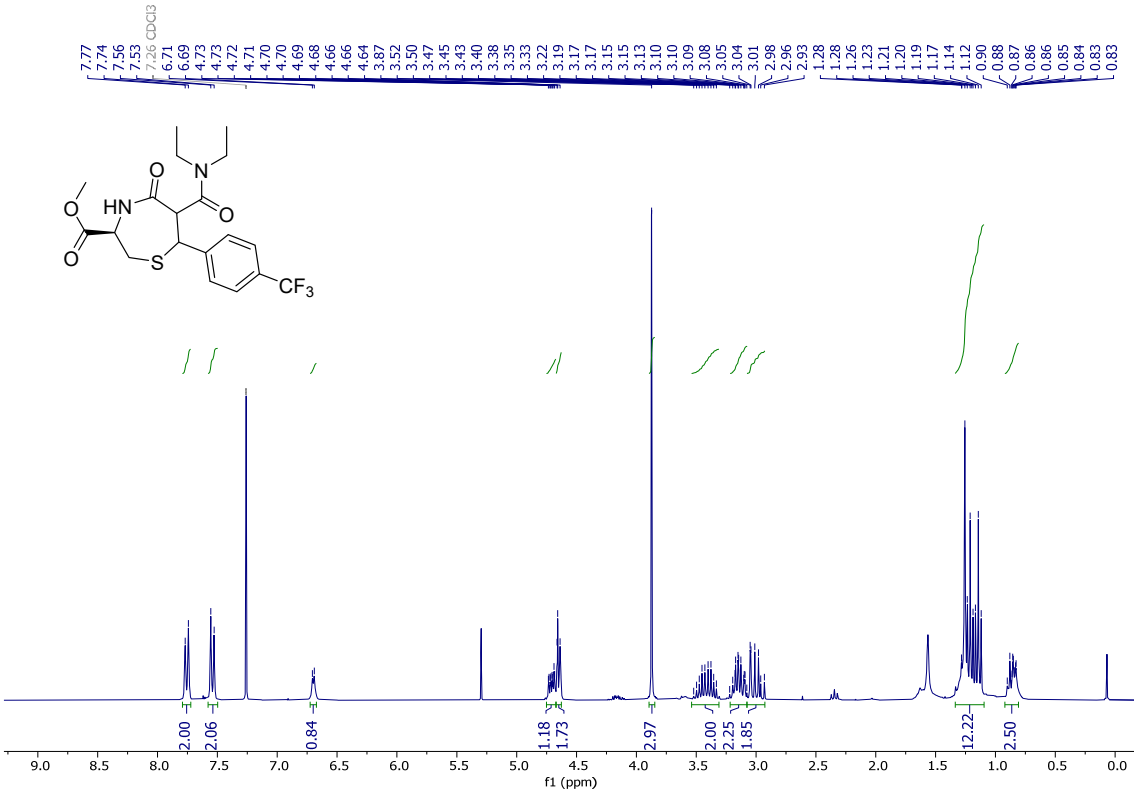

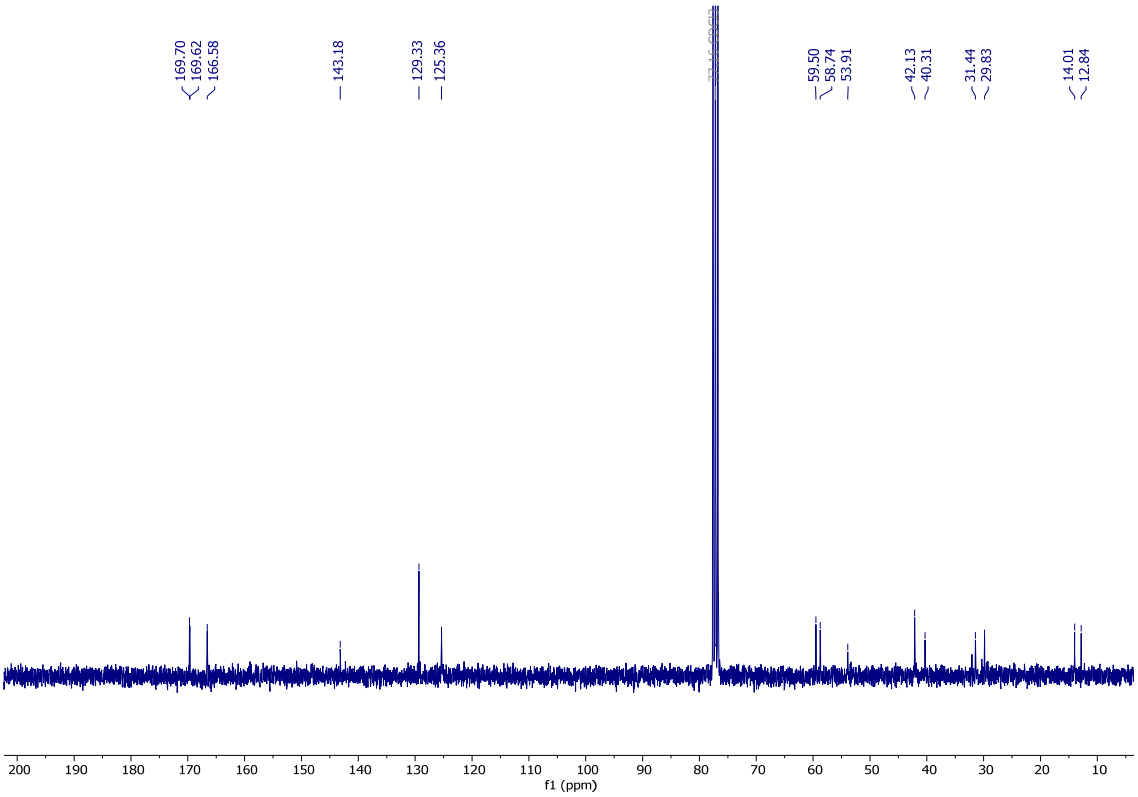

Figure S 114. ^{1}H-NMR and ^{13}C-NMR of compound **11 (fraction A)** in $CDCl_3$.

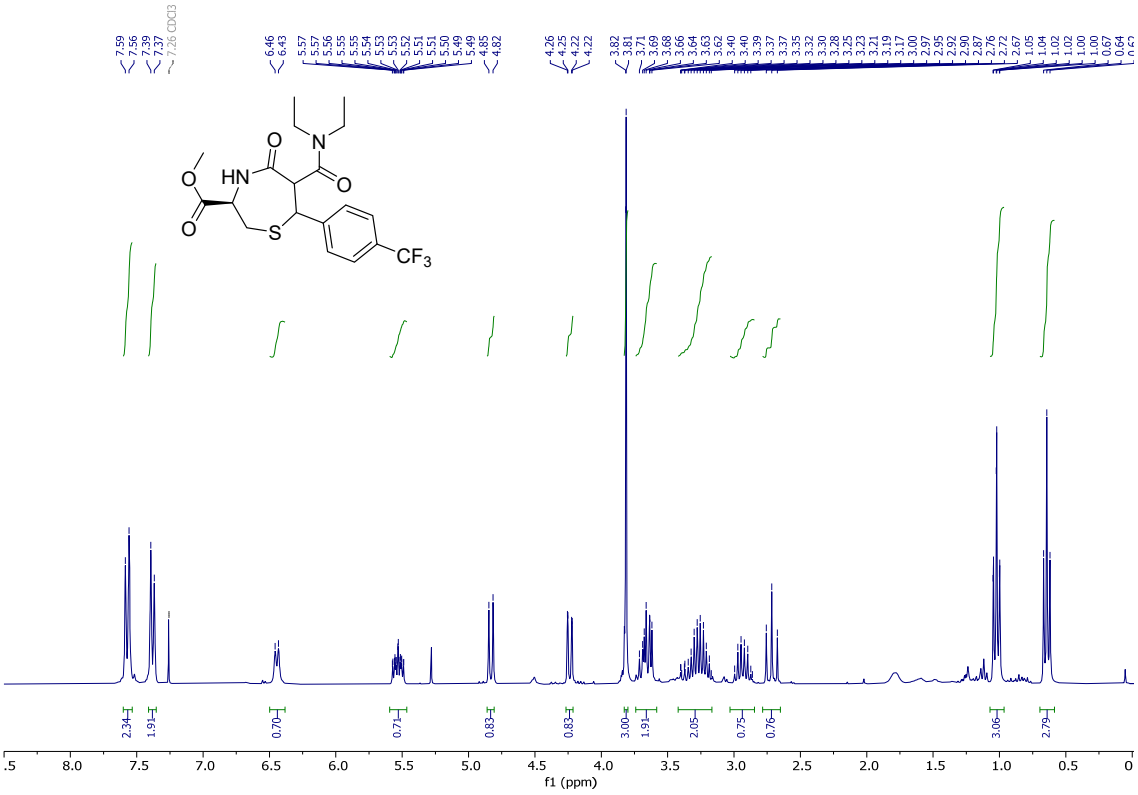

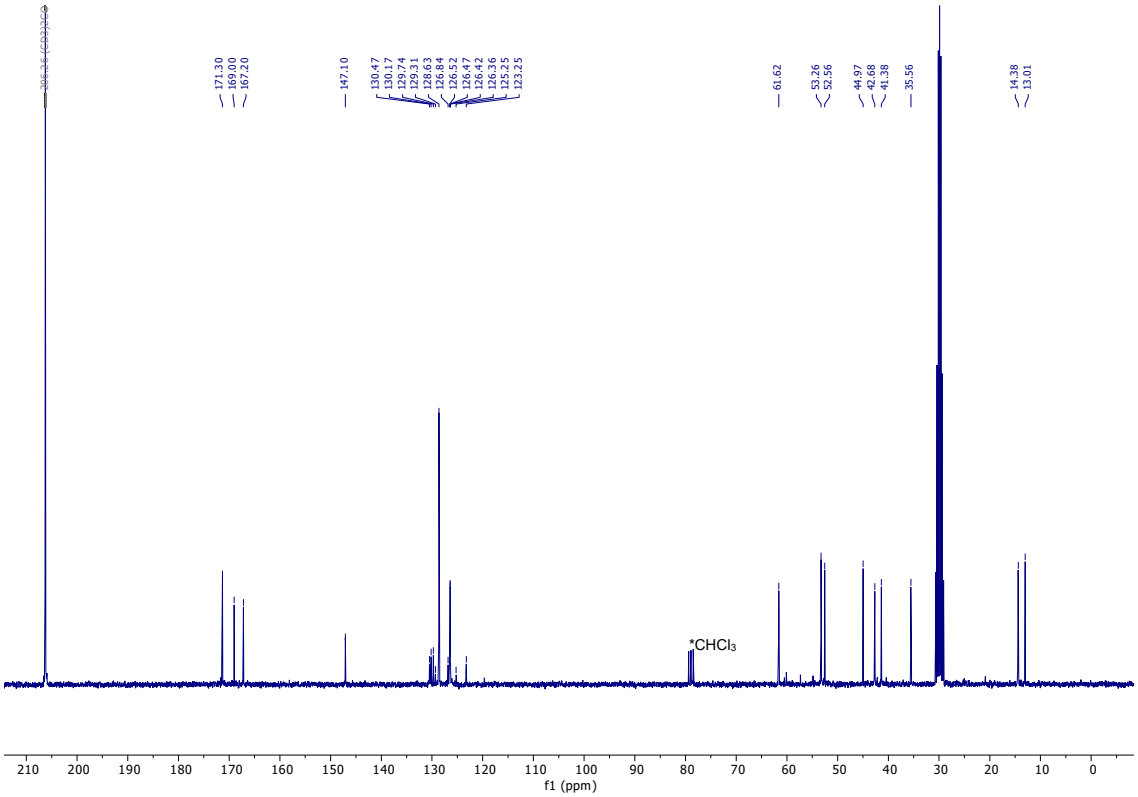

Figure S 115. ^{1}H-NMR (in $CDCl_3$) and ^{13}C-NMR (in Acetone-d_6) of compound **11 (fraction B)**.

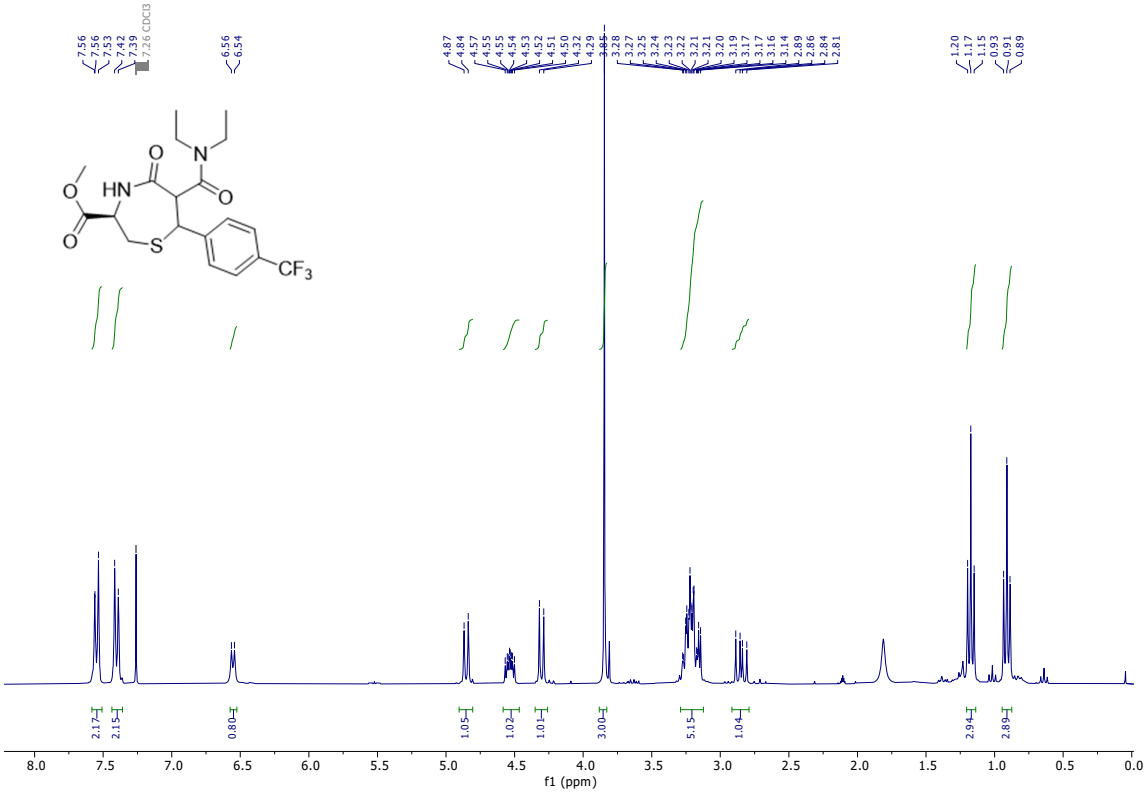

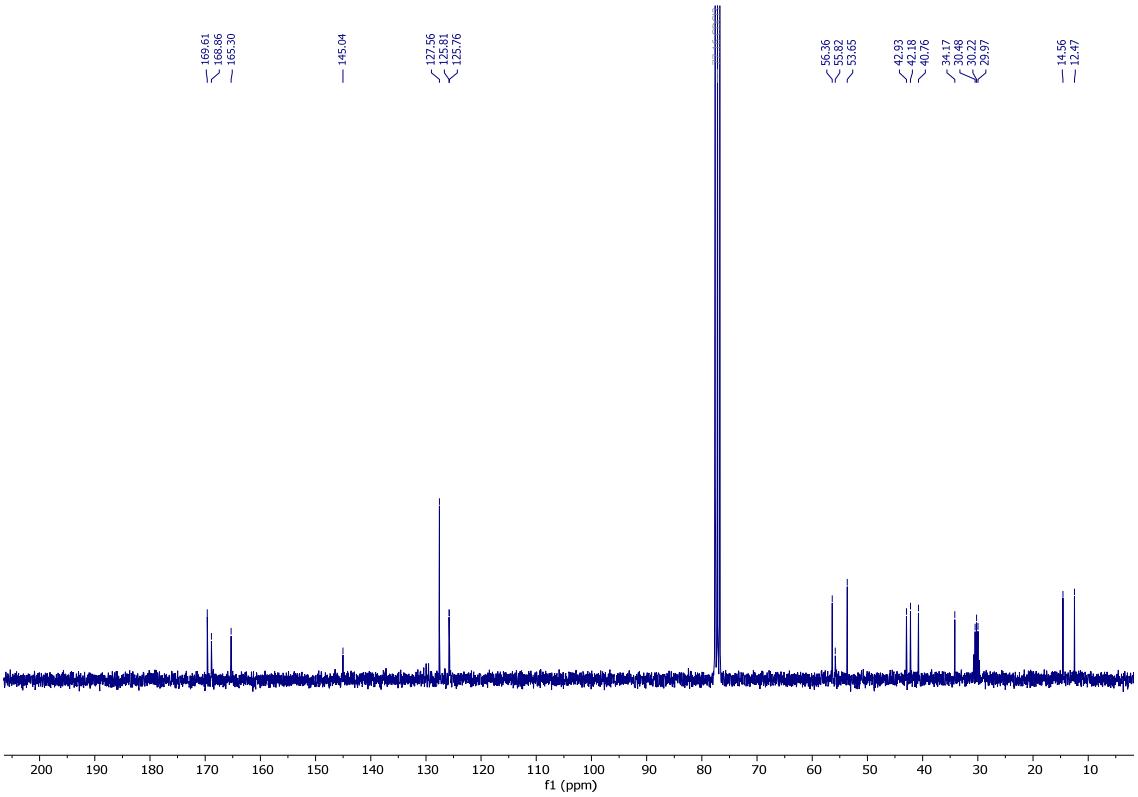

Figure S 116. ^{1}H-NMR and ^{13}C-NMR of compound **11 (fraction C)** in $CDCl_3$.

19. References

1. R. Heathcote, J. A. S. Howell, N. Jennings, D. Cartlidge, L. Cobden, S. Coles and M. Hursthouse, *Dalton Trans.*, 2007, 1309.
2. D. Lahav, B. Liu, R. J. B. H. N. van den Berg, A. M. C. H. van den Nieuwendijk, T. Wennekes, A. T. Ghisaidoobe, I. Breen, M. J. Ferraz, C.-L. Kuo, L. Wu, P. P. Geurink, H. Ovaa, G. A. van der Marel, M. van der Stelt, R. G. Boot, G. J. Davies, J. M. F. G. Aerts and H. S. Overkleeft, *J. Am. Chem. Soc.*, 2017, **139**, 14192.
3. S. Svedhem, C.-Å. Hollander, J. Shi, P. Konradsson, B. Liedberg and S. C. T. Svensson, *J. Org. Chem.*, 2001, **66**, 4494.
4. *US Pat.,* 39301951B2, 2016.
5. R. Tuba and F. Ungváry, *J. Mol. Catal. A Chem.*, 2003, **203**, 59.
6. Y. Kobayashi and T. Harayama, *Tetrahedron Lett.*, 2009, **50**, 6665.
7. X. Wang, J. Zhou, F. Yang, Z. Xue and N. Xu, *J. Chem. Res.*, 2016, **40**, 604.
8. V. Froidevaux, M. Borne, E. Laborbe, R. Auvergne, A. Gandini and B. Boutevin, *RSC Adv.*, 2015, **5**, 37742.
9. E. Ros, M. Bellido, X. Verdaguer, L. Ribas de Pouplana and A. Riera, *Bioconjugate Chem.*, 2020, **31**, 933.